

Synthesis and evaluation of novel NQO2 inhibitors

A thesis submitted to the University of Manchester for the degree of Doctor
of Philosophy in the Manchester Pharmacy School

October/ 2013

Soraya Ma'moun Othman Alnabulsi

Manchester Pharmacy School

TABLE OF CONTENTS

Contents	2
List of Figures	11
List of Schemes	15
List of Tables	19
List of Abbreviations	20
Abstract	21
Declaration	22
Copyright	22
Acknowledgement	23
Dedication	25
Chapter I. Introduction	
1. Cancer	26
1.1. Cancer Chemotherapy	26
1.1.1. Antimetabolites	27
1.1.1.1. Folate antagonists	27
1.1.1.2. Nucleoside analogues	28
1.1.1.2.1. 5-Fluorouracil and its nucleoside metabolites	29
1.1.1.2.2. Deoxycytidine derivatives	30
1.1.1.2.3. 6-Thioguanine and 6-mercaptopurine nucleosides	30
1.1.2. Alkylating agents	30
1.1.3. Topoisomerase enzymes inhibitors	33
1.1.4. DNA Intercalators	35
1.1.4.1. Acridines	36
1.1.4.2. Anthracyclines	36
1.1.5. Microtubules-targeting anticancer drugs	37
1.1.6. L-Asparaginase	37
1.1.7. Drugs that target the cell cycle	38
1.2. Cancer resistance to chemotherapy- the need for new targets and approaches	39
1.3. Cancer chemoprevention- first line of defence	39
2. Quinones as carcinogenic compounds	41
2.1. Quinone reductases (QRs)	42
2.1.1. NAD(P)H: quinone reductase 1 (NQO1) enzyme	43
2.1.2. <i>N</i> -Ribosyl dihydronicotinamide (NRH): quinone	44

oxidoreductase 2 (NQO2) enzyme	
2.1.3. NQO1 and NQO2: similarities and differences	48
2.1.4. The catalytic consequences of NQO1 and NQO2 on cells	50
2.1.5. Importance of NQO1 and NQO2 enzymes in cancer-targeted therapy	51
3. NQO2 enzyme and its role in human diseases	53
3.1. NQO2 inhibitors	54
3.1.1. Flavones	55
3.1.2. Resveratrol	56
3.1.3. Aminoquinolines	56
3.1.4. MT-3 ligands	56
3.1.5. Imatinib (Glivec®)	57
3.1.6. Dabigartan and its ethyl ester prodrug	58
3.1.7. Casimiroin and its analogues	58
3.1.8. Triazoloacridin-6-ones	60
3.1.9. Imidazoloacridin-6-ones	60
3.1.10. Indolequinones	61
3.1.11. Quinoline and pyrroloquinoline ammosamide analogues	62
3.1.12. 9-Aminoacridine	63
3.1.13. Ellipticine	63
3.1.14. Quinolines	64
3.1.15. Furan-amidines	65
3.1.16. Mode of binding of the NQO2 inhibitors in the active site	65
4. Amidine functional group	67
4.1. Amidine-containing pharmacologically active molecules	68
4.1.1. Fibrogen antagonists	69
4.1.2. Anticoagulant drugs	69
5. Aim and objectives of the research	69
Chapter II. Results and Discussion/ Chemistry	
1. Introduction	71

2. Synthesis of the furan-amidine scaffold	71
3. Synthesis of the asymmetric furan-amidine scaffold: synthetic pathway optimization	74
3.1. Mannich base reaction	75
3.2. Aryl 1,4-diketones synthesis	75
3.2.1. Synthesis of 5-(2-hydroxy)-3,4-dimethyl-1,3-thiazolium iodide catalyst 128	82
3.3. 2,5-Diarylfuran synthesis	83
3.4. Carboximidate synthesis	87
3.5. Amidine functional group synthesis	90
3.6. Conclusion	94
4. Applications of the optimized multi-step synthetic pathway	95
4.1. Asymmetric aryl 1,4-diketones synthesis	96
4.1.1. Spectroscopic characterization of the 1,4-diketones 165-174	99
4.1.2. Synthesis of the methyl aryl ketones 163 and 164	102
4.1.3. Synthesis of α -bromomethyl aryl ketone 175	103
4.2. Synthesis of the aryl 1,4-diketone with a <i>meta</i> -nitrile group 179	104
4.3. Synthesis of the ethyl imidate intermediates	105
4.4. Synthesis of the targeted amidines	105
4.5. Physical properties of the amidines 144-154	106
5. Asymmetric furan-amidine isosteres	108
5.1. Hydrophilicity optimization	108
5.1.1. Synthesis of substituted 2,5-diarylpyrrole-amidines 191 and 192	109
5.1.2. Synthesis of substituted imidazole-amidines 193 and 194	115
5.1.3. Synthesis of oxazole-amidine 195	122
5.2. Hypothesized correlation between compound structure and NQO2 inhibitory activity	127
5.2.1. Synthesis of an asymmetric 3,4-disubstituted furan-amidine	127
5.2.2. Synthesis of the asymmetric 2,5-diarylthiophene-amidine 226	133

5.3. Amidine isosteres: Bioavailability optimization	138
5.3.1. Amidine isosteres: Synthesis of 1,4-diketones substrates	139
5.3.2. Amidine isosteres: 2,5-Diarylfuarns syntheses	140
5.3.3. Amidine isosteres: 2,5-Diarylthiophenes syntheses	140
5.3.4. Amidine isosteres: Reduction of the nitro-groups into aromatic amines	141
5.3.5. Amidine isosteres: <i>N</i> -aryl amidines “reversed amidines” syntheses	143
5.3.5.1. Synthesis of <i>S</i> -2-naphthylmethyl thioacetimidate hydrobromide 251	144
5.3.6. Amidine isosteres: <i>N</i> -Aryl amides syntheses	145
5.3.7. Amidine isosteres: Carboximidate synthesis	146
5.3.8. Amidine isosteres: Amidoxime synthesis	148
6. Furan analogue of resveratrol	150
6.1. Synthesis of 3',5'-dihydroxy-2-bromoacetophenone 252	153
6.2. Synthesis of 4'-(acetyloxy)acetophenone 253	154
6.3. Synthesis of 3',5'-di(acetyloxy)acetophenone 254	154
6.4. Synthesis of 2-bromo-4'-(acetyloxy)acetophenone 255	155
7. Synthesis of <i>N</i>-ribosyl dihydronicotinamide NRH	158
Chapter II. Results and Discussion/ NQO2 Inhibitory Activity	
1. Inhibition of recombinant human NQO2 enzyme activity	160
Chapter II. Results and Discussion/ Docking	
1. Docking: Correlation between the predicted and real NQO2 inhibitory activity of the synthesized compounds	166
Chapter II. Results and Discussion/ DNA Melting	
1. Introduction	171
2. DNA binding: Is it an off-target effect for the synthesized asymmetric furan- and <i>N</i> -methylpyrrole-amidines?	172
3. DNA binding: Reversed amidines and DNA binding affinities	176
Chapter II. Results and Discussion/ Conclusion	
1. Conclusion on synthesis and evaluation of novel NQO2 inhibitors	177
Chapter II. Results and Discussion/ Future work	
1. Isosteric replacement of the basic amidine group with the acidic carboxylic acid	179

2. Synthesis of 3-fluoro diarylimidazole-amidine	179
3. Positron Emission Tomography (PET): Study of NQO2 biological role and consequences of its inhibition in tumour cells	179
Chapter III. Experimental/ Chemistry	
1. Chemicals and materials	181
2. Synthesis	181
2.1. Mannich bases 121 and 125	181
2.1.1. <i>N,N</i> -Dimethyl 1-(4-cyanophenyl)-1-oxopropan-3-ammonium chloride 121	182
2.1.2. <i>N,N</i> -Dimethyl 1-oxo-1-phenylpropan-3-ammonium chloride 123	182
2.2. Aryl 1,4-diketones 123 and 126	182
2.2.1. General procedure for Stetter reaction	183
2.2.1.1. 1,4-Bis(4-cyanophenyl)-1,4-butadione 123	183
2.2.1.2. 1-(4-Cyanophenyl)-4-phenyl-1,4-butadione 126	183
2.2.1.3. 5-(2-Hydroxyethyl)-3,4-dimethyl-1,3-thiazolium iodide catalyst 128	184
2.2.2. General procedure for the coupling between methyl aryl ketones and α -bromomethyl aryl ketones	184
2.2.2.1. 1,4-Bis(4-cyanophenyl)-1,4-butadione 123	185
2.2.2.2. 1-(4-Cyanophenyl)-4-phenyl-1,4-butadione 126	185
2.3. General procedure for the synthesis of 2,5-diarylfurans 118 and 127	185
2.3.1. 4,4'-(Furan-2,5-diaryl)benzotrile 118	185
2.3.2. 4-(5-Phenylfuran-2-yl)benzotrile 127	186
2.4. General procedure for the synthesis of furan-imidates 119 and 143	186
2.4.1. Diethyl 4,4'-(furan-2,5-diyl)dibenzimidate dihydrochlorides 119	186
2.4.2. Ethyl 4-(5-phenylfuran-2-yl)benzimidate hydrochloride 143	187
2.5. General procedure for the synthesis of furan-amidines 110 and 111	187
2.5.1. 4-(5-Phenylfuran-2-yl)benzamidine acetate 110	187
2.5.2. 4,4'-(Furan-2,5-diyl)dibenzamidine acetate 111	188
2.6. General procedure for the synthesis of asymmetric aryl 1,4-	188

diketones 165-174	
2.6.1.	1-(4-Cyanophenyl)-4-(3-fluorophenyl)-1,4-butadione 165 189
2.6.2.	1-(4-Cyanophenyl)-4-(4-fluorophenyl)-1,4-butadione 166 189
2.6.3.	1-(4-Cyanophenyl)-4-(4-bromophenyl)-1,4-butadione 167 190
2.6.4.	1-(4-Cyanophenyl)-4-(3-nitrophenyl)-1,4-butadione 168 190
2.6.5.	1-(4-Cyanophenyl)-4-(4-nitrophenyl)-1,4-butadione 169 191
2.6.6.	1-(4-Cyanophenyl)-4-(4-methoxyphenyl)-1,4-butadione 170 191
2.6.7.	1-(4-Cyanophenyl)-4-(4-methylphenyl)-1,4-butadione 171 192
2.6.8.	1-(4-Cyanophenyl)-4-(4-ethylphenyl)-1,4-butadione 172 193
2.6.9.	1-(4-Cyanophenyl)-4-(4-isopropylphenyl)-1,4-butadione 173 194
2.6.10.	1-(4-Cyanophenyl)-4-(4- <i>tert</i> -butylphenyl)-1,4-butadione 174 194
2.7.	1-(3-Cyanophenyl)-4-phenyl-1,4-butadione 179 195
2.8.	General procedure for the synthesis of methyl aryl ketones 163 and 164 196
2.8.1.	4-Isopropylacetophenone 163 196
2.8.2.	4- <i>tert</i> -Butylacetophenone 164 196
2.9.	2-Bromo-1-(4-ethylphenyl)ethanone 175 197
2.10.	4-(5-Phenyl-1H-pyrrol-2-yl)benzotrile 198 197
2.11.	4-(1-Methyl-5-phenyl-1H-pyrrol-2-yl)benzotrile 199 198
2.12.	General procedure for the synthesis of ethylfuran- 180-190 , pyrrole- 200 , and <i>N</i> -methylpyrrole-imidate hydrochloride 201 intermediates 198
2.12.1.	Ethyl 4-(5-(3-fluorophenylfuran-2-yl)benzimidate hydrochloride 180 199
2.12.2.	Ethyl 4-(5-(4-fluorophenylfuran-2-yl)benzimidate hydrochloride 181 199
2.12.3.	Ethyl 4-(5-(4-bromophenylfuran-2-yl)benzimidate hydrochloride 182 200
2.12.4.	Ethyl 4-(5-(3-nitrophenylfuran-2-yl)benzimidate hydrochloride 183 200
2.12.5.	Ethyl 4-(5-(4-nitrophenylfuran-2-yl)benzimidate hydrochloride 184 201

2.12.6. Ethyl 4-(5-(methoxyphenylfuran-2-yl)benzimidate hydrochloride 185	201
2.12.7. Ethyl 4-(5-(4-methylphenylfuran-2-yl)benzimidate hydrochloride 186	201
2.12.8. Ethyl 4-(5-(4-ethylphenylfuran-2-yl)benzimidate hydrochloride 187	202
2.12.9. Ethyl 4-(5-(4-isopropylphenylfuran-2-yl)benzimidate hydrochloride 188	202
2.12.10. Ethyl 4-(5-(4- <i>tert</i> -butylphenylfuran-2-yl)benzimidate hydrochloride 189	203
2.12.11. Ethyl 3-(5-phenylfuran-2-yl)benzimidate hydrochloride 190	203
2.12.12. Ethyl 4-(5-phenyl-1 <i>H</i> -pyrrol-2-yl)benzimidate hydrochloride 200	204
2.12.13. Ethyl 4-(1-methyl-5-phenyl-1 <i>H</i> -pyrrol-2-yl)benzimidate hydrochloride 201	204
2.13. General procedure for the synthesis of furan- 144-154 , pyrrole- 191 , and <i>N</i> -methylpyrrole-amidine acetates 192	205
2.13.1. 4-(5-(3-Fluorophenyl)furan-2-yl)benzamidine acetate 144	205
2.13.2. 4-(5-(4-Fluorophenyl)furan-2-yl)benzamidine acetate 145	205
2.13.3. 4-(5-(4-Bromophenyl)furan-2-yl)benzamidine acetate 146	206
2.13.4. 4-(5-(3-Nitrophenyl)furan-2-yl)benzamidine acetate 147	206
2.13.5. 4-(5-(4-Nitrophenyl)furan-2-yl)benzamidine acetate 148	207
2.13.6. 4-(5-(4-Methoxyphenyl)furan-2-yl)benzamidine acetate 149	207
2.13.7. 4-(5-(4-Methylphenyl)furan-2-yl)benzamidine acetate 150	208
2.13.8. 4-(5-(4-Ethylphenyl)furan-2-yl)benzamidine acetate 151	208
2.13.9. 4-(5-(4-Isopropylphenyl)furan-2-yl)benzamidine acetate 152	209
2.13.10. 4-(5-(4- <i>tert</i> -Butylphenyl)furan-2-yl)benzamidine acetate 153	209
2.13.11. 3-(5-Phenylfuran-2-yl)benzamidine acetate 154	210
2.13.12. 4-(5-Phenyl-1 <i>H</i> -pyrrol-2-yl)benzamidine acetate 191	210
2.13.13. 4-(1-Methyl-5-phenyl-1 <i>H</i> -pyrrol-2-yl)benzamidine acetate 192	211
2.14. 4-(4-Phenyl-1 <i>H</i> -imidazol-2-yl)benzonitrile 203	211

2.15.	4-(1-Methyl-4-phenyl-1 <i>H</i> -imidazol-2-yl)benzotrile	205A	212
	2.16.1.	4-(5-Phenyloxazol-2-yl)benzamidine acetate	211
			212
	2.16.2.	4-Cyano- <i>N</i> -(2-oxo-2-phenylethyl)benzamide	209
			213
2.17.	4-(4-Methyl-5-phenylfuran-2-yl)benzotrile	224	213
2.18.	4-(5-Phenylthiophen-2-yl)benzotrile	228	214
2.19.	General procedure for the synthesis of <i>N</i> -hydroxyamidines (amidoximes)	204, 206, 212, 225, 233 and 240	214
	2.19.1.	<i>N</i> -Hydroxy-4-(4-phenyl-1 <i>H</i> -imidazol-2-yl)benzamidine	204
			215
	2.19.2.	<i>N</i> -Hydroxy-4-(1-methyl-4-phenyl-1 <i>H</i> -imidazol-2-yl)benzamidine	206
			215
	2.19.3.	<i>N</i> -Hydroxy-4-(4-phenyloxazol-2-yl)benzamidine	212
			216
	2.19.4.	<i>N</i> -Hydroxy-4-(4-methyl-5-furan-2-yl)benzamidine	225
			216
	2.19.5.	<i>N</i> -Hydroxy-4-(5-phenylthiophen-2-yl)benzamidine	233
			217
	2.19.6.	<i>N</i> -Hydroxy-4-(5-phenylfuran-2-yl)benzamidine	240
			217
2.20.	General procedure for the synthesis of amidines	193-195	218
	2.20.1.	4-(Phenyl-1 <i>H</i> -imidazol-2-yl)benzamidine acetate	193
			218
	2.20.2.	4-(1-Methyl-4-phenyl-1 <i>H</i> -imidazol-2-yl)benzamidine acetate	194
			219
	2.20.3.	4-(4-Phenyloxazol-2-yl)benzamidine acetate	195
			219
	2.20.4.	4-(4-Methyl-5-phenylfuran-2-yl)benzamidine acetate	223
			220
2.21.	4-(4-Methyl-5-phenylthiophen-2-yl)benzamidine acetate	226	220
2.22.	Methyl 4-(5-phenylfuran-2-yl)benzimidate hydrochloride	234	221
2.23.	General procedure for the synthesis of the aryl 1,4-diketones	241 and 242	221
	2.23.1.	1-(3-Nitrophenyl)-4-phenyl-1,4-butadione	241
			222
	2.23.1.	1-(4-Nitrophenyl)-4-phenyl-1,4-butadione	242
			222
2.24.	General procedure for the synthesis of 2,5-diarylfurans	243 and 244	223
	2.24.1.	2-(3-Nitrophenyl)-5-phenylfuran	243
			223
	2.24.2.	2-(4-Nitrophenyl)-5-phenylfuran	244
			223
2.25.	General procedure for the synthesis of 2,5-diarylthiophenes	245 and 246	224
	2.25.1.	2-(3-Nitrophenyl)-5-phenylthiophene	245
			224
	2.25.2.	2-(4-Nitrophenyl)-5-phenylthiophene	246
			225
2.26.	General procedure for the synthesis of amines	247-250	225
	2.26.1.	3-(5-Phenylfuran-2-yl)aniline	247
			225
	2.26.2.	4-(5-Phenylfuran-2-yl)aniline	248
			226
	2.26.3.	3-(5-Phenylthiophen-2-yl)aniline	249
			226
	2.26.4.	4-(5-Phenylthiophen-2-yl)aniline	250
			227
2.27.	General procedure for the synthesis of <i>N</i> -aryl amidines (reversed amidines)	235 and 236	227
	2.27.1.	<i>N</i> -(4-(5-Phenylfuran-2-yl)phenyl)acetimidate hydrobromide	235
			227
	2.27.2.	<i>N</i> -(4-(5-Phenylthiophen-2-yl)phenyl)acetimidate hydrobromide	236
			228
	2.27.3.	<i>S</i> -2-Naphthylmethylthioacetimidate hydrobromide	251
			228
2.28.	General procedure for the synthesis of <i>N</i> -aryl amides	237-239	229
	2.28.1.	<i>N</i> -(3-(5-Phenylfuran-2-yl)phenyl)acetamide	237
			229

2.28.2. <i>N</i> -(4-(5-Phenylfuran-2-yl)phenyl)acetamide	238	229
2.28.3. <i>N</i> -(3-(5-Phenylthiophen-2-yl)phenyl)acetamide	239	230
2.29. Furan analogue of resveratrol		230
2.29.1. 4'-(Acetyloxy)acetophenone	253	230
2.29.2. 3',5'-Di(acetyloxy)acetophenone	254	231
2.29.3. 2-Bromo-4'-(acetyloxy)acetophenone	255	231
2.3. <i>N</i> -Ribosyl dihydronicotinamide	NRH	232
Chapter III. Experimental/ NQO2 Inhibitory Activity		
1. Materials and methods		233
2. General procedure		233
Chapter III. Experimental/ Docking		
1. Materials and methods		234
2. General procedure		234
Chapter III. Experimental/ DNA Melting		
1. Materials and methods		235
2. Calf thymus DNA preparation		235
3. General procedure for DNA melting temperatures measurement		235
Chapter IV. References		
		236

LIST OF FIGURES

Figure 1. The structure of methotrexate (1).	27
Figure 2. Structures of methotrexate analogues, trimetrexate (2) and edatrexate (3).	28
Figure 3. The structure of 5-fluorouracil (4).	29
Figure 4. Structures of 6-thioguanine (5) and 6-mercaptopurine (6).	30
Figure 5. Structures of the topoisomerase I enzyme inhibitors, camptothecin (7), topotecan (8) and irinotecan (9).	33
Figure 6. Structures of epipodophyllotoxin anticancer drugs, teniposide (10), etoposide (11) and podophyllotoxin (12).	34
Figure 7. Structures of novel topoisomerase II inhibitors.	35
Figure 8. Structures of acridine DNA intercalators, nitracrine (18) and amsacrine (19).	36
Figure 9. Structures of doxorubicin (20) and daunorubicin (21).	37
Figure 10. Structures of anticancer drugs that target the cell cycle, flavopiridol (22) and UCN-01 (23).	39
Figure 11. Structures of FMN (27) and FAD (28) cofactors.	42
Figure 12. The 3D structure of NQO2 enzyme (PDB code 1QR2; Resolution at 2.10 Å).	45
Figure 13. NQO2 enzyme active site (PDB code 1QR2; Resolution at 2.10 Å).	46
Figure 14. Structures of NQO2 enzyme co-substrates, <i>N</i> -ribosyl (29), <i>N</i> -methyl (30), <i>N</i> -(<i>n</i> -propyl) (31) and <i>N</i> -benzyl (32) dihydronicotinamide.	47
Figure 15. Structures of the NQO2 substrates, menadione (33), coenzyme Q0 (34), estrone (35) and estradiol (36).	47
Figure 16. Enzyme's active site: A- NQO1 (PDB code 2F1O; Resolution at 2.75 Å); B- NQO2 (PDB code 1QR2; Resolution at 2.10 Å).	49
Figure 17. First known inhibitors of quinone reductase enzymes, benzo(a)pyrene (39), 7-methylbenzo(a)anthracene (40) and dicoumarol (41).	49
Figure 18. Structures of NADH (42) and NADPH (43).	50
Figure 19. Structures of anti-tumour prodrugs, CB 1954 (44) and nitro-cryptolepine derivatives (45).	51
Figure 20. The structure of 2-fluoro-7,9-dinitro-cryptolepine (47).	52
Figure 21. Structures of the anticancer drugs: mitomycin C (48), EO9 (49) and BMY25067 (50).	53
Figure 22. Structures of tyrosine kinase inhibitors, Imatinib (51) and nilotinib (52).	54
Figure 23. Structures of first reported NQO2 inhibitors, Quinacrine (53), Chlorpromazine (54) and benzo(a)anthracene (55).	55
Figure 24. Structures of flavonoid inhibitors of NQO2, Epigenin (56), Genistein (57), Kaempferol (58) and Quercetin (59).	55
Figure 25. The structure of resveratrol (60).	56
Figure 26. Structures of aminoquinoline inhibitors of NQO2, Primaquine (61) and Chloroquine (62).	56

Figure 27. Structures of MT3 receptor ligands.	57
Figure 28. Structures of the anticoagulants, dabigatran (71) and its ethyl ester (72).	58
Figure 29. The structure of casimiroin (73).	58
Figure 30. The structure of triazoloacridin-6-one NSC645827 (85).	60
Figure 31. The structure of imidazoloacridin-6-one NSC660841 (89).	61
Figure 32. Indolequinone scaffold (94).	62
Figure 33. The structure of ammosamide B (95).	62
Figure 34. Bicyclic (96) and tricyclic (97) analogues of ammosamide B.	62
Figure 35. The structure of the most potent analogue of ammosamide B (98).	62
Figure 36. The structure of 9-aminoacridine (99).	63
Figure 37. Casimirion (73) occupies two thirds of the active site of NQO2 (PDB code 3GAM; Resolution at 1.98 Å).	66
Figure 38. Resveratrol (60) occupies the whole area of the active site of NQO2 (PDB code 1SG0; Resolution at 1.50 Å).	67
Figure 39. Amidine and its carbonyl analogues.	67
Figure 40. The protonation states of amidine and guanidine.	68
Figure 41. Structures of amidine fibrogen antagonists, Ro 43-5054 (113) and Ro 44-9883 (114).	69
Figure 42. The structure of factor Xa inhibitor, DX-90659 (115).	69
Figure 43. The infrared spectrum of the 1,4-diketone 126 .	78
Figure 44. ¹ H NMR (CDCl ₃) spectrum of 1-(4-cyanophenyl)-4-phenyl-1,4-butadione 126 .	81
Figure 45. ¹ H NMR (DMSO-d ₆) spectrum of 5-(2-hydroxyethyl)-3,4-dimethyl-1,3-thiazolium iodide 128 .	83
Figure 46. ¹ H NMR (CDCl ₃) spectrum of 4-(5-phenylfuran-2-yl)benzotrile 127 .	85
Figure 47. ¹ H NMR (DMSO-d ₆) spectrum of 4,4'-(furan-2,5-diyl)benzotrile 118 .	86
Figure 48. Structure of the expected ethyl imidate hydrochloride salt 142 .	88
Figure 49. NMR (DMSO-d ₆) spectra of 4-(5-phenylfuran-2-yl)benzamidine acetate 110 : A- ¹ H NMR; B- ¹³ C NMR.	93
Figure 50. NMR (CDCl ₃) spectra of 1-(4-cyanophenyl)-4-(3-fluorophenyl)-1,4-butadione 165 : A- ¹ H NMR; B- ¹³ C NMR.	100
Figure 51. NMR (CDCl ₃) spectra of 1-(4-cyanophenyl)-4-(4-fluorophenyl)-1,4-butadione 166 : A- ¹ H NMR; B- ¹³ C NMR.	102
Figure 52. ¹ H NMR (CDCl ₃) spectrum of 4-(5-phenyl- <i>H</i> -pyrrol-2-yl)benzotrile 198 .	111
Figure 53. The W arrangement of <i>N</i> -H, H-3' and H-4' protons in 4-(5-	111

phenyl- <i>H</i> -pyrrol-2-yl)benzotrile 198 .	
Figure 54. ¹ H NMR spectrum of <i>N</i> -H, H-3' and H-4' protons of 4-(5-phenyl- <i>H</i> -pyrrol-2-yl)benzotrile 198 ; A-CDCl ₃ ; B- D ₂ O + CDCl ₃	112
Figure 55. ¹ H NMR (DMSO-d ₆) spectrum of 4-(1-methyl-5-phenyl- <i>H</i> -pyrrol-2-yl)benzotrile 199 .	113
Figure 56. ¹³ C NMR (DMSO-d ₆) spectrum of 4-(1-methyl-5-phenyl- <i>H</i> -pyrrol-2-yl)benzotrile 199 .	114
Figure 57. ¹ H NMR (DMSO-d ₆) spectrum of 4-(4-phenyl-1 <i>H</i> -imidazol-2-yl)benzotrile 203 .	116
Figure 58. ¹ H NMR (DMSO-d ₆) spectrum of <i>N</i> -hydroxy-4-(4-phenyl-1 <i>H</i> -imidazol-2-yl)benzamidine 204 .	118
Figure 59. IR spectrum of <i>N</i> -hydroxy-4-(4-phenyl-1 <i>H</i> -imidazol-2-yl)benzamidine 204 .	119
Figure 60. ¹ H NMR (DMSO-d ₆) spectrum of <i>N</i> -methylimidazole regioisomers 205A and 205B .	120
Figure 61. The NOESY (DMSO-d ₆) spectrum of 4-(1-methyl-4-phenyl-1 <i>H</i> -imidazol-2-yl)benzotrile 205A .	121
Figure 62. ¹ H NMR (DMSO-d ₆) spectrum of 4-cyano- <i>N</i> -(2-oxo-2-phenylethyl)benzamide 209 .	123
Figure 63. ¹ H NMR (DMSO-d ₆) spectrum of 4-(5-phenyloxazol-2-yl)benzotrile 211 .	126
Figure 64. Structures of the symmetric furan-amidine 112 and the proposed asymmetric 3,4-dimethylfuran-amidine 213 .	127
Figure 65. ¹ H NMR (DMSO-d ₆) spectrum for the furan compound 4-(4-methyl-5-phenylfuran-2-yl)benzotrile 224 .	130
Figure 66. IR spectrum of 4-(4-methyl-5-phenylfuran-2-yl)benzotrile 224 .	131
Figure 67. The structure of thiophene-amidine 226 .	133
Figure 68. IR spectrum of 4-(5-phenylthiophen-2-yl)benzotrile 228 .	136
Figure 69. A- ¹ H NMR (CDCl ₃) spectrum of A- 2-(3-nitrophenyl)-5-phenylfuran 243 ; B- ¹ H NMR (DMSO-d ₆) spectrum of 3-(5-phenylfuran-2-yl)aniline 247 .	142
Figure 70. Resonance states of the aryl ring A in 3-(5-phenylfuran-2-yl)aniline 247 .	143
Figure 71. ¹ H NMR (DMSO-d ₆) spectrum of <i>N</i> -(4-(5-phenylfuran-2-yl)phenyl)acetamide 238 .	146
Figure 72. NMR (CDCl ₃) spectra of methyl 4-(5-phenylfuran-2-yl)benzimidate hydrochloride 234 ; A- ¹ H NMR; B- ¹³ C NMR.	148
Figure 73. ¹ H NMR (DMSO-d ₆) spectrum of <i>N</i> -hydroxy-4-(5-phenylfuran-2-yl)benzamidine 240 .	150
Figure 74. The structures of resveratrol (60) and the furan-analogue of resveratrol (250).	150
Figure 75. ¹ H NMR (CDCl ₃) spectrum of 3-(acetyloxy)-5-hydroxyacetophenone 256 .	153
Figure 76. ¹ H NMR (CDCl ₃) spectrum of 2,4'-di(acetyloxy)acetophenone 261 .	157
Figure 77. The structures of the furan-amidine 110 and its furan- 235 and thiophene-reversed amidine 236 .	165
Figure 78. The most energetically favourable docking binding mode in the NQO2 active site (PDB code 1QR2; Resolution at 2.10 Å) for: A-	167

Asymmetric furan-amidine 150 ; B- Asymmetric pyrrole-amidine 191 ; C- Asymmetric <i>N</i> -methylpyrrole-amidine 192 ; D- Asymmetric thiophene-amidine 226 .	
Figure 79. Experimental (ΔG_{exp} ; KJ/mol) and calculated (ΔG_{cacl} ; KJ/mol) binding affinities for the synthesized inhibitors binding to NQO2.	168
Figure 80. Experimental (ΔG_{exp} ; KJ/mol) and calculated (ΔG_{cacl} ; KJ/mol) binding affinities for the synthesized inhibitors 110 , 150 , 151 and 153 binding to NQO2.	169
Figure 81. Experimental (ΔG_{exp} ; KJ/mol) and calculated (ΔG_{cacl} ; KJ/mol) binding affinities for the synthesized inhibitors 110 , 191 , 192 , 193 and 226 binding to NQO2.	169
Figure 82. Experimental (ΔG_{exp} ; KJ/mol) and calculated (ΔG_{cacl} ; KJ/mol) binding affinities for the synthesized inhibitors 110 , 191 , 192 and 193 binding to NQO2.	170
Figure 83. Thermal denaturation sigmoidal curve for DNA.	171
Figure 84. DNA melting temperature (T_m) measurement.	172
Figure 85. DNA thermal denaturation first derivative curve, asymmetric furan-amidine 144 .	173
Figure 86. DNA melting temperature: The plot of relative absorbance <i>versus</i> temperature.	175
Figure 87. Structures of the most active asymmetric furan-amidines 147 and 148 .	177
Figure 88. Structures of the asymmetric furan-amidine 110 and its 5-membered heterocycle analogues.	178
Figure 89. Structure of the potential prodrug 240 of the asymmetric furan-amidine 110 .	178
Figure 90. Structure of asymmetric furan-amidine 110 and its carboxylic acid isostere 265 .	179
Figure 91. Structure of asymmetric furan-amidine 144 and 3-fluoro diarylimidazole-amidine 266 .	179
Figure 92. Structures of PET candidate compounds 144 and 149 .	180

LIST OF SCHEMES

Scheme 1. The site of action of 5-fluorouracil.	30
Scheme 2. The mechanism of the alkylating agent mechlorethamine inside the cell.	31
Scheme 3. The reaction catalysed by L-asparaginase enzyme.	38
Scheme 4. The one-electron and two-electron reduction of quinone (24).	41
Scheme 5. Ping-pong mechanism of quinone reduction by NQO1 enzyme.	44
Scheme 6. Reduction of benzo(a)pyrenediones (37) into benzo(a)pyrenediol (38).	48
Scheme 7. Reduction of the cytotoxic compound CB 1954 (44) by NQO2 enzyme.	52
Scheme 8. Synthetic pathway for symmetric furan-amidine 111 ; Reagents and conditions: i- H ₂ SO ₄ , Ac ₂ O, reflux; ii- CuCN, quinolone, reflux; iii- EtOH, HCl (g), CHCl ₃ , 0 °C - rt; iv- NH ₃ (g), CHCl ₃ , rt.	72
Scheme 9. Proposed synthetic pathway for symmetric furan-amidine 111 ; Reagents and conditions: i- Paraformaldehyde, HN(CH ₃) ₂ .HCl, EtOH, reflux; ii- 5-(2-Hydroxyethyl)-3,4-dimethyl-1,3-thiazolium iodide 128 , NEt ₃ , dry THF, reflux; iii- H ₂ SO ₄ , Ac ₂ O, reflux	73
Scheme 10. Proposed synthetic pathway for the asymmetric furan-amidine 110 ; Reagents and conditions: i- Paraformaldehyde, NH(CH ₃) ₂ .HCl, EtOH, reflux; ii- 5-(2-Hydroxyethyl)-3,4-dimethyl-1,3-thiazolium iodide 128 , NEt ₃ , dry THF , reflux; iii- H ₂ SO ₄ , Ac ₂ O, reflux.	74
Scheme 11. The mechanism of the preparation of Mannich base 125 .	75
Scheme 12. The mechanism of the Stetter reaction in the synthesis of the 1,4-diketone 126 .	77
Scheme 13. Synthesis of 1-(4-cyanophenyl)-4-phenyl-1,4-butadione 126 through the coupling between methyl aryl ketone 120 and α-bromomethyl aryl ketone 133 ; Reagents and conditions: i- ZnCl ₂ , NEt ₃ , EtOH, dry toluene, rt.	79
Scheme 14. The mechanism of the synthesis of 1-(4-cyanophenyl)-4-phenyl-1,4-butadione by the coupling between methyl aryl ketone 120 and α-bromomethyl aryl ketone 133 .	80
Scheme 15. The synthetic pathway for the symmetric 1,4-diketone 123 through the coupling between methyl aryl ketone 120 and α-bromomethyl aryl ketone 136 ; Reagents and conditions: i- ZnCl ₂ , NEt ₃ , EtOH, dry toluene, rt.	81
Scheme 16. Route for the synthesis of the thiazolium catalyst 128 ; Reagents and conditions: i- CH ₃ I, dry CH ₃ CN, reflux.	82
Scheme 17. Mechanism of Paal-Knorr furan synthesis.	84
Scheme 18. Synthetic pathway to give 4,4'-(furan-2,5-diyl)benzotrile 127 ; Reagents and conditions: i- Ac ₂ O, H ₂ SO ₄ , reflux.	84
Scheme 19. Synthetic pathway for 4,4'-(furan-2,5-diyl)benzotrile 118 ; Reagents and conditions: i- Ac ₂ O, H ₂ SO ₄ , reflux.	85
Scheme 20. Synthetic pathway for 4,4'-(furan-2,5-diyl)benzotrile 127 using <i>in situ</i> generated dry hydrogen chloride gas.	87
Scheme 21. Pathways for the synthesis of carboximidates.	87
Scheme 22. Mechanism of formation of carboximide by hydrogen chloride gas	88

and ethanol.	
Scheme 23. Synthesis of ethyl 4-(5-phenylfuran-2-yl)benzimidate hydrochloride 143 .	89
Scheme 24. Synthetic pathway for diethyl 4,4'-(furan-2,5-diyl)dibenzimidate dihydrochloride 119 ; Reagents and conditions: i- $\text{HCl}_{(g)}$, EtOH, CHCl_3 , 0 °C- rt.	90
Scheme 25. Pinner synthesis of unsubstituted amidine.	90
Scheme 26. Synthesis of an unsubstituted amidine from nitrile <i>via</i> the thioimidate.	91
Scheme 27. Synthesis of an unsubstituted amidine from nitrile using ammonium salts in liquid ammonia.	91
Scheme 28. Unsubstituted amidine synthesis using aluminum amide reagents.	91
Scheme 29. Substituted amidine synthesis using copper (I) chloride.	91
Scheme 30. Synthetic pathway to give 4-(5-phenylfuran-2-yl)benzamidine acetate 110 and 4,4'-(furan-2,5-diyl)dibenzamidine acetate 111 ; Reagents and conditions: i- $\text{CH}_3\text{COO}^+\text{NH}_4$, EtOH, rt.	92
Scheme 31. General synthetic pathway for the preparation of asymmetric furan-amidines; A- starting from methyl aryl ketone having a nitrile group; B- starting from α -bromomethyl aryl ketone having a nitrile group; Reagents and conditions: i- ZnCl_2 , NEt_3 , EtOH, dry toluene or THF, rt; ii- $\text{HCl}_{(g)}$, EtOH, CHCl_3 , 0 °C- rt; iii- $\text{CH}_3\text{COO}^+\text{NH}_4$, EtOH, rt.	94
Scheme 32. Pathway for the synthesis 1,4-diketones 165-174 ; Reagents and conditions: i- ZnCl_2 , NEt_3 , EtOH, dry toluene or THF, rt.	97
Scheme 33. Alternative pathway for the synthesis 1,4-diketone 172 ; Reagents and conditions: i- ZnCl_2 , NEt_3 , EtOH, dry toluene, rt.	98
Scheme 34. Pathway for the synthesis of 163 and 164 using a Friedel-Craft acylation; Reagents and conditions: i- AcCl , AlCl_3 , dry DCM, 0 °C - rt.	102
Scheme 35. Friedel-Craft acylation mechanism.	103
Scheme 36. Pathway for the synthesis of 2-bromo-1-(4-ethylphenyl)ethanone 175 .	103
Scheme 37. Mechanism of bromination of ketone 162 using NBS in the presence of PTSA.	104
Scheme 38. Synthesis of the 1,4-diketone 179 ; Reagents and conditions: i- ZnCl_2 , NEt_3 , EtOH, dry toluene, rt.	105
Scheme 39. Pathway for the synthesis of the ethyl imidate hydrochloride intermediates; 180-190 ; Reagents and conditions: i- $\text{HCl}_{(g)}$, EtOH, CHCl_3 , 0 °C - rt .	105
Scheme 40. Synthetic pathway of the targeted amidines; 144-154 ; Reagents and conditions: i- $\text{CH}_3\text{COO}^+\text{NH}_4$, EtOH, rt.	106
Scheme 41. Pathways for the synthesis of: A- 4-(5-phenyl-1 <i>H</i> -pyrrol-2-yl)benzimidine acetate 198 ; B- 4-(1-methyl-5-phenyl-1 <i>H</i> -pyrrol-2-yl)benzimidine acetate 199 .	110
Scheme 42. Pathway for the synthesis of 4-(5-phenyl- <i>H</i> -pyrrol-2-yl)benzimidine acetate 191 and 4-(1-methyl-5-phenyl- <i>H</i> -pyrrol-2-yl)benzimidine acetate 192 ; Reagents and conditions: i- $\text{HCl}_{(g)}$, EtOH, CHCl_3 , 0 °C - rt; ii- $\text{CH}_3\text{COO}^+\text{NH}_4$, EtOH, rt.	114
Scheme 43. Synthetic pathway of 4-(4-phenyl-1 <i>H</i> -imidazol-2-yl)benzimidine acetate 203 ; Reagents and conditions: i- $\text{CH}_3\text{COO}^+\text{NH}_4$, MeOH, rt.	115

Scheme 44. Pathway for the synthesis of 4-(4-phenyl-1 <i>H</i> -imidazol-2-yl)benzamidinium acetate 193 ; Reagents and conditions: i- NH ₂ OH.HCl, <i>t</i> -BuOK, dry DMSO, 0 °C - rt; ii- HCOO ⁻ NH ₄ ⁺ , Pd/C, AcOH, reflux.	117
Scheme 45. Pathway for the synthesis of the <i>N</i> -methylimidazole regioisomers 205A and 205B ; Reagents and conditions: i- CH ₃ I, KOH, acetone, rt.	120
Scheme 46. Synthetic pathway for 4-(1-methyl-4-phenyl-1 <i>H</i> -imidazol-2-yl)benzamidinium acetate 194 ; Reagents and conditions: i- NH ₂ OH.HCl, <i>t</i> -BuOK, dry DMSO, 0 °C - rt; ii- HCOO ⁻ NH ₄ ⁺ , Pd/C, AcOH, reflux.	122
Scheme 47. Reaction for the synthesis of 4-cyano- <i>N</i> -(2-oxo-2-phenylethyl)benzamide 209 ; Reagents and conditions: i- NaHCO ₃ , DCM, 0 °C - rt.	122
Scheme 48. Synthetic pathway for 4-((2-oxo-2-phenylethyl)carbamoyl)benzimidate hydrochloride 210 ; Reagents and conditions: i- HCl _(g) , EtOH, CHCl ₃ , 0 °C - rt.	124
Scheme 49. Pathway for the synthesis of 4-(5-phenyloxazol-2-yl)benzimidate 211 ; Reagents and conditions: i- Ac ₂ O, conc. H ₂ SO ₄ , rt.	124
Scheme 50. The mechanism for the synthesis of 2,5-diaryloxazole 211 .	125
Scheme 51. Pathway for the synthesis of 4-(5-phenyloxazol-2-yl)benzimidate acetate 195 ; Reagents and conditions: i- NH ₂ OH.HCl, <i>t</i> -BuOK, dry DMSO, 0 °C - rt; ii- HCOO ⁻ NH ₄ ⁺ , Pd/C, AcOH, reflux.	126
Scheme 52. Synthetic pathway for the preparation of 4-(3,4-dimethyl-5-phenylfuran-2-yl)benzimidate 213 ; Reagents and conditions: i- Ac ₂ O, H ₂ SO ₄ , reflux; ii- paraformaldehyde, 33% wt HBr in AcOH, reflux; iii- LiAlH ₄ , dry THF, rt; iv- CuCN, quinoline, reflux.	128
Scheme 53. Proposed alternative synthetic pathway for the preparation of 4-(3,4-dimethyl-5-phenylfuran-2-yl)benzimidate 213 ; Reagents and conditions: i- Ac ₂ O, H ₂ SO ₄ , reflux .	129
Scheme 54. Synthetic pathway of the 1,4-diketone 219 ; Reagents and conditions: i- EtMgBr, Et ₂ NH, dry THF, 0 °C - rt.	129
Scheme 55. Pathway for the synthesis of 4-(4-methyl-5-phenylfuran-2-yl)benzimidate 223 ; Reagents and conditions: i- EtMgBr, Et ₂ NH, dry THF, 0 °C - rt.	130
Scheme 56. Mechanism for the synthesis of 4-(4-methyl-5-phenylfuran-2-yl)benzimidate 224 .	132
Scheme 57. Pathway for the synthesis of 4-(4-methyl-5-phenylfuran-2-yl)benzimidate 223 via amidoxime intermediate 225 ; Reagents and conditions: i- Ac ₂ O, conc. H ₂ SO ₄ , reflux; ii- NH ₂ OH. HCl, <i>t</i> -BuOK, dry DMSO, 0 °C - rt.	133
Scheme 58. Synthetic pathway for the preparation of the asymmetric 4-(5-phenylthiophen-2-yl)benzimidate 226 .	134
Scheme 59. Mechanism of synthesis of 2,5-diarylthiophene 228 compound using Lawesson's reagent 227 .	135
Scheme 60. Attempted synthesis of ethyl 4-(5-phenylthiophen-2-yl)benzimidate hydrochloride 232 ; Reagents and conditions: i- HCl _(g) , EtOH, CHCl ₃ , 0 °C - rt.	136
Scheme 61. The alternative synthetic pathway for 4-(5-phenylthiophen-2-yl)benzimidate 226 ; Reagents and conditions: i- NH ₂ OH.HCl, <i>t</i> -BuOK, dry DMSO, 0 °C - rt; ii- HCOO ⁻ NH ₄ ⁺ , Pd/C, AcOH, reflux.	137
Scheme 62. The reduction of <i>N</i> -hydroxy 4-(5-phenylthiophen-2-yl)benzimidate 226 using catalytic transfer hydrogenation.	137
Scheme 63. Pathway for the synthesis of 1,4-diketones 241 and 242 ; Reagents	139

and conditions: i- ZnCl ₂ , NEt ₃ , EtOH, dry toluene, rt.	
Scheme 64. Pathway for the synthesis of 2-(3-nitrophenyl)-5-phenylfuran 243 and 2-(4-nitrophenyl)-5-phenylfuran 244 ; Reagents and conditions: i- HCl _(g) , CHCl ₃ , 0 °C - rt.	140
Scheme 65. Pathway for the synthesis of 2-(3-nitrophenyl)-5-phenylthiophene 245 and 2-(4-nitrophenyl)-5-phenylthiophene 246 ; Reagents: i- Lawesson's reagent 227 , THF, 55 °C.	140
Scheme 66. Reduction of the nitro-group in compounds 243-246 to give amines 247-250 ; Reagents and conditions: i- NaBH ₄ , CuSO ₄ , EtOH, 0 °C - rt.	141
Scheme 67. Routes for the synthesis of <i>N</i> -(4-(5-phenylfuran-2-yl)phenyl)acetamide hydrobromide 235 , X = O and <i>N</i> -(4-(5-phenylthiophen-2-yl)phenyl)acetamide hydrobromide 236 , X = S.	144
Scheme 68. Pathway for the synthesis of <i>S</i> -2-naphthylmethyl thioacetimidate hydrobromide 251 .	145
Scheme 69. Synthetic pathway of <i>N</i> -aryl amides 237-239 ; Reagents and conditions: i- AcCl, dry CH ₃ CN, rt.	145
Scheme 70. Reaction of 143 gave methyl 4-(5-phenylfuran-2-yl)benzimidate hydrochloride 234 and not 110 ; Reagents and conditions: i- NH ₄ Cl, MeOH/H ₂ O, reflux.	147
Scheme 71. Pathway for the synthesis of <i>N</i> -hydroxy-4-(5-phenylfuran-2-yl)benzimidine 240 ; Reagents and conditions: i- Ac ₂ O, conc. H ₂ SO ₄ , reflux; ii- NH ₂ OH. HCl, <i>t</i> -BuOK, dry DMSO, 0 °C - rt.	149
Scheme 72. Pathway for the synthesis of 5(5-(4-hydroxyphenyl)furan-2-yl)benzene-1,3-diol 250 ; Reagents and conditions: i- HCl _(g) , CHCl ₃ , 0 °C - rt.	151
Scheme 73. Pathways for the synthesis of 1-(3,5-di(acetyloxy)phenyl)-4-(acetyloxyphenyl)-1,4-butadione 251 .	151
Scheme 74. Pathways attempted for the synthesis of 1-(3,5-di(acetyloxy)phenyl)-4-(acetyloxyphenyl)-1,4-butadione 251 ; Reagents and conditions: i- <i>t</i> -BuOMgBr, dry THF, 0 °C- rt.	152
Scheme 75. Synthetic pathway for α-bromo-compound 252 ; Reagents and conditions: i- CuBr ₂ , EtOAc/DCM, reflux.	153
Scheme 76. Pathway for the synthesis of 4'-(acetyloxy)acetophenone 253 ; Reagents: i- Ac ₂ O, DMAP, NEt ₃ , DCM, 0 °C - rt .	154
Scheme 77. Pathway for the synthesis of 3',5'-di(acetyloxy)acetophenone 254 ; Reagents: i- Ac ₂ O, DMAP, NEt ₃ , DCM, 0 °C - rt.	154
Scheme 78. α-Bromination of 4'-hydroxyacetophenone 258 ; Reagents and conditions: i- CuBr ₂ , EtOAc/DCM, reflux.	155
Scheme 79. Pathway for the synthesis of 2,4'-di(acetyloxy)acetophenone 261 and 2,2-dibromo-4'-acetyloxyacetophenone 262 ; Reagents: i- Ac ₂ O, DMAP, NEt ₃ , DCM, 0 °C - rt.	156
Scheme 80. Pathway for the synthesis of 2-bromo-4'-(acetyloxy)acetophenone 255 ; Reagents and conditions: i- Br ₂ / AlCl ₃ , THF, 0 °C - rt.	157
Scheme 81. Pathway for the enzymatic synthesis of the co-substrate <i>N</i> -ribosyl dihydronicotinamide NRH .	159
Scheme 82. Reduction of DCPIP 263 by NQO2 in the presence of NRH (R=ribose).	160

LIST OF TABLES

Table 1. The structures of nitrogenous bases and sugars constituting the natural nucleoside	29
Table 2. The classes of alkylating agents and examples of each class	32
Table 3. Microtubule-targeting drugs as anti-cancer chemotherapeutic agents	37
Table 4. Cancer chemo-preventive agents	40
Table 5. NQO2 inhibitors data for casimiroin and its analogues	59
Table 6. NQO2 inhibition data for <i>N</i> -oxide derivatives of triazoloacridin-6-one	60
Table 7. NQO2 inhibition data for <i>N</i> -oxide derivatives of imidazoloacridin-6-one	61
Table 8. NQO2 inhibition data for ellipticine compounds	63
Table 9. NQO2 inhibition data for quinoline compounds	64
Table 10. Furan-amidine lead compounds as inhibitors NQO2	65
Table 11. The differences between the two synthetic pathways used for the preparation of the 1,4-diketones 123 and 126	82
Table 12. The structures of the synthesized targeted furan-amidines.	96
Table 13. The reaction times and % yields for the synthesis of the 1,4-diketones 165-174 .	97
Table 14. The calculated log P values of the synthesized asymmetric furan-amidines 110 and 144-154 .	107
Table 15. Calculated log P values of the proposed asymmetric furan-amidine isosteric analogues of the asymmetric furan-amidine 110	108
Table 16. The structures of the amidine-isosteres of 110 .	138
Table 17. The IC ₅₀ values of resveratrol and the synthesized furan-amidine compounds.	161
Table 18. The IC ₅₀ values of the asymmetric furan-amidine 110 and its alkyl-substituted analogues.	162
Table 19. The IC ₅₀ values of the asymmetric furan-amidine 110 and its furan isosteric analogues.	163
Table 20. The IC ₅₀ values of the asymmetric furan-amidine 110 and its amidine isosteric analogues.	164
Table 21. The experimental (ΔG_{exp} ; KJ/mol) and calculated (ΔG_{cacl} ; KJ/mol) binding affinities of the asymmetric furan-amidine 110 and its alkyl-substituted analogues 150 , 151 and 153 .	168
Table 22. DNA melting temperatures of doxorubicin, symmetric and asymmetric furan-amidines and asymmetric <i>N</i> -methylpyrrole-amidine in low salt solution.	173
Table 23. DNA melting temperatures of doxorubicin, symmetric and asymmetric furan-amidines and asymmetric <i>N</i> -methylpyrrole-amidine in high salt solution.	176

LIST OF ABBREVIATIONS

Å: Angstrom 10^{-10} m

Abs.: Absolute

Asn: Asparagine

Asp: Aspartic acid

APCI: Atmospheric-pressure chemical ionization spectrometry

CDCl₃: Deuterated chloroform

DCM: Dichloromethane

DMSO: Dimethyl sulfoxide

DMSO-d₆: Deuterated dimethyl sulfoxide

ESIMS: Electrospray ionization mass spectrometry

EtOAc: Ethyl acetate

FAD: Flavin adenine dinucleotide

Gly: Glycine

IR: Infra-red spectroscopy

Ile: Isoleucine

Leu: Leucine

Met: Methionine

MT3: Melatonin-binding site 3

NADH: Reduced adenine dinucleotide

NADPH: Reduced adenine phosphate dinucleotide

NCI: National Cancer Institute

NF-κB: Nuclear factor-kappa B

NRH: *N*-ribosyl dihydronicotinamide

Ppm: Parts per million

Phe: Phenylalanine

rt: Room temperature

R_f: Retardation factor

Cys: Cysteine

THF: Tetrahydrofuran

Thr: Threonine

TNF: Tumor necrosis factor

Trp: Tryptophan

Tyr: Tyrosine

The University of Manchester
Soraya Ma'moun Othman Alnabulsi
Doctor of Philosophy
Synthesis and Evaluation of Novel NQO2 Inhibitors
2013

Abstract

The NRH: quinone oxidoreductase 2 enzyme (NQO2) is a potential therapeutic target in cancer, malaria and neurodegenerative diseases. The inhibition of NQO2 enzyme activity may have a role in cancer chemoprevention and chemotherapy.

The objective of this research is the design, synthesis and evaluation of novel selective NQO2 inhibitors with no off-target effects, for example binding to DNA. From previous virtual screening studies of the NCI database, symmetric and asymmetric furan-amidines were identified as lead inhibitors of the NQO2 enzyme, with IC₅₀ values of 630 nM for 4,4'-(furan-2,5-diyl)dibenzamidine, 50 nM for 4,4'-(3,4-dimethylfuran-2,5-diyl)dibenzamidine and 140 nM for 4-(5-phenylfuran-2-yl)benzamidine.

A synthetic pathway for the synthesis of the asymmetric furan-amidines was established, which involved the cyclisation of the 1,4-diketone intermediates to give the furan ring. Several furan analogues with a range of substituents on the aromatic ring (e.g. fluoro, bromo, nitro, methyl, ethyl, isopropyl, *tert*-butyl, methoxy) were prepared. In addition, isosteres of the amidine group were made, including imidate, *N*-aryl amidine (reversed amidine), *N*-aryl amide and *N*-hydroxyamidine (amidoxime). The furan ring was replaced with other 5-membered heterocycles, including pyrrole, *N*-methylpyrrole, thiophene, imidazole, *N*-methylimidazole and oxazole. All compounds were fully characterized by ¹H and ¹³C NMR spectroscopy, IR spectroscopy and mass spectrometry.

The synthesized asymmetric furan-amidines and their analogues showed potent NQO2 inhibition activity with IC₅₀ values in the nano-molar range. The most active compounds were asymmetric furan-amidines with *meta*- and *para*-nitro substitution on the aromatic ring, with IC₅₀ values of 15 nM.

In contrast to the symmetric furan-amidines, which showed potent intercalation in the minor grooves of DNA, the synthesized asymmetric furan-amidines and *N*-methylpyrrole-amidine showed no affinity towards DNA, as shown by DNA melting temperature experiment.

The high NQO2 inhibition activity of some analogues together with their high toxicity against several breast cancer cell lines, make these lead compounds worthy of further development and optimization as potential drugs.

Declaration

No portion of the work referred to in the thesis has been submitted in support of an application for another degree or qualification of this or any other university or other institute of learning

Copyright

1. The author of this thesis (including any appendices and/or schedules to this thesis) owns certain copyright or related rights in it (the “Copyright”) and s/he has given The University of Manchester certain rights to use such Copyright, including for administrative purposes.
2. Copies of this thesis, either in full or in extracts and whether in hard or electronic copy, may be made only in accordance with the Copyright, Designs and Patents Act 1988 (as amended) and regulations issued under it or, where appropriate, in accordance with licensing agreements which the University has from time to time.
3. The ownership of certain Copyright, patents, designs, trade marks and other intellectual property (the “Intellectual Property”) and any reproductions of copyright works in the thesis, for example graphs and tables (“Reproductions”), which may be described in this thesis, may not be owned by the author and may be owned by third parties. Such Intellectual Property and Reproductions cannot and must not be made available for use without the prior written permission of the owner(s) of the relevant Intellectual Property and/or Reproductions.
4. Further information on the conditions under which disclosure, publication and commercialisation of this thesis, the Copyright and any Intellectual Property and/or Reproductions described in it may take place is available in the University IP Policy (see <http://documents.manchester.ac.uk/DocuInfo.aspx?DocID=487>), in any relevant Thesis restriction declarations deposited in the University Library, The University Library’s regulations (see <http://www.manchester.ac.uk/library/aboutus/regulations>) and in The University’s policy on Presentation of Theses.

Acknowledgement

My sincere thanks go to my great supervisors Dr. Sally Freeman and Professor Ian Stratford for giving me the opportunity to be a PhD student under their supervision and for their continuous support and help during my PhD research. Also, I would like to thank Dr. Richard Bryce for his help in the docking experiments, Dr. Elena Bichenkova for her help in DNA melting experiments and support with the NMR spectrometer, and Dr. Roger Whitehead for the use of his chemistry laboratory for the synthesis of NRH.

I would like to thank my colleague and my friend Dr. Manikandan Kadirvel for his friendship, continuous help and support during my work in the medicinal chemistry lab and my stay in the UK. Also, I would like to thank Dr. Mary Clare Caraher for teaching me the measurement of IC_{50} values for the synthesized compounds. Many thanks go to my colleague Elham Santina for measuring the IC_{50} values of the synthesized compounds.

I would like to thank my colleague in the medicinal chemistry lab Fariba FaniMarvasti for the great time we spent together.

I would like to thank my friends Farah El-Mohtadi and Buthianah Hussein for their endless courage and support. I would like to say for both of them that joining me in the UK in the last months of my PhD study was a gift for me as you both fulfilled my life with your great friendship, fun, joy and great memorable moments. Many thanks go to my friend Wadiaa Baniamer for her great friendship, motivation and continuous support.

I would like to thank my colleagues in the molecular modelling group, biophysics group, oncology group and Caren Soo Mei from the chemistry group.

I would like to thank Rehana Sung and Gareth Smith from the mass spectrometry unit in the School of Chemistry for the prompt recording of the mass spectra for my samples.

Special thanks go to Dr. Amjad Qandil, who inspired me to pursue my postgraduate study, supported me since I was an undergraduate student at Jordan University of Science and Technology and for his continuous support all through my PhD study.

My great thanks for my lovely husband Dr. Rami Al-Khatib for his sacrifice, continuous support and courage. I would like to say that you are my dream-maker. Also, my great thanks to my lovely mother Sabah and lovely father Ma'moun for their continuous prayers, motivation and support. I would like to say for both of them,

without both of you and your support I would not be here. I cannot forget my lovely little angels Ahmad and Larina who accompanied me during my journey and made my life full of fun. Many thanks go to my brothers, Esam, Mo'tasem, Mohammad-Zeid and Ahmad, and my lovely sister Suzan and my sister-in-law Remaz. I would like to thank my late grandmother, who supported me to start this journey and she would be happy to see me finish it.

Also, I would like to thank my brother-in-law Dr. Luai Al-Khatib and his wife Madeleine ElTigani for their continuous help and support during my stay in UK. You were my family in UK.

Finally, I would like to thank my sponsor Jordan University of Science and Technology for their financial sponsorship.

I dedicate my thesis to my lovely family

Chapter I. Introduction

1. Cancer

Cancer is a life-threatening illness that accounts for high mortality in the world.¹ Cancer is a disease of uncontrolled cell proliferation² that initiates as a result of the modification or damage of the genetic material that controls and regulates cell cycle.³ The process by which the normal cell transforms into cancerous cell is called carcinogenesis, which occurs through three stages: initiation, promotion and progression. The uncontrolled division and replication of cancer cells will result in the formation of a group of cells known as a tumour.⁴ Malignant tumour cells can travel from their initial site and invade other parts of the body leading to cancer metastasis.⁵

Tumours are classified into solid and liquid tumours. Solid tumours are defined as a solid mass of cancer cells that grow in organs and can occur anywhere in the human body. Two types of solid tumours can occur: epithelial tumours (also called carcinomas) and connective tissue tumours (also called sarcomas). On the other hand, liquid tumours occur in the blood (lymphoma, which starts in the immune system as a liquid tumour and transforms to a solid tumour), bone marrow (leukaemia) and lymph nodes (cancer of plasma cells).⁶ The treatment of tumours involves surgery, radiotherapy or systemic administration of chemotherapeutic drugs known as antineoplastic agents. It is chemotherapy that is the focus of this research.

1.1. Cancer chemotherapy

Cancer chemotherapy is the use of drugs to selectively inhibit or kill proliferating cancer cells without affecting normal cells. Cancer chemotherapy started in the 1940s with the use of nitrogen mustards and antifolate drugs to cure cancer.⁷

Chemotherapeutic drugs can be classified depending on their mechanism of action:

- 1- Antimetabolite drugs: Folate antagonists or antifolate drugs and nucleoside analogues
- 2- Alkylating agents
- 3- DNA topoisomerase inhibitors
- 4- DNA intercalators
- 5- Microtubule-targeting anticancer drugs
- 6- L-Asparaginase
- 7- Drugs that target the cell cycle

A detailed discussion about each group is given in the following sections

Chapter I. Introduction

1.1.1. Antimetabolites

Antimetabolite drugs were amongst the first effective chemotherapeutic agents discovered and are folic acid, pyrimidine or purine analogues. They have similar structures as naturally occurring molecules used in nucleic acid (DNA and RNA) synthesis. Antimetabolites are similar to chemicals needed for normal biochemical activity, but differ sufficiently so that they interfere with normal cell function. Generally, antimetabolites induce cell death during the S phase of cell growth when incorporated into RNA and DNA or inhibit enzymes needed for nucleic acid production. These agents are used for a variety of cancer therapies including leukaemia, breast, ovarian and gastro-intestinal cancers.⁸

1.1.1.1. Folate antagonists

Methotrexate (amethopterin) **1** (Figure 1) was first used as a chemotherapeutic drug in 1948 to treat acute leukaemia in children.⁹ Methotrexate was shown to have antitumour activity in a range of epithelial malignancies, including breast, ovarian, bladder, head and neck cancers. Also, methotrexate was the first drug administered systemically to cure solid tumour such as choriocarcinoma.⁷

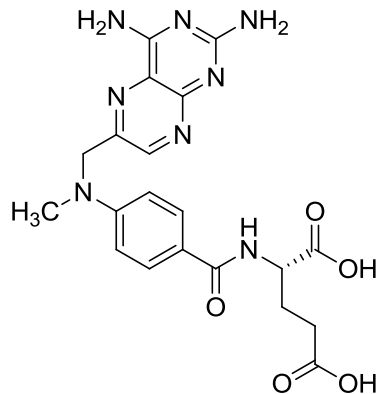


Figure 1. The structure of methotrexate (**1**).

Methotrexate is a competitive inhibitor of the enzyme dihydrofolate reductase. Dihydrofolate reductase is responsible for the reduction of dihydrofolate into tetrahydrofolate, which is the one-carbon carrier in purine and thymidine base biosynthesis. The depletion of tetrahydrofolate leads to inhibition of thymidylate (TMP) synthesis and subsequently inhibition of DNA synthesis. Also, methotrexate inhibits purine biosynthesis both directly and by inhibiting tetrahydrofolate formation.¹⁰

Chapter I. Introduction

Trimetrexate **2** and edatrexate **3** (Figure 2) are antifolate drugs that are used as alternatives to methotrexate in case of the resistance of cancerous cells to methotrexate.¹¹

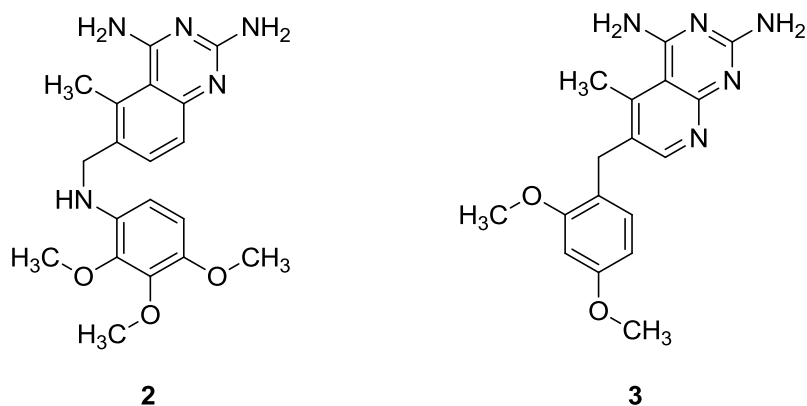


Figure 2. Structures of methotrexate analogues, trimetrexate (**2**) and edatrexate (**3**).

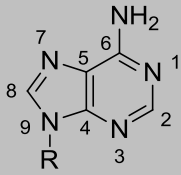
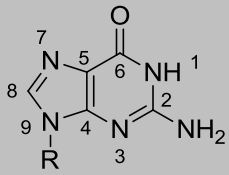
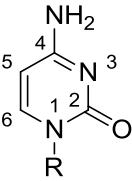
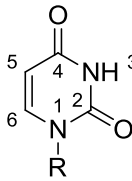
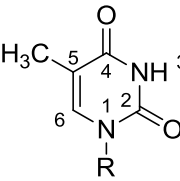
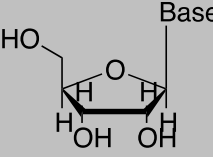
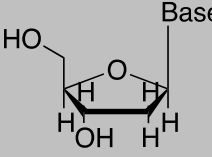
1.1.1.2. Nucleoside analogues

Natural nucleosides are nitrogen base compounds with purine (adenine and guanine) or pyrimidine (cytosine, uracil and thymine) scaffolds bound to a ribose or deoxyribose sugar (Table 1). The natural nucleosides are important in the molecular mechanisms of conservation, replication and transcription of the genetic information.¹²

Nucleoside analogues are cytotoxic agents, which exert their cytotoxic activity by interfering with the nucleic acids, DNA and RNA in different ways. These drugs incorporate into and alter nucleic acids, interfere with various enzymes involved in nucleic acid biosynthesis and modify metabolism of physiological nucleosides.¹³

Chapter I. Introduction

Table 1. The structures of nitrogenous bases and sugars constituting the natural nucleoside

	Structure		
Purine			
	Adenine	Guanine	
Pyrimidine			
	Cytosine	Uracil	Thymine
	Sugar		
Ribose		Deoxyribose	

1.1.1.2.1. 5-Fluorouracil and its nucleoside metabolites

5-Fluorouracil (5-FU) **4** is structurally similar to the pyrimidine base uracil in which the hydrogen on C-5 of uracil is isosterically replaced by a fluoro-atom in 5-FU (Figure 3).

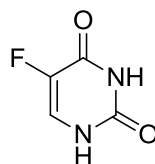
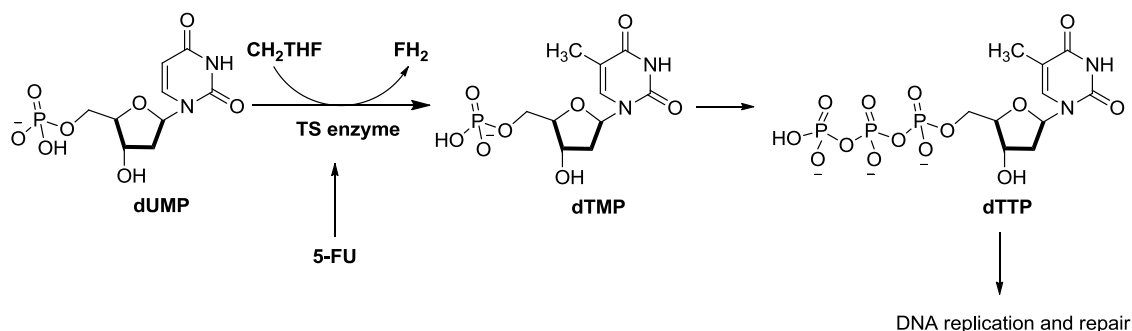


Figure 3. The structure of 5-fluorouracil (**4**).

5-FU is metabolized inside the cell into different active nucleoside and nucleotide metabolites that exert their action by disrupting RNA synthesis and inhibiting the enzyme thymidylate synthase (TS). Thymidylate synthase catalyses the reductive methylation of deoxyuridine monophosphate (dUMP) to deoxythymidine monophosphate (dTMP) using 5,10-methylenetetrahydrofolate (CH₂THF) as the methyl

Chapter I. Introduction

donor (Scheme 1). This reaction provides the thymidylate, which is important in DNA synthesis and repair.¹⁴



Scheme 1. The site of action of 5-fluorouracil.

1.1.1.2.2. Deoxycytidine derivatives

Cytarabine is a deoxycytidine analogue used in the treatment of haematological malignant disease, namely acute myeloid leukaemia. Cytarabine directly inhibits DNA polymerase and its arabinosyl CTP derivative is incorporated into DNA leading to inhibition of DNA synthesis.¹³

1.1.1.2.3. 6-Thioguanine and 6-mercaptopurine nucleosides

6-Thioguanine **5** and 6-mercaptopurine **6** are thio-analogues of the naturally occurring 6-ketopurine bases, guanine and hypoxanthine, respectively (Figure 4). 6-Mercaptopurine was initially evaluated for the treatment of leukaemia in the early 1950s.¹⁵

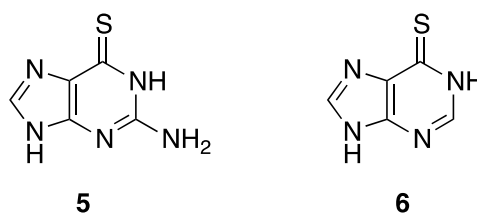


Figure 4. Structures of 6-thioguanine (**5**) and 6-mercaptopurine (**6**).

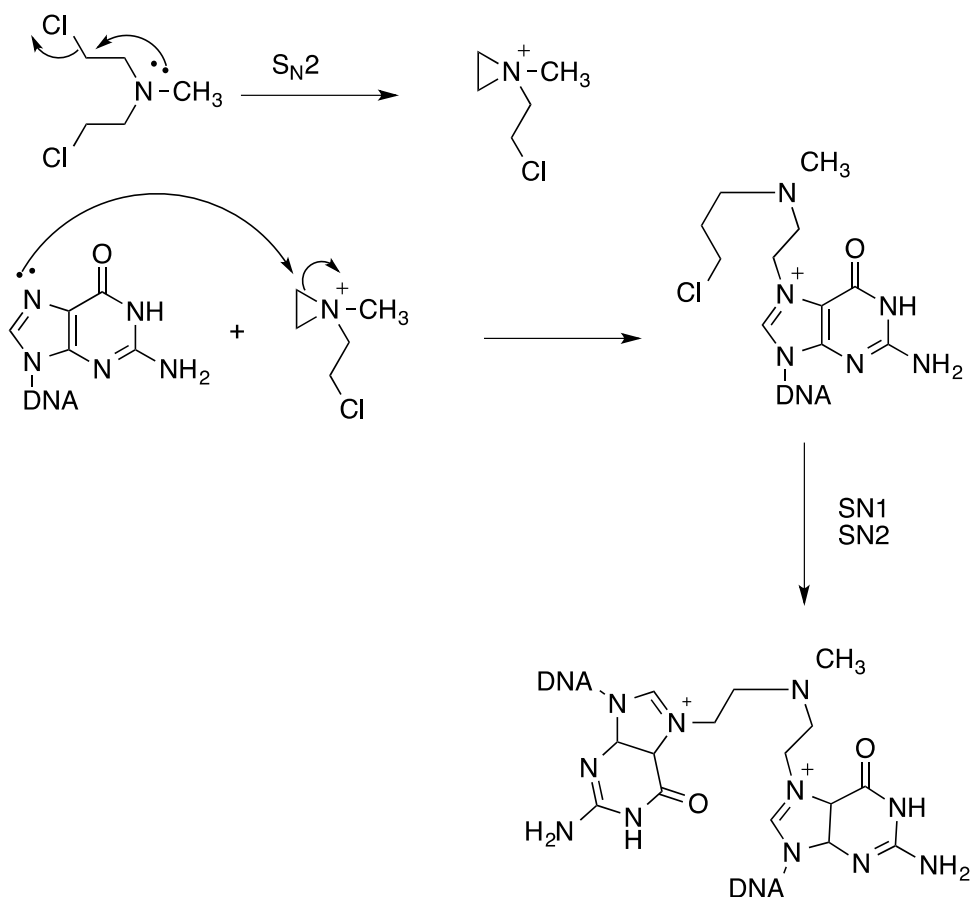
1.1.2. Alkylating agents

The use of alkylating agents in cancer chemotherapy was started in the early 1940s. Alkylating agents are used to treat a wide variety of cancers, most effectively on solid tumours and leukaemia. They are cytotoxic agents known to act during all phases of the cell cycle. They exert their action directly on DNA leading to the crosslinking

Chapter I. Introduction

between DNA strands and causing the formation of DNA strand breaks. Consequently, cell division will be inhibited and cell apoptosis will be induced.¹⁶

In general, the alkylating agents exert their action inside the cell by the formation of highly reactive cation species. For example, the nitrogen mustard mechlorethamine, undergoes S_N2 cyclization step followed by nucleophilic attack of N-7 guanine residue of DNA forming a covalent bond with DNA, followed by crosslinking between the DNA strands (Scheme 2).¹⁷

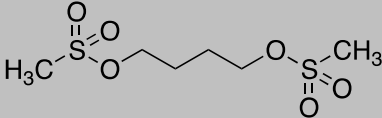
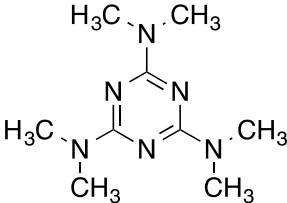
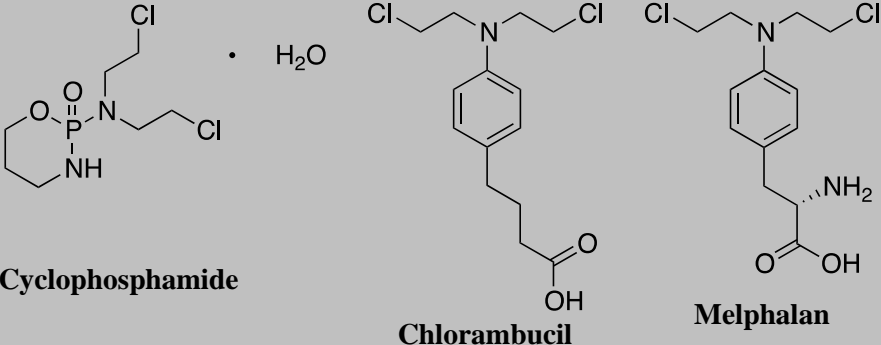
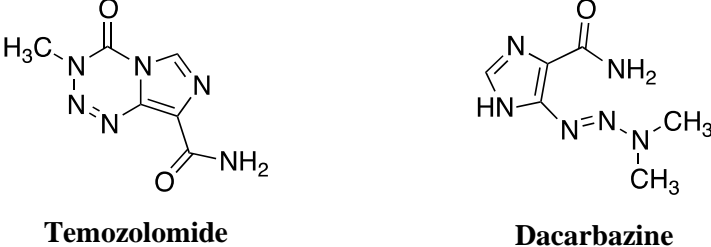
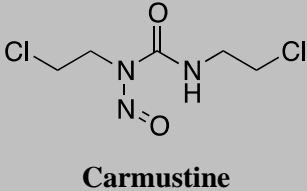
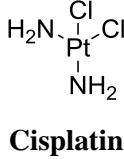


Scheme 2. The mechanism of the alkylating agent mechlorethamine inside the cell.

Alkylating agents are classified into six groups, as shown with examples, in Table 2.

Chapter I. Introduction

Table 2. The classes of alkylating agents and examples of each class¹⁸

Alkylating agent group	Examples
Alkyl sulfonates	 <p data-bbox="975 510 1091 539">Busulfan</p>
Methylmelamine	 <p data-bbox="895 790 1173 819">Hexamethylmelamine</p>
Nitrogen mustard	 <p data-bbox="587 1111 831 1140">Cyclophosphamide</p> <p data-bbox="991 1167 1166 1196">Chlorambucil</p> <p data-bbox="1286 1144 1430 1173">Melphalan</p>
Triazenes	 <p data-bbox="711 1440 898 1469">Temozolomide</p> <p data-bbox="1185 1440 1350 1469">Dacarbazine</p>
Nitrosoureas	 <p data-bbox="959 1659 1107 1688">Carmustine</p>
Platinum drugs	 <p data-bbox="975 1839 1091 1868">Cisplatin</p>

Chapter I. Introduction

1.1.3. Topoisomerase enzymes inhibitors

Topoisomerase enzymes control the topology of DNA function at several steps in the replication of cells. These enzymes remove the negative and positive supercoils of DNA, which result from DNA duplex-unwinding. The enzymes are classified into topoisomerase I and II, which are different in their mechanism of action. Topoisomerase I cuts a single strand of the DNA double helix while topoisomerase II cuts both strands of DNA, using adenosine triphosphate (ATP) for fuel. The rest of the process by which the two enzymes work is very similar. The process entails the relaxation of the coil of the two DNA strands, and then after the cuts are made and replication or repair is complete, the strands are ligated back together and reform a coil.¹⁹

Topoisomerase enzymes are potential targets in the treatment of cancer because their inhibition results in cell death. Therefore inhibitors of the topoisomerase enzymes have the ability to kill all cells undergoing DNA replication, reading of the DNA for protein production or undergoing repair of DNA damage. Since cancer cells divide much more rapidly than normal cells, the cancer cells will be killed by the topoisomerase inhibitors, though some normal cells with topoisomerase activity will also be killed.

Camptothecin **7** and its derivatives topotecan **8** and irinotecan **9** (Figure 5) are alkaloids with anticancer activity. They exert their action through the inhibition of topoisomerase I.²⁰

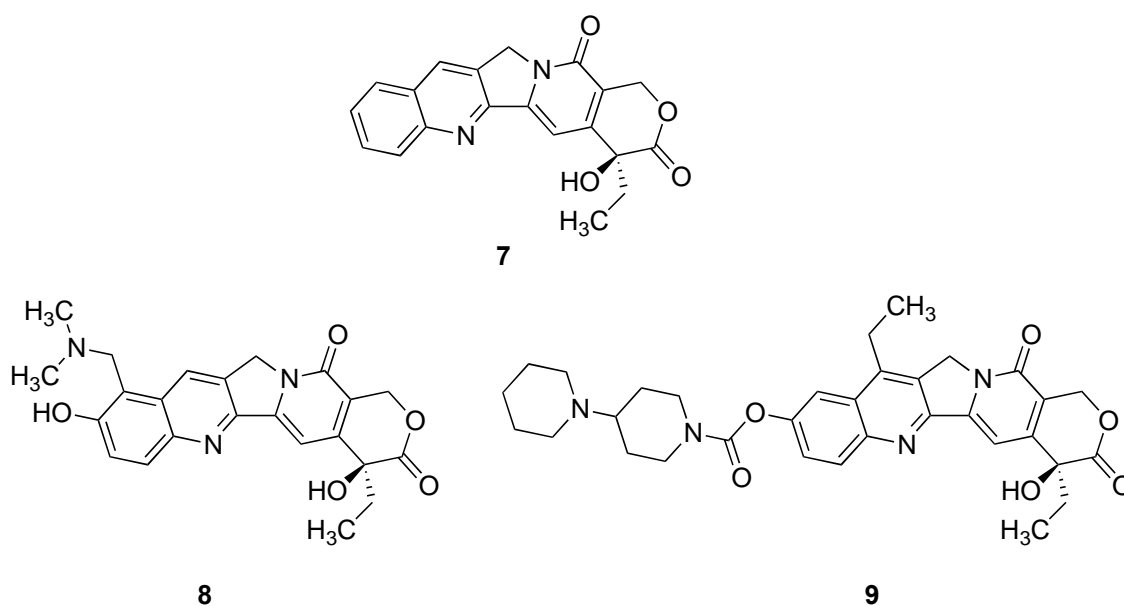


Figure 5. Structures of the topoisomerase I enzyme inhibitors, camptothecin (**7**), topotecan (**8**) and irinotecan (**9**).

Chapter I. Introduction

On the other hand, topoisomerase II is considered a potential target for widely used anticancer drugs currently in clinical use. These drugs include anthracyclines (discussed in section 1.1.1.4.) and epipodophyllotoxins. Teniposide **10** and etoposide **11** are anticancer drugs that share the podophyllotoxin scaffold **12** (Figure 6).²¹

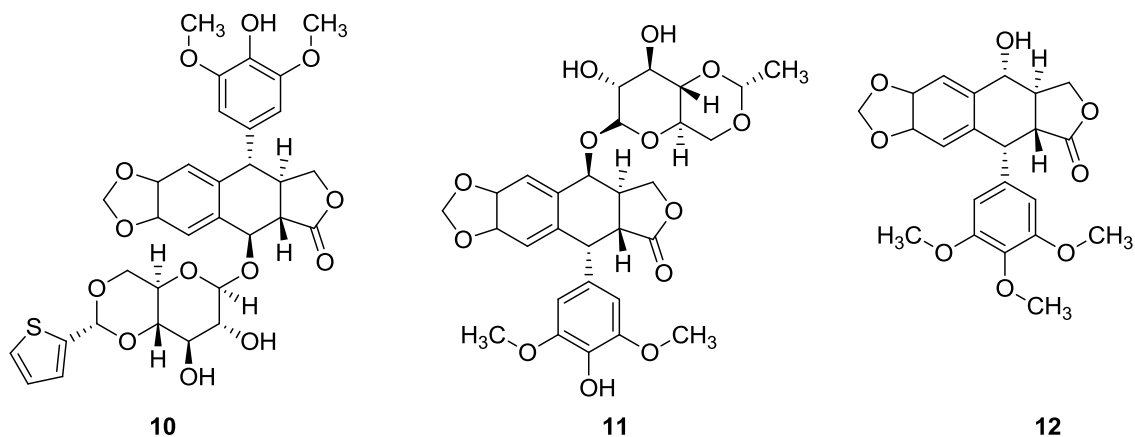


Figure 6. Structures of epipodophyllotoxin anticancer drugs, teniposide (**10**), etoposide (**11**) and podophyllotoxin (**12**).

Several compounds were approved as novel topoisomerase II enzyme inhibitors (Figure 7)²¹

- 1- Merbarone (NSC 336628) **13**: a conjugate of thiobarbituric acid and aniline joined by an amide linkage.
- 2- Suramin **14**: is a polyanionic sulphonate compound.
- 3- Fostriecin **15**: is a polyene lactone phosphate ester.
- 4- Quinolone derivatives: Quinolones are widely used antibiotics, which exert their action through the inhibition of the bacterial topoisomerase II enzyme (DNA gyrase). Quinolone derivatives, namely quinobenzoxazines showed good cytotoxic activity toward tumour cell lines such as HT-29 human colon carcinoma and A546 human breast carcinoma. Examples of these cytotoxic agents are A-62176 **16** and A-74932 **17**.

Chapter I. Introduction

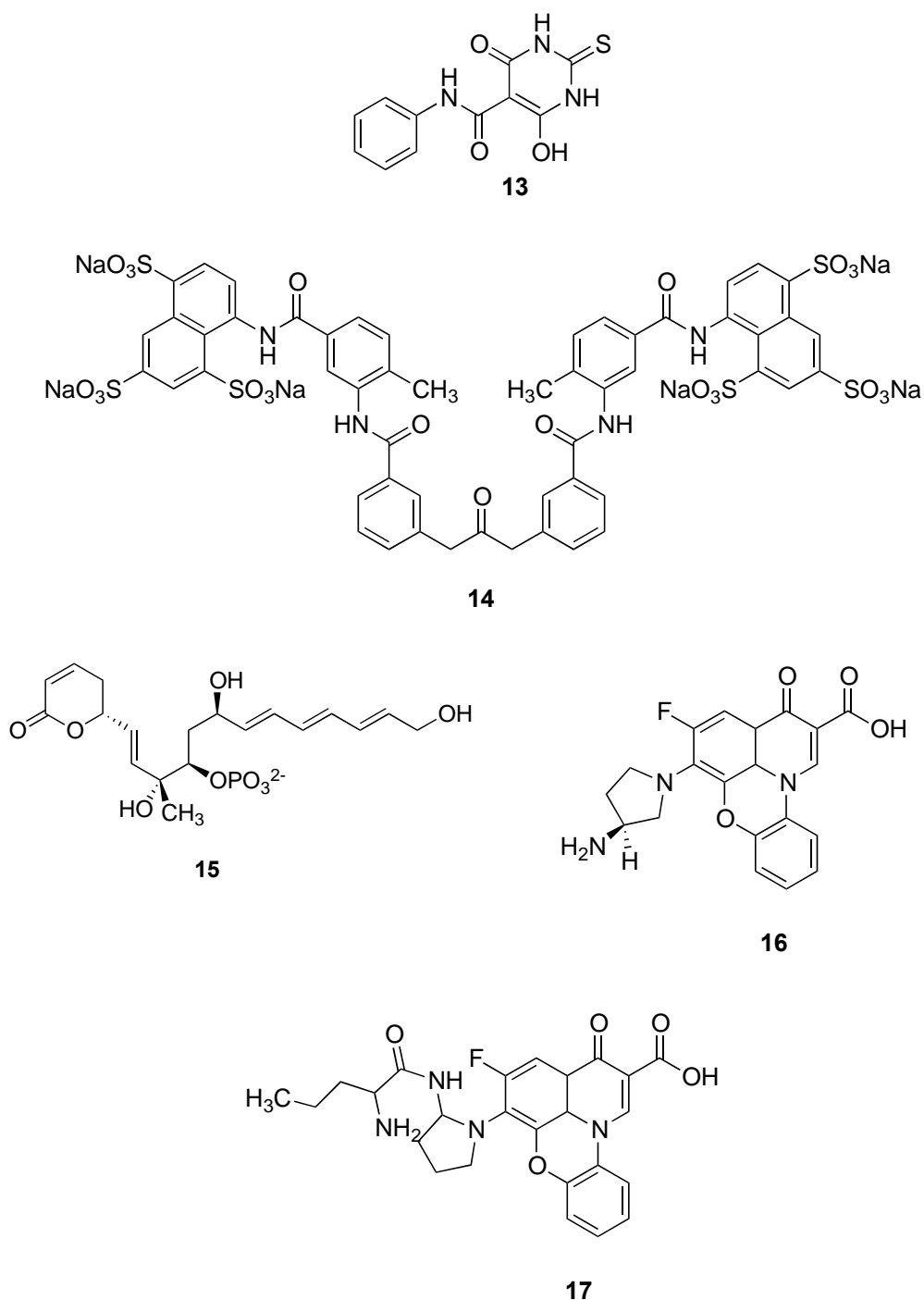


Figure 7. Structures of topoisomerase II inhibitors.

1.1.4. DNA intercalators

DNA intercalation is the insertion of a planar molecule in the space between two base pairs of DNA without breaking the H-bonding between DNA strands. This process induces local structural changes to the DNA including unwinding of the double helix and lengthening of the DNA strand. As a consequence, the transcription and replication of DNA will be retarded or inhibited.²²

Chapter I. Introduction

The drugs known to exert their cytotoxic activity through DNA intercalation are acridines and anthracyclines.

1.1.4.1. Acridines²³

Acridines intercalate DNA via π - π stacking interactions with DNA base pairs. In 1970s, nitracrine **18** and amsacrine **19** (Figure 8) were the first acridines developed for the treatment of cancer. Nitracrine is 1-nitroacridine derivative and amsacrine is a 9-anilinoacridine derivative.

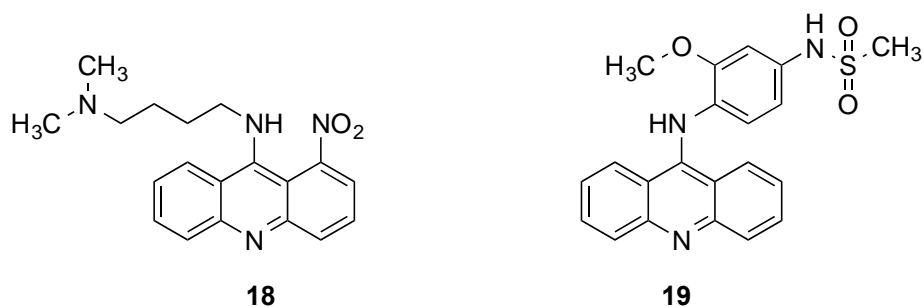


Figure 8. Structures of acridine DNA intercalators, nitracrine (**18**) and amsacrine (**19**).

1.1.4.2. Anthracyclines²⁴

Anthracyclines are planar polycyclic compounds that intercalate DNA. The cytotoxic activity of anthracyclines is believed to occur through different mechanisms of action beside their ability to intercalate DNA:

1. Generation of free radicals through the one-electron reduction of the quinone part. The generated free radicals lead to DNA damage and lipid peroxidation.
2. DNA binding and alkylation
3. DNA cross-linking
4. Interference with DNA unwinding or DNA strand separation
5. The inhibition of topoisomerase II enzyme causing induction of cell apoptosis.

The first anthracyclines were doxorubicin **20** and daunorubicin **21** (Figure 9), which were isolated from *Streptomyces peucetius* in the 1960s.²⁵ Doxorubicin is used for the treatment of breast cancer, childhood solid tumours, soft tissue sarcomas and aggressive lymphomas. On the other hand, daunorubicin is used to cure acute lymphoblastic or myeloblastic leukaemias.

Chapter I. Introduction

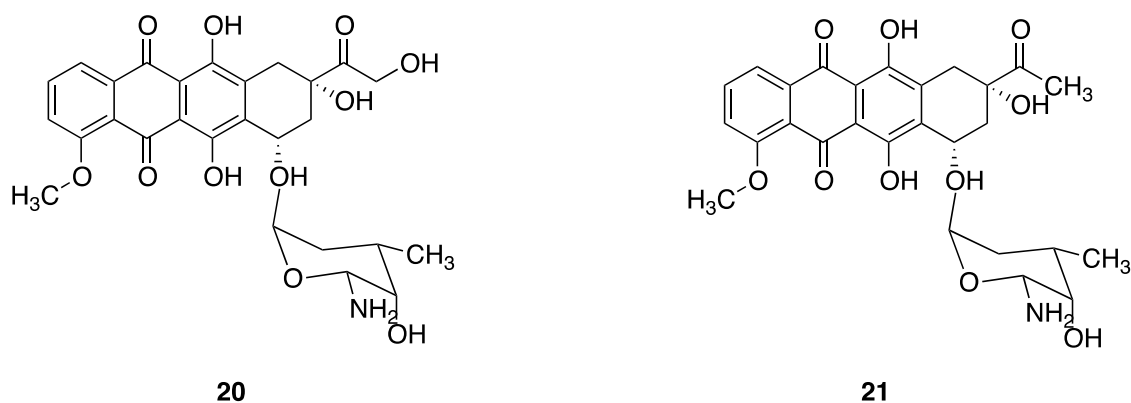


Figure 9. Structures of doxorubicin (**20**) and daunorubicin (**21**).

1.1.5. Microtubule-targeting anticancer drugs²⁶

Microtubules are long, filamentous, tube-shaped proteins present in all eukaryotic cells. They are important in the development and maintenance of cell shape, in cell signalling and in cell division and mitosis.

Microtubules are potential target in cancer because of their high importance in the process of cell mitosis: the drugs that target microtubules are named as antimitotic drugs. Microtubules are mainly targeted by naturally occurring alkaloids derived from plants and animals. Table 3 summarizes the anti-microtubules drugs and the cancer type for their activity.

Table 3. Microtubule-targeting drugs as anti-cancer chemotherapeutic agents^{26b}

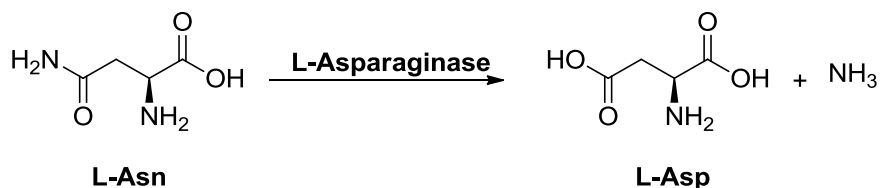
Drug	Cancer type
Vinblastine	Hodgkin's disease, testicular germ-cell cancer
Vincristine	Leukaemia, lymphomas
Paclitaxel	Ovarian, breast and lung tumours
Combretastatins	Clinical studies on anaplastic thyroid cancer
2-Methoxyestradiol	Clinical studies on breast cancer
Estramustine	Prostate

1.1.6. L-Asparaginase¹⁸

The enzyme L-asparaginase is a chemotherapeutic agent used in the treatment of acute lymphoblastic leukaemia and other lymphoid malignancies. It was first used

Chapter I. Introduction

clinically in 1966. L-Asparaginase catalyzes the hydrolysis of L-asparagine (L-Asn) into L-aspartic acid (L-Asp) and ammonia (Scheme 3).



Scheme 3. The reaction catalysed by L-asparaginase enzyme.

The effectiveness of L-asparaginase as a chemotherapeutic agent rose from the fact that lymphoblasts and certain other tumour cells do not synthesize L-Asn *de novo*. The inability of the tumour cells to synthesize L-Asn causes them to rely on L-Asn supplied from serum for survival. As a consequence, the depletion in the supply of L-Asn to the tumour cells will lead to cell death.

1.1.7. Drugs that target the cell cycle

The cell cycle is a complex process which is divided into four distinct phases:

- 1- G1 phase (first gap phase): cell is preparing for DNA synthesis.
- 2- S phase (Synthesis phase): cell is synthesizing DNA.
- 3- G2 phase (second gap phase): cell is preparing for mitosis.
- 4- M phase (mitosis phase): cell divides into two daughter cells.

The cell is considered in G₀ phase (quiescent phase) when the cell is not in the cycle, but it has the potential to divide.²⁷

The process of the cell cycle is usually regulated by cyclin proteins and by cyclin-dependent kinases.²⁷ The inhibition of cyclin-dependent kinases leads to cell cycle arrest and induction of apoptosis. Flavopiridol **22** and UCN-01 **23** are examples of drugs that inhibit cyclin-dependent kinases (Figure 10).²⁸

Chapter I. Introduction

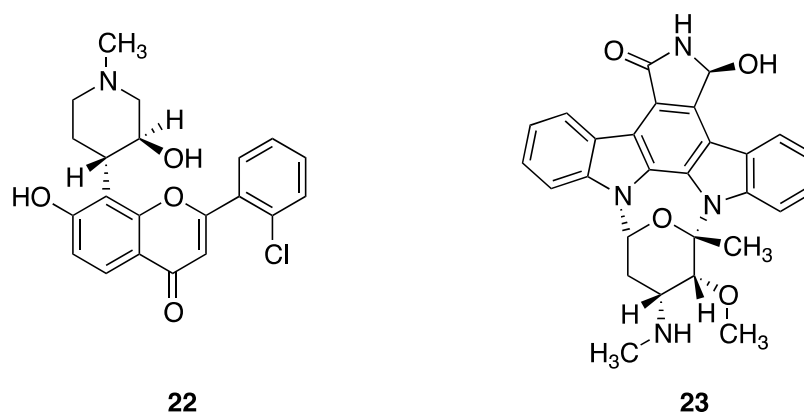


Figure 10. Structures of anticancer drugs that target the cell cycle: flavopiridol (**22**) and UCN-01 (**23**).

1.2. Cancer resistance to chemotherapy- the need for new targets and approaches²⁹

The major problem facing the use of chemotherapeutic drugs for the treatment of cancer is the resistance of cancerous cells to these drugs. The resistance develops because of the rapid metabolic changes occurring in cancer cells, and the hypoxic conditions of the tumour environment, specifically in solid tumours. The hypoxic conditions affect the action of most chemotherapeutic agents, which need molecular oxygen to generate free radicals that induce cell toxicity.

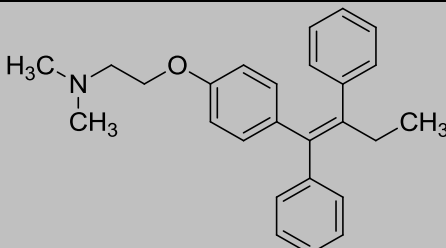
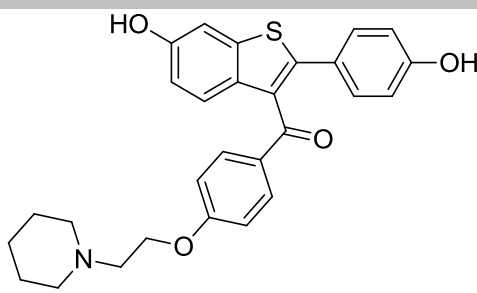
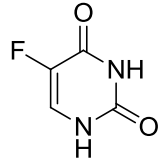
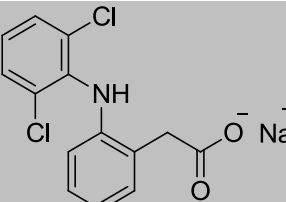
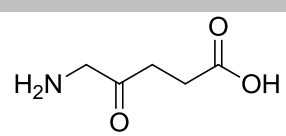
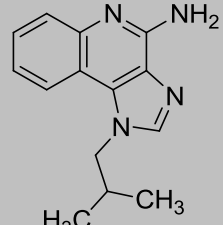
The understanding of signal-transduction pathways involved in carcinogenesis pathways led to the discovery of new targets. This aids in the rational drug design of compounds that can modify the action of these targets leading to the discovery of new chemotherapeutic drugs.

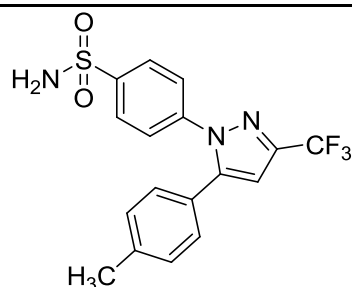
1.3. Cancer chemoprevention- first line of defence

The high toxicity of conventional anticancer drugs and the failure to reduce the mortality rate for some cancers, means that chemoprevention of cancer is of great importance.³⁰ Cancer chemoprevention is the use of a synthetic or natural product which has the ability to modulate the progress of normal cells into tumour cells.³¹ Table 4 summarizes the chemoprevention agents that have been approved for use in the clinic by the Food and Drug Administration.³²

Chapter I. Introduction

Table 4. Cancer chemo-preventive agents

Drug name	Structure	Cancer type	Year first approved
Tamoxifen ³³		Breast	1998
Raloxifene ³⁴		Breast	2007
HPV vaccine ³⁵	---	Cervix, vagina, anus	2006
5-Fluorouracil ³⁶		Skin	1970
Diclofenac sodium ³⁶		Skin	2000
5-Aminolevulinic acid ³⁶		Skin	1999
Imiquimod ³⁶		Skin	2004

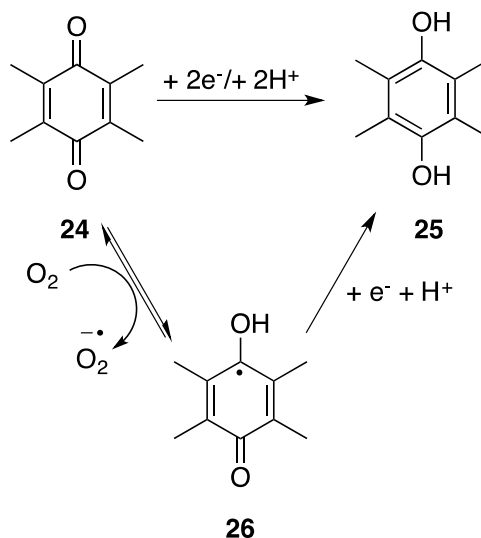
Celecoxib³⁶

Colon

1988

2. Quinones as carcinogenic compounds

Quinones **24** are organic cyclic compounds present as endogenous biochemical in pro- and eukaryotic cells and they are abundant in the environment. Quinones are cytotoxic compounds as they are highly electrophilic compounds that can react with the nucleophilic sites of DNA, nucleophilic residues of proteins and glutathione (GSH) leading to protein alkylation and GSH depletion.³⁷ In mammalian cells, quinones are reduced into either more stable derivatives known as hydroquinones **25** or to reactive species known as semiquinones **26**. Hydroquinones are produced from two-electron transfer, but semiquinones from one-electron transfer (Scheme 4).³⁸



Scheme 4. The one-electron and two-electron reduction of quinone (**24**).

The one-electron transfer is catalysed by flavin- or metal-dependent catalytic enzymes, such as NADH-cytochrome *b5* reductase, NADPH-cytochrome P450 reductase and chloroplast ferredoxin-NADP⁺ reductase.³⁹ The semiquinone species **26**, which result from the one-electron reduction of quinones have a role in the oxidative stress in cells. This can be explained by their high toxicity, which forces the cells to detoxify them through the reaction with oxygen molecules. Reaction of the semiquinone

Chapter I. Introduction

species with oxygen molecules leads to the formation of superoxide radicals, which can damage DNA. The increase in the production of these superoxide radicals can lead to cancer.^{38, 40}

The two-electron reduction of quinones into hydroquinones, which is catalysed by flavo-quinone reductase enzymes (QRs) competes with the one-electron reduction of quinones. The resulting hydroquinones **25**, which are relatively stable compounds, are removed from cells by conjugation with glutathione and UDP-glucuronic acid.⁴¹ The quinone reductase enzymes utilize either flavin mononucleotide (FMN) **27** or flavin adenine dinucleotide (FAD) **28** as a cofactor (Figure 11). The role of the cofactor in the reduction process is the transfer of the hydride ion from an electron donor, such as NAD(P)H to the quinone substrate.³⁸

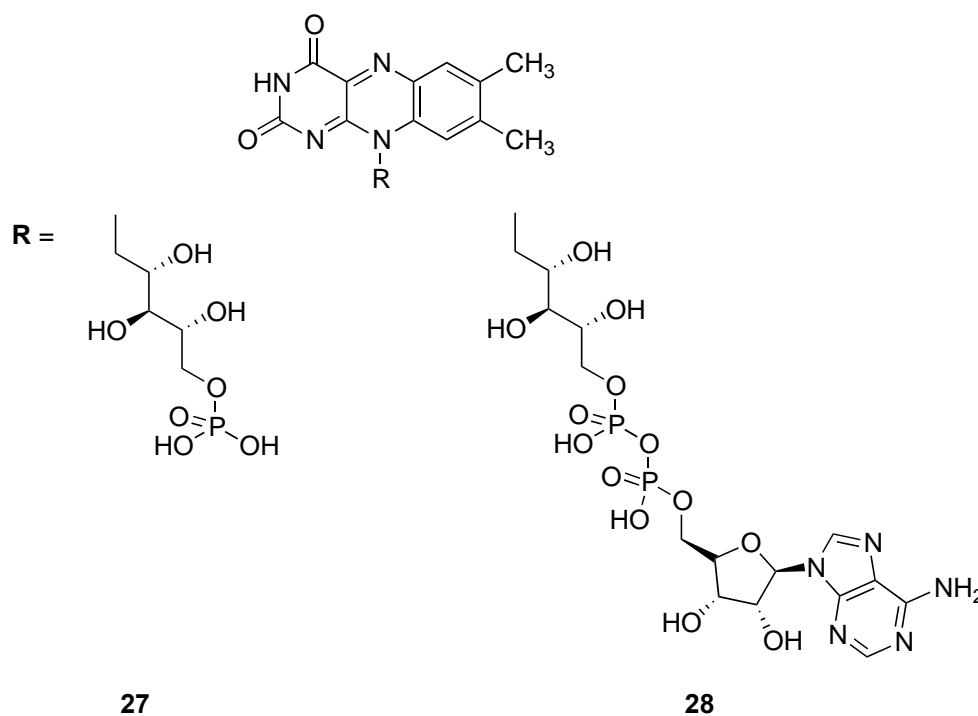


Figure 11. Structures of FMN (**27**) and FAD (**28**) cofactors.

2.1. Quinone reductases (QRs)

NAD(P)H: quinone oxidoreductase 1 (NQO1) and NRH: quinone oxidoreductase 2 (NQO2) are examples of mammalian quinone reductase enzymes. Both enzymes are homodimeric with two FAD molecules bound non-covalently to the enzymes. The isoalloxazine ring of the FAD molecule forms the floor of both enzyme active sites. The FAD molecules are involved in the reduction processes catalysed by the two enzymes, each of which will be discussed further.

Chapter I. Introduction

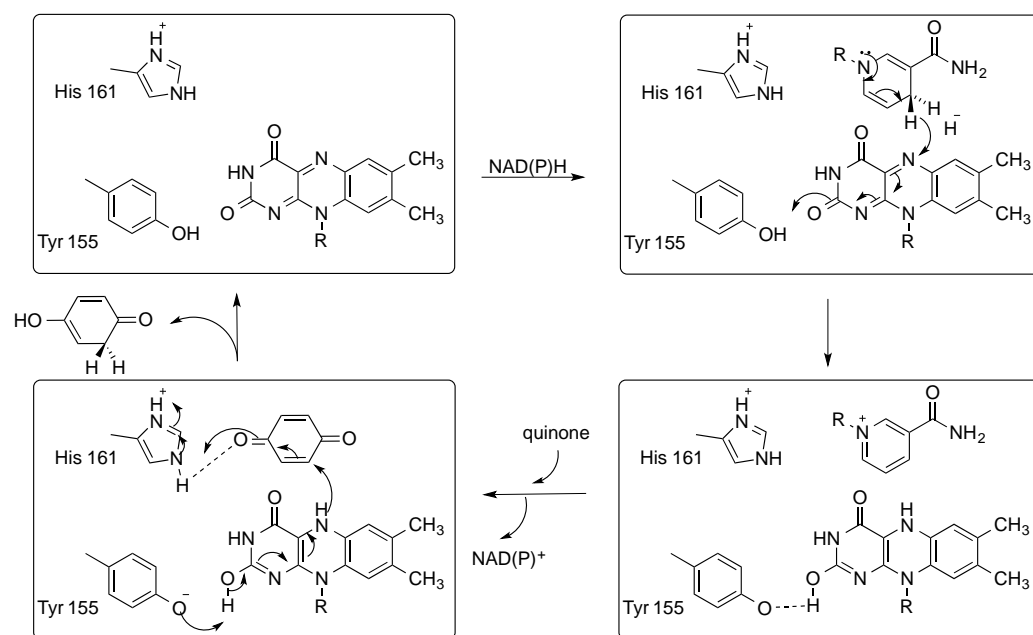
2.1.1. NAD(P)H: quinone oxidoreductase 1 (NQO1) enzyme

NQO1 (EC 1.6.99.2) is a cytosolic flavoprotein first isolated from rat liver by Ernster and co-workers in 1958.⁴² NQO1 is also known as DT-diaphorase as the enzyme which non-specifically catalyses the oxidation of reduced di- and tri-phosphopyridine nucleotide NADH and NADPH, respectively.⁴² NQO1 is highly expressed in liver, brain, kidney, heart, lungs and testis in human.⁴³ Besides that, NQO1 is highly expressed in most human solid tumours,⁴⁴ particularly in non-small cell lung, prostate, pancreatic and breast tumours.⁴⁵

NQO1 is a homodimeric protein with a molecular weight of around 55,000 Da,⁴⁶ which is composed from two monomers. Each 273-amino acid monomer is divided into two domains: a large catalytic domain contains the amino acid residues 1-220 and a small C-terminal domain contains the amino acid residues 221-273. The NQO1 enzyme has two FAD molecules bound to the catalytic domain of each monomer.⁴⁷ The FAD molecules are anchored through hydrogen bonding with the amino acid residues Trp¹⁰⁵, Phe¹⁰⁶, Tyr¹⁵⁵, Gly¹⁵⁰, Gly¹⁴⁹, Leu¹⁰³, Thr¹⁴⁷, Asp¹⁸, Arg²⁰⁰, Gln⁶⁶, His¹¹ and Tyr¹⁰⁴.⁴⁸

More than 90% of the enzyme's catalytic activity was found to be cytosolic and minor portions are associated with mitochondria and microsomes.^{43a} NQO1 catalyses the two-electron reduction of quinones and converts them into hydroquinones. The reduction process proceeds through a ping-pong mechanism (Scheme 5). This mechanism involves the complete transfer of two electrons and protons from NQO1 co-substrate, NAD(P)H to its cofactor flavin adenine dinucleotide (FAD⁺) molecule forming reduced flavin adenine dinucleotide (FADH₂) (Scheme 5).⁴⁹ Subsequently, a hydride ion will transfer from FADH₂ to the quinone substrate.⁵⁰

Chapter I. Introduction



Scheme 5. Ping-pong mechanism of quinone reduction by the NQO1 enzyme.

NQO1 is considered as a detoxifying enzyme as its role in the reduction of quinones aids in the protection of cells from harmful effects of quinones.⁴¹

2.1.2. *N*-Ribosyl dihydronicotinamide (NRH): quinone oxidoreductase 2 (NQO2) enzyme

NRH: quinone oxidoreductase 2 (NQO2) enzyme is a cytosolic flavoprotein enzyme discovered by Liao and Williams-Ashman in 1961.⁵¹ It is widely distributed in human tissue, mainly in heart, brain, lung, liver and skeletal muscle.⁵² NQO2 is a homodimeric protein⁵³ consisting of 231-amino acids.⁵⁴ Each monomer is divided into two domains: the N-terminal domain (1-220 amino acid residues) and the C-terminal domain (221-231 amino acid residues) (Figure 12).⁵⁵

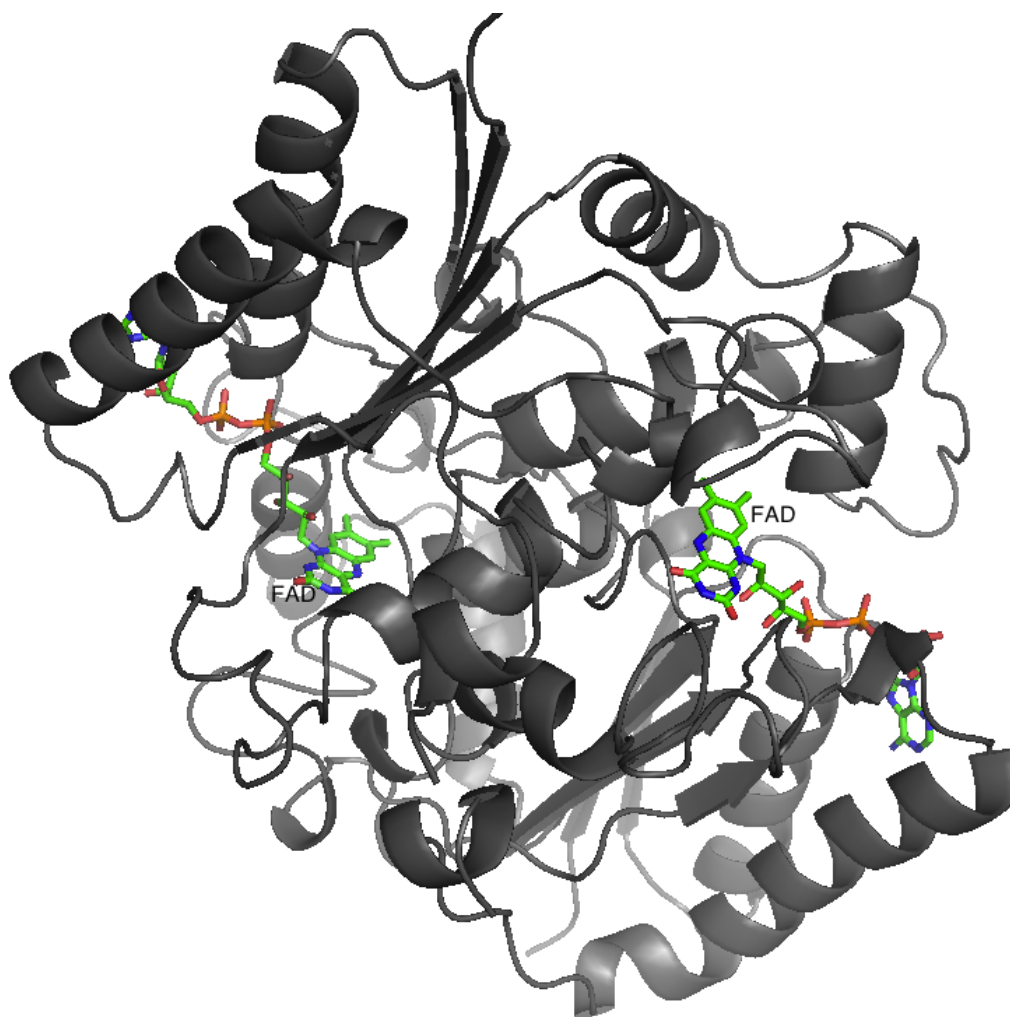


Figure 12. The 3D structure of NQO2 enzyme (PDB code 1QR2; Resolution at 2.10 Å).⁵⁴

The NQO2 enzyme active site is a narrow deep hydrophobic cavity,⁵⁵ which is surrounded by the side chains of Tyr^{132'}, Phe^{178'}, Phe^{126'}, Met^{154'} and Cys^{121'} amino acid residues from one monomer and Tyr¹⁵⁵ and Phe¹⁰⁶ amino acid residues from the other monomer.⁵⁶ The isoalloxazine ring of the FAD molecule⁵⁴ and the side chain of Trp¹⁰⁵ amino acid form the floor of the cavity.⁵⁶ The side chain of Asn¹⁶¹ and the hydroxyl groups of Tyr¹⁵⁵ and Tyr¹³² amino acid residues form a hydrophilic surface at one end of the cavity.⁵⁶ The hydroxyl group of Thr⁷¹ and the main chain of Gly⁶⁸ and Asp¹¹⁷ amino acid residues point towards the other end of the cavity.⁵⁶ The positions of these amino acid residues indicate that both ends have numerous functional groups accessible for hydrogen bonding. The fourth side is accessible to solvent (Figure 13).⁵⁶

Chapter I. Introduction

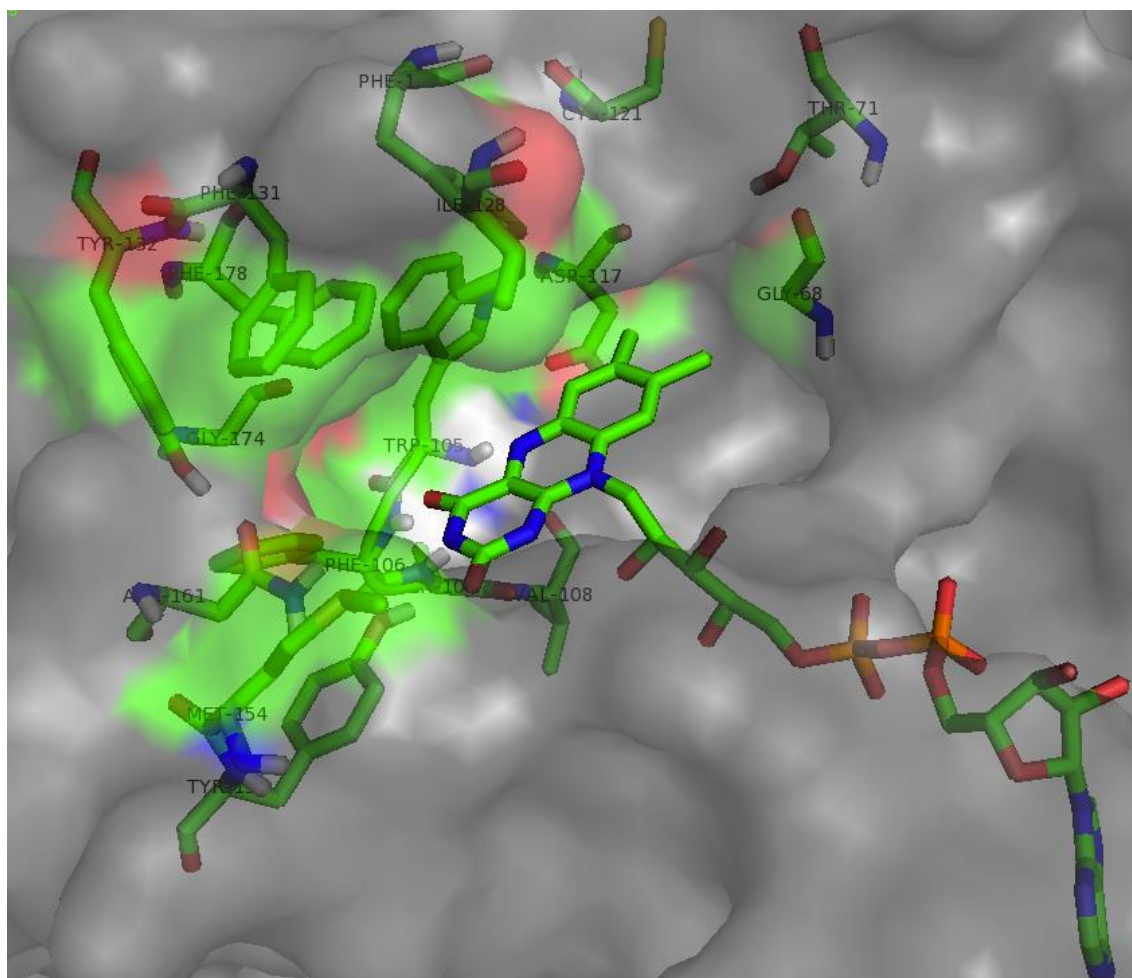


Figure 13. NQO2 enzyme active site (PDB code 1QR2; Resolution at 2.10 Å).⁵⁴

NQO2 catalyzes the two-electron reduction of quinones *via* a ping-pong mechanism similar to the NQO1 enzyme.⁵⁷ NQO2 utilizes non-naturally occurring *N*-ribosyl dihydronicotinamide (NRH) co-substrate **29** as an electron donor in the reduction processes.⁵⁸ The *N*-methyl **30**, *N*-(*n*-propyl) **31**, and *N*-benzyl **32** analogues of NRH (Figure 14) were studied as alternative co-substrates of NQO2.⁵⁹ It was found that NQO2 has a high affinity for the *N*-benzyl nicotinamide analogue **32**.⁶⁰

Chapter I. Introduction

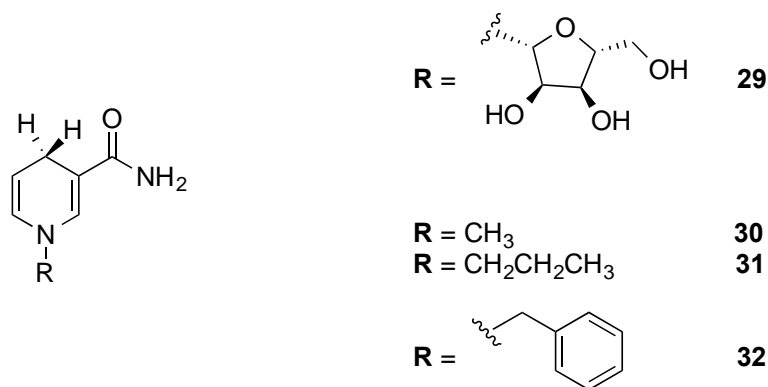


Figure 14. Structures of NQO2 enzyme co-substrates, *N*-riboseyl (**29**), *N*-methyl (**30**), *N*-(*n*-propyl) (**31**) and *N*-benzyl (**32**) dihydropyridinamide.

The substrates for the NQO2 enzyme are either *para*-quinones, such as menadione (vitamin K3, menadione) **33**,⁵¹ coenzyme Q0 **34**,⁶⁰ or *ortho*-quinones (catechol quinones),⁶¹ such as the estrogen *ortho*-quinone metabolites, estrone **35** and estradiol **36** (Figure 15).⁶² Menadione (2-methyl-1,4-naphthaquinone, Vitamin K3, **33**) is activated by NQO2 leading to hepatic toxicity.⁶³

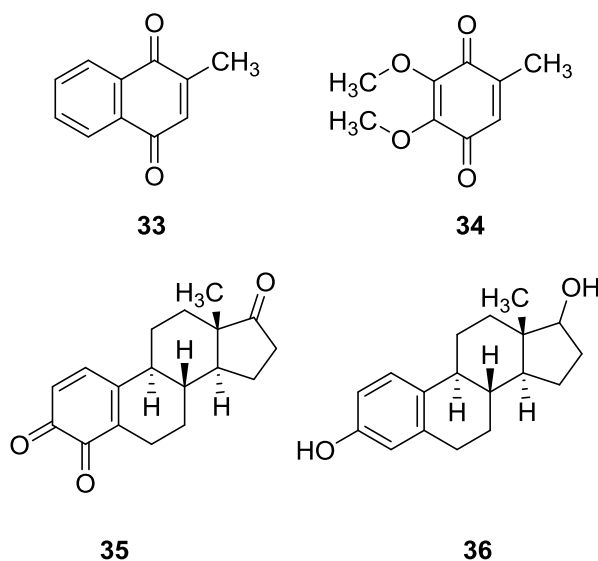
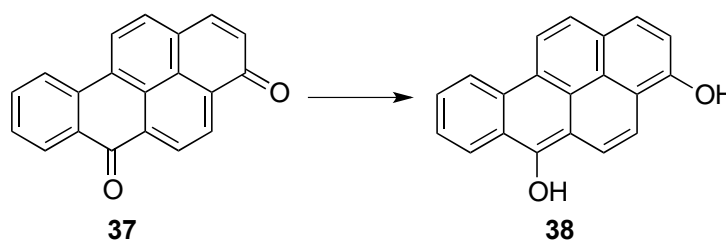


Figure 15. Structures of the NQO2 substrates, menadione (**33**), coenzyme Q0 (**34**), estrone (**35**) and estradiol (**36**).

The role of NQO2 in the reduction of estrogen *ortho*-quinones is considered a detoxification reaction. The estrogen quinones are electrophilic compounds that react with DNA and they are related to carcinogenesis of breast cancer.⁶²

Chapter I. Introduction

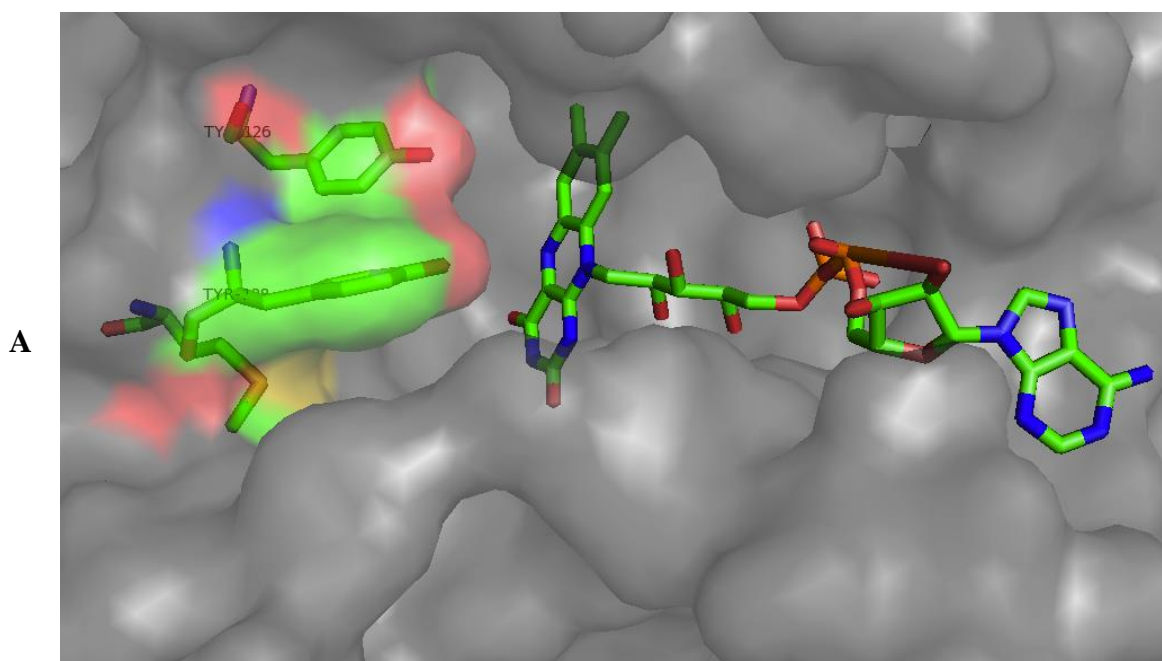
On the other hand, NQO2 is considered as an activating enzyme as its role in the reduction of benzo[a]pyrene-3,6-quinone **37**⁴¹ is related to cell toxicity. The reduction of benzo[a]pyrene-3,6-quinone **37** yields benzo[a]pyrenediol product **38**. Benzo[a]pyrenediol product can re-oxidize back to benzo[a]pyrenediones generating hydrogen peroxide, hydroxyl and semiquinone radicals (Scheme 6) that can attack cell macromolecules⁶⁴ leading to mutagenicity.⁶⁵



Scheme 6. Reduction of benzo(a)pyrenediones (**37**) into benzo(a)pyrenediol (**38**).

2.1.3. NQO1 and NQO2: similarities and differences

The overall topology of NQO2 is highly similar to its homologous enzyme NQO1, with 54% and 49% similarity between human NQO2 and NQO1 cDNA and protein, respectively.⁵³ Both enzymes are homodimeric binding two FAD cofactors⁶⁶ and they share the same active site.⁵⁴ The active sites are hydrophobic, favouring the binding of hydrophobic substrates and inhibitors.⁵⁷ The NQO2 active site is slightly larger and more hydrophobic than the NQO1 active site because Tyr¹²⁶, Tyr¹²⁸ and Met¹³¹ residues in NQO1 are replaced by Phe¹²⁶, Ile¹²⁸ and Phe¹³¹ in NQO2 (Figure 16).⁵⁴



Chapter I. Introduction

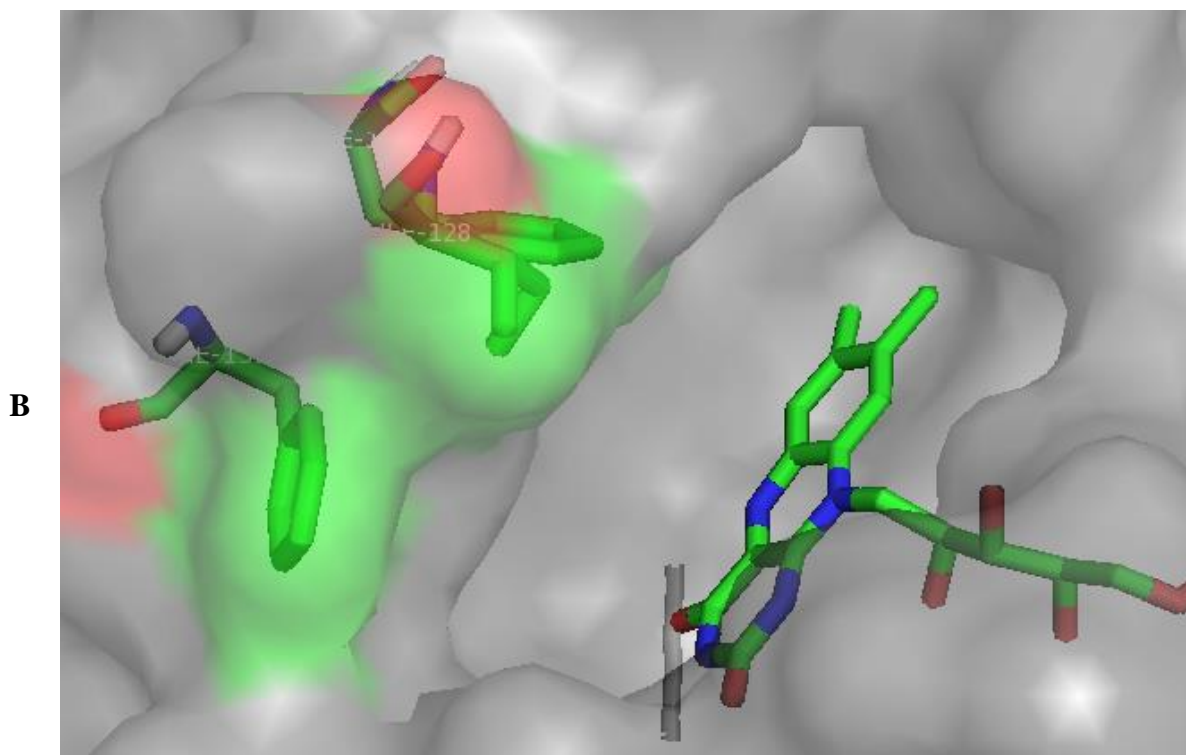


Figure 16. Enzyme's active site: A- NQO1 (PDB code 2F1O; Resolution at 2.75 Å); B- NQO2 (PDB code 1QR2; Resolution at 2.10 Å).

The difference in the binding sites' nature and size between NQO1 and NQO2 enzymes has an impact on the inhibitor specificity for each enzyme. The potent polycyclic aromatic hydrocarbon inhibitors of NQO2, such as benzo(a)pyrene **39** and 7-methylbenzo(a)anthracene **40** (Figure 17), do not inhibit the NQO1 enzyme.^{57, 59, 67} Also, NQO2 is not inhibited by the potent NQO1 inhibitor dicoumarol **41** (Figure 17).

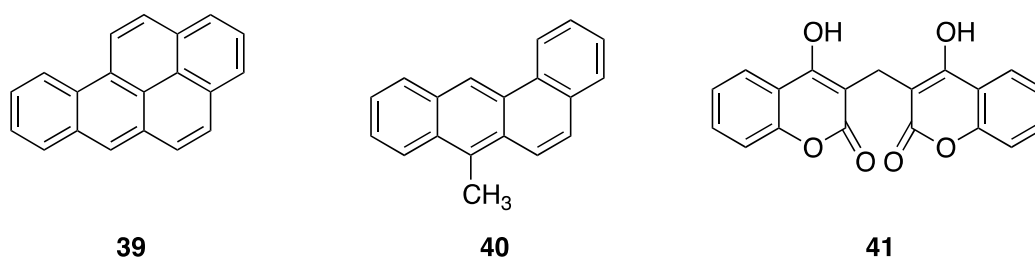


Figure 17. First known inhibitors of quinone reductase enzymes, benzo(a)pyrene (**39**), 7-methylbenzo(a)anthracene (**40**) and dicoumarol (**41**).

Both NQO1 and NQO2 catalyse the two-electron reduction of quinone and four-electron reduction of nitro-compounds,^{66b} with differences in the co-substrate that each

Chapter I. Introduction

enzyme uses as electron donor. NQO2 uses reduced non-phosphorylated derivatives of nicotinamides such as NRH **29** and its analogues **30-32**, but it is completely inert toward the phosphorylated derivatives of nicotinamide such as NADH **42** or NADPH **43** (Figure 18) ⁵⁹ that are used by NQO1.

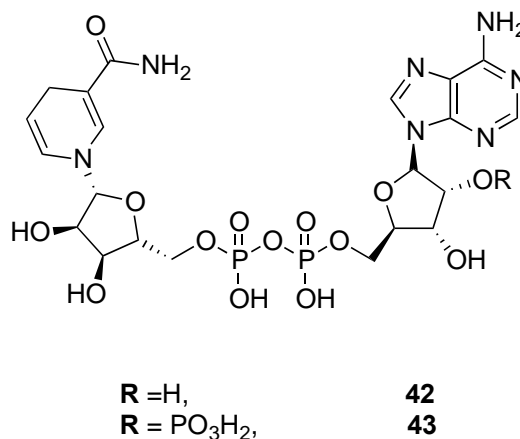


Figure 18. Structures of NADH (**42**) and NADPH (**43**).

The difference in co-substrate affinity between NQO1 and NQO2 enzymes can be explained by the lack of 43 amino acids in the C-terminal domain in NQO2.⁵⁷ This C-terminal domain in NQO1 provides the site for binding of the pyrophosphate-ribose-adenine moiety of phosphorylated nicotinamides **42** and **43**.⁵⁷ For the same reason, NQO2 cannot be inhibited by dicoumarol **41**, a known potent inhibitor of NQO1, because it exerts its action by competing with the NAD(P)H binding site.⁵⁷

2.1.4. The catalytic consequences of NQO1 and NQO2 on cells

The impact of the catalytic function of NQO1 and NQO2 in cells is different between the two enzymes. NQO1 is considered as a protective detoxifying enzyme, but NQO2 is an activating enzyme with some detoxification activity against estrogen *ortho*-quinones. NQO2-null mice exhibited myeloid hyperplasia and hyperactivity of bone marrow.⁶³ The reduction of menadione by NQO1 and NQO2 has a different impact on the cells. The reduction of menadione into menadiol by NQO1 leads to the decrease of its toxicity on cells as menadiol will be removed by conjugation with glutathione and UDP-glucuronic acid.³⁷ On the other hand, the reduction of menadione by NQO2 leads to hepatic toxicity.⁶³

NQO1 and NQO2 enzymes act as chaperone proteins by binding to the tumour suppressor factor p53 leading to its stabilization against 20S proteasomal degradation.⁶⁸ Tumour suppressor factor p53 ‘the guardian of the genome’ regulates and controls cell

Chapter I. Introduction

growth and protects cells against adverse effects of radiation and chemicals by the induction of cell growth arrest or programmed cell death (apoptosis).⁶⁹

2.1.5. Importance of NQO1 and NQO2 enzymes in cancer-targeted therapy

The targeted anti-cancer prodrug therapy is an approach used to increase the local delivery of the parent cytotoxic drugs to the cancer cells in humans. This targeting depends on the activation of the prodrugs by a certain enzyme, which is over-expressed in the cancer cells. This has an advantage of limiting the side effects of the cytotoxic drugs on normal cells of the human.⁷⁰ Prodrugs are compounds that must be transformed *in vivo* to exert their pharmacological activity.

The high expression of NQO1⁷¹ and NQO2 enzymes in tumour cells⁷² and their ability to reduce quinone and nitro compounds was utilized for the targeting of prodrugs such as CB1954 **44** and nitro-cryptolepine derivatives **45** (Figure 19) to the cancer cells.⁷²⁻

73

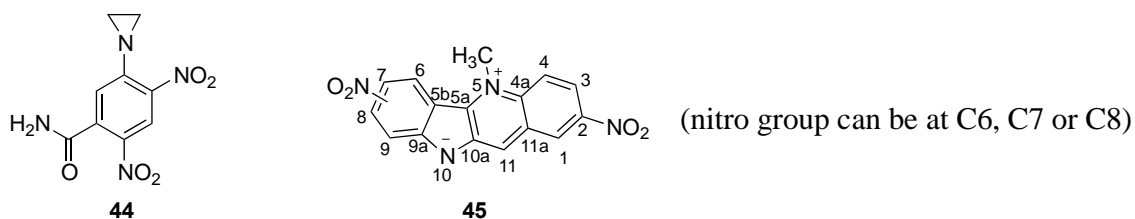
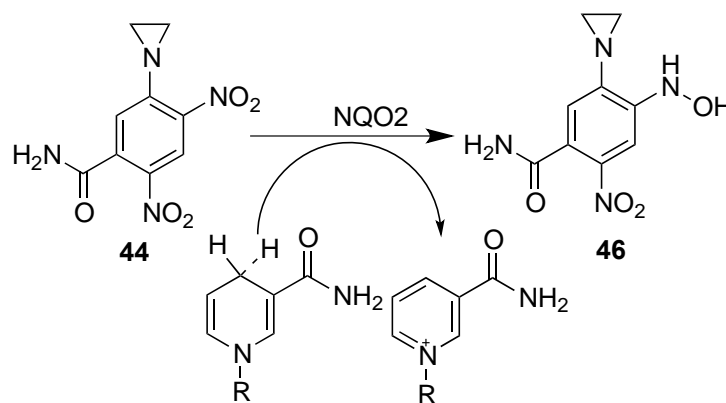


Figure 19. Structures of anti-tumour prodrugs, CB1954 (**44**) and nitro-cryptolepine derivatives (**45**).

The bio-activation of cytotoxic prodrugs into cancer cells produces highly toxic derivatives able to covalently bind macromolecules, especially DNA, leading to cell toxicity and death. The catalytic efficiency of the two enzymes is different: NQO2 is 3000 times more efficient than NQO1^{66b} in the four-electron reduction such as CB1954 [5-(aziridin-1-yl)-2,4-dinitrobenzamide, **44**] into DNA alkylating 4-hydroxylamine derivative **46** (Scheme 7).^{66b, 72}

Chapter I. Introduction



Scheme 7. Reduction of the cytotoxic compound CB1954 (**44**) by NQO2 enzyme.

Nitro-cryptolepine derivatives are activated by NQO1 and not NQO2 with the exception of the compound 2-fluoro-7,9-dinitrocryptolepine **47** (Figure 20). Compound **47** was found to exhibit higher toxicity in the RT112 cell line (high in NQO2) in the presence of *N*-ribosyl dihydronicotinamide **29** (NRH).⁷³

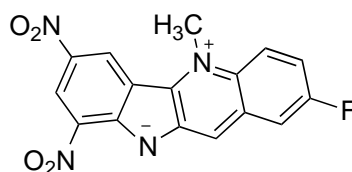


Figure 20. The structure of 2-fluoro-7,9-dinitrocryptolepine (**47**).

The anticancer prodrug mitomycin C **48** (Figure 21) is activated by the two enzymes through two-electron transfer forming a highly electrophilic hydroquinone metabolite, which has the ability to cross-link DNA.⁷⁴ However, NQO1 has poor affinity for mitomycin C⁷⁵ and the product of this reduction can irreversibly bind NQO1 leading to its inhibition.⁷⁶ Mitomycin C analogues namely, EO9 **49** can be activated by NQO1⁷⁷ and NQO2⁴¹, and BMY25067 **50** (Figure 21) can be activated by NQO2 only.⁴¹

Chapter I. Introduction

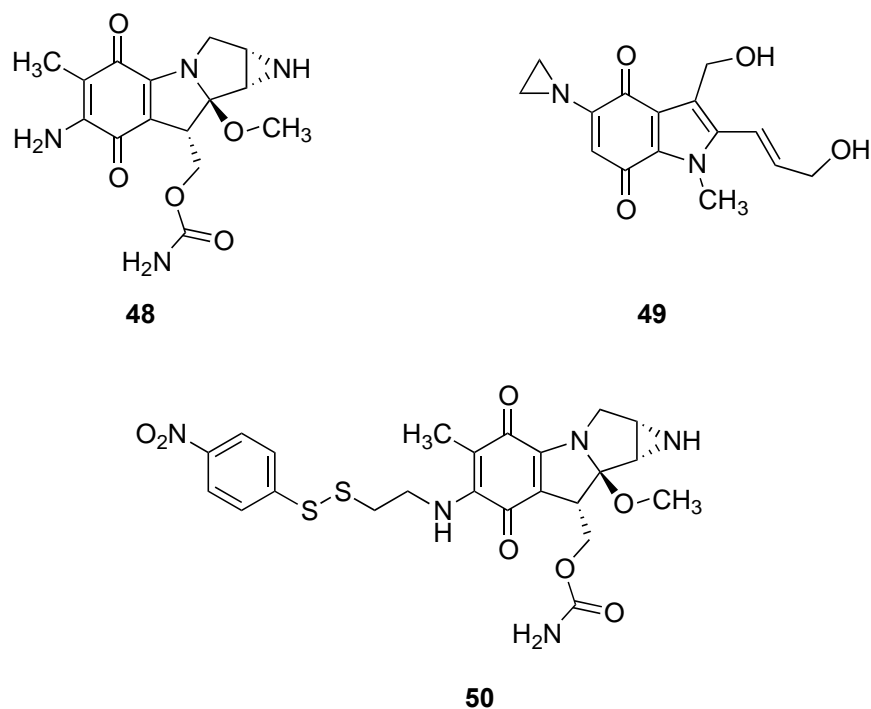


Figure 21. Structures of the anticancer drugs: mitomycin C (**48**), EO9 (**49**) and BMY25067 (**50**).

3. NQO2 Enzyme and its role in human diseases

The NQO2 enzyme is considered a potential therapeutic target in cancer and this importance has arisen for a number of reasons.

NQO2 is highly expressed in tumour cells,⁷² and its role in the reduction of quinones is related to cell toxicity^{41, 63} and mutagenicity.⁶⁵ NQO2 is required for the tumour necrosis factor (TNF)-induced activation of NF- κ B.⁷⁸ NF- κ B is a transcription factor, which controls the genes responsible for cell proliferation and survival. The activation of NF- κ B by the cytokine TNF results in the suppression of cell apoptosis⁷⁹ and the protection of tumour cells from chemotherapeutic drugs and ionizing radiation.⁸⁰

NQO2 binds some anti-tumour drugs as their off-target effect. It was found that Imatinib (2-phenylaminopyrimidine compound, **51**) and nilotinib (4-pyridyl-2-phenylaminopyrimidine compound, **52**) (Figure 22) bind to the active site of NQO2 enzyme leading to its inhibition. Imatinib and nilotinib are tyrosine kinase inhibitors used to treat leukaemia.⁸¹

Chapter I. Introduction

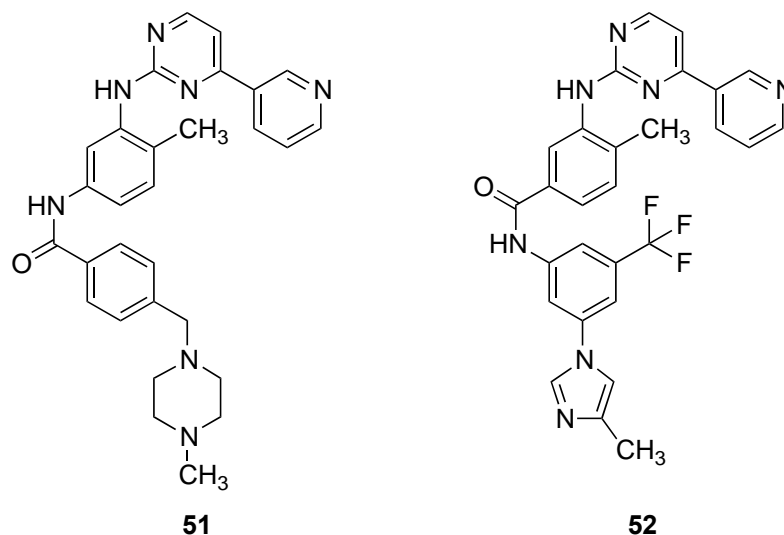


Figure 22. Structures of tyrosine kinase inhibitors, Imatinib (**51**) and nilotinib (**52**).

The inhibition of the NQO2 enzyme activity has a role in the chemoprevention⁵⁵ and chemotherapy of cancer. The inhibition of the NQO2 enzyme activity leads to the modulation of NF-kB signalling.⁸² The modulation of NF-kB signalling has an effect on tumour cell proliferation⁸³ and the potentiation of the activity of chemotherapeutic drugs and ionizing radiation leading to induction of tumour cell apoptosis.^{80, 84}

In addition, the high expression of NQO2 enzymes in tumour cells⁷² and its ability to reduce quinone and nitro compounds was utilized for the targeting of bioreducible cytotoxic agents such CB1954 and nitro-cryptolepine analogues to the tumour cells.⁷²⁻⁷³

Also, the NQO2 enzyme has a role in other human diseases neurodegenerative diseases, for example Parkinson's disease,⁸⁵ schizophrenia⁸⁶ and Alzheimer's disease. NQO2 gene polymorphism is correlated with Parkinson's disease⁸⁵ and schizophrenia.⁸⁶ On the other hand, the levels of the NQO2 enzyme in the hippocampus of Alzheimer's disease patients was found to be high, but still the relation between Alzheimer's disease and NQO2 has not yet been determined.⁸⁷

The NQO2 enzyme in human red blood cells has been identified as a potential target of the anti-malarial aminoquinoline compounds primaquine and chloroquine,⁸⁸ which can selectively inhibit this enzyme in the low micro-molar range.⁵⁰

3.1. NQO2 inhibitors

The first compounds studied as inhibitors for NQO2, with the aim to determine the enzyme properties, were quinacrine (Atabrine®, **53**) and chlorpromazine **54** (Figure

Chapter I. Introduction

23) which can inhibit NQO2 at concentration of 20.0 μM .⁵¹ Polycyclic aromatic hydrocarbons such as benzo[a]pyrene **39** (Figure 17) and benzo[a]anthracene **55** (Figure 23), can also potently inhibit the NQO2 enzyme with an IC_{50} value less than 10 nM.⁵¹

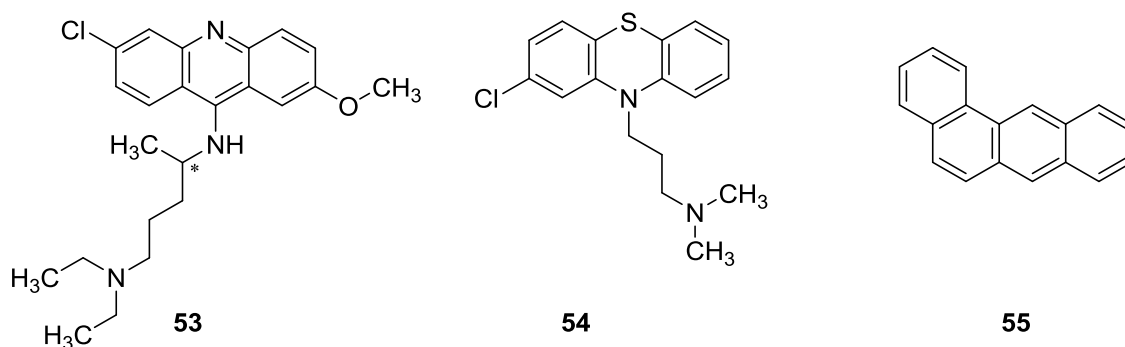


Figure 23. Structures of first reported NQO2 inhibitors, quinacrine (**53**), Chlorpromazine (**54**) and benzo(a)anthracene (**55**).

3.1.1. Flavones

Flavones are polyphenol compounds that can inhibit NQO2 competitively with respect to NRH.^{66b} In the literature many of these compounds were reported as potent inhibitor of NQO2 through exerting their inhibition action in the 100 nM range such as Epigenin **56**, Genistein **57**, and Kaempferol **58**.⁶⁰ The most potent flavone inhibitor known is Quercetin (2-(3,4-dihydroxyphenyl)-3,5,7-trihydroxy-4*H*-chromen-4-one, **59**) (Figure 24) that can inhibit NQO2 with an IC_{50} value of 80 nM.^{66b}

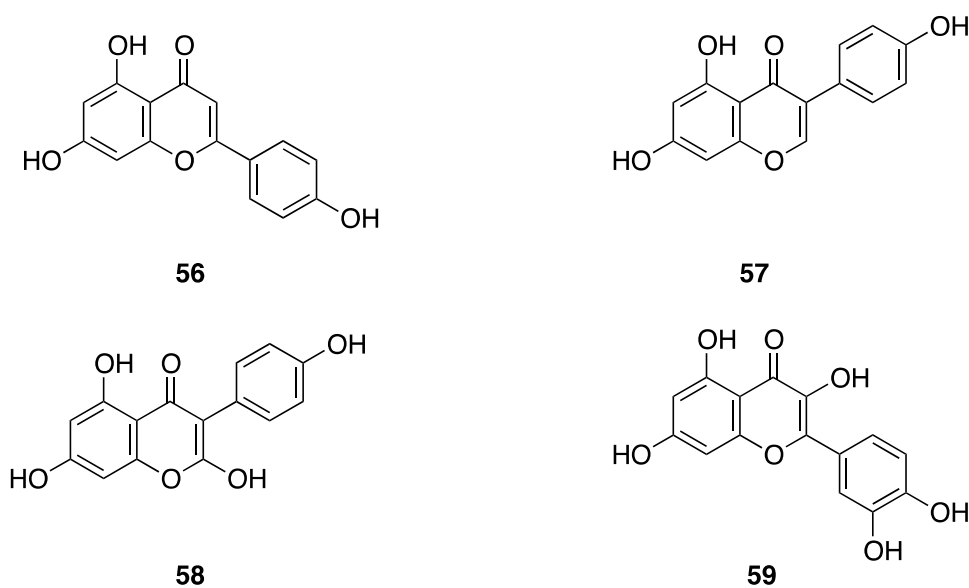


Figure 24. Structures of flavonoid inhibitors of NQO2, Epigenin (**56**), Genistein (**57**), Kaempferol (**58**) and Quercetin (**59**).

Chapter I. Introduction

3.1.2. Resveratrol

Resveratrol (*trans*-3,4',5-trihydroxystilbene, **60**), a constituent of red grapes (Figure 25), is a chemopreventive compound that can affect the three stages in carcinogenesis, namely, tumour initiation, promotion and progression. Its action as a chemopreventive agent was first reported with its inhibition of cyclooxygenase at a concentration of $\sim 15 \mu\text{M}$.⁸⁹ The chemopreventive action of resveratrol is also linked to the inhibition of the NQO2 enzyme through binding to the enzyme active site competing with the substrate.⁵⁵

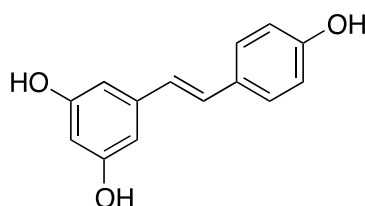


Figure 25. The structure of resveratrol (**60**).

3.1.3. Aminoquinolines

The antimalarial aminoquinoline compounds namely, quinacrine **53** (Figure 23), primaquine **61** and chloroquine **62** (Figure 26) showed high affinity for inhibition of NQO2 enzyme in the $1 \mu\text{M}$ range.^{50,90}

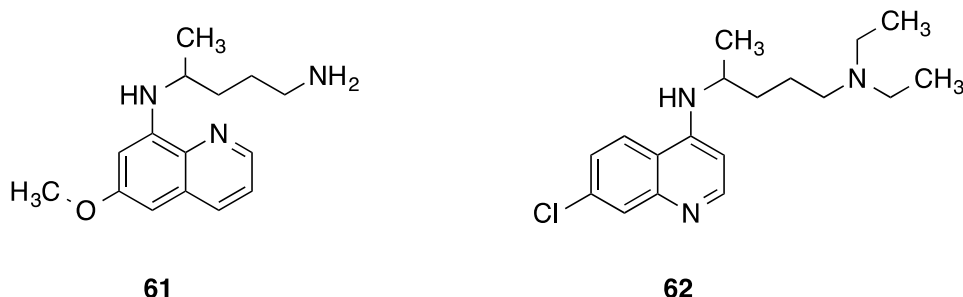


Figure 26. Structures of aminoquinoline inhibitors of NQO2, Primaquine (**61**) and Chloroquine (**62**).

3.1.4. MT3-ligands

Melatonin (N-acetyl-5-methoxytryptamine, **63**) (Figure 27) is a neurohormone secreted from the pineal glands. It exerts its action in the body by binding two G protein coupled receptors, namely MT1 and MT2, and a non G-protein coupled receptor with enzymatic properties identified and characterized as NQO2 (MT3).⁹¹ Melatonin **63** and its analogue iodomelatonin **64** can bind to the active site of the NQO2 enzyme leading to its inhibition with IC_{50} values of 11.3 and $1.1 \mu\text{M}$, respectively.⁹² Several MT3

Chapter I. Introduction

receptor ligands are reported in the literature as potent NQO2 inhibitors.⁹³ These ligands (Figure 27) can specifically inhibit the NQO2 enzyme in the low nanomolar range. The most potent ligand is compound S29434 **67** that can inhibit NQO2 with an IC₅₀ value of 2.4 nM.⁹³⁻⁹⁴

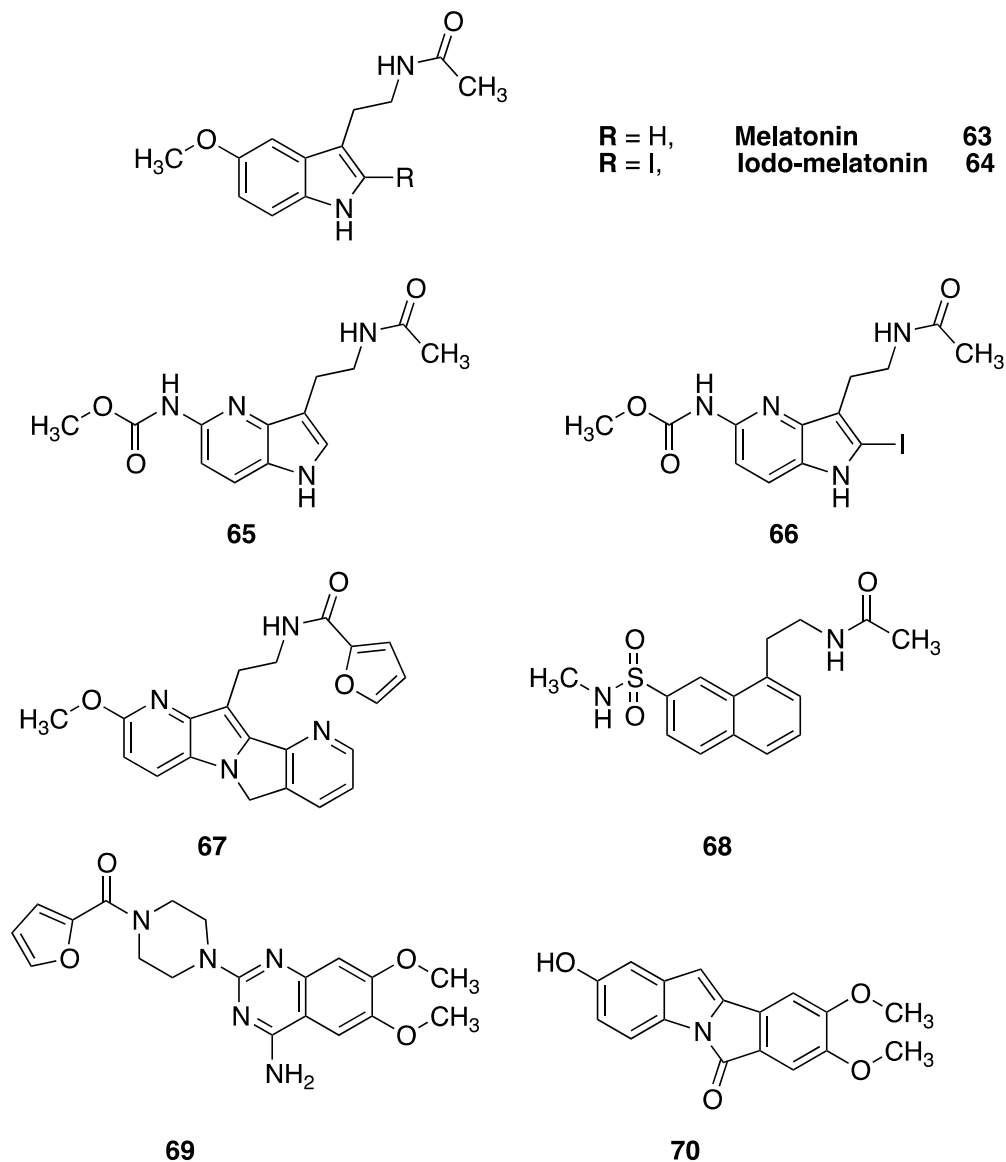


Figure 27. Structures of MT3 receptor ligands.

3.1.5. Imatinib (Glivec®)

The anti-leukaemic drug Imatinib **51** (Figure 22) is a tyrosine kinase inhibitor that can inhibit the NQO2 enzyme with an IC₅₀ value of 80 nM. It competes with the substrate for the active site which is considered as an off-target effect for this drug.⁸¹

Chapter I. Introduction

3.1.6. Dabigatran and its ethyl ester prodrug⁹⁵

Dabigatran **71** and dabigatran ethyl ester **72** (Figure 28) are anti-coagulant drugs, which exert their action through the inhibition of thrombin. Michaelis and co-workers reported that these drugs have similar NQO2 inhibitory potency as Imatinib **51**.

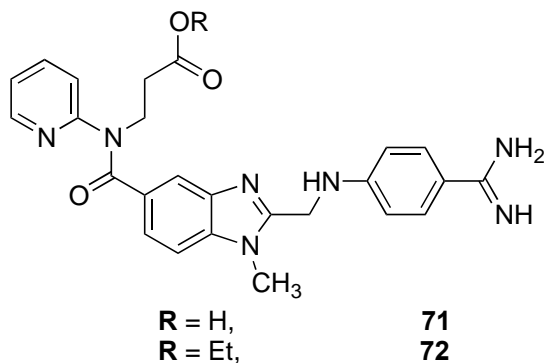


Figure 28. Structures of the anticoagulants, dabigatran (**71**) and its ethyl ester (**72**).

3.1.7. Casimiroin and its analogues⁵⁶

Casimiroin **73** (Figure 29) is a natural product derived from the fruit of the *Casimiroa edulis Rutaceae* plant. It is a lead quinolinone compound investigated for its potential chemopreventive and chemotherapeutic activity, which can be explained by its ability to inhibit the NQO2 enzyme with an IC_{50} of 54.1 μ M. To optimize its NQO2 inhibition activity many analogues were synthesized (Table 5) and the most potent, compound **78** exerted its activity with an IC_{50} of 1.9 μ M.

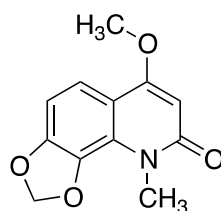


Figure 29. The structure of casimiroin (**73**).

Table 5. NQO2 inhibition data for casimiroin and its analogues.⁵⁶

Compound ID	R ₁	R ₂	R ₃	R ₄	R ₅	IC ₅₀ (μM)
Casimiroin 73			----			54.1 ± 6.7
74	-OCH ₂ O-		H	H	CH ₃	6.2 ± 0.8
75	OCH ₃	H	H	H	CH ₃	5.8 ± 0.9
76	OCH ₃	OCH ₃	H	H	CH ₃	9.3 ± 2.3
77	OCH ₃	H	OCH ₃	H	H	8.8 ± 1.1
78	OCH ₃	H	OCH ₃	H	CH ₃	1.9 ± 0.2
79	OCH ₃	H	H	OCH ₃	H	10.8 ± 1.5
80	OCH ₃	H	H	OCH ₃	CH ₃	4.1 ± 0.6
81	OCH ₃	OCH ₃	OCH ₃	H	CH ₃	7.0 ± 1.1
82	OCH ₃	H	OCH ₃	OCH ₃	H	6.0 ± 0.6
83	OCH ₃	OCH ₃	OCH ₃	OCH ₃	H	> 500
84	OCH ₃	OCH ₃	OCH ₃	OCH ₃	CH ₃	> 500

Casimiroin and its analogues bind deeply in the NQO2 enzyme active site through hydrophobic interactions between the quinoline ring and Trp¹⁰⁵, Gly⁶⁸, Phe¹²⁶, Phe¹⁷⁸ amino acids residues and the isoalloxazine ring of FAD.

These analogues are more potent than casimiroin in their NQO2 inhibition: replacement of methoxy group at position 4 by a methyl group increases the potency of analogues, e.g. compound **74** is 8 times more potent than casimiroin. *N*-Methylated analogues are more potent than non *N*-methylated analogues, e.g. compounds **78** and **80** are more active than compounds **77** and **79**. Di- and tri-methoxy analogues are more potent than casimiroin, but tetramethoxy analogues are inactive because of an increase in the steric bulk of these groups, which affects the co-planarity with the FAD isoalloxazine ring disfavoring π - π stacking with the benzene ring.

Chapter I. Introduction

3.1.8. Triazoloacridin-6-ones⁹⁶

NSC645827 **85** (Figure 30) is a triazoloacridin-6-one compound that was identified by Stratford and co-workers using virtual screening of the NCI databases to be a lead NQO1 inhibitor in the low micro-molar potency range.

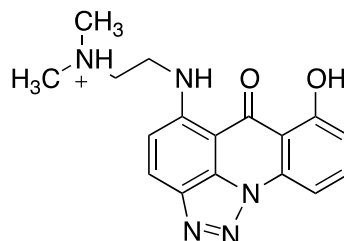
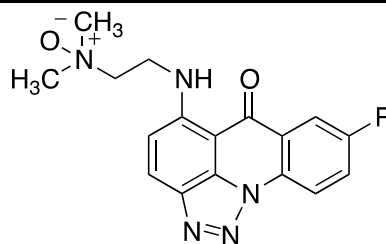


Figure 30. The structure of triazoloacridin-6-one NSC645827 (**85**).

Analogues of the lead **85** were synthesized and evaluated for their NQO1 and also NQO2 inhibition activity. This resulted in introducing three *N*-oxide derivatives (Table 6) that can specifically and potently inhibit NQO2 in the low 100 nM range.

Table 6. NQO2 inhibition data for *N*-oxide derivatives of triazoloacridin-6-one



Compound ID	R	IC ₅₀ (nM)
86	H	167 ± 42
87	Br	117 ± 29
88	OCH ₃	98 ± 10

3.1.9. Imidazoloacridin-6-ones

Series of the National Cancer Institute (NCI) compounds with imidazoloacridin-6-one scaffold were tested for their ability to inhibit the NQO2 enzyme by Stratford and co-workers. The imidazoloacridin-6-one NSC660841 **89** (Figure 31) was identified as a lead NQO2 inhibitor with an IC₅₀ of 6 nM.⁹⁷

Chapter I. Introduction

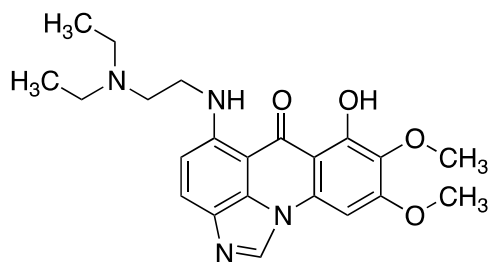
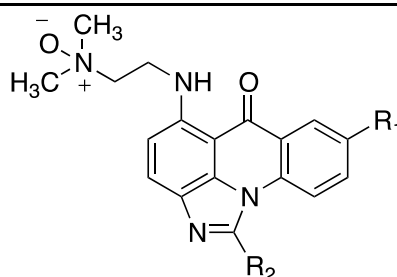


Figure 31. The structure of imidazoloacridin-6-one NSC660841 (**89**).

In order to develop potentially potent NQO2 inhibitors, analogues containing the imidazoloacridin-6-one scaffold were synthesized. An *N*-oxide moiety was introduced to many imidazoloacridin-6-ones to ensure their selectivity as NQO2 inhibitors without DNA binding effects (Table 7). The imidazoloacridin-6-ones with the *N*-oxide moiety proved to be potent inhibitors of the NQO2 enzyme in cells at non-toxic concentrations.⁹⁸

Table 7. NQO2 inhibition data for *N*-oxide derivatives of imidazoloacridin-6-one⁹⁸



Compound ID	R ₁	R ₂	IC ₅₀ (nM)
90	OCH ₃	H	14 ± 4
91	OH	H	42 ± 6
92	Br	CH ₃	47 ± 12
93	H	CH ₃	56 ± 10

3.1.10. Indolequinones⁹⁹

The compounds with the indolequinone scaffold **94** (Figure 32) can inhibit the NQO2 enzyme selectively. The observed selective inhibition of NQO2 is mechanism-based (suicide substrate) involving irreversible modification of the protein.

Chapter I. Introduction

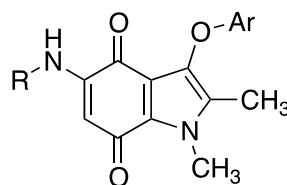


Figure 32. Indolequinone scaffold (**94**).

3.1.11. Quinoline and pyrroloquinoline ammosamide analogues¹⁰⁰

Ammosamide B **95** (Figure 33) is a natural product isolated from marine *Streptomyces* strain CNR-698. Ammosamide B potently inhibits NQO2 with an IC₅₀ value of 61.0 nM.

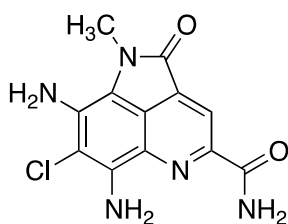


Figure 33. The structure of ammosamide B (**95**).

Several bicyclic **96** and tricyclic **97** analogues of ammosamide B (Figure 34) were synthesized to explore the structural requirements for NQO2 inhibitory activity.

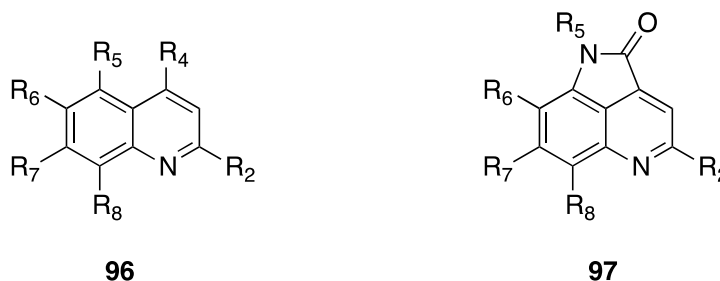


Figure 34. Bicyclic (**96**) and tricyclic (**97**) analogues of ammosamide B.

The IC₅₀ values for the synthesized compounds ranged from 4.1-25.2 μ M. The compounds that were structurally distinct from the scaffold of ammosamide B were not active as NQO2 inhibitors. The most potent compound was the *N*-methyl derivative at C-8 of ammosamide B **98** (Figure 35), with an IC₅₀ value of 4.1 nM.

Chapter I. Introduction

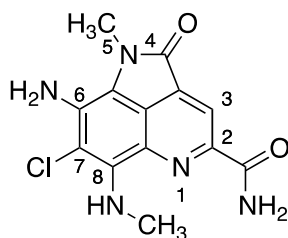


Figure 35. The structure of the most potent analogue of ammosamide B (**98**).

3.1.12. 9-Aminoacridine ⁸²

NSC13000 **99** (Figure 36) is a 9-aminoacridine compound that was identified by Stratford and co-workers using virtual screening of the NCI database to be a lead NQO2 inhibitor with an IC₅₀ of 420 nM.

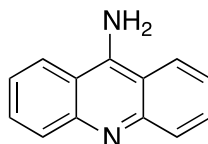


Figure 36. The structure of 9-aminoacridine (**99**).

3.1.13. Ellipticine ⁸²

Virtual screening of the NCI database by Stratford and co-workers, led to the discovery of ellipticine compounds as NQO2 inhibitors with an IC₅₀ range of 20-160 nM (Table 8).

Table 8. NQO2 inhibition data for ellipticine compounds

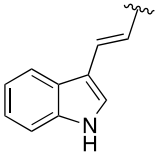
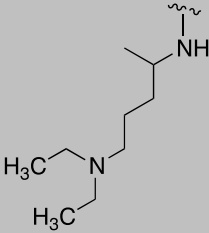
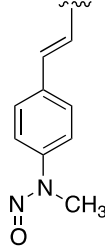
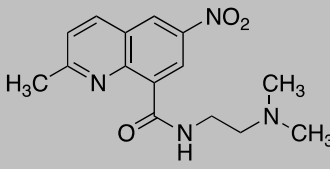
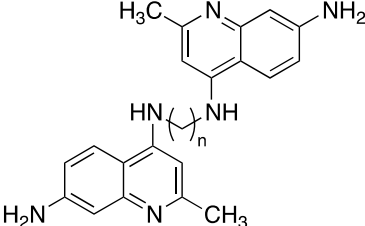
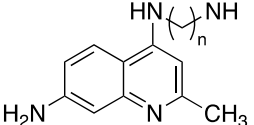
Compound ID	R	IC ₅₀ (nM)
NSC71795 (100)	H	50 ± 10
NSC164016 (101)	(CH ₂) ₂ NHCH ₂ C ₆ H ₅	20 ± 10
NSC322087 (102)	CH ₂ C ₆ H ₅	30 ± 0.0
NSC12547 (103)		160 ± 50

Chapter I. Introduction

3.1.14. Quinolines⁸²

Series of quinolines were found to inhibit NQO2 in the low nanomolar range. The virtual screening of the NCI database by Stratford and co-workers, led to the discovery of several quinoline compounds as NQO2 inhibitors with IC₅₀ values of 40-640 nM (Table 9).

Table 9. NQO2 inhibition data for quinoline compounds

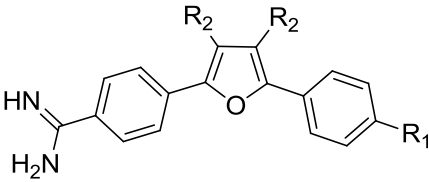
NSC No.	R ₁	R ₂	R ₃	IC ₅₀ (nM)
				
76750 (104)		H	H	500 ± 60
13484 (105)	Ph	OCH ₃		550 ± 50
101984 (106)	H	H		640 ± 50
617933 (107)				40 ± 10
273829 (108)				n = 7 250 ± 50
270904 (109)				n = 8 170 ± 90

Chapter I. Introduction

3.1.15. Furan-amidines⁸²

The virtual screening of the NCI database and NQO2 enzyme studies performed by Nolan and co-workers identified three compounds with furan-amidine scaffold as lead NQO2 inhibitors (Table 10). The scaffold of furan-amidines can be classified into symmetric (compounds **111** and **112**) or asymmetric (compound **110**).

Table 10. Furan-amidine lead compounds as inhibitors of NQO2⁸²



	R ₁	R ₂	NQO2 Inhibition IC ₅₀ (nM)
NSC17602 (110)	H	H	140 ± 40
NSC305831 (111)	C(=NH)NH ₂	H	630 ± 70
NSC305836 (112)	C(=NH)NH ₂	CH ₃	50 ± 10

3.1.16. Mode of binding of the NQO2 inhibitors in the active site

The binding of the inhibitors in the active site of the NQO2 protein was studied. The inhibitors of the NQO2 enzyme exhibit a flat conformation in order to fit inside the narrow cavity of the active site.^{41, 55} They bind deeply inside the active site cavity coplanar with the isoalloxazine ring of the FAD molecule.^{55-56, 96-97} FAD is involved in the enzyme reduction activity.⁵⁰ The co-planarity of the inhibitors with the isoalloxazine ring of FAD is essential for their action.^{41, 55-56} Any structural modification which disfavors this position will lead to inactive compounds, e.g. tetramethoxy analogues of casimiroin are inactive compared to mono-, di-, and tri-methoxy analogues because of the steric bulk of the fourth methoxy groups that disturbs the co-planarity.⁵⁶

The occupancy of the active site area is different among the known NQO2 inhibitors. Small inhibitors such as, casimiroin **73** (Figure 37) and its analogues occupy two thirds of the active site area.⁵⁶ Larger inhibitors such as flavones, resveratrol **60**⁵⁵ (Figure 38), triazoloacridin-6-ones,⁹⁶ and imidazoloacridin-6-ones⁹⁷ occupy the whole

Chapter I. Introduction

area of the active site. All the inhibitors maintain their co-planar situation with the FAD molecule through hydrophobic interactions with the isoalloxazine ring of the FAD molecule and the side chains of the amino acid residues lining the inner surface of the cavity. The hydrophobic interaction between the enzyme and the inhibitors is very important because of the highly hydrophobic nature of the active site cavity.⁵⁴ In addition, the inhibitors form hydrogen bonds with hydrophilic amino acids at the sides of the cavity either directly or through water bridges.⁹²

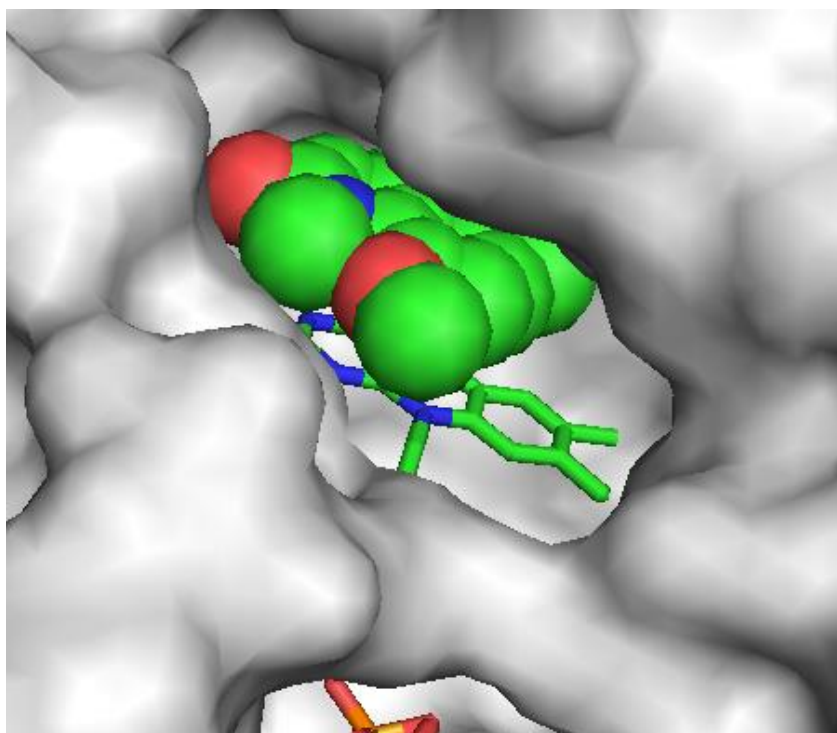


Figure 37. Casimiroin (73) occupies two thirds of the active site area of NQO2 (PDB code 3GAM; Resolution at 1.98 Å).⁵⁶

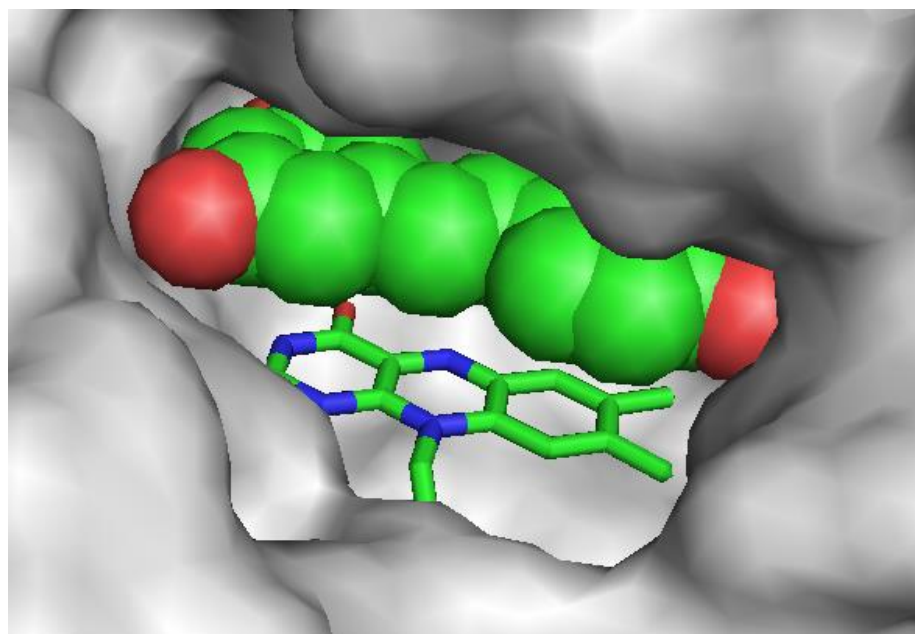


Figure 38. Resveratrol (**60**) occupies the whole area of the active site area of NQO2 (PDB code 1SG0; Resolution at 1.50 Å).⁵⁵

4. Amidine functional group

Amidine is a binitrogen analogue of the carboxylic acid and ester groups (Figure 39). The amino nitrogen free electrons are in conjugation with the π -electrons of the imine (C=N) double bond. The bonds between the central carbon and the two nitrogen atoms have partial double bond properties because of resonance. Amidine combines the properties of azomethine-like C=N double bond and amide-like C-N single bond.¹⁰¹

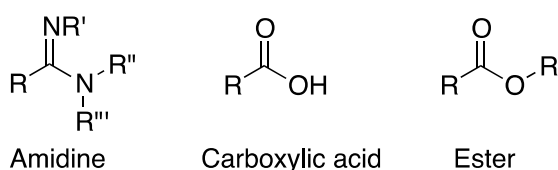


Figure 39. Amidine and its carbonyl analogues.

Amidine is an organo-superbase with pK_a range 5.0-12.0. The basicity of the amidine depends on the extent and type of substitution at the imino and amino nitrogen atoms and the central carbon atom. The protonation occurs at the imino nitrogen atom, so the substitution at this nitrogen atom has the largest influence on the pK_a value of amidines followed by substitution at the functional carbon atom.¹⁰²

Amidine is more basic than the amine functional group and less basic than guanidine. The pK_a values of methylamine, acetamidine and guanidine are 10.6, 12.4

Chapter I. Introduction

and 13.6, respectively. The high basicity of amidine and guanidine is due to the formation of a highly effective conjugation system after the protonation (Figure 40).¹⁰²

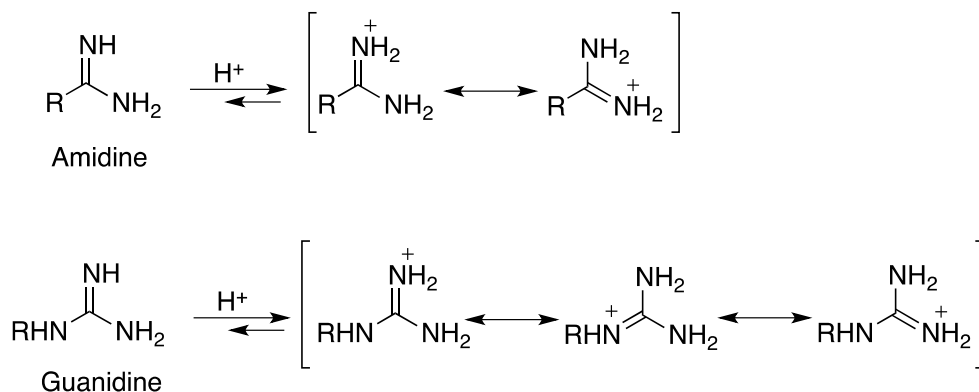
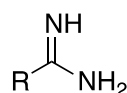


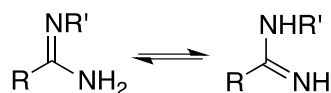
Figure 40. The protonation states of amidine and guanidine.

Amidines can be classified into five general types depending on the number and the distribution of the substituents on the amino- and imino-nitrogen atoms.¹⁰³ These types are:

1. Unsubstituted



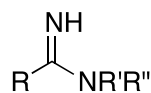
2. Mono-substituted



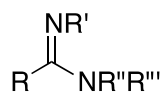
3. Symmetric di-substituted



4. Asymmetric di-substituted



5. Tri-substituted



4.1. Amidine-containing pharmacologically active molecules

The amidine group is present in different pharmacologically active molecules. Some examples are given in the following sections.

Chapter I. Introduction

4.1.1. Fibrinogen antagonists¹⁰⁴

The peptidomimetic low molecular weight fibrinogen antagonists named, as Ro 43-5054 **113** and Ro 44-9883 **114** are amidine compounds (Figure 41). These two amidine compounds inhibit the binding of fibrinogen to glycoprotein IIb-IIIa leading to the prevention of platelet aggregation. *p*-Amidino-compounds **113** and **114** are potent fibrinogen antagonists with IC₅₀ values of 60 and 30 nM, respectively.

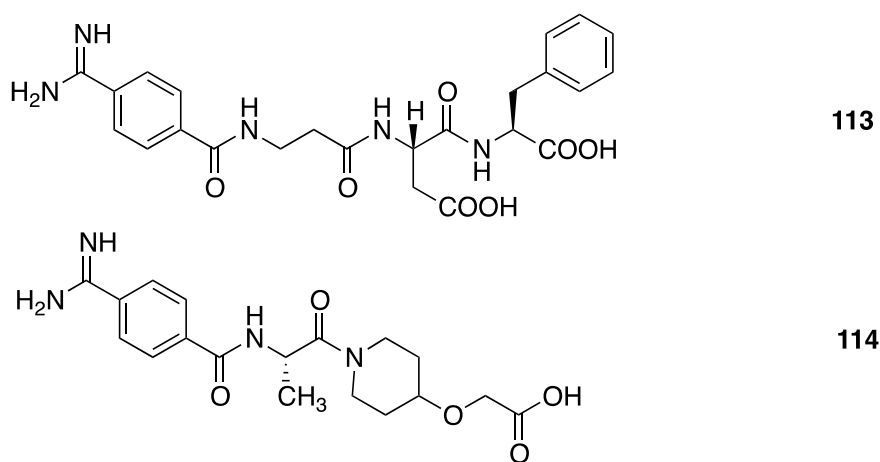


Figure 41. Structures of amidine fibrinogen antagonists, Ro 43-5054 (**113**) and Ro 44-9883 (**114**).

4.1.2. Anticoagulant drugs¹⁰⁵

Dibasic (amidinoaryl)propionic acid derivatives are identified as lead anticoagulant compounds. These low molecular weight, non-peptidic and orally active inhibitors are potent and selective inhibitors of factor Xa. The best inhibitor is DX-90659 **115** (Figure 42), which can inhibit factor Xa with an IC₅₀ value of 70 nM.

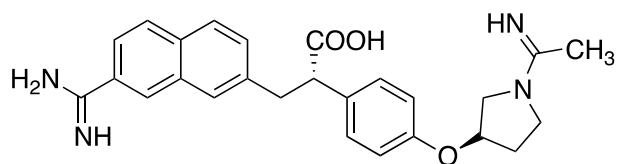


Figure 42. The structure of factor Xa inhibitor, DX-90659 (**115**).

5. Aim and objectives of the research

The overall objective of this research is the optimization of the furan-amidino leads (see section 3.1.15 and Table 10) as novel selective NQO2 inhibitors with no off-target effect, for example DNA intercalation. The research involves the design and synthesis of a series of asymmetric furan-amidino and analogues with potential NQO2 inhibition and good drug-like properties.

Chapter I. Introduction

To ensure selectivity of the designed compounds for NQO2, the focus will be on the design of asymmetric furan-amidines and their analogues. To ensure desirable pharmacokinetic properties of the designed inhibitors, the amidine group will be replaced with isosterically similar groups.

Symmetric and asymmetric furan-amidines possess different distribution properties inside the cell, which depends on the number of the positive charges on the compounds. The high basicity of the amidine group leads to its total protonation at physiological pH.¹⁰¹ The symmetric furan-amidines with two amidine groups, distribute inside the nucleus and bind to DNA.¹⁰⁶ In contrast, the asymmetric furan-amidines with one amidine group distributes in the cytoplasm, into mitochondria, without nuclear accumulation.^{106a}

Chapter II. Results and Discussion/ Chemistry

1. Introduction

The synthesis of the lead furan-amidines **110** and **111**, identified as inhibitors of NQO2 from the published virtual screening of the NCI database by Nolan and coworkers,⁸² was the first objective in this research. The synthesis of these known compounds was required to complete their further biological evaluation; however it also allowed method development of a new synthetic pathway to prepare a range of symmetric and asymmetric furan-amidines and their analogues.

The effect of the isosteric replacements of the furan ring in **110** on NQO2 inhibition activity and water solubility was studied. The furan ring was replaced with a wide range of 5-membered heterocycles such as pyrrole, *N*-methylpyrrole, thiophene, imidazole, *N*-methylimidazole and oxazole.

All of the synthesized furan-amidines and their analogues have the highly basic amidine groups. These aryl amidine groups are known to give a low oral bio-availability, which can be explained by their high ionization at physiological pH. The reported pK_a of benzamidine is 11.89 ± 0.50 ,¹⁰¹ which makes this compound totally ionized at pH 7.4. The isosteric replacements of the amidine group by less basic imidate (iminoether) (pK_a = 6.2)¹⁰⁷, *N*-aryl amide (neutral), *N*-aryl amidine (reversed amidine, pK_a = 9.64 ± 0.50) and amidoxime (*N*-hydroxy amidine, pK_a = 6.53 ± 0.69) groups were completed to study the effect of these changes firstly on NQO2 inhibition ability. These less basic analogues, having more of the neutral form at physiological pH, may enhance the oral bio-availability of the NQO2 inhibitors.

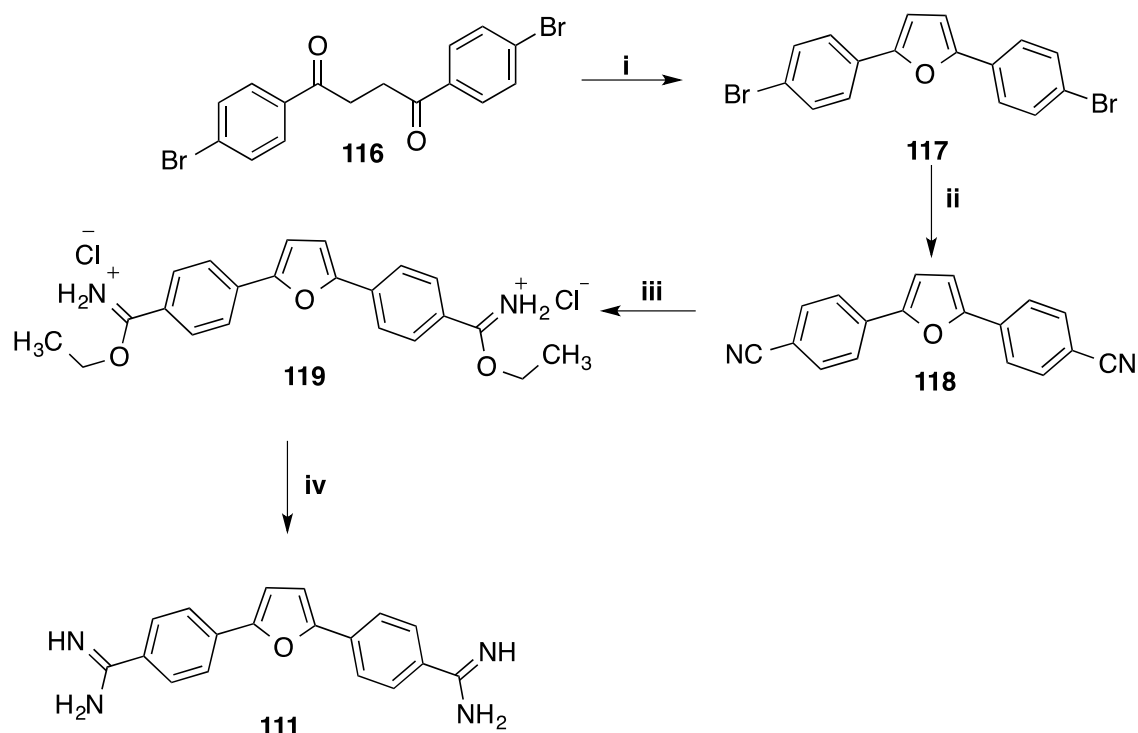
The details of the synthetic routes of all of the targeted compounds are discussed in the following sections.

2. Synthesis of the furan-amidine scaffold

The literature synthetic pathway for the preparation of the furan-amidines, specifically the symmetric furan-amidines, requires the initial preparation of the symmetric 1,4-diketone 4-bromo substituents **116** (Scheme 8).¹⁰⁸ The bromine atoms in the 1,4-diketone **116** are substituted later by nitrile groups using a cyanide-containing reagent, such as copper (I) cyanide. This substitution step is usually done after the cyclization of the 1,4-diketones **116** into furan **117**. The nitrile groups in compound **118** are the precursors for amidine groups. The conversion of the nitrile groups **118** into amidines **111** is typically completed through the preparation of an imidate hydrochloride (iminoether) intermediate **119**. The reaction between imidate

Chapter II. Results and Discussion/ Chemistry

hydrochloride intermediate with ammonia gas results in the formation of amidine group **111**.



Scheme 8. Synthetic pathway for symmetric furan-amidine **111**; Reagents and conditions: i- H₂SO₄, Ac₂O, reflux; ii- CuCN, quinolone, reflux; iii- EtOH, HCl (g), CHCl₃, 0 °C - rt; iv- NH₃ (g), CHCl₃, rt.

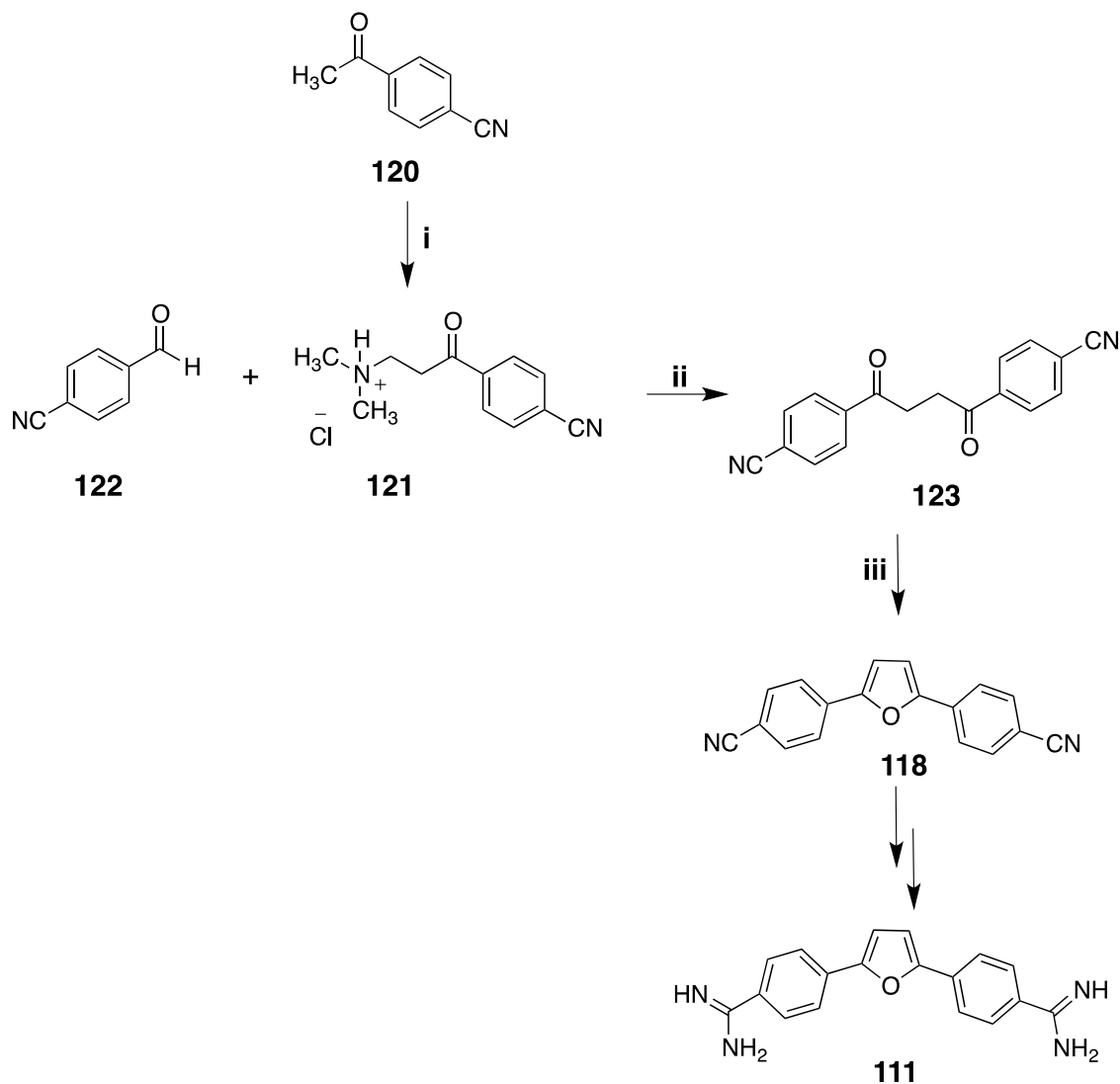
The limitations for the use of this synthetic pathway for the synthesis of the symmetric furan-amidines generally and asymmetric furan-amidines specifically are:

1. The use of a highly toxic cyanide reagent to substitute the bromine in step ii. Upon the acidic work-up of this step, the highly toxic hydrogen cyanide gas is formed, therefore, this reagent will not be used unless absolutely necessary.
2. The use of a large volume of dry hydrogen chloride gas to saturate the reaction in step iii. The traditional method of generating hydrogen chloride gas is done by the reaction between concentrated sulfuric acid and sodium chloride salt.¹⁰⁹ The disposal of large quantities of concentrated sulfuric acid is not preferable. The alternative use of hydrogen chloride gas cylinders may be an issue because of the highly corrosive properties of hydrogen chloride gas.
3. The use of ammonia gas.

These limitations led to the search for a safer and simpler synthetic pathway for the synthesis of the furan-amidines. An alternative multi-step synthetic pathway for the

Chapter II. Results and Discussion/ Chemistry

synthesis of the furan-amidines was proposed. This pathway depends on the approach described by Suthiwangcharoen and Stephens¹¹⁰ (Scheme 9), which starts from reagents already possessing the aryl nitrile groups. The aryl nitrile groups in the starting materials serve as precursors for the aryl amidine groups later.

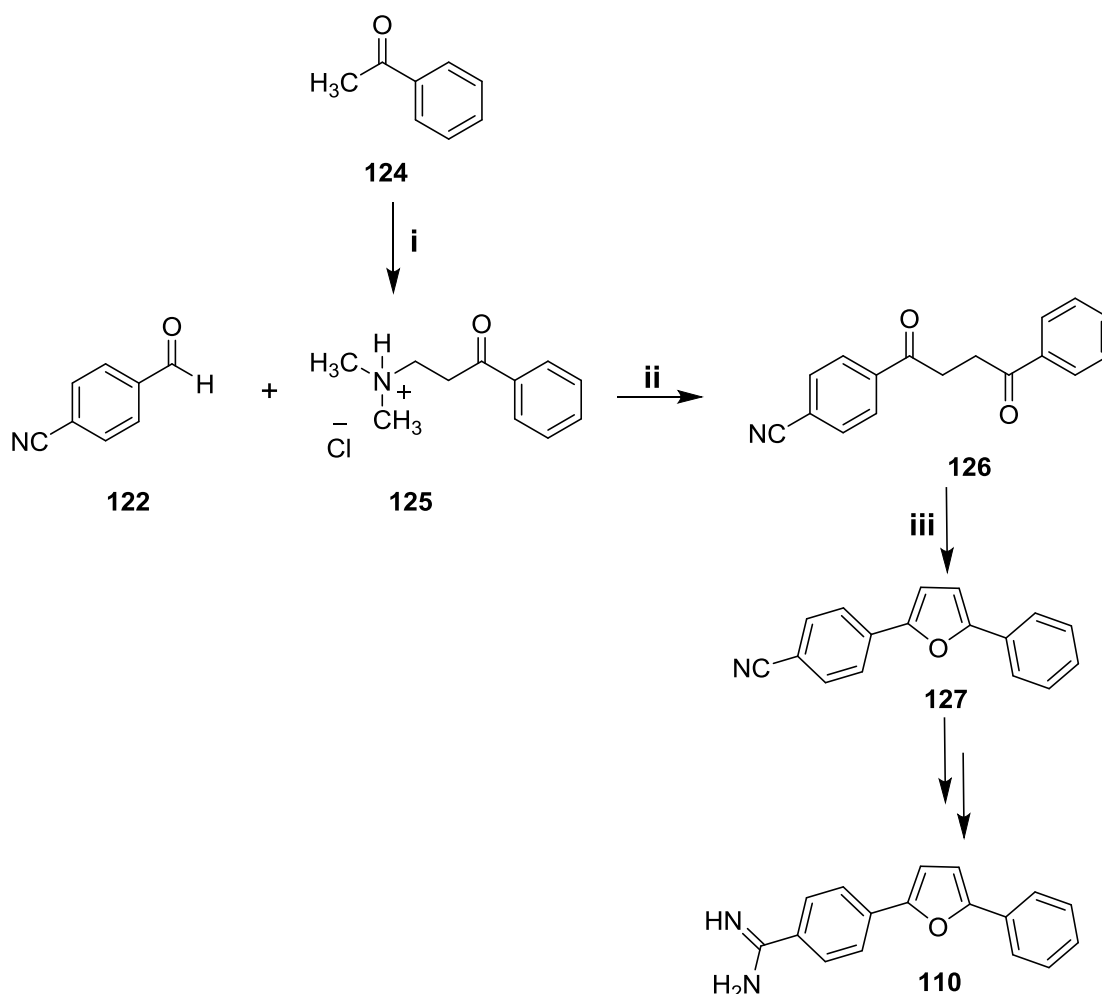


Scheme 9. Proposed synthetic pathway for symmetric furan-amidine **111**; Reagents and conditions: i- Paraformaldehyde, $\text{HN}(\text{CH}_3)_2 \cdot \text{HCl}$, EtOH, reflux; ii- 5-(2-Hydroxyethyl)-3,4-dimethyl-1,3-thiazolium iodide **128**, NEt_3 , dry THF, reflux.; iii- H_2SO_4 , Ac_2O , reflux.

The proposed alternative synthetic pathway was applied for the synthesis of the asymmetric furan-amidine **110**. The multi-step synthetic pathway was optimized and used later to synthesize the symmetric furan-amidine **111**.

3. Synthesis of asymmetric furan-amidine scaffold: Synthetic pathway optimization

The asymmetric furan-amidine **110** was synthesized using a modified approach to the one described by Suthiwangcharoen and Stephens.¹¹⁰ The 1,4-diketone **126** was first synthesised through the coupling between Mannich base **125** and 4-formylbenzonitrile **122** under Stetter reaction conditions (Scheme 10). Mannich base **125** was firstly prepared from the reaction between acetophenone **124**, paraformaldehyde and dimethylamine hydrochloride under anhydrous acidic conditions. Each step in the synthesis of the asymmetric furan-amidine **110** was discussed in detail in the following sections.

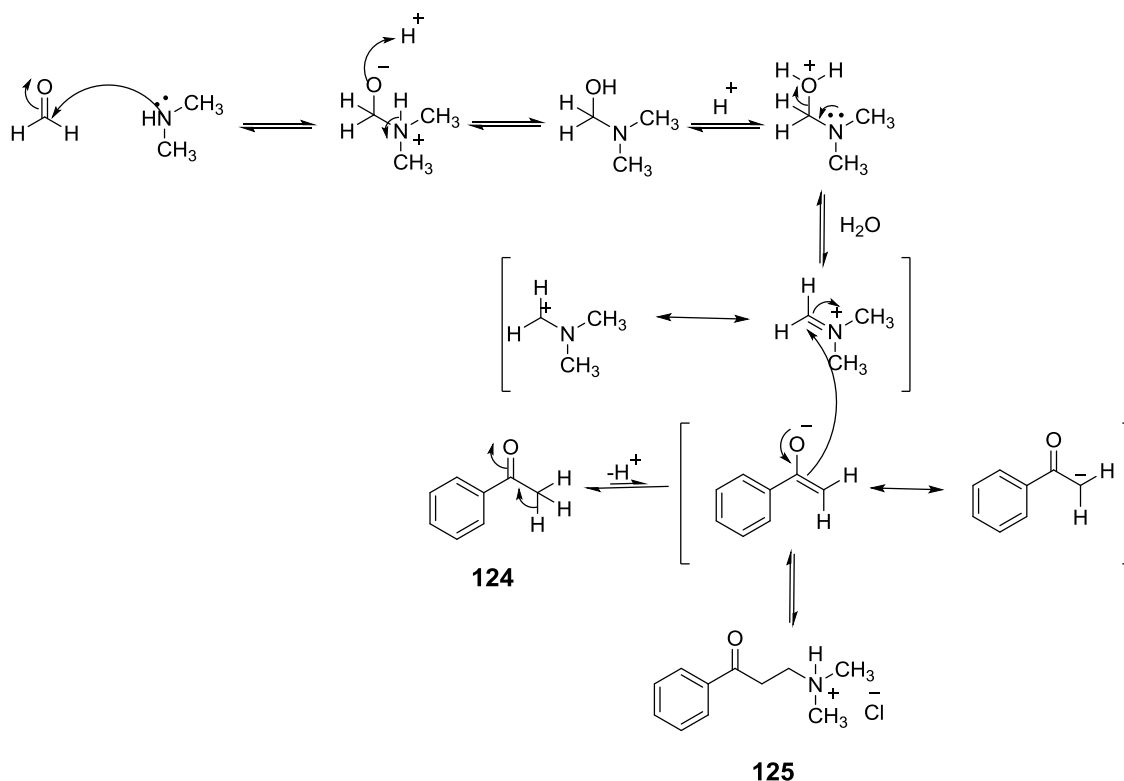


Scheme 10. Proposed synthetic pathway for the asymmetric furan-amidine **110**; Reagents and conditions: i- Paraformaldehyde, $\text{NH}(\text{CH}_3)_2 \cdot \text{HCl}$, EtOH, reflux; ii- 5-(2-Hydroxyethyl)-3,4-dimethyl-1,3-thiazolium iodide **128**, NEt_3 , dry THF, reflux; iii- H_2SO_4 , Ac_2O , reflux.

Chapter II. Results and Discussion/ Chemistry

3.1. Mannich base reaction

The Mannich base reaction is an equilibrium reaction, which starts by the formation of Schiff base from the reaction of paraformaldehyde and dimethylamine hydrochloride under acidic conditions. The resulting imine reacts as an electrophile, which is attacked by the enolate form of the methyl aryl ketone (Scheme 11). The best molar ratio to be used for the Mannich base reaction is 1 methyl aryl ketone: 1.5 paraformaldehyde: 1.5 dimethylamine hydrochloride.



Scheme 11. The mechanism of the preparation of Mannich base 125.

3.2. Aryl 1,4-diketones synthesis

Aryl 1,4-diketones or γ -diketones are useful intermediates used in the preparation of 5-membered heterocyclic rings such as furan, pyrrole and thiophene. Aryl 1,4-diketones are synthesized by carbon-carbon coupling between two carbonyl compounds. Aryl 1,4-diketones can be classified as symmetric and asymmetric depending on the starting carbonyl compounds used in their synthesis.

The synthesis of the asymmetric 1,4-diketones is challenging when compared to the synthesis of the symmetric 1,4-diketones. This is attributed to the cross reactions between the two different starting carbonyl compounds, which can lead to the formation of different products.

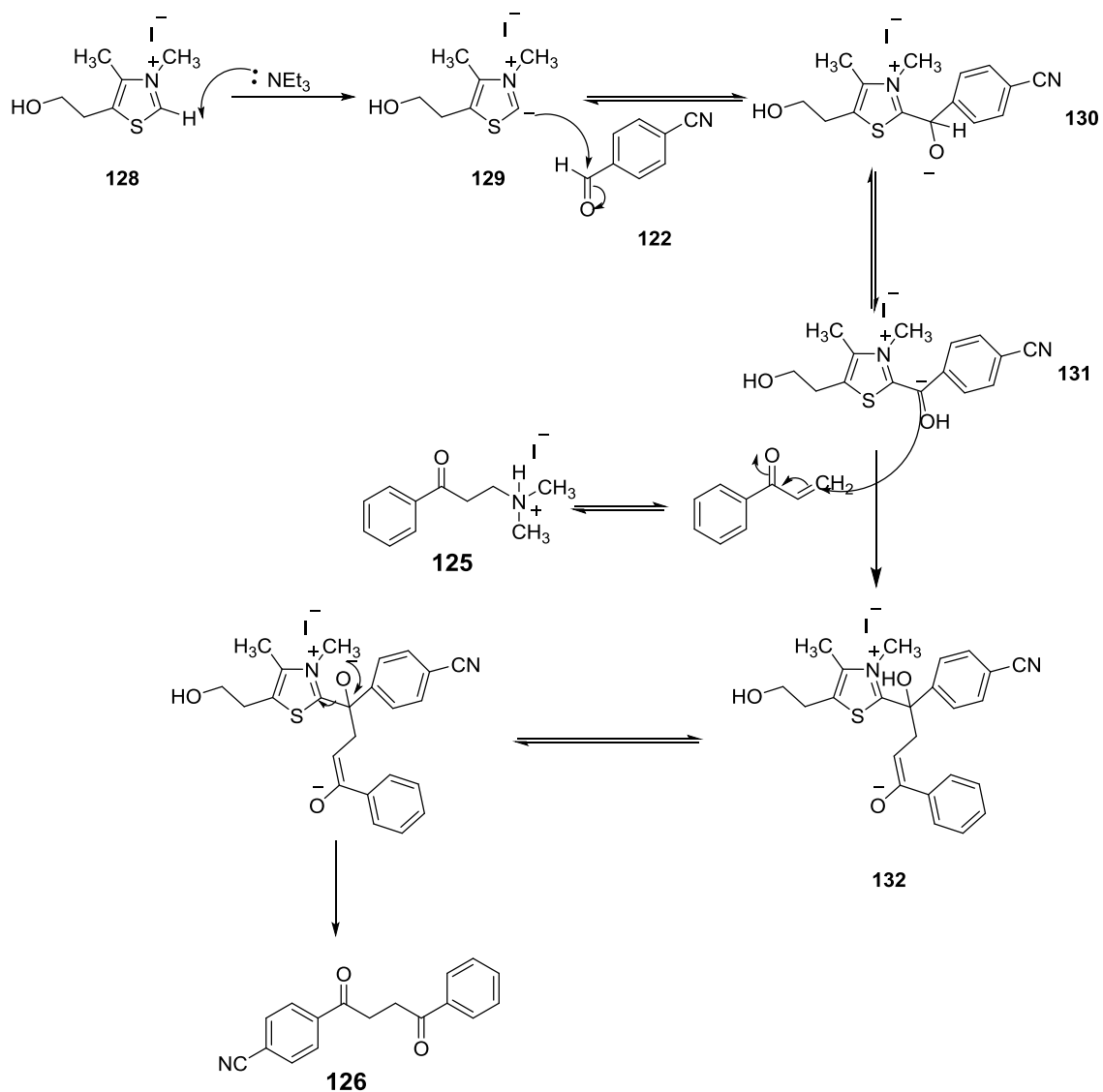
Chapter II. Results and Discussion/ Chemistry

Two synthetic pathways were used to synthesize the 1,4-diketone **126**, the key intermediate in the synthesis of the targeted asymmetric furan-amidine **110**. The first synthetic pathway used was the Stetter reaction, which implies the coupling between Mannich base **125** and 4-formylbenzotrile **122**. The Stetter Reaction is a 1,4-addition (conjugate addition) of an aldehyde to an α,β -unsaturated compound, catalyzed by cyanide or a thiazolium salt. This reaction competes with the corresponding 1,2-addition, which is known as the benzoin condensation. The benzoin-condensation is a reversible reaction, but the Stetter reaction leads to more stable products.¹¹¹ The main product derived from this reaction is the 1,4-diketone **126**.

The key step in the reaction mechanism is the conversion of the aldehyde carbonyl group from an electrophile to a nucleophile in an umpolung process (Scheme 12) through the use of 5-(2-hydroxyethyl)-3,4-dimethyl-1,3-thiazolium iodide **128** as a catalyst. Catalyst **128** for the Stetter reaction needed to be synthesized which is detailed in section 3.2.1.

The reaction is initiated by the activation of the quaternary thiazolium iodide **128** into ylide **129** through the deprotonation of the aryl hydrogen by triethylamine. Then, the nucleophilic ylide **129** attacks the carbonyl group in 4-cyanobenzaldehyde **122** forming the tetrahedral intermediate **130**. The 1,2-rearrangement of the methylene proton in **130** results in the formation of the carbanion **131**. The carbanion **131** reacts with the enone derived from the Mannich bases **125** forming the adduct **132**. Finally, the thiazolium compound **128** is expelled generating the 1,4-diketone **126** and completing the catalytic cycle (Scheme 12).¹¹¹

The Stetter reaction must be carried out in an aprotic solvent and under anhydrous conditions. The best solvent to get a good yield from this heterogeneous reaction is 1,2-dimethoxyethane. Dry DMF, toluene and THF were tried as alternatives to this solvent because of the high toxicity of 1,2-dimethoxyethane on fertility. Dry THF was the best solvent used to prepare the 1,4-diketone **126**.



Scheme 12. The mechanism of the Stetter reaction in the synthesis of the 1,4-diketone **126**.

The nitrile groups in the 1,4-diketone **126** serve as precursors for the amidine groups. In this synthetic pathway the nitrile group has not been affected by the reaction conditions. In the infrared spectrum, the stretching frequency of the nitrile group in **126** appeared as a strong peak at 2229.3 cm^{-1} (Figure 43).

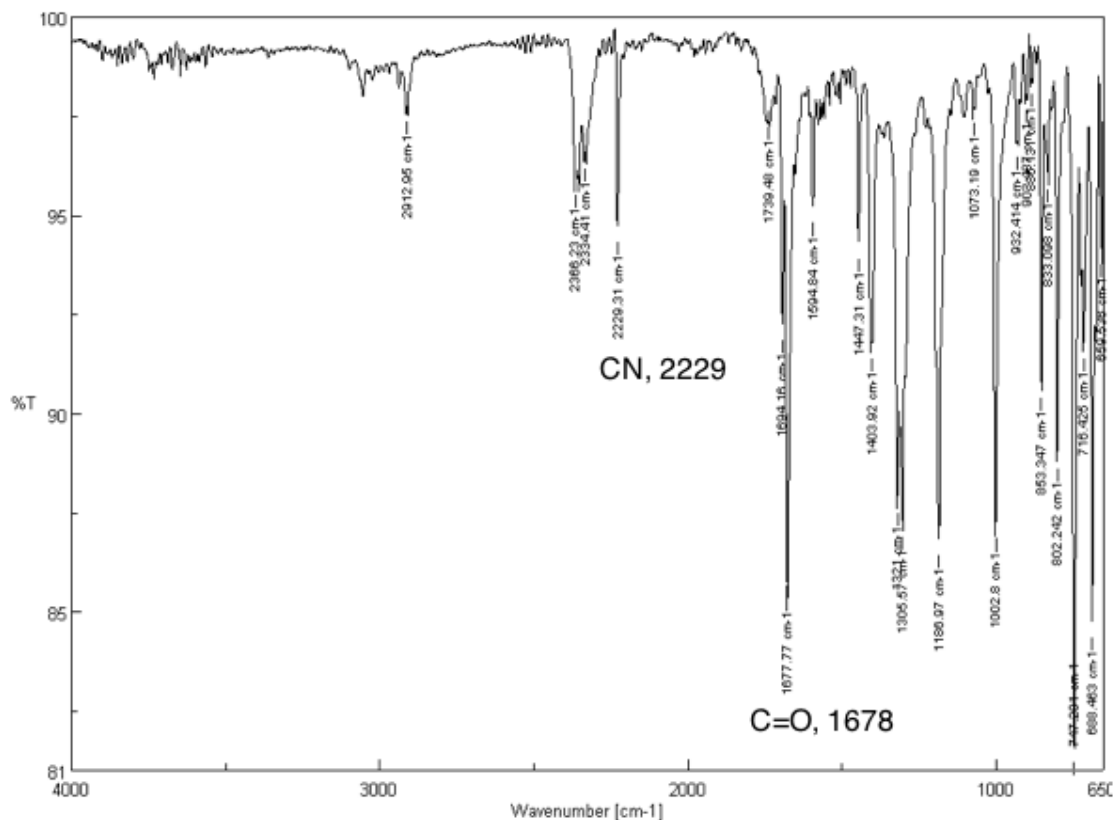


Figure 43. The infrared spectrum of the 1,4-diketone **126**.

The use of the Stetter reaction as the main synthetic pathway in the preparation of the 1,4-diketones **126** had some limitations:

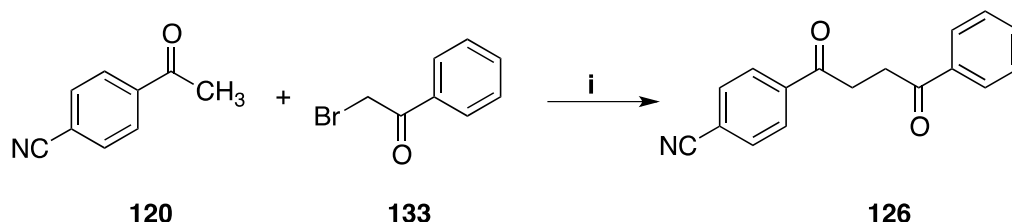
1. The long reaction time of the Stetter reaction under reflux, which is 24-72 hr.
2. The difficult purification of the 1,4-diketones from the Stetter heterogeneous reaction mixture.
3. The poor yield of the 1,4-diketone **126**, which was 36%.

The 1,4-diketone **126** was used as a model compound to optimize the conditions needed to synthesize the targeted 1,4-diketone intermediates. The ease in the synthesis of the 1,4-diketones together with a good yield are essential issues to be considered in choosing general synthetic pathway to be applied for the preparation of different 1,4-diketones with different substituents. Also, the symmetrical 1,4-diketone **123** was synthesized using the Stetter reaction in a yield of only 20%.

The new synthetic pathway to synthesize the 1,4-diketone **126** was proposed adapting the method described by Nevar and co-workers.¹¹² This synthetic pathway requires the coupling between methyl aryl ketone and α -bromomethyl aryl ketones using zinc chloride, triethylamine and t-butanol as a condensation reagent (Scheme 13).

Chapter II. Results and Discussion/ Chemistry

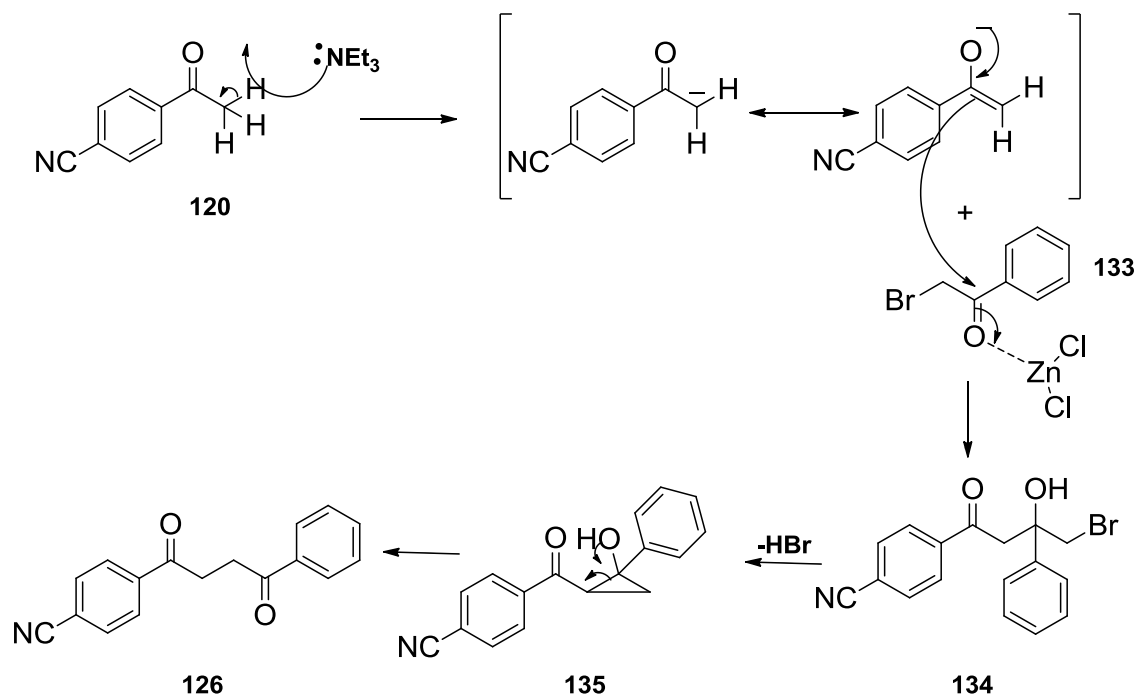
Ethanol was used as an alternative to *tert*-butanol because of the lower boiling point of ethanol compared to *tert*-butanol and its easier evaporation during the work-up step. The 1,4-diketone **126** was prepared using this synthetic pathway by the coupling between the methyl aryl ketone **120** and the α -bromomethyl aryl ketone **133** (Scheme 13).



Scheme 13. Synthesis of 1-(4-cyanophenyl)-4-phenyl-1,4-butanedione **126** through the coupling between methyl aryl ketone **120** and α -bromomethyl aryl ketone **133**;

Reagents and conditions: i- ZnCl_2 , NEt_3 , EtOH, dry toluene, rt.

In general, the methyl aryl ketone reacts as a nucleophile and α -bromomethyl aryl ketone reacts as an electrophile (Scheme 14). The aldol condensation between the enolate form of the methyl aryl ketone **120** and the α -bromomethyl aryl ketone **133** leads to the formation of the 4-bromo-3-hydroxyketone intermediate **134**. The intermediate **134** subsequently rearranges to a 1,4-diketone through the formation of activated cyclopropane intermediate **135**.¹¹²



Scheme 14. The mechanism of the synthesis of 1-(4-cyanophenyl)-4-phenyl-1,4-butadione by the coupling between methyl aryl ketone **120** and α -bromomethyl aryl ketone **133**.

The formation of unsymmetrical 1-(4-cyanophenyl)-4-phenyl-1,4-butadione **126** using the two synthetic pathways detailed above was confirmed by the use of ^1H NMR spectroscopy. In the ^1H NMR spectrum, the chemical shift of the $\text{COCH}_2\text{CH}_2\text{CO}$ protons (H-2 and H-3 protons) were observed as two triplets merged to form a multiplet in the region between 3.42 ppm to 3.52 ppm with an integration of 4 protons (Figure 44).

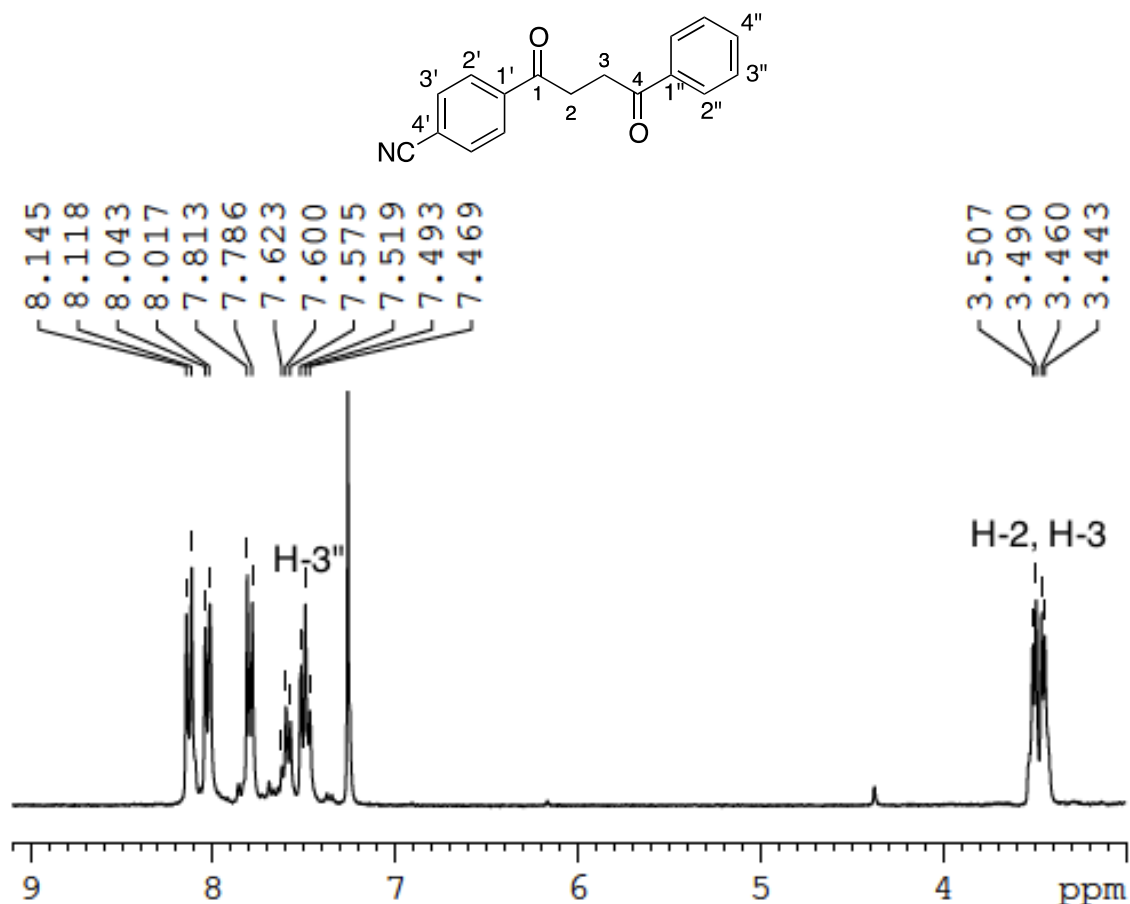
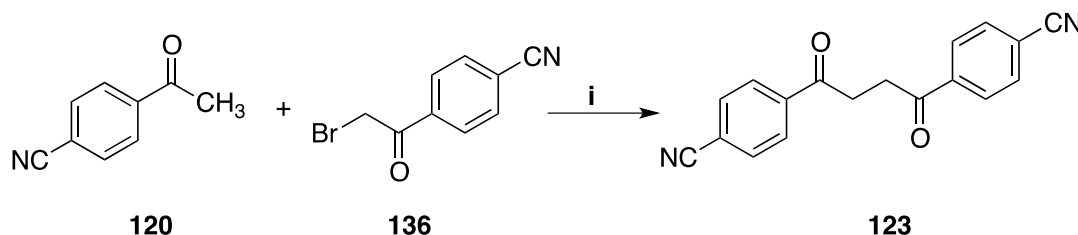


Figure 44. ¹H NMR (CDCl₃) spectrum of 1-(4-cyanophenyl)-4-phenyl-1,4-butanedione **126**.

Also, the symmetric 1,4-diketone **123** was synthesized through the coupling between the methyl aryl ketone **120** and the α -bromomethyl aryl ketone **136** (Scheme 15).



Scheme 15. The synthetic pathway for the symmetric 1,4-diketone **123** through the coupling between methyl aryl ketone **120** and α -bromomethyl aryl ketone **136**;

Reagents and conditions: *i*- ZnCl₂, NEt₃, EtOH, dry toluene, rt.

Table 11 shows the differences between the two synthetic pathways used in the preparation of 1,4-diketones **123** and **126**.

Chapter II. Results and Discussion/ Chemistry

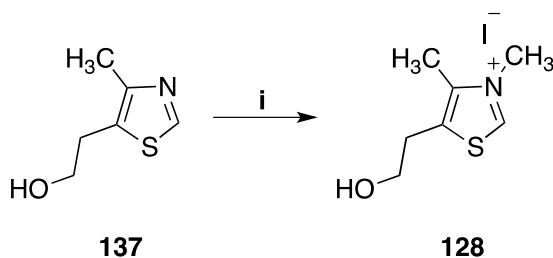
Table 11. The differences between the two synthetic pathways used for the preparation of the 1,4-diketones **123** and **126**

	Stetter reaction	Methyl aryl ketone and the α -bromomethyl aryl ketones coupling
Reaction conditions	Reflux	Room temperature
Reaction time	2-3 days	3-4 days
1,4-diketones purification	Column chromatography	Crystallization
%Yield of 123	20	61
%Yield of 126	36	39

Considering these results, the coupling between the methyl aryl ketones and α -bromomethyl aryl ketones was used as the main route for the synthesis of other 1,4-diketones intermediates, required to prepare the target heterocyclic compounds.

3.2.1. Synthesis of 5-(2-hydroxyethyl)-3,4-dimethyl-1,3-thiazolium iodide catalyst **128**

Thiazolium catalyst **128** was synthesized by heating the compound **137** at reflux with iodomethane under anhydrous conditions (Scheme 16). The structure of the thiazolium catalyst **128** was confirmed by ^1H (Figure 45), ^{13}C and DEPT135 NMR and IR spectroscopy. The purity of the catalyst **128** was confirmed using thin layer chromatography (TLC). The catalyst was used in the Stetter reaction step (as detailed in section 3.2.) without any further purification.



Scheme 16. Route for the synthesis of the thiazolium catalyst **128**; Reagents and conditions: i- CH_3I , dry CH_3CN , reflux.

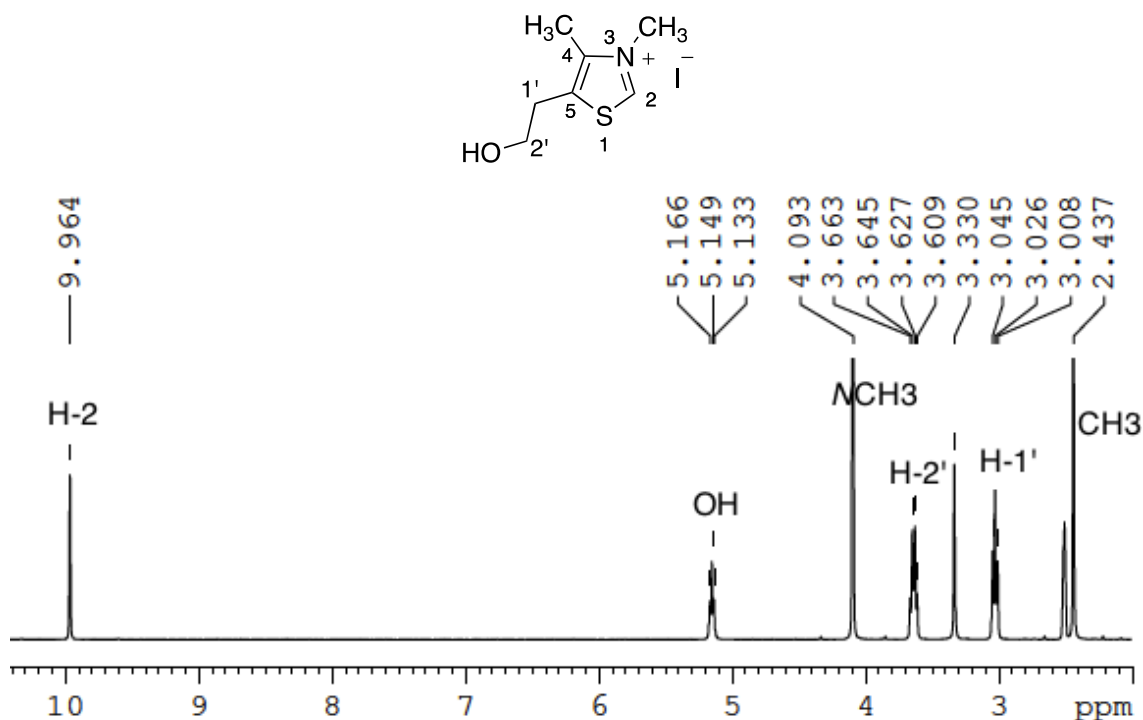
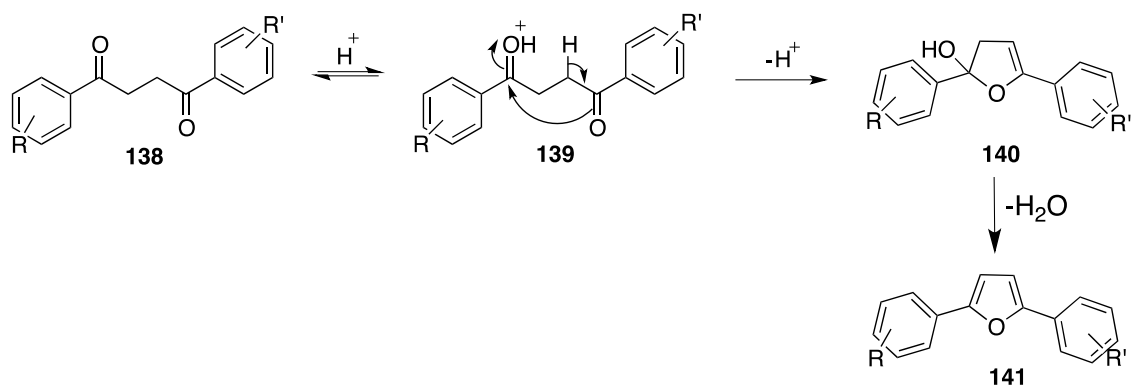


Figure 45. ¹H NMR (DMSO-d₆) spectrum of 5-(2-hydroxyethyl)-3,4-dimethyl-1,3-thiazolium iodide **128**.

3.3. 2,5-Diarylfuran synthesis

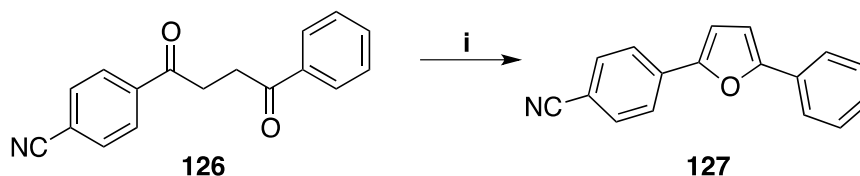
Substituted 2,5-diarylfurans are aromatic compounds synthesized starting from 1,4-dicarbonyl compounds, such as 1,4-diketones. The 1,4-diketones are cyclized into a furan ring in the presence of acid. The acid-catalyzed cyclization of 1,4-diketones into furans is known as the Paal-Knorr furan synthesis (Scheme 17).¹¹³ The first step in the reaction is the rapid and reversible protonation of one of the carbonyls **138** forming the positively charged intermediate **139**. Intermediate **139** undergoes a concerted enolization and ring closure to give **140**, which is the slowest step in the reaction. The dehydration of **140** leads to the formation of 2,5-diarylfuran **141**. The dehydration step is rapid and irreversible due to the aromatization.¹¹³

Chapter II. Results and Discussion/ Chemistry



Scheme 17. Mechanism of Paal-Knorr furan synthesis.

The acid-catalyzed cyclization of 1,4-diketone **126** to give the 2,5-diarylfuran **127** was accomplished using two synthetic pathways. The first synthetic pathway requires the heating of the 1,4-diketone **126** in acetic anhydride in the presence of few drops of sulfuric acid (Scheme 18).¹¹³



Scheme 18. Synthetic pathway to give 4,4'-(furan-2,5-diyl)benzonitrile **127**; Reagents and conditions: i- Ac_2O , H_2SO_4 , reflux.

Using this synthetic pathway 4-(5-phenylfuran-2-yl)benzonitrile **127** was obtained in a high yield of 78.0%. The formation of **127** was confirmed by 1H NMR spectroscopy. The formation of the furan ring was confirmed by 1H NMR spectroscopy as the furan protons H-3' and H-4' were observed as doublets at 6.81 ppm (J 3.6 Hz) and 6.93 ppm (J 3.3 Hz). The phenyl protons H-2'', H-3'' and H-4'' were observed as a doublet at 7.78 ppm (J 7.2 Hz), a triplet at 7.45 ppm (J 7.8 Hz) and a triplet at 7.34 ppm (J 7.5 Hz), respectively. The phenyl protons H-2 and H-3 were observed as doublets at 7.70 ppm (J 8.4 Hz) and at 7.83 ppm (J 8.4 Hz) (Figure 46).

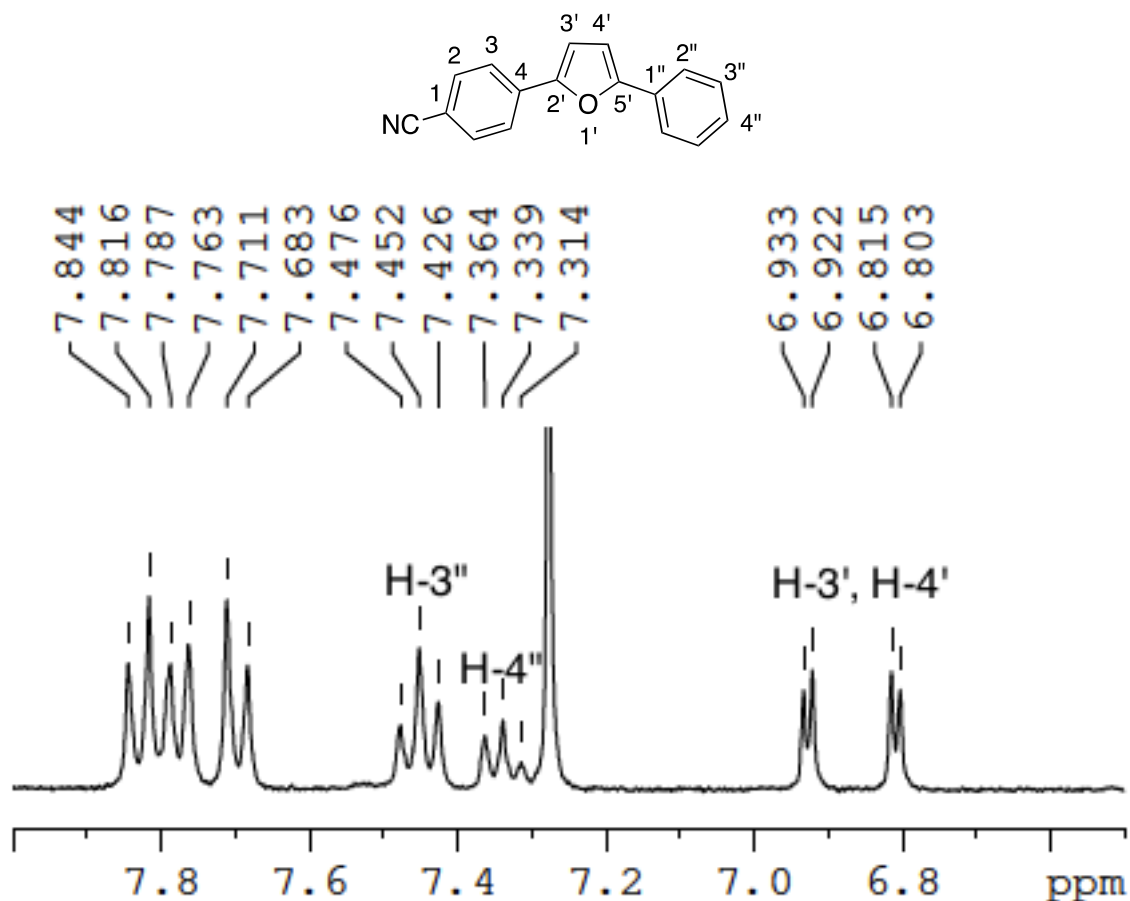
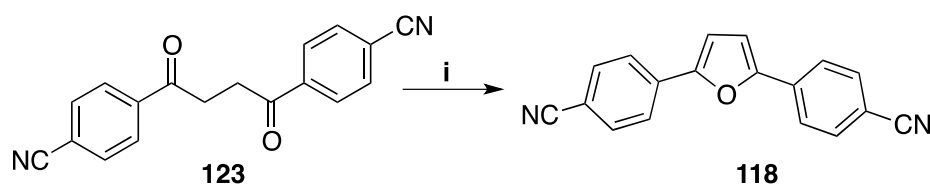


Figure 46. ^1H NMR (CDCl_3) spectrum of 4-(5-phenylfuran-2-yl)benzonitrile **127**.

The harsh acidic conditions of the reaction did not affect the nitrile group. The stretching frequency of the nitrile group **127** was present at 2225 cm^{-1} in the IR spectrum and at 119.0 ppm in the ^{13}C -NMR spectrum.

A symmetric 2,5-diarylfuran **118** was also synthesized by heating the 1,4-diketone **123** in acetic anhydride in the presence of concentrated sulfuric acid (Scheme 19).



Scheme 19. Synthetic pathway for 4,4'-(furan-2,5-diyl)benzonitrile **118**; Reagents and conditions: i- Ac_2O , H_2SO_4 , reflux.

The structure of **118** was characterized by ^1H NMR spectroscopy. Because of the plane of symmetry in the compounds, the protons H-3' and H-4' of the furan ring

Chapter II. Results and Discussion/ Chemistry

were observed as a singlet at 7.44 ppm. The protons H-2 and H-3 of the phenyl rings were observed as doublets at 7.92 ppm (J 8.1 Hz) and 8.06 ppm (J 8.4 Hz) (Figure 47).

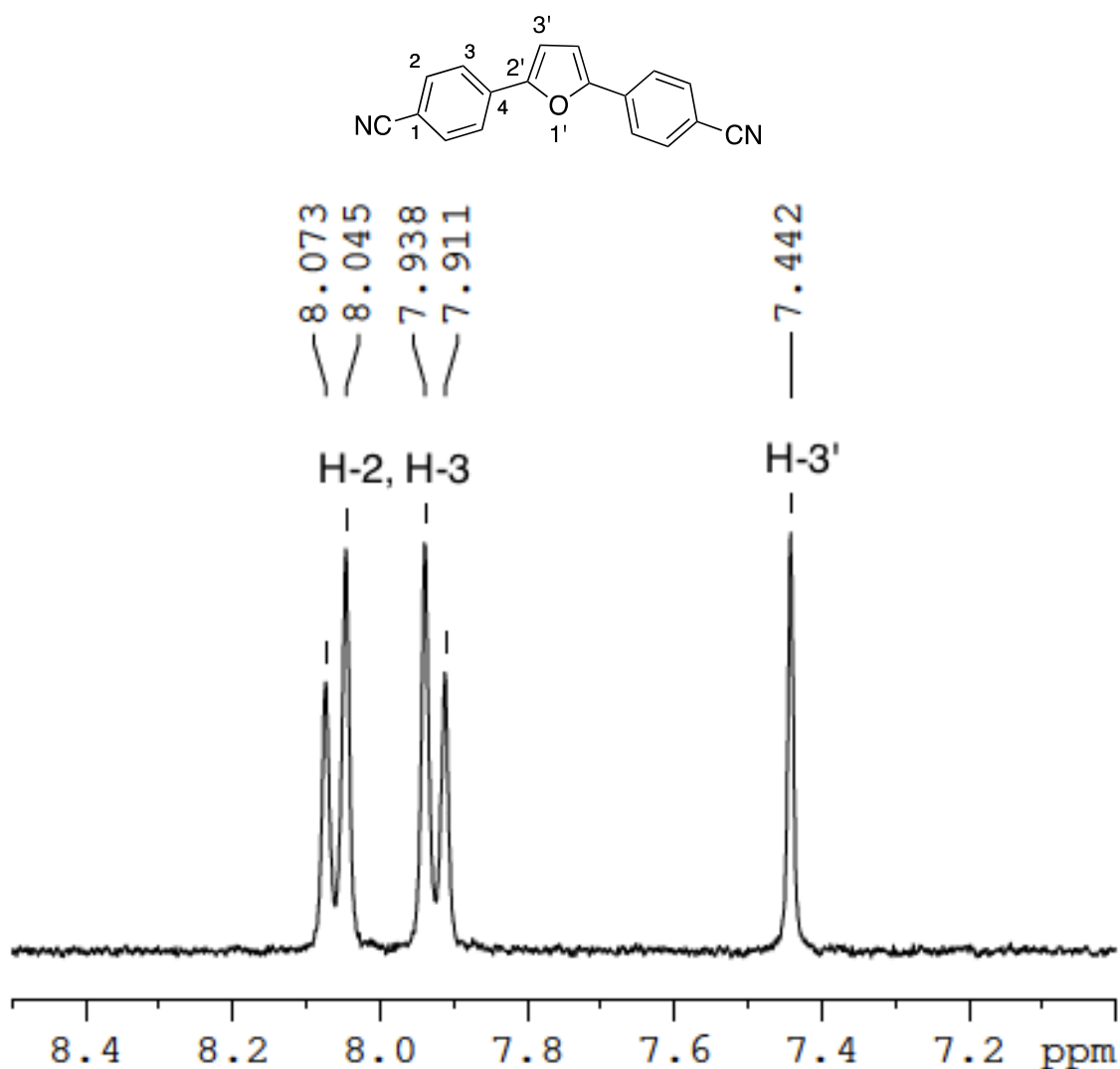
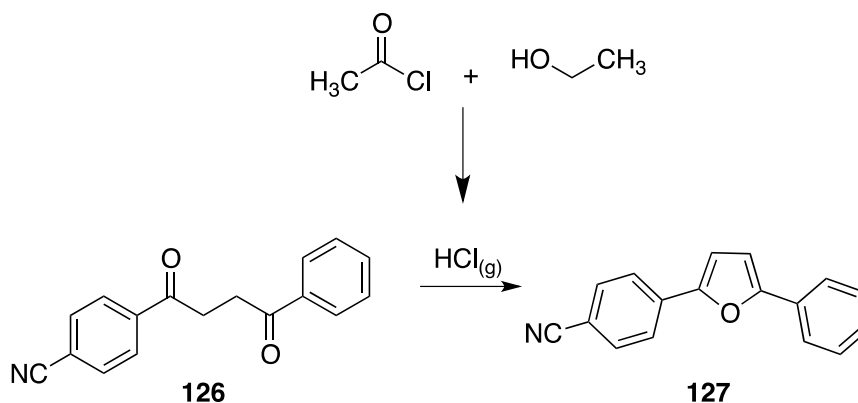


Figure 47. ¹H NMR (DMSO-d₆) spectrum of 4,4'-(furan-2,5-diyl)benzodinitrile **118**.

The second synthetic pathway used to synthesize **127** depends on the use of hydrogen chloride gas generated *in situ* from the reaction between ethanol and acetyl chloride (Scheme 20). The molar ratio that was used from acetyl chloride and ethanol was 8:12 for each 1.0 mole of the 1,4-diketone compound.

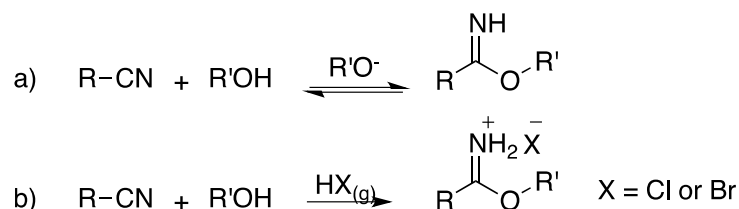


Scheme 20. Synthetic pathway for 4,4'-(furan-2,5-diyl)benzonitrile **127** using *in situ* generated dry hydrogen chloride gas.

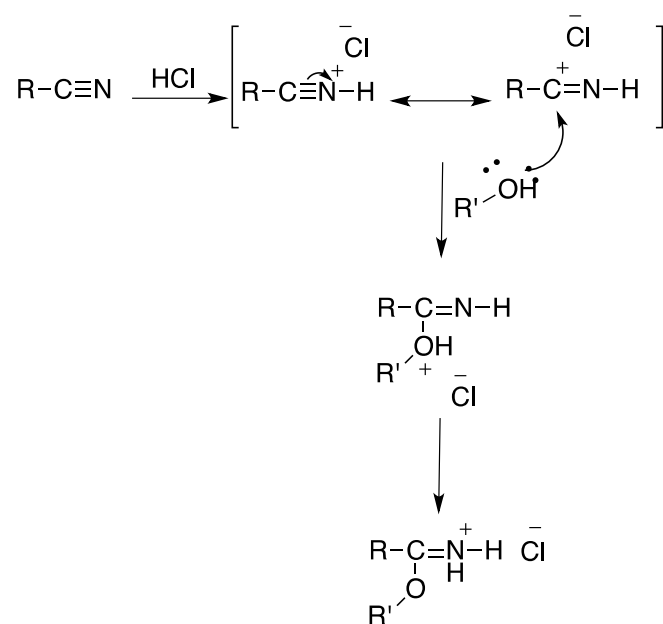
This *in situ* hydrogen chloride gas generation method was used as an alternative to the typical method, which uses concentrated sulfuric acid.¹⁰⁹ This was an attempt to avoid handling and disposal of concentrated sulfuric acid.

3.4. Carboximidate synthesis

Carboximidates are organic compounds with the general formula $RC(=NR')OR'$. They are also known as imino ethers as an imine group ($C=N$), together with an oxygen atom are connected to the carbon atom. Carboximidates are prepared as intermediates for the preparation of unsubstituted amidines from nitriles. Carboximidates intermediates can be prepared by either base-catalyzed reaction of nitriles with alcohols (Scheme 21a)¹¹⁴ or the Pinner synthesis, which consists of condensing a nitrile and an alcohol under anhydrous conditions in the presence of hydrogen chloride or hydrogen bromide gas (Scheme 21b).¹¹⁵ In the Pinner synthesis the hydrogen chloride gas activates the nitrile group making it liable to be attacked by alcohol leading to the formation of carboximidate hydrochlorides (Scheme 22).



Scheme 21. Pathways for the synthesis of carboximidates.



Scheme 22. Mechanism for the formation of carboximidates using hydrogen chloride gas and ethanol.

According to the research reported by Yadav and Babu for the synthesis of an imidate hydrochloride salt from a nitrile group using dry hydrogen chloride gas, the best molar ratio to use was 1 (nitrile): 8 (acetyl chloride): 12 (alcohol). Utilizing these conditions, it was expected that the reaction between hydrogen chloride gas, ethanol and the 1,4-diketones **126** will form the ethyl imidate hydrochloride compound **142** (Figure 48),¹¹⁶ however the furan **127** was formed in this reaction (see Scheme 23).

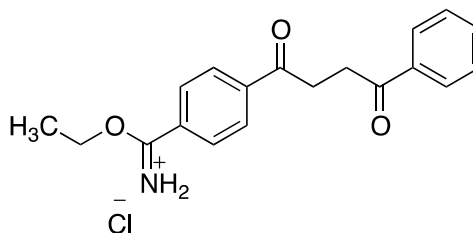


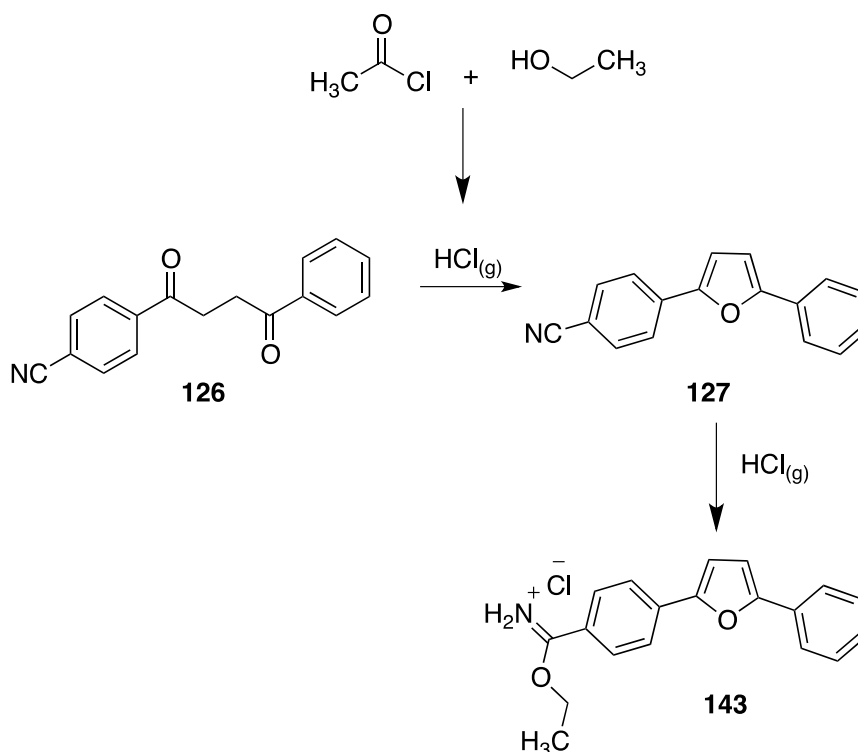
Figure 48. Structure of the expected ethyl imidate hydrochloride salt **142**.

This can be explained by the higher reactivity of the ketone groups towards protonation compared to the nitrile group. The effect of the number of hydrogen chloride gas moles on the product formed from the reaction with 1,4-diketones compounds bearing the nitrile group was studied further.

According to the results reported by Yadav and Babu,¹¹⁶ the nitrile group reacted with 8 moles of hydrogen chloride gas (generated *in situ* from the reaction between 8 moles of acetyl chloride and 12 moles of alcohol), giving 4 moles of alcohol

Chapter II. Results and Discussion/ Chemistry

to provide the nucleophile to attack the nitrile group to form the imidate hydrochloride. In this reaction, as the ketone groups were more reactive towards hydrogen chloride gas than the nitrile, the moles needed from acetyl chloride and alcohol were doubled. Using 16 moles of acetyl chloride and 24 moles of ethanol with each mole of the 1,4-diketone **126** resulted in both the cyclization to the furan and the conversion of the nitrile group into the ethyl imidate hydrochloride **143** (Scheme 23). Monitoring of the reaction using ^1H NMR spectroscopy, showed that the furan ring formed first, followed by the conversion of the nitrile group to ethyl imidate hydrochloride.

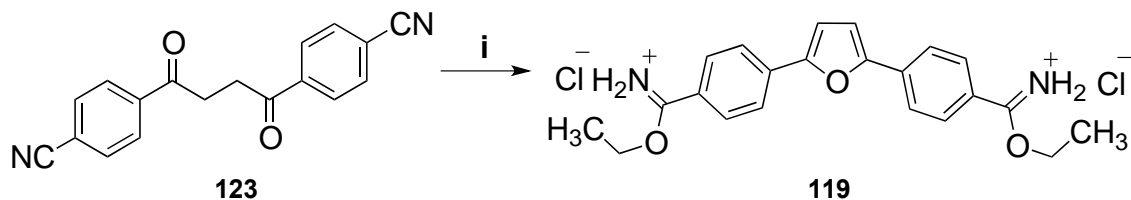


Scheme 23. Synthesis of ethyl 4-(5-phenylfuran-2-yl)benzimidate hydrochloride **143**.

The structure of **143** was confirmed by ^1H NMR and IR spectroscopy. The furan protons H-3' and H-4' were observed as doublets at 7.22 ppm (J 3.3 Hz) and 7.45 ppm (J 3.6 Hz). The phenyl protons H-2'', H-3'' and H-4'' were observed as a doublet at 7.90 ppm (J 7.8 Hz), triplet at 7.49 ppm (J 7.5 Hz) and triplet at 7.37 ppm (J 7.5 Hz), respectively. The phenyl protons H-2 and H-3 were observed as doublets at 8.08 ppm (J 8.7 Hz) and at 8.17 ppm (J 8.4 Hz). IR spectroscopy confirmed that the nitrile group had been converted to the imidate group, with a new carbon-nitrogen double bond stretch at 1606 cm^{-1} .

Chapter II. Results and Discussion/ Chemistry

This imidate Pinner synthesis was also used to synthesize the symmetrical diethyl 4,4'-(furan-2,5-diyl)dibenzimidate hydrochloride **119**. Compound **119** was synthesized starting from the 1,4-diketone **123** (Scheme 24).

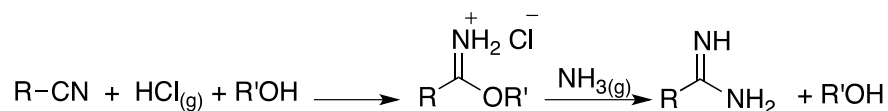


Scheme 24. Synthetic pathway for diethyl 4,4'-(furan-2,5-diyl)dibenzimidate dihydrochloride **119**; Reagents and conditions: i- HCl_(g), EtOH, CHCl₃, 0 °C- rt.

In order to ensure the synthesis of diethyl 4,4'-(furan-2,5-diyl)dibenzimidate **119** starting from the 1,4-diketones **123**, 24 equivalents of hydrogen chloride gas were used to affect the transformation of the two-nitrile groups into ethyl imidate hydrochloride. The symmetrical structure of **119** was confirmed by ¹H NMR spectroscopy. The protons for the ethyl groups were observed as a triplet at 1.52 ppm (*J* 6.9 Hz) and a quartet at 4.66 ppm (*J* 6.9 Hz). The furan protons H-3' were observed as a singlet at 7.54 ppm. The aryl protons H-2 and H-3 were observed as two doublets at 8.15 ppm (*J* 8.1 Hz) and 8.25 ppm (*J* 8.4 Hz).

3.5. Amidine functional group synthesis

The most common route reported in the literature for the synthesis of unsubstituted amidines is the Pinner method. As described in the previous section, the Pinner method transforms the nitrile group into the carboximidate by reacting it with hydrogen chloride gas and alcohol. The carboximidate intermediate can then be transformed into the amidine group by the action of ammonia (Scheme 25).¹⁰³

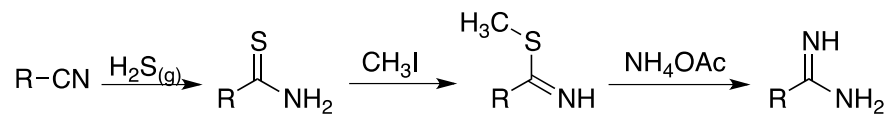


Scheme 25. Pinner synthesis of unsubstituted amidine.

An alternative synthesis of the amidine group involves transformation of the nitrile group into the thioamide using hydrogen sulfide gas. The thioimidate can then be

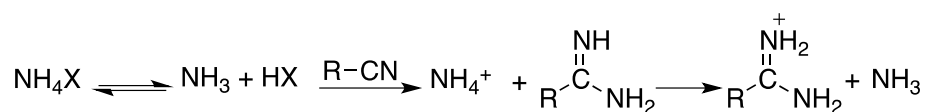
Chapter II. Results and Discussion/ Chemistry

converted into the unsubstituted amidines using methyl iodide followed by ammonium acetate (Scheme 26).¹¹⁷



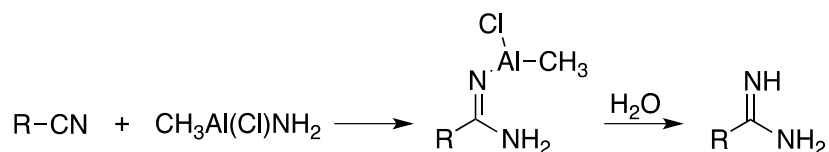
Scheme 26. Synthesis of an unsubstituted amidine from nitrile *via* the thioimidate.

In addition, unsubstituted amidines can be synthesized directly from nitrile by heating the nitrile-containing compound with an ammonium salt in liquid ammonia at a high temperature (150-200 °C) (Scheme 27).¹¹⁸



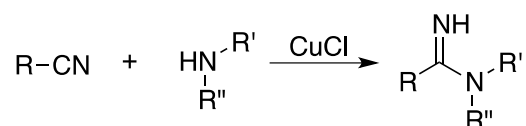
Scheme 27. Synthesis of an unsubstituted amidine from nitrile using ammonium salts in liquid ammonia.

The nucleophilic addition of amine to a nitrile group using methyl chloro aluminum amide can also afford amidine under mild conditions (Scheme 28).¹¹⁹



Scheme 28. Unsubstituted amidine synthesis using aluminum amide reagents.

In another approach, substituted amidine can be synthesized from the reaction of a nitrile with substituted amines. The reaction is catalyzed by copper (I) chloride (Scheme 29).¹²⁰

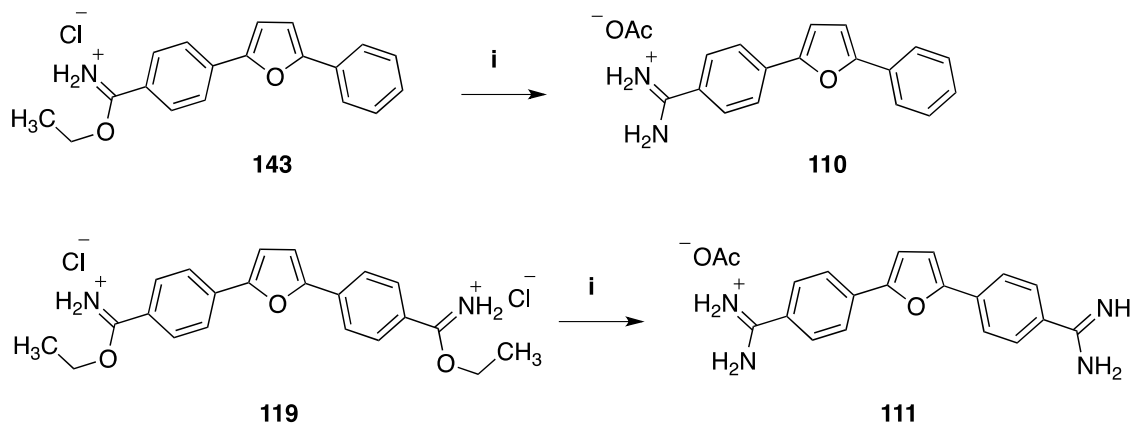


Scheme 29. Substituted amidine synthesis using copper (I) chloride.

In this research the Pinner synthesis was used to transform the ethyl benzimidate intermediates **143** and **119** into unsubstituted amidines 4-(5-phenylfuran-2-yl)benzamidinium acetate **110** and 4,4'-(furan-2,5-diyl)dibenzamidinium acetate **111**,

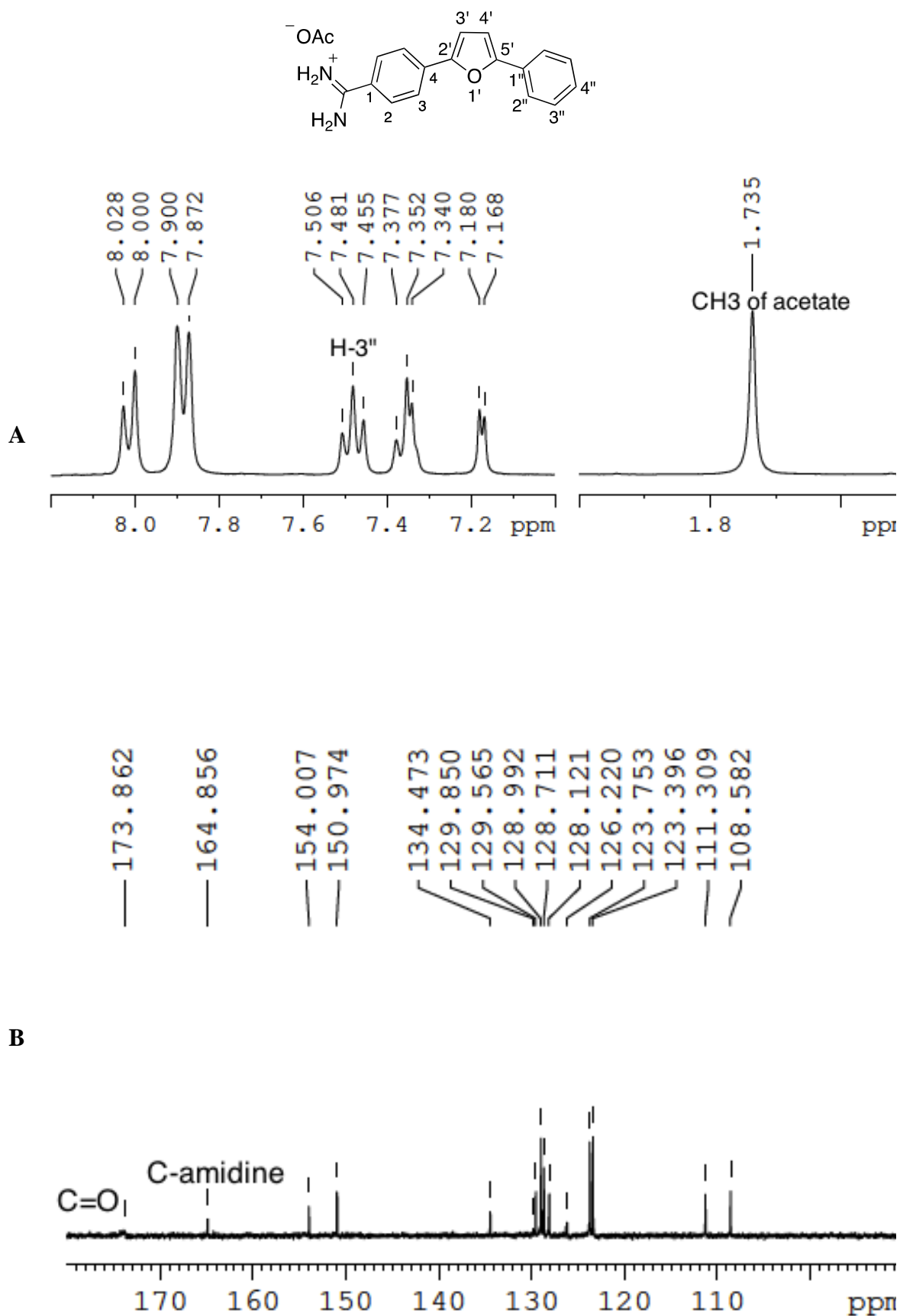
Chapter II. Results and Discussion/ Chemistry

respectively. The ethyl benzimidates **143** and **119** reacted with ammonium acetate (the source of ammonia) in ethanol at room temperature (Scheme 30).¹²¹



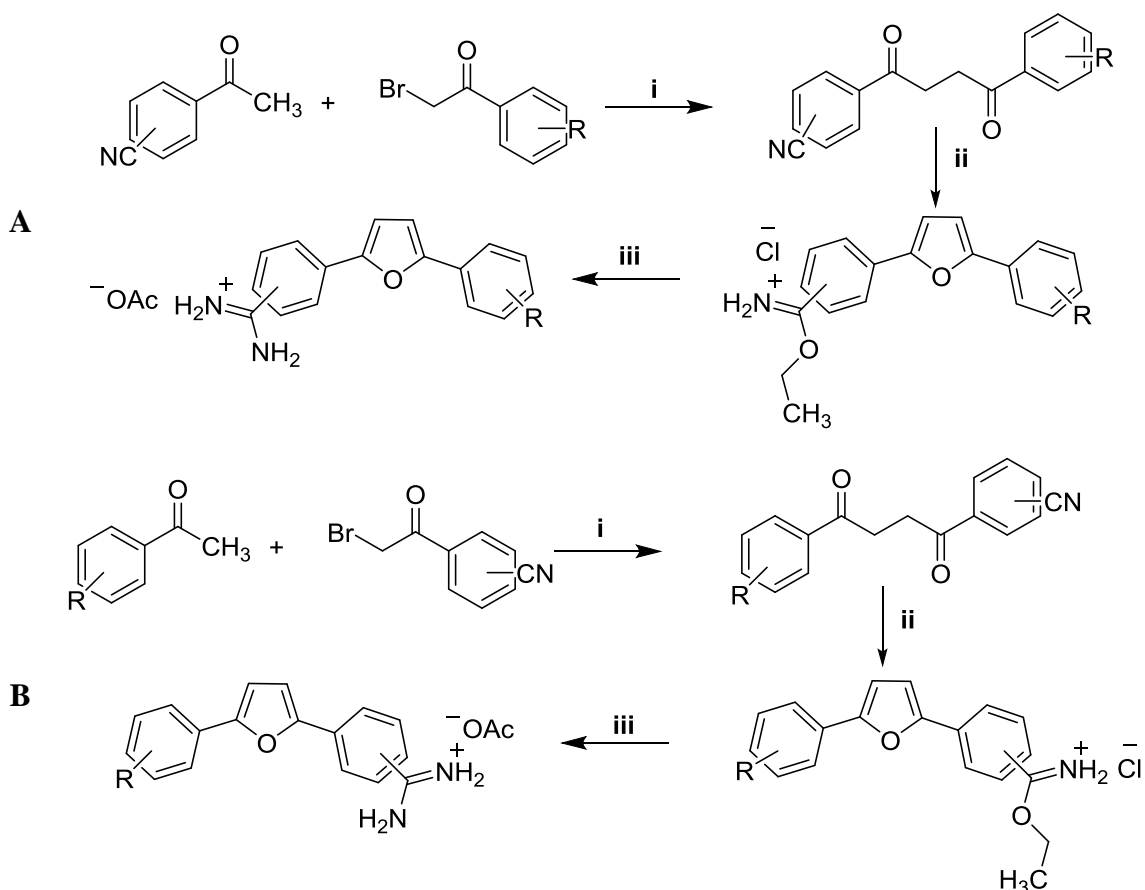
Scheme 30. Synthetic pathway to give 4-(5-phenylfuran-2-yl)benzamidinium acetate **110** and 4,4'-(furan-2,5-diyl)dibenzamidinium acetate **111**; Reagents and conditions: i- $\text{CH}_3\text{COO}^-\text{NH}_4^+$, EtOH, rt.

The formation of the amidine groups in **110** and **111** was confirmed by the disappearance of the ethyl peaks for ethyl benzimidates **143** and **119** in the ^1H NMR and ^{13}C NMR spectra and the appearance of the amidine carbons in the ^{13}C NMR spectrum at 164.9 and 164.8 ppm, respectively (Figure 49).



3.6. Conclusion

A general multi-step synthetic pathway for the synthesis of asymmetric furan-amidines with different substituents (R group) was developed (Scheme 31). The synthetic pathway depends on the use of commercially available methyl aryl ketones and α -bromomethyl aryl ketones as starting materials in the synthesis of the 1,4-diketone intermediates. One of the starting materials has a nitrile group that serves as the precursor for the target amidine group. The 1,4-diketone intermediates are then cyclized to give the furan ring and the nitrile group is transformed into ethyl benzimidate hydrochloride. The imidate group is an intermediate functional group between the nitrile group and the final amidine group. Finally the ethyl imidate hydrochloride intermediates are converted into amidine by the use of ammonium acetate.



Scheme 31. General synthetic pathway for the preparation of asymmetric furan-amidines; A- starting from methyl aryl ketone having a nitrile group; B- starting from α -bromomethyl aryl ketone having a nitrile group; Reagents and conditions: i- ZnCl_2 , NEt_3 , EtOH, dry toluene or THF, rt; ii- $\text{HCl}_{(g)}$, EtOH, CHCl_3 , $0\text{ }^\circ\text{C}$ - rt; iii- $\text{CH}_3\text{COO}^- \text{NH}_4^+$, EtOH, rt.

Chapter II. Results and Discussion/ Chemistry

4. Applications of the optimized multi-step synthetic pathway

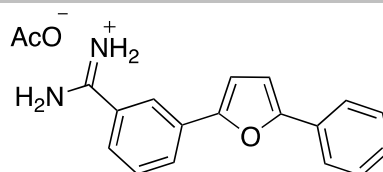
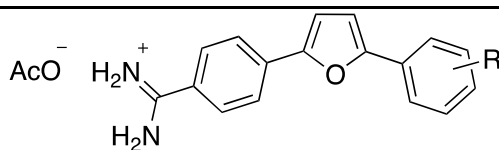
The multi-step synthetic pathway developed in section 3, was used to synthesise a range of asymmetric furan-amidines with different substituents on the phenyl ring. This was completed to study the effect of different substituents (electronics and size) on the NQO2 inhibition activity.

The asymmetric furan amidines synthesized are summarized in Table 12. Different substituents were introduced, which can be classified as electron-withdrawing or electron-donating groups. The effect of the electron-withdrawing groups, namely, fluoro **144** and **145**, bromo **146** and nitro groups **147** and **148** on NQO2 inhibition activity was studied. The regio-effect for the fluoro- and nitro-groups on NQO2 inhibition activity was also considered through the preparation of different regio-isomers, with *meta* **144** and **147** and *para* **145** and **148** analogues. In addition, the effect of the electron-donating groups, namely, methoxy **149**, methyl **150**, ethyl **151**, isopropyl **152** and *t*-butyl **153** groups on NQO2 inhibition ability was also studied. The length and size of the alkyl chains was evaluated through the preparation of a series of methyl, ethyl, isopropyl and *t*-butyl substituents.

In addition, one compound with a meta-amidine group **154** was prepared to study the effect of the amidine position on the NQO2 inhibition activity.

Table 12. The synthesized targeted furan-amidines.

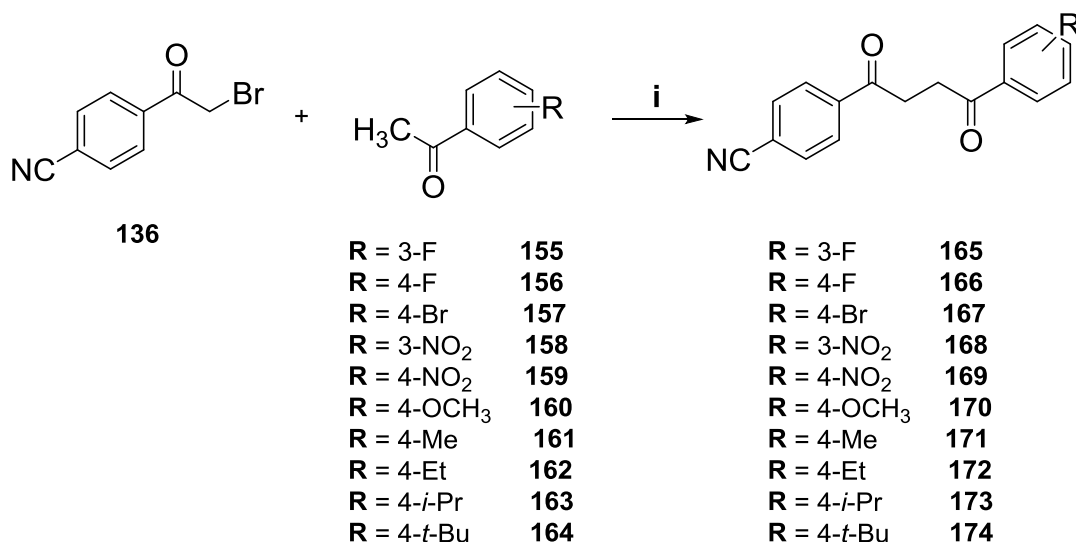
Compound ID	R
144	3-F
145	4-F
146	4-Br
147	3-NO ₂
148	4-NO ₂
149	4-OCH ₃
150	4-CH ₃
151	4-CH ₂ CH ₃
152	4-CH(CH ₃) ₂
153	4-C(CH ₃) ₃
154	----



The detailed synthesis of the target asymmetric furan-amidines and their precursors is discussed in the following sections.

4.1. Asymmetric aryl 1,4-diketones synthesis

The 1,4-diketones **165-174** with different substituents on the aromatic ring were synthesized from the coupling reaction between the methyl aryl ketones **155-164** and the α -bromomethyl aryl ketone **136** (Scheme 32).



Scheme 32. Pathway for the synthesis 1,4-diketones **165-174**; Reagents and conditions:

i- ZnCl₂, NEt₃, EtOH, dry toluene or THF, rt.

The preparation of the 1,4-diketone intermediates **165-174** is the key step in the synthetic pathway of the target amidine compounds; their preparation in good yields is desirable. Variable yields of the 1,4-diketone intermediates **165-174** were obtained depending on the substituent on the phenyl group of the precursor methyl aryl ketones **155-164** (Table 13).

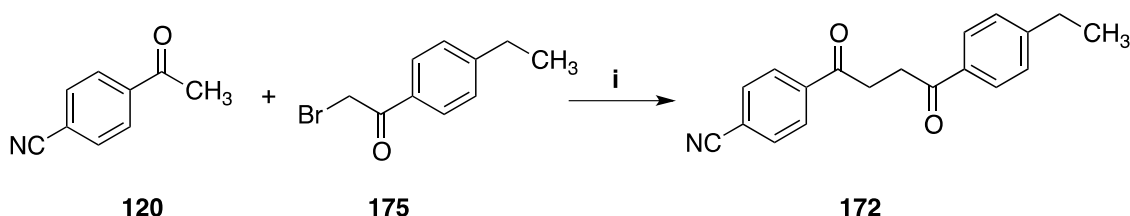
Table 13. The reaction times and % yields for the synthesis of the 1,4-diketones **165-174**.

1,4-diketone ID	Reaction time	%Yield
165	4 days	16
166	3 days	26
167	3 days	56
168	3 days	47
169	3 days	51
170	7 days	27
171	7 days	9
172	7 days	15
173	7 days	11
174	7 days	9

Chapter II. Results and Discussion/ Chemistry

The first step in this synthetic pathway is the formation of the enolate anion (conjugate base) of the methyl aryl ketones (see Scheme 14). This slow step is base-catalysed and it was accomplished using triethylamine. Shorter reaction times were observed in the case of starting with the methyl aryl ketones **157-159** giving the 1,4-diketones **167-169** in the best yields. This is attributed to the starting methyl aryl ketones **157-159** having large electron-withdrawing groups on the aryl rings increasing the acidity of the α -hydrogens adjacent to the carbonyl group of the ketone, leading to the stabilization of the negative charge on the enolate anion. In contrast, low yields of 1,4-diketones **171-174** were obtained and attributed to the methyl aryl ketones precursors bearing electron-donating groups **161-164**. This can also be explained by the inductive effect of the electron-donating alkyl groups on de-stabilizing the enolate intermediate formed during the reaction.

An attempt to increase the yields of the 1,4-diketones, which were synthesized from the methyl aryl ketones with electron-donating groups, was investigated. The synthesis of the 1,4-diketone **172** was attempted through the coupling between methyl 4-cyanophenyl ketone **120** and the α -bromomethyl 4-ethylphenyl ketone **175** (Scheme 33). In this synthetic pathway, the starting ketone **120** had the electron-withdrawing nitrile group, whereas in the earlier synthesis methyl 4-ethylphenyl ketone **162** had an ethyl electron-donating group.



Scheme 33. Alternative pathway for the synthesis 1,4-diketone **172**; Reagents and conditions: i- ZnCl₂, NEt₃, EtOH, dry toluene, rt.

The percentage yield of the 1,4-diketone **172** obtained from this reaction was 18.0 % compared to 15.0 % obtained from the first synthetic pathway. No improvement can be seen either starting from the methyl aryl ketone **162** or **120**. The α -bromomethyl aryl ketone **175** was synthesized as discussed in section 4.1.3.

The methyl aryl ketones **163** and **164** were required to be synthesized, as described in section 4.1.2.

Chapter II. Results and Discussion/ Chemistry

4.1.1. Spectroscopic characterization of the 1,4-diketones 165-174

The structures of the 1,4-diketones **165-174** were characterized by ^1H , ^{13}C NMR IR spectroscopy and mass spectrometry. The formation of the 1,4-diketones **165-174** was confirmed by the appearance of two triplet peaks merged as a multiplet or a singlet peak in the aliphatic region (3.42 ppm to 3.52 ppm) of the ^1H NMR spectra for the $\text{COCH}_2\text{CH}_2\text{CO}$ protons integrating to 4H.

The presence of the aryl nitrile group (CN) in the 1,4-diketones **165-174** was confirmed by ^{13}C NMR and IR spectroscopy. The aryl nitrile group is usually observed in the 118-119 ppm region in the ^{13}C NMR spectrum and the peak is absent from the ^{13}C -DEPT135 spectrum. In the IR spectrum the nitrile group has a distinct sharp peak with a frequency in the region $2220\text{-}2230\text{ cm}^{-1}$.

The 1,4-diketones **165** and **166** with *meta*-fluoro and *para*-fluoro atoms, respectively, showed coupling between the fluoro-atom and the protons in the ^1H NMR spectrum and carbons in the ^{13}C NMR spectrum.

The ^1H NMR spectrum of 1-(4-cyanophenyl)-4-(3-fluorophenyl)-1,4-butadione **165** showed the coupling between the fluorine atom and the *ortho*-protons H-2'' and H-4'' and the *meta*-proton H-5'' (Figure 50A). The H-2'', H-4'' and H-5'' were observed as doublet at 7.71 ppm ($^3J_{\text{HF}} = 9.6\text{ Hz}$), triplet (formally dd) at 7.33 ppm ($^3J_{\text{HF}} = J_{\text{HH}} = 8.4\text{ Hz}$) and quartet (formally ddd) at 7.50 ppm ($^4J_{\text{HF}} = J_{\text{HH}} = 6.0\text{ Hz}$), respectively. ^{13}C - ^{19}F Coupling was also observed in the ^{13}C NMR spectrum of **170** (Figure 50B). The coupling between the fluorine atom and C-1'', C-2'', C-3'', C-4'', C-5'' and C-6'' was observed as doublets with different coupling constants depending on the proximity of the fluorine to the carbon. The carbons C-1'', C-2'', C-3'', C-4'', C-5'' and C-6'' were observed at 138.5 ppm ($^3J_{\text{CF}} 6.0\text{ Hz}$), 120.4 ppm ($^2J_{\text{CF}} 21.0\text{ Hz}$), 162.9 ppm ($^1J_{\text{CF}} 247.0\text{ Hz}$), 114.9 ppm ($^2J_{\text{CF}} 22.0\text{ Hz}$), 130.4 ppm ($^3J_{\text{CF}} 8.0\text{ Hz}$) and 123.9 ppm ($^4J_{\text{CF}} 3.0\text{ Hz}$), respectively.

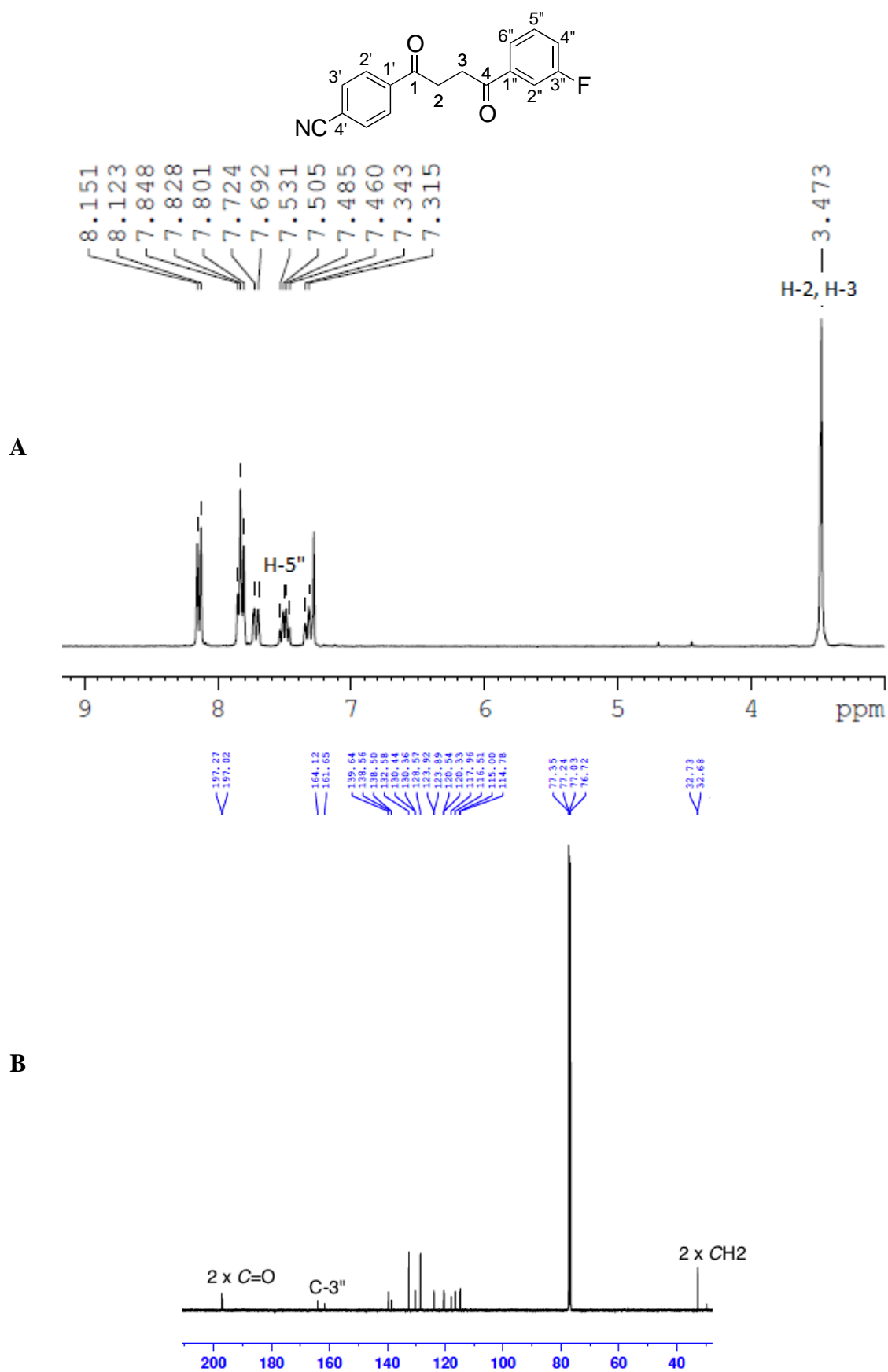
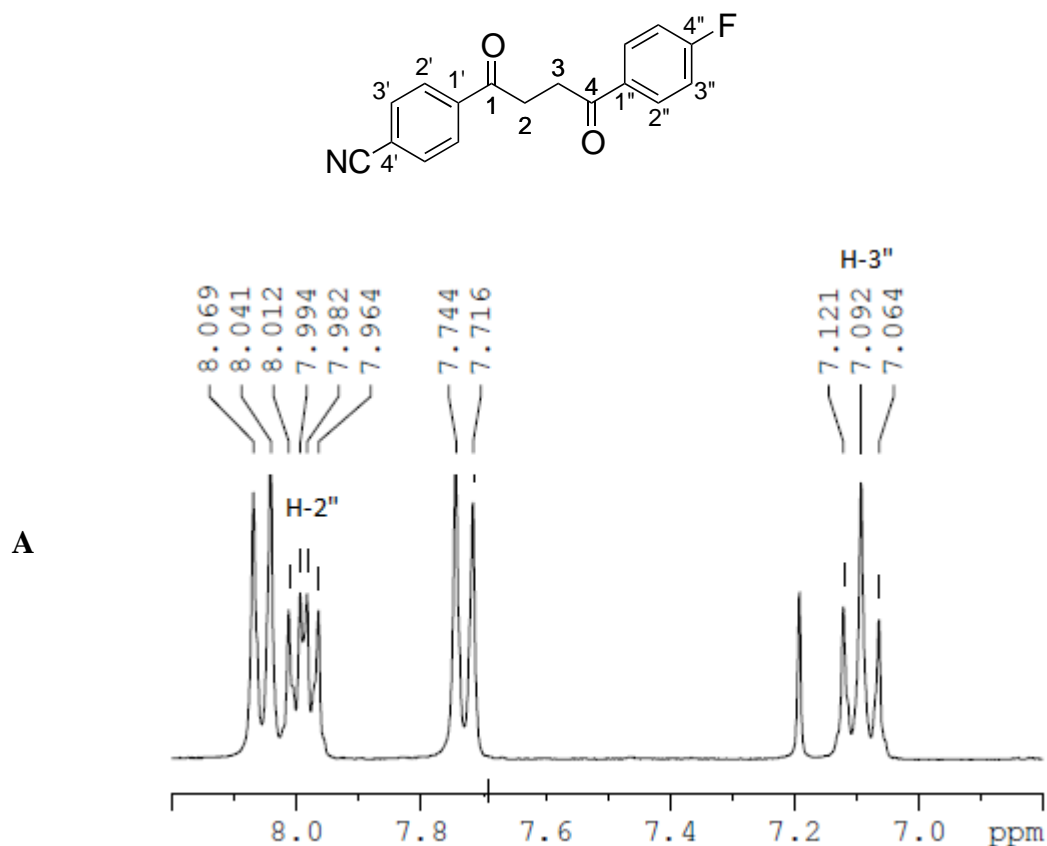


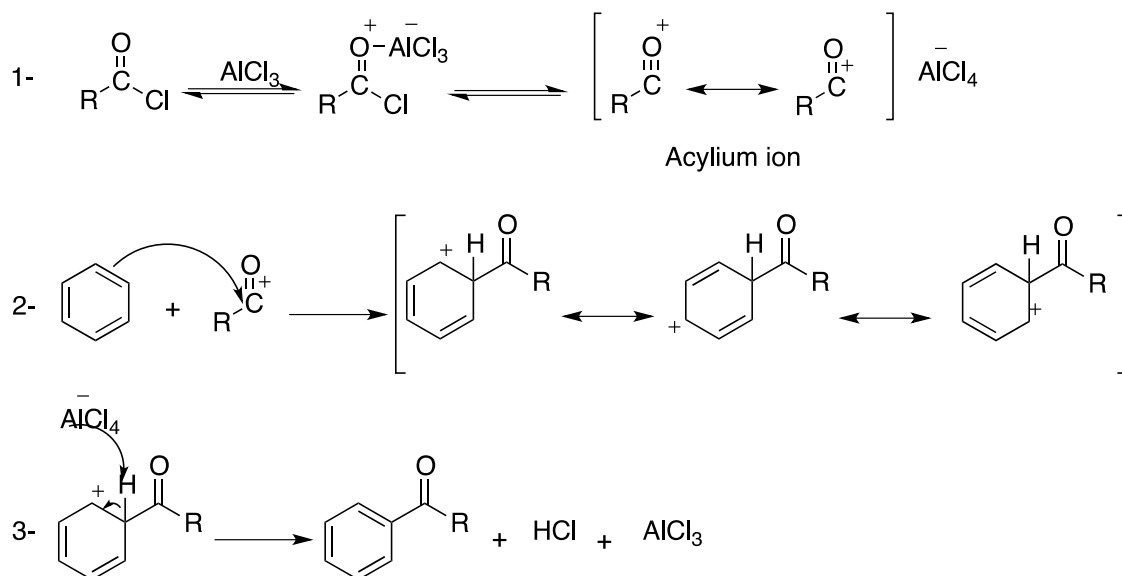
Figure 50. NMR (CDCl₃) spectra of 1-(4-cyanophenyl)-4-(3-fluorophenyl)-1,4-butanedione **165**: A- ¹H NMR; B- ¹³C NMR.

Chapter II. Results and Discussion/ Chemistry

The ^1H -NMR spectrum of 1-(4-cyanophenyl)-4-(4-fluorophenyl)-1,4-butadione **166** showed the coupling between the fluorine atom and the *ortho*-protons H-3'' and *meta*-protons H-2'' (Figure 51A). The H-3'' protons were observed as a triplet at 7.09 ($^3J_{\text{HF}} = J_{\text{HH}} = 8.4$ Hz) and the protons H-2'' were observed as a doublet of doublets at 7.99 ppm ($^4J_{\text{HF}} = J_{\text{HH}} = 7.8$ Hz). The ^{13}C -NMR spectrum of 1-(4-cyanophenyl)-4-(3-fluorophenyl)-1,4-butadione **166** showed the coupling between the fluorine atom and the carbon atoms through 1, 2, 3 and 4 bonds. The C-1'', C-2'', C-3'' and C-4'' carbons were observed as doublets at 132.9 ppm ($^4J_{\text{CF}} 3.0$ Hz), 130.8 ppm ($^3J_{\text{CF}} 9.0$ Hz), 115.8 ppm ($^2J_{\text{CF}} 22.0$ Hz) and 165.9 ppm ($^1J_{\text{CF}} 253.0$ Hz), respectively (Figure 51B). ^{19}F -NMR spectroscopy showed the presence of one aryl-fluoro atom in the 1,4-diketones **165** and **166** at -111.7 and -104.7 ppm.



Chapter II. Results and Discussion/ Chemistry

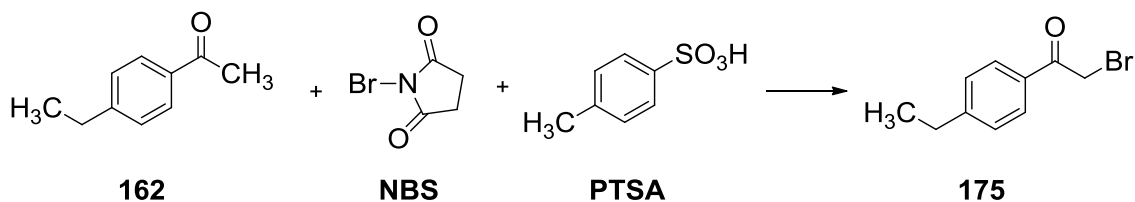


Scheme 35. Friedel-Craft acylation mechanism.

The substituents on the aromatic ring will direct the reaction position. Alkyl groups are known to be *ortho*- and *para*-directing groups because of the stabilization of the positive charge by inductive effect. Because of the bulkiness of the isopropyl and *tert*-butyl groups, by t.l.c the acylation gave only one product, forming only the methyl aryl ketones **163** and **164**, respectively. The structures of 4-isopropylacetophenone **163** and 4-*tert*-butylacetophenone **164** were confirmed by $^1\text{H-NMR}$ spectroscopy.

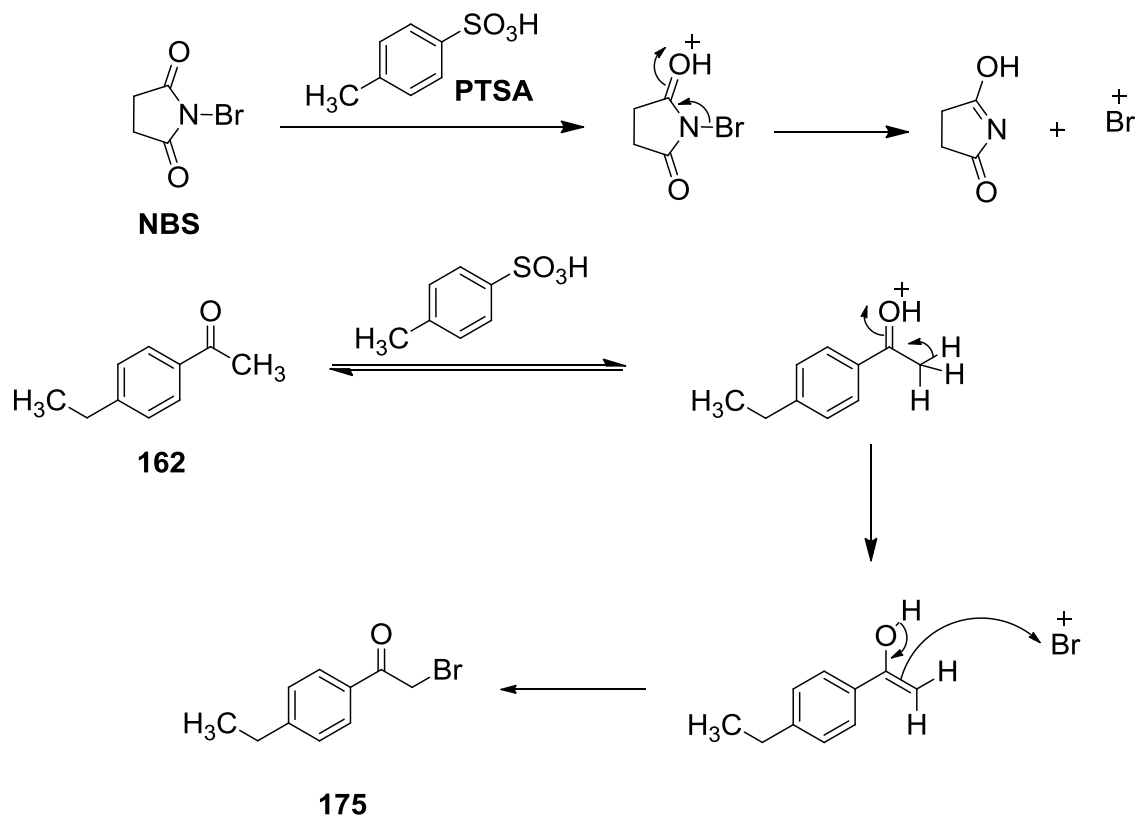
4.1.3. Synthesis of α -bromomethyl aryl ketone **175**

α -Bromomethyl aryl ketone **175** was synthesized from the reaction of 4-ethylacetophenone **162** with *N*-bromosuccinimide (NBS) in the presence of *p*-toluenesulfonic acid (PTSA) as a catalyst (Scheme 36).¹²³



Scheme 36. Pathway for the synthesis of 2-bromo-1-(4-ethylphenyl)ethanone **175**.

p-Toluenesulfonic acid was used in large amount to aid in the formation of the bromonium ion (Br^+), which reacted with the enol of **162** (Scheme 37).



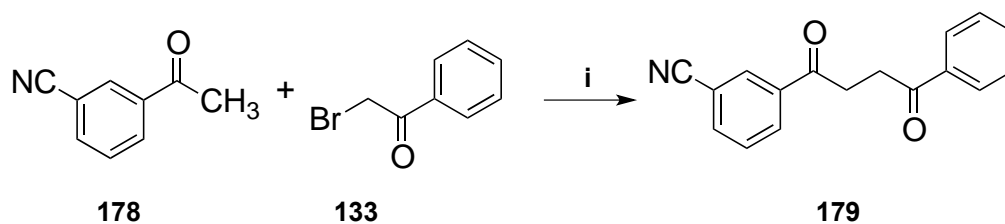
Scheme 37. Mechanism of bromination of ketone **162** using NBS in the presence of PTSA.

The structure of 2-bromo-1-(4-ethylphenyl)ethanone **175** was confirmed by ^1H NMR spectroscopy.

4.2. Synthesis of the aryl 1,4-diketone with a *meta*-nitrile group **179**

Aryl 1,4-diketone **179** was synthesized by the coupling between 3-acetylbenzotrile **178** and 2-bromoacetophenone **133** using zinc chloride, triethylamine and ethanol as condensation agent (Scheme 38) in a yield of 15.2%. 1-(3-Cyanophenyl)-4-phenyl-1,4-butadione **179** is an asymmetric 1,4-diketone with a *meta*-nitrile group. This compound was synthesized as an intermediate to prepare the asymmetric furan-amidine **154** described in section 4.4. The *meta*-aryl amidine group is reported to have lower binding affinity towards DNA compared to the *para*-aryl amidine.¹²⁴ If the furan-amidine **154** shows good NQO2 inhibition activity, this compound could be a selective NQO2 inhibitor.

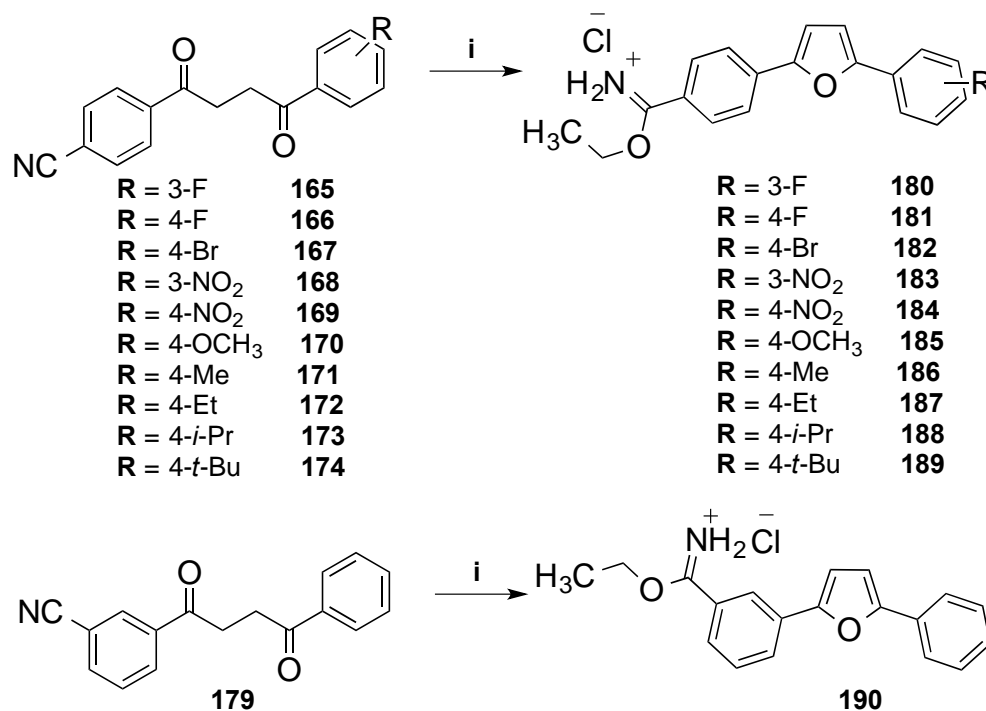
Chapter II. Results and Discussion/ Chemistry



Scheme 38. Synthesis of the 1,4-diketone **179**; Reagents and conditions: i- ZnCl₂, NEt₃, EtOH, dry toluene, rt.

4.3. Synthesis of the ethyl imidate intermediates

The ethyl imidate hydrochloride intermediates **180-190** were synthesized by reacting the 1,4-diketones **165-174** and **179** with dry hydrogen chloride and ethanol (Scheme 39). Sixteen equivalents of hydrogen chloride gas were used to ensure firstly the cyclization of the 1,4-diketones and secondly the transformation of the nitrile group into carboximidate, to give the furan- ethyl imidate intermediates.



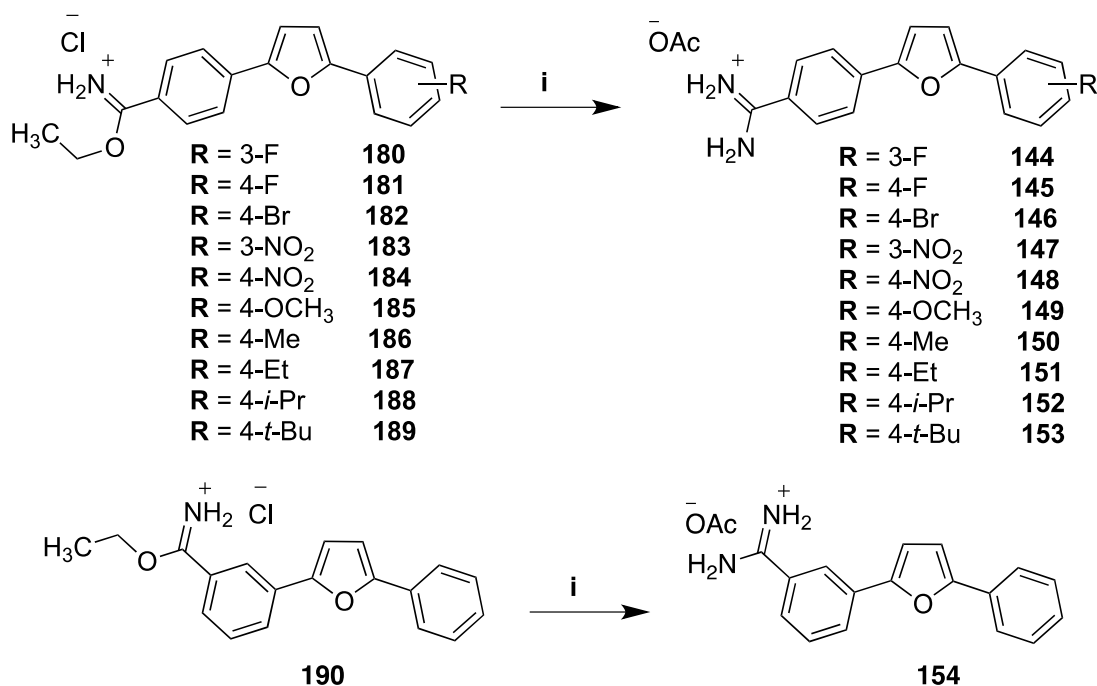
Scheme 39. Pathway for the synthesis of the ethyl imidate hydrochloride intermediates; **180-190**; Reagents and conditions: i- HCl_(g), EtOH, CHCl₃, 0 °C - rt .

4.4. Synthesis of the targeted amidines

The target amidines **144-154** were synthesized by treating the ethyl imidate hydrochloride intermediates **180-190** with ammonium acetate in ethanol (Scheme 40).

Chapter II. Results and Discussion/ Chemistry

Good to excellent yields of the amidines **144-154**, except for **146** (18.2%) were obtained.



Scheme 40. Synthetic pathway of the targeted amidines; **144-154**; Reagents and conditions: i- CH₃COO⁺NH₄, EtOH, rt.

4.5. Physical properties of the amidines 144-154

The synthesized asymmetric furan-amidines **110** and **144-154** showed different solubilities in water (hydrophilicity). A drug candidate must have optimal hydrophilicity properties to be tested in a cell system. The calculated log *P* value for a drug candidate can be used as an indication for its hydrophilicity. The Log *P* value of a drug is the logarithm of its (n-octanol-water) partition coefficient $P_{(o/w)}$.¹²⁵ The partition coefficient for a substance X can be given by the following equation:

$$P_{(o/w)} = [X]_o / [X]_w$$

In general, the synthesized amidines **110** and **144-154** showed poor water solubility and the least soluble were the furan-amidines **147** and **148**. The study of the predicted log *P* values (Table 14) for the base-form of the synthesized asymmetric furan-amidines **110** and **144-154** aided in addressing the problem of low water solubility of the synthesized amidines.

Chapter II. Results and Discussion/ Chemistry

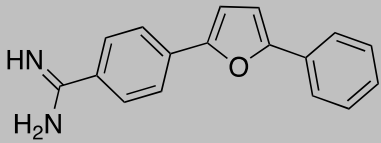
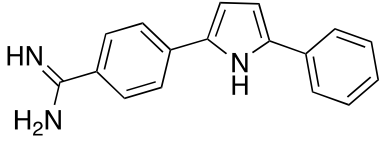
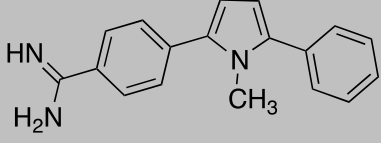
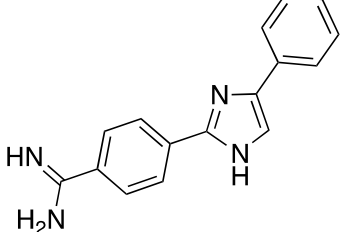
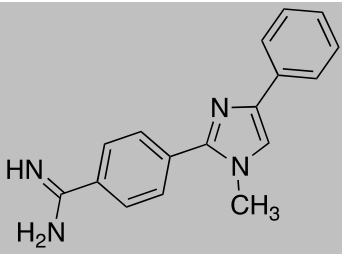
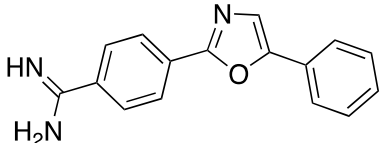
Table 14. The calculated log *P* values¹²⁶ of the synthesized asymmetric furan-amidines **110** and **144-154**.

ID	R	Calculated log <i>P</i>
110	H	2.8
144	3-F	2.9
145	4-F	2.9
146	4-Br	3.5
147	3-NO ₂	2.7
148	4-NO ₂	2.7
149	4-OCH ₃	2.7
150	4-CH ₃	3.2
151	4-CH ₂ CH ₃	3.5
152	4-CH(CH ₃) ₂	3.9
153	4-C(CH ₃) ₃	4.4
154	----	2.8

One of the ways that was used to increase the hydrophilicity of the asymmetric furan-amidines was to exchange the furan ring into more water-soluble heterocycles. Pyrrole, *N*-methylpyrrole, imidazole, *N*-methylimidazole and oxazole were the heterocycles that were chosen. The calculated log *P* values for the proposed heterocycle-isosteres of the asymmetric furan-amidine **110** are listed in Table 15, all of which are lower than the furan analogue.

Chapter II. Results and Discussion/ Chemistry

Table 15. Calculated $\log P$ values¹²⁶ of the proposed asymmetric furan-amidine isosteric analogues of the asymmetric furan-amidine **110**

ID	Compound structure	Calculated $\log P$
110		2.8
191		2.5
192		2.4
193		1.8
194		1.7
195		2.2

5. Asymmetric furan-amidines isosteres

5.1. Hydrophilicity optimization

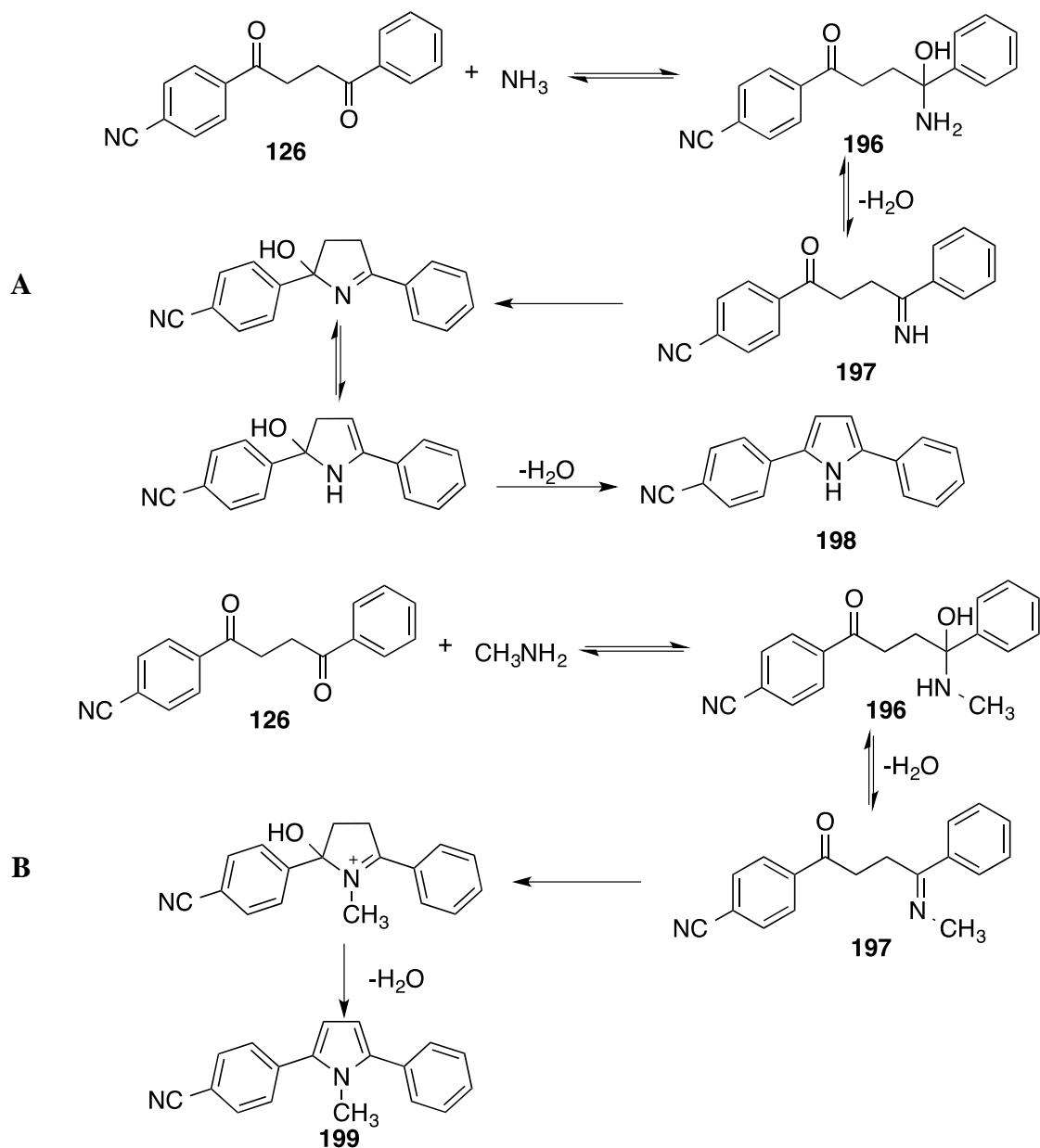
The isosteres **191-195** of the asymmetric furan-amidine **110** were synthesized with the aim to optimize the water solubility of the potential NQO2 inhibitors. The details of the synthesis of the heterocyclic amidines **191-195** are discussed in the following sections.

Chapter II. Results and Discussion/ Chemistry

5.1.1. Synthesis of substituted 2,5-diarylpyrrole-amidines **191** and **192**

The pyrrole ring is a very abundant heterocycle in nature and in commercially available drugs. In general, pyrroles are synthesized from the condensation reaction between a 1,4-dicarbonyl compound and a primary amine, which is known as the Paal-Knorr pyrrole synthesis.¹²⁷

The first step in the synthesis of the pyrrole- **191** and *N*-methylpyrrole-amidines **192** was the cyclization of the 1,4-diketones **126** into pyrrole **198** and *N*-methylpyrrole **199**. The condensation between the aryl 1,4-diketone **126** and an amine results in the formation of the hemiaminal **196** intermediate. The elimination of water molecule from the hemiaminal **196** gives the imine **197**. Finally, the ring closure and elimination of a water molecule yields 2,5-diarylpyrrole compounds **198** (Scheme 41A) and **199** (Scheme 41B). The amines, which were used to synthesize **198** and **199**, were ammonium acetate and methylamine, respectively.



Scheme 41. Pathways for the synthesis of: A- 4-(5-phenyl-1*H*-pyrrol-2-yl)benzonitrile **198**; B- 4-(1-methyl-5-phenyl-1*H*-pyrrol-2-yl)benzonitrile **199**.

The structure of 4-(5-phenyl-*H*-pyrrol-2-yl)benzonitrile **198** was confirmed by ^1H NMR spectroscopy. The *N*-H proton was observed as a broad singlet at 8.65 ppm. H-2 and H-3 protons were observed as doublets at 7.68 ppm (J 8.7 Hz) and in the region of 7.56-7.62 ppm merged with H-2'' proton of the second aryl ring. H-3'' and H-4'' were observed as triplets at 7.44 ppm (J 7.8 Hz) and 7.30 ppm (J 7.5 Hz), respectively (Figure 52).

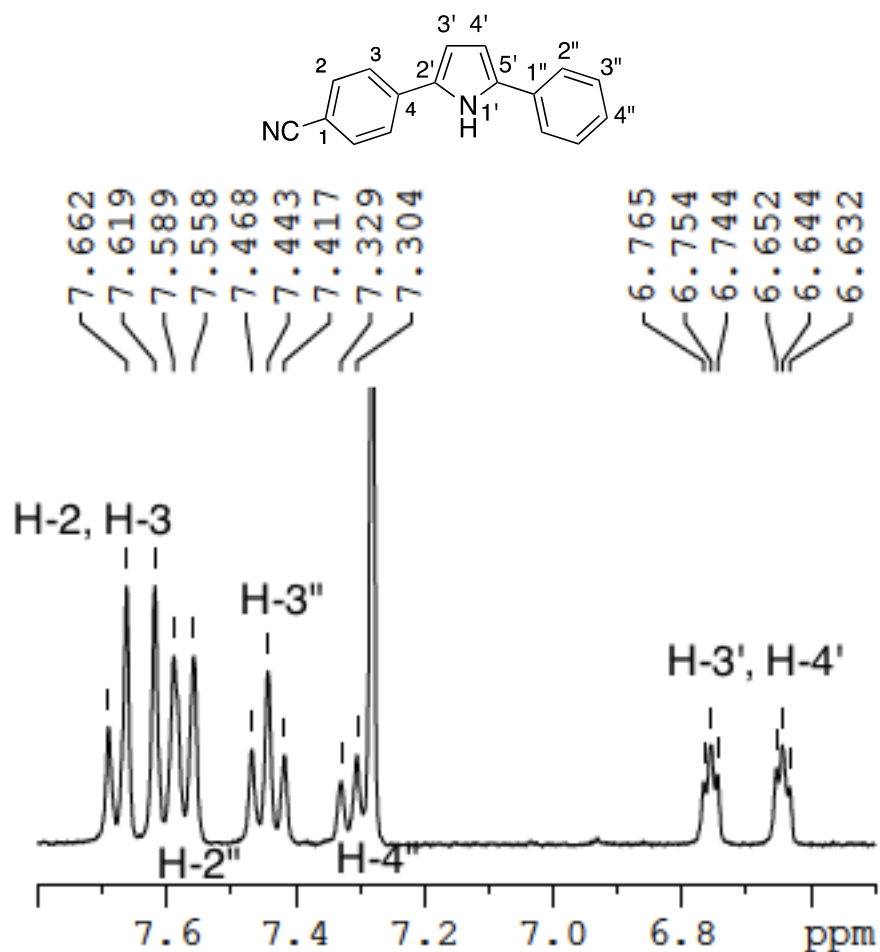


Figure 52. ^1H NMR (CDCl_3) spectrum of 4-(5-phenyl-*H*-pyrrol-2-yl)benzonitrile **198**.

The H-3' and H-4' protons were observed as triplets at 6.64 ppm and 6.75 ppm. A long-range coupling through four bonds ($J = 2.4\text{-}3.0$ Hz) was observed between *N*-H and the H-3'/ H-4' protons, possible as they adopt a W arrangement (Figure 53).

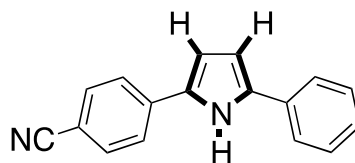


Figure 53. The W arrangement of *N*-H, H-3' and H-4' protons in 4-(5-phenyl-*H*-pyrrol-2-yl)benzonitrile **198**.

To confirm the long-range coupling between *N*-H, H-3' and H-4' protons, a D_2O exchange experiment was completed. Four drops of D_2O were added to the NMR tube and the tube was shaken. The deuterium from D_2O replaces the exchangeable *N*-H proton, which could no longer be observed. Due to the lack of *N*-H coupling, H-3' and

Chapter II. Results and Discussion/ Chemistry

H-4' were each observed as a doublet at 6.65 ppm and 6.81 ppm with J values of 3.9 Hz and 3.6 Hz (Figure 54B).

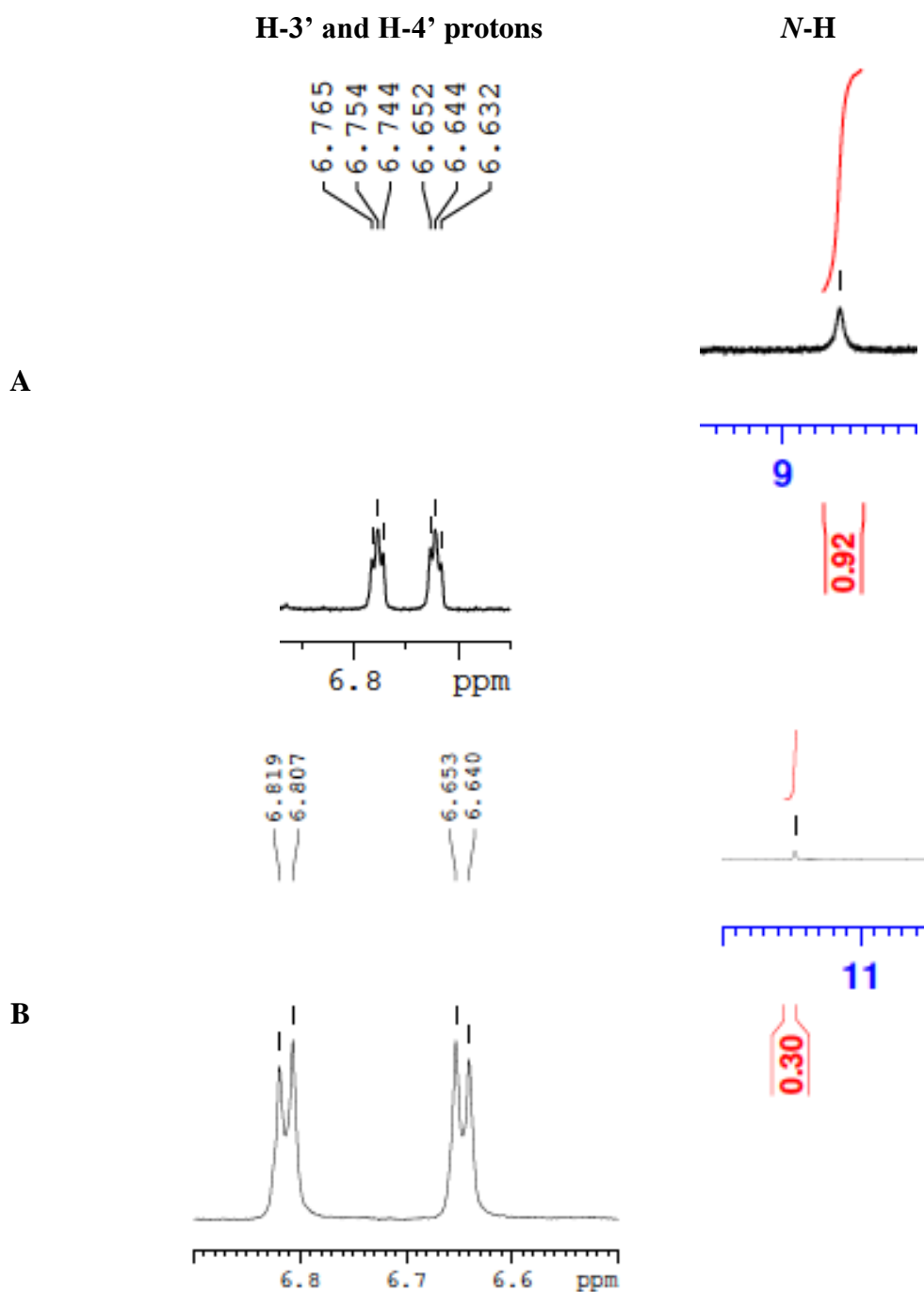


Figure 54. ^1H NMR spectrum of N -H, H-3' and H-4' protons of 4-(5-phenyl- H -pyrrol-2-yl)benzotrile **198**; A-CDCl₃; B- 4 drops of D₂O + CDCl₃.

^{13}C NMR spectroscopy also confirmed the structure of 4-(5-phenyl- H -pyrrol-2-yl)benzotrile **198**. The peaks of C-3' and C-4' of the pyrrole ring were observed at 107.0 ppm and 108.4 ppm and the aryl nitrile peak was observed at 119.3 ppm. Also,

Chapter II. Results and Discussion/ Chemistry

the nitrile peak was observed at 2214 cm^{-1} in the infrared spectrum, which means that the nitrile group remained intact during the reaction conditions.

The structure of 4-(1-methyl-5-phenyl-1*H*-pyrrol-2-yl)benzotrile **199** was confirmed by $^1\text{H-NMR}$ spectroscopy. The protons of the *N*-methyl group were observed as singlet at 3.63 ppm and the H-3' and H-4' protons were observed as doublets at 6.35 ppm (J 3.6 Hz) and 6.51 ppm (J 3.6 Hz). H-2 and H-3 protons were observed as doublets at 7.72 ppm (J 8.1 Hz) and 7.89 ppm (J 8.4 Hz). On the other hand, H-2'' and H-3'' were observed as a multiplet at 7.45-7.54 ppm and H-4'' as a triplet at 7.36 ppm (J 7.2 Hz) (Figure 55).

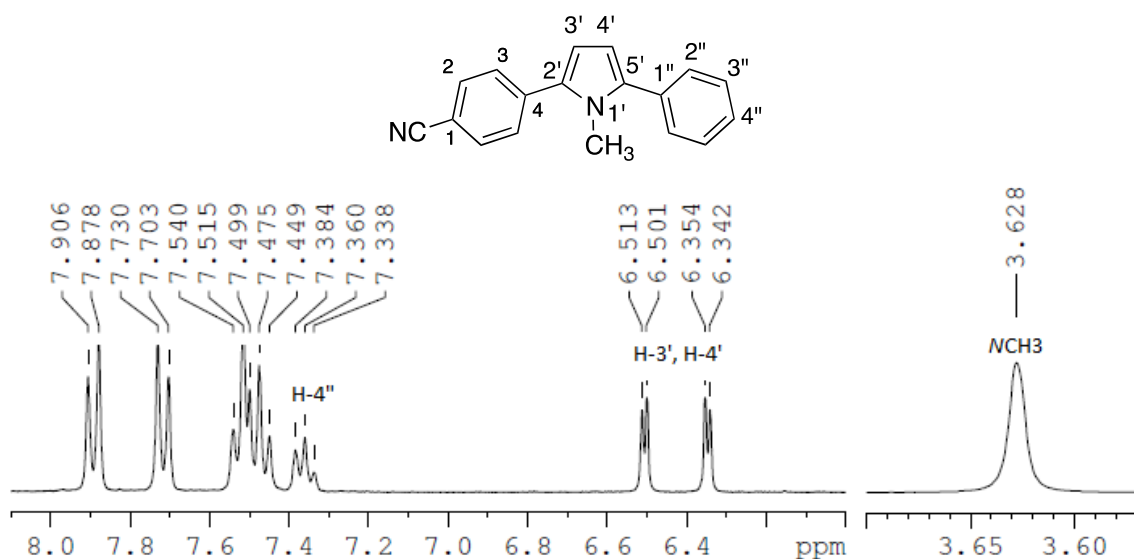
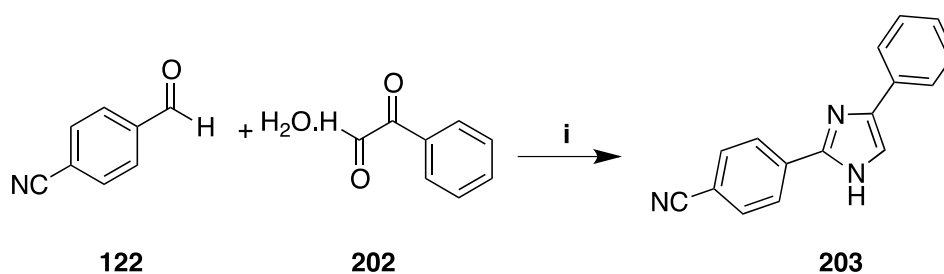


Figure 55. $^1\text{H NMR}$ (DMSO- d_6) spectrum of 4-(1-methyl-5-phenyl-*H*-pyrrol-2-yl)benzotrile **199**.

$^{13}\text{C-NMR}$ spectroscopy confirmed the structure of the 4-(1-methyl-5-phenyl-1*H*-pyrrol-2-yl)benzotrile **199**. The peaks of C-3' and C-4' of the pyrrole ring were observed at 108.2 ppm and 109.2 ppm (Figure 56).

5.1.2. Synthesis of substituted imidazole-amidines **193** and **194**

Two imidazole-amidines, 4-(4-phenyl-1*H*-imidazol-2-yl)benzamidine acetate **193** and *N*-methylimidazole-amidine **194** were synthesized. The first step in the preparation of **193** and **194** was the synthesis of the diarylimidazole **203**. The imidazole **203** was synthesized from the reaction between 4-cyanobenzaldehyde **122** and phenylglyoxal monohydrate **202** in the presence of ammonium acetate (Scheme 43).¹²⁸



Scheme 43. Synthetic pathway of 4-(4-phenyl-1*H*-imidazol-2-yl)benzonitrile **203**;

Reagents and conditions: i- $\text{CH}_3\text{COO}^+\text{NH}_4$, MeOH, rt.

The structure of 4-(4-phenyl-1*H*-imidazol-2-yl)benzonitrile **203** was confirmed by ¹H NMR spectroscopy. The H-3'' and H-4'' were observed as triplets at 7.41 ppm (*J* 7.5 Hz) and 7.25 ppm (*J* 6.9 Hz), respectively. The aryl protons; H-2, H-3, H-4' and H-2'' were present in the range 7.86-8.20 ppm. The *N*-H proton was observed as a broad singlet at 12.98 ppm (Figure 57). The addition of 2 drops of deuterium dioxide led to the disappearance of the *N*-H proton from the ¹H NMR spectrum.

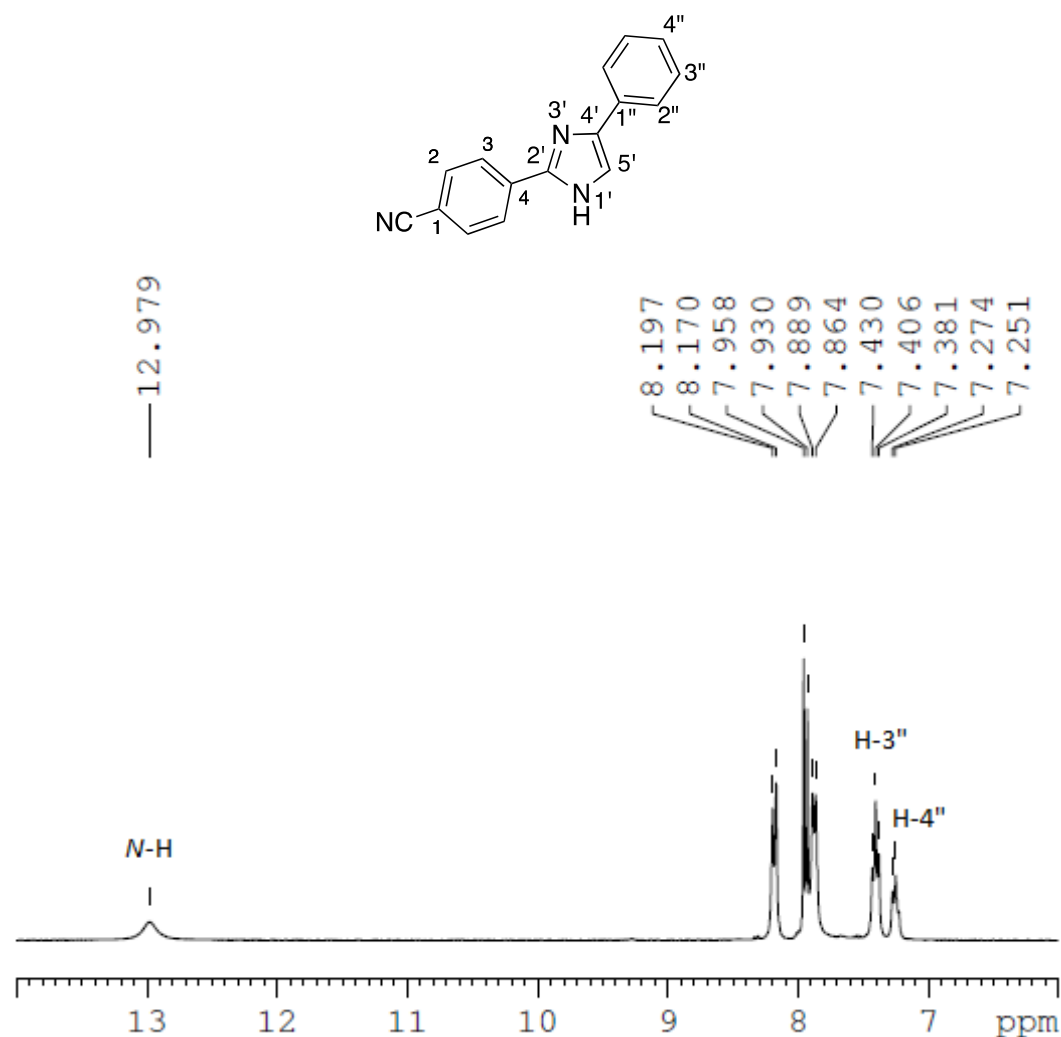
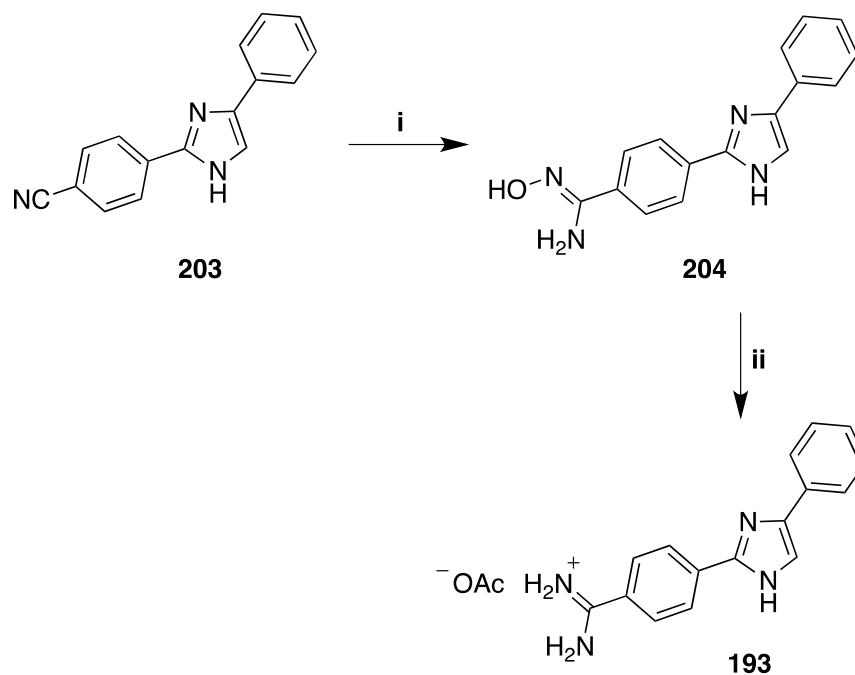


Figure 57. ¹H NMR (DMSO-d₆) spectrum of 4-(4-phenyl-1H-imidazol-2-yl)benzonitrile **203**.

The conversion of the aryl nitrile group in **203** to the amidine using the Pinner synthesis did not work. Attempts to synthesize the ethyl imidate hydrochloride intermediate failed because of the basicity of the nitrogen atom of the imidazole ring (pK_a of the conjugate acid = 6.9). Compound **203** precipitated as hydrochloride salt at the beginning of the reaction in a large range of organic solvents such as chloroform, ethanol and tetrahydrofuran.

The imidazole-amidine **193** was prepared through the conversion of the aryl nitrile in **203** into an amidoxime (*N*-hydroxyamidine) intermediate **204**.¹²⁹ The intermediate **204** was then reduced to afford the imidazole-amidine **193** (Scheme 44).¹³⁰



Scheme 44. Pathway for the synthesis of 4-(4-phenyl-1*H*-imidazol-2-yl)benzamidinium acetate **193**; Reagents and conditions: i- $\text{NH}_2\text{OH}\cdot\text{HCl}$, *t*-BuOK, dry DMSO, 0 °C - rt; ii- $\text{HCOO}^- \text{NH}_4^+$, Pd/C, AcOH, reflux.

The structure of *N*-hydroxy-4-(4-phenyl-1*H*-imidazol-2-yl)benzamidinium **204** was confirmed by ^1H NMR spectroscopy. The *N*-OH and NH_2 protons were observed at 9.75 and 5.85 ppm, respectively (Figure 58), which exchanged with deuterium oxide in the NMR tube.

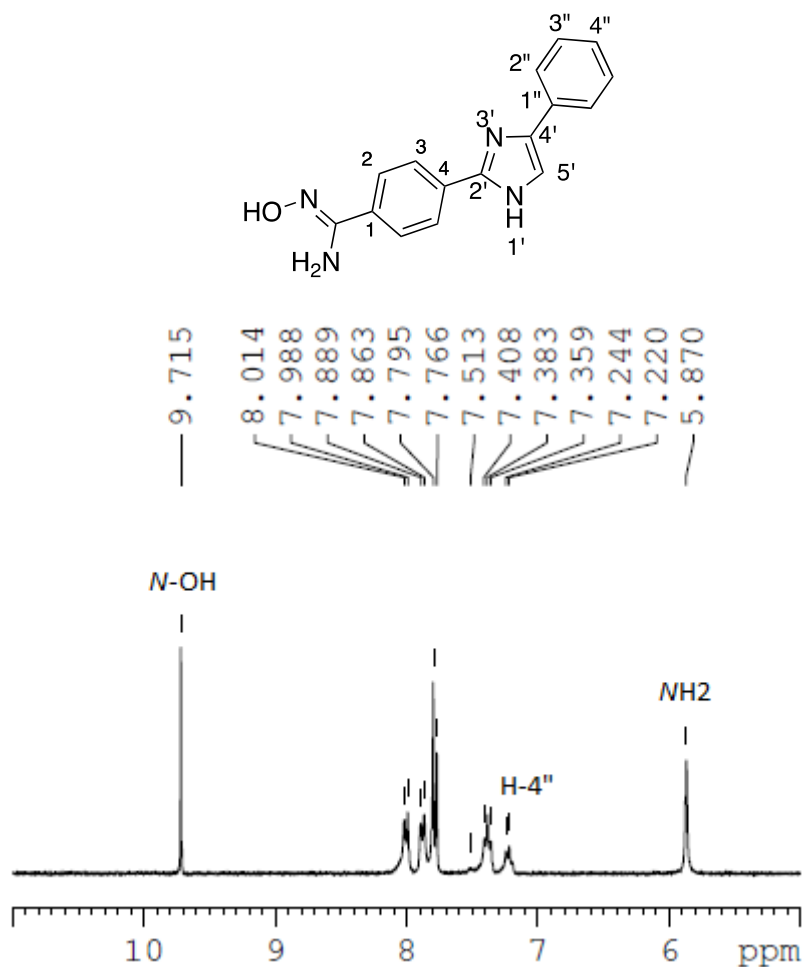


Figure 58. ¹H NMR (DMSO-d₆) spectrum of *N*-hydroxy-4-(4-phenyl-1*H*-imidazol-2-yl)benzamidine **204**.

The reaction of the nitrile group **203** with hydroxylamine to form the amidoxime **204** was confirmed by the absence of the nitrile peak in the IR spectrum (Figure 59). The nitrile stretching frequency was observed at 2228.3 cm⁻¹ in the IR spectrum of **203**.

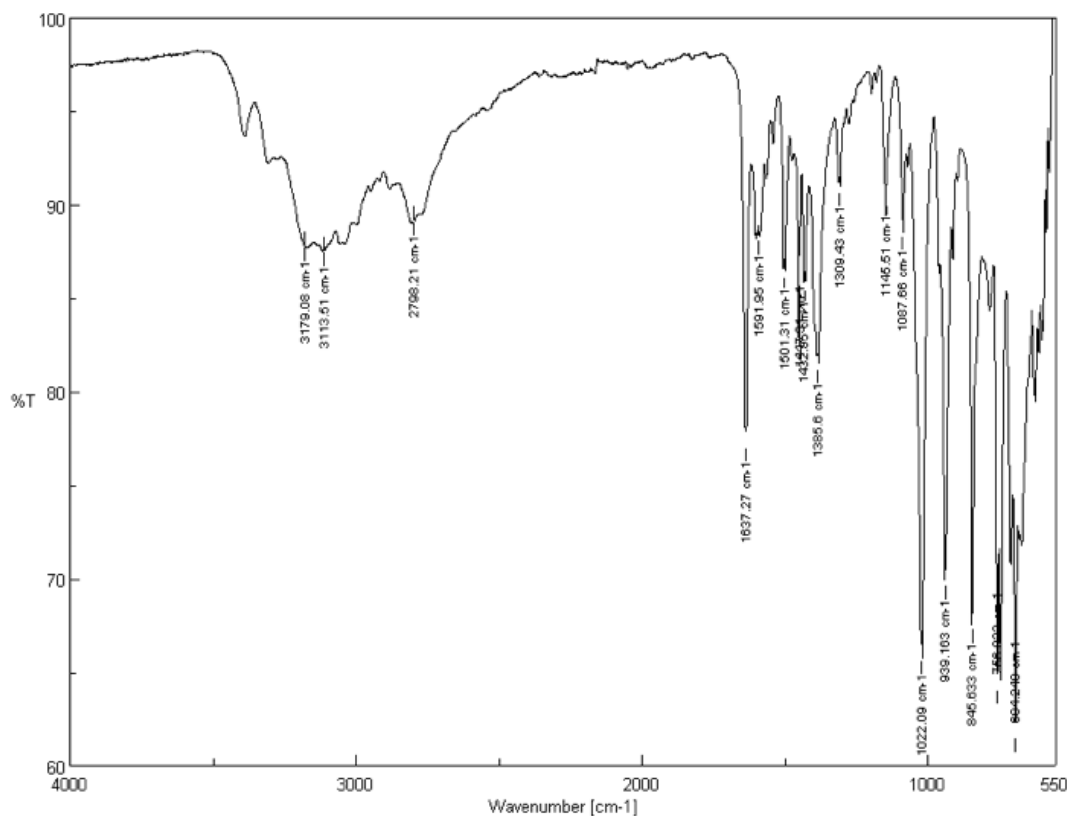
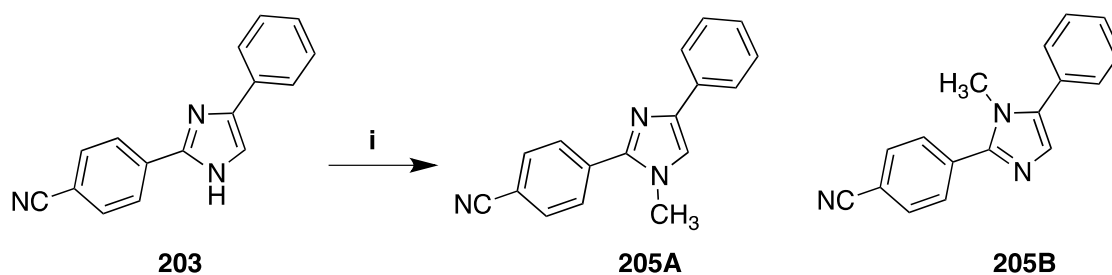


Figure 59. IR spectrum of *N*-hydroxy-4-(4-phenyl-1*H*-imidazol-2-yl)benzamidinium **204**.

The conversion of amidoxime **204** into amidine **193** was accomplished by catalytic hydrogen-transfer using ammonium formate as the source of hydrogen. The catalytic hydrogen-transfer is the use of an organic molecule as a donor for hydrogen in the presence of a metal catalyst.¹³¹ The structure of 4-(4-phenyl-1*H*-imidazol-2-yl)benzamidinium acetate **193** was confirmed by observing the amidine carbon in the ¹³C-NMR spectrum at 165.4 ppm. The carbon of the amidoxime group in **204** was observed at 150.3 ppm in the ¹³C-NMR spectrum.

N-Methylimidazole **205** was synthesized from the reaction of 4-(4-phenyl-1*H*-imidazol-2-yl)benzimidinium acetate **203** with iodomethane (Scheme 45). There is a possibility to get two regioisomers **205A** or **205B** from the reaction of 4-(4-phenyl-1*H*-imidazol-2-yl)benzimidinium acetate **203** with iodomethane.

Chapter II. Results and Discussion/ Chemistry



Scheme 45. Pathway for the synthesis of the *N*-methylimidazole regioisomers **205A** and **205B**; Reagents and conditions: *i*- CH₃I, KOH, acetone, rt.

Depending on the ¹H NMR spectrum of the imidazole **205**, the methyl group was added to the acidic nitrogen of the imidazole tautomer **203**. ¹H NMR spectrum of **205** (Figure 60) showed the disappearance of the *N*-H proton that was observed in the ¹H-NMR spectrum of **203** at 12.98 ppm (see Figure 57). The protons H_a and H_b were observed as doublets at 7.97 ppm (*J* 8.7 Hz) and 8.00 ppm (*J* 8.7 Hz). The protons H_c, H_d, H_e and H_f were observed as a singlet at 7.86 ppm, a doublet at 7.81 ppm (*J* 7.2 Hz), a triplet at 7.39 ppm (*J* 7.8 Hz) and a triplet at 7.23 ppm (*J* 7.2 Hz), respectively.

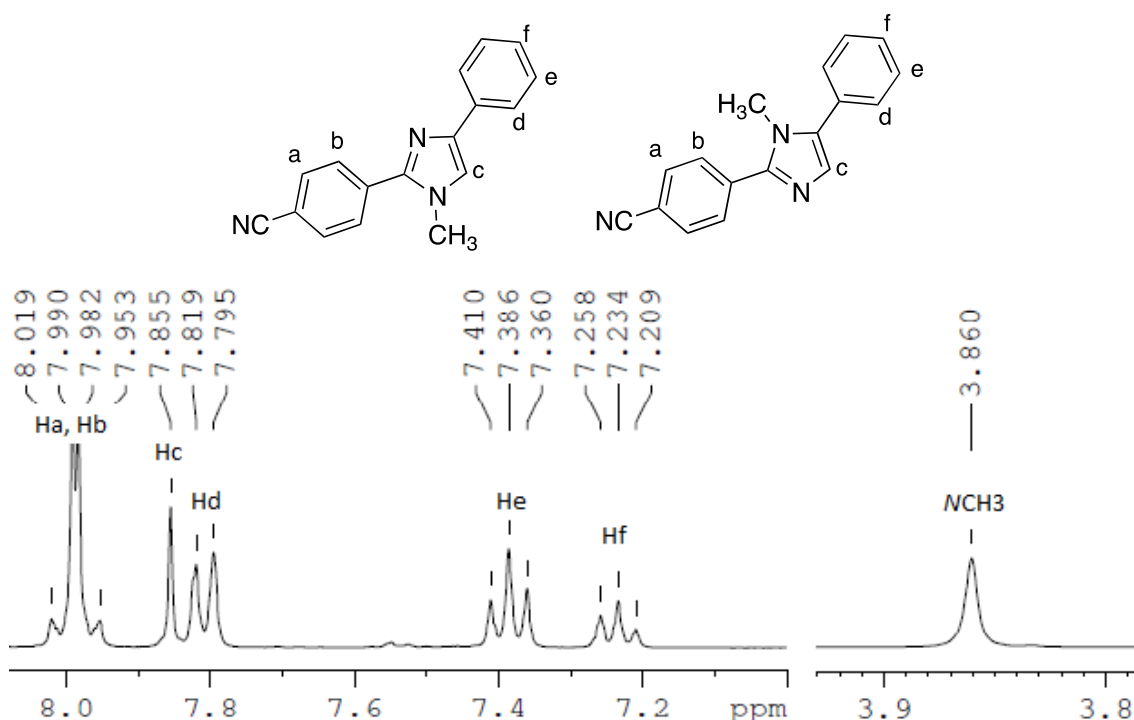


Figure 60. ¹H NMR (DMSO-d₆) spectrum of *N*-methylimidazole regioisomers **205A** and **205B**.

Chapter II. Results and Discussion/ Chemistry

The regioisomer **205A** was formed from the reaction of 4-(4-phenyl-1*H*-imidazol-2-yl)benzonitrile **203** with iodomethane as confirmed by the NOESY spectrum (Figure 61). A long-range interaction between the *N*-methyl protons and H-5' can be observed from the NOESY spectrum. The formation of the regioisomer **205A** can be explained by an easier attack of *N*-1' by iodomethane, as *N*-3' is more sterically hindered as it is adjacent to two aryl rings.

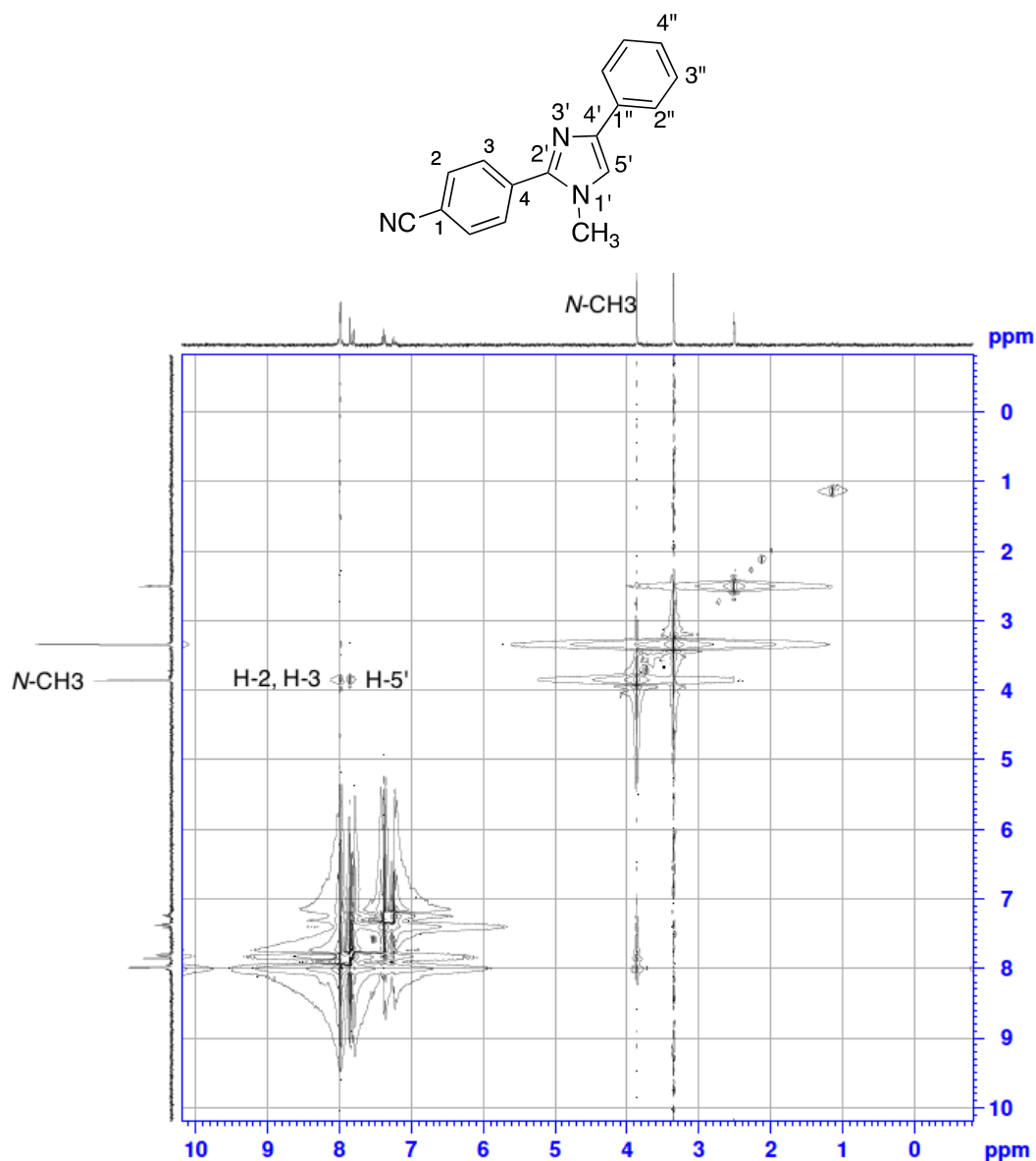
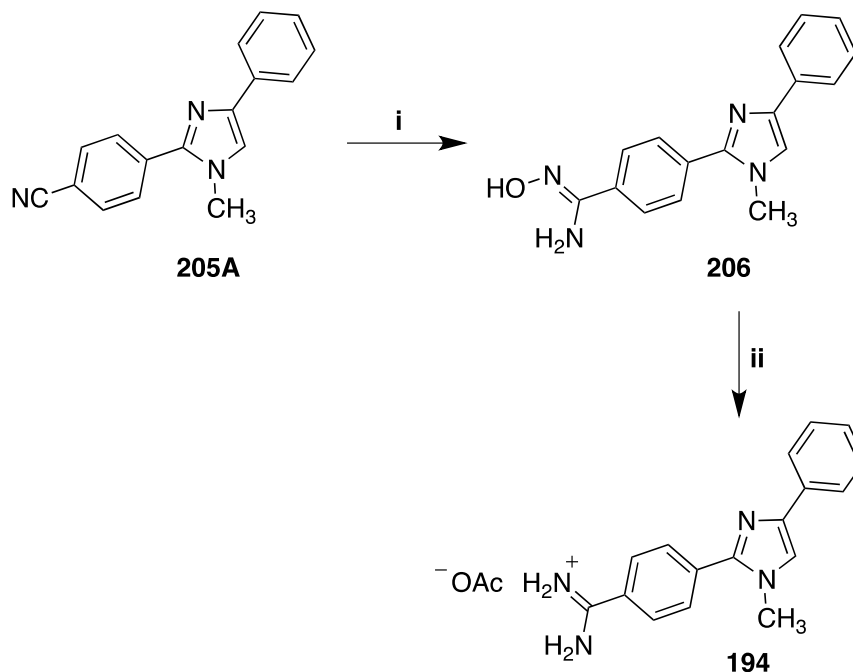


Figure 61. The NOESY (DMSO-*d*₆) spectrum of 4-(1-methyl-4-phenyl-1*H*-imidazol-2-yl)benzonitrile **205A**.

Chapter II. Results and Discussion/ Chemistry

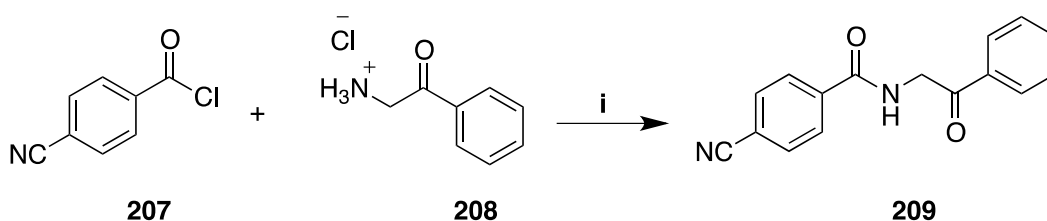
4-(1-Methyl-4-phenyl-1*H*-imidazol-2-yl)benzamidine **194** was synthesized from 4-(1-methyl-4-phenyl-1*H*-imidazol-2-yl)benzonitrile **205A** through the formation of the *N*-hydroxyamidine intermediate **206** (Scheme 46).



Scheme 46. Synthetic pathway for 4-(1-methyl-4-phenyl-1*H*-imidazol-2-yl)benzamidine acetate **194**; Reagents and conditions: i- $\text{NH}_2\text{OH}\cdot\text{HCl}$, $t\text{-BuOK}$, dry DMSO, $0\text{ }^\circ\text{C}$ - rt; ii- $\text{HCOO}^- \text{NH}_4^+$, Pd/C, AcOH, reflux.

5.1.3. Synthesis of oxazole-amidine **195**

The oxazole-amidine **195** was synthesized from the key precursor 4-cyano-*N*-(2-oxo-2-phenylethyl)benzamide **209**. First the benzamide **209** was prepared from the coupling between 4-cyanobenzoyl chloride **207** and 2-amino-1-phenylethanone hydrochloride **208** in the presence of sodium bicarbonate as the base (Scheme 47).¹³²



Scheme 47. Reaction for the synthesis of 4-cyano-*N*-(2-oxo-2-phenylethyl)benzamide **209**; Reagents and conditions: i- NaHCO_3 , DCM, $0\text{ }^\circ\text{C}$ - rt.

Chapter II. Results and Discussion/ Chemistry

The identification of 4-cyano-*N*-(2-oxo-2-phenylethyl)benzamide **209** was confirmed by ^1H NMR spectroscopy. The protons *N*-H, H-1', H-3'', H-4'' were observed as a triplet at 9.16 ppm (J 5.7 Hz), a doublet at 4.83 ppm (J 5.7 Hz), a triplet at 7.58 ppm (J 7.8 Hz) and a triplet at 7.70 ppm (J 7.2 Hz), respectively. The protons H-2, H-3 and H-2'' were observed as a multiplet at 7.99-8.08 ppm (Figure 62).

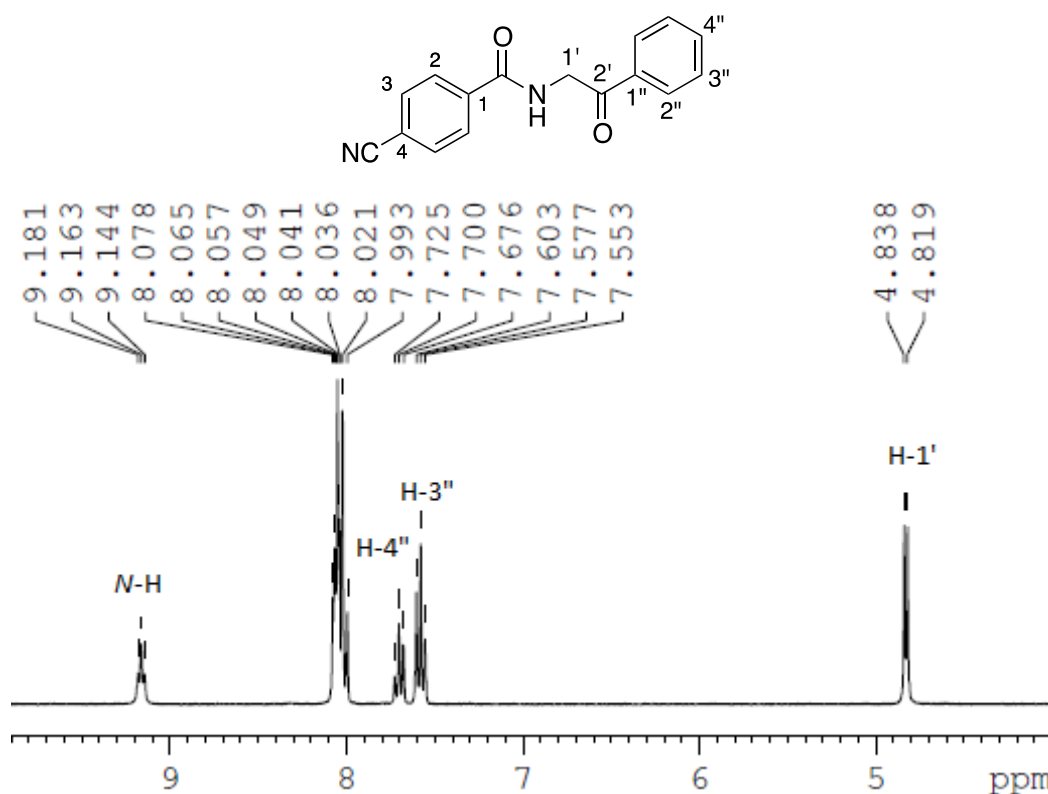
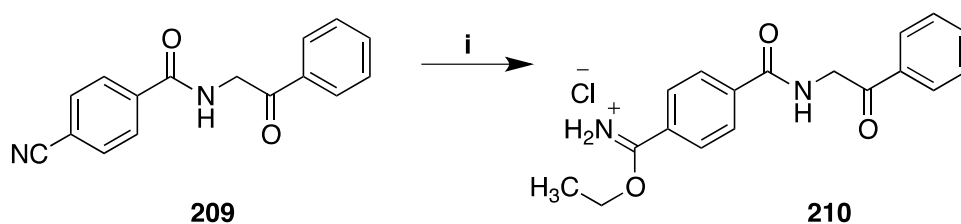


Figure 62. ^1H NMR (DMSO- d_6) spectrum of 4-cyano-*N*-(2-oxo-2-phenylethyl)benzamide **209**.

It was then anticipated that hydrogen chloride gas would both cyclize **209** to the oxazole and convert the aryl nitrile to the imidate, however only ethyl 4-((2-oxo-2-phenylethyl)carbamoyle)benzimidate hydrochloride **210** was formed without the cyclization of the oxazole heterocycle (Scheme 48). The structure of **210** was confirmed by ^1H NMR spectroscopy and IR spectroscopy. The formation of ethyl imidate **210** was confirmed by the appearance of methyl and methylene proton peaks as a triplet at 1.51 ppm (J 6.9 Hz) and a quartet at 4.66 ppm (J 6.9 Hz), respectively, in ^1H NMR spectrum. IR spectroscopy confirmed the disappearance of the nitrile peak, but also the presence of two carbonyl groups (ketone stretching was observed at 1694 cm^{-1} and secondary amide stretching was observed at 1647 cm^{-1} and 1533 cm^{-1}) for the non-cyclized

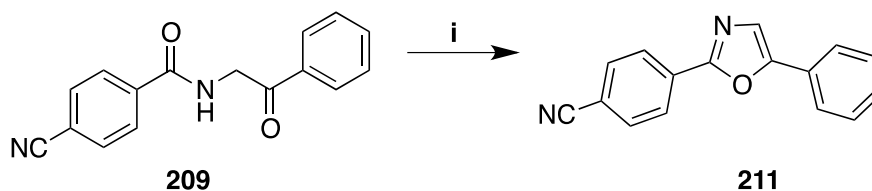
Chapter II. Results and Discussion/ Chemistry

compound. The absence of cyclization was also consistent with a doublet peak in the ^1H NMR spectrum at 4.84 ppm (J 5.7 Hz) integrating to 2H for H-1”.



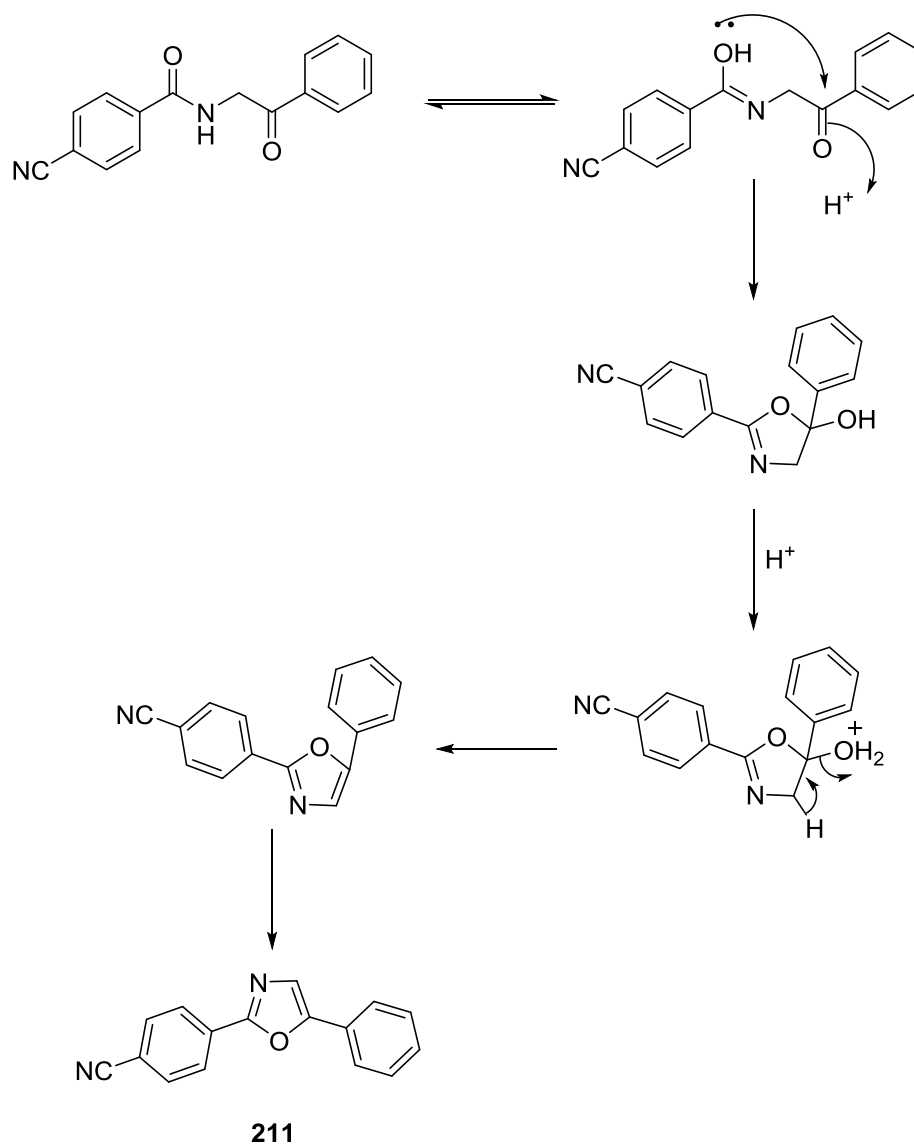
Scheme 48. Synthetic pathway for 4-((2-oxo-2-phenylethyl)carbamoyl)benzimidate hydrochloride **210**; Reagents and conditions: i- $\text{HCl}_{(\text{g})}$, EtOH, CHCl_3 , $0\text{ }^\circ\text{C}$ - rt.

The cyclization to the oxazole was accomplished under alternative conditions: the reaction of 4-cyano-*N*-(2-oxo-2-phenylethyl)benzamide **209** in acetic anhydride with a few drops of concentrated sulfuric acid at room temperature led to the formation of the 2,5-diphenyloxazole ring **211** within minutes (Scheme 49).



Scheme 49. Pathway for the synthesis of 4-(5-phenyloxazol-2-yl)benzonitrile **211**; Reagents and conditions: i- Ac_2O , conc. H_2SO_4 , rt.

The formation of an oxazole from the dehydration of 2-acylaminoketone is known as Robinson-Gabriel synthesis.¹³³ The study of the mechanism of the reaction showed that the oxygen of the amide is involved in the oxazole ring formation and the oxygen of the ketone group is expelled during the reaction (Scheme 50).¹³⁴



Scheme 50. The mechanism for the synthesis of 2,5-diaryloxazole **211**.

The product 4-(5-phenyloxazol-2-yl)benzonitrile **211** was characterized by ^1H NMR spectroscopy. The H-4' proton of the oxazole ring was observed as a singlet at 7.97 ppm (Figure 63). The nitrile had not reacted, as confirmed by the IR spectrum.

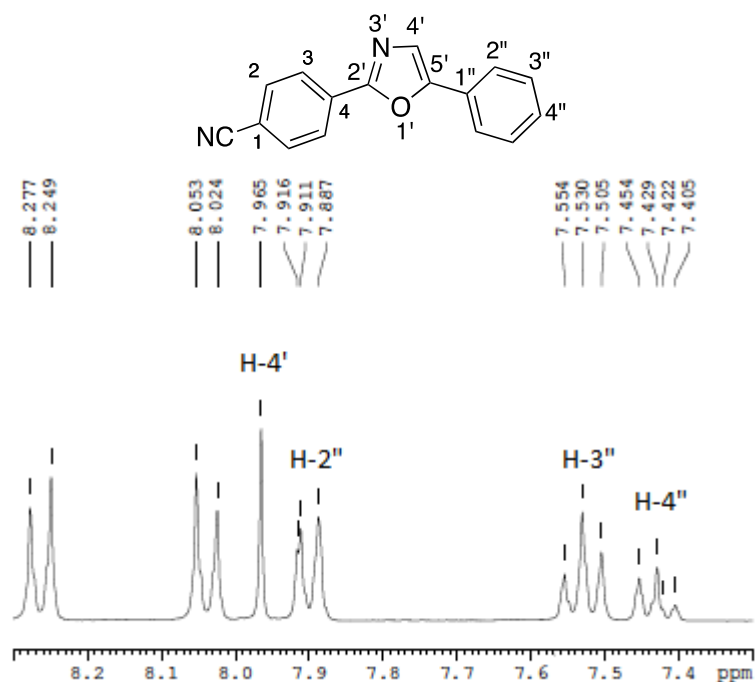
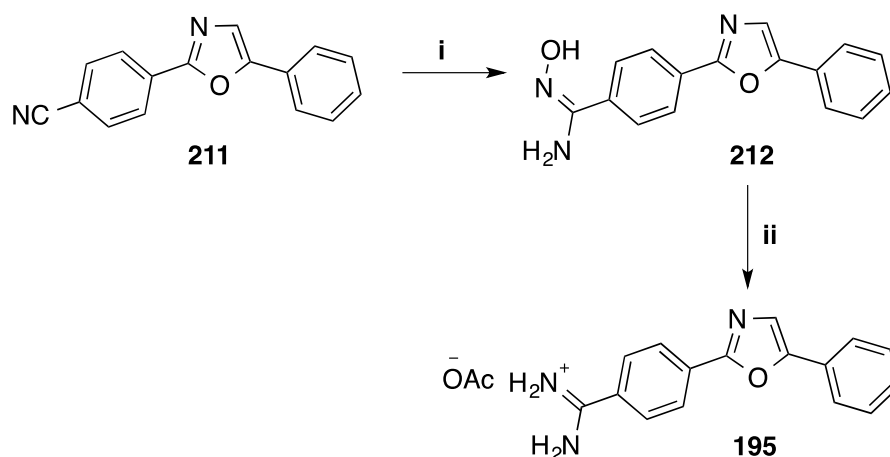


Figure 63. ^1H NMR (DMSO- d_6) spectrum of 4-(5-phenyloxazol-2-yl)benzonitrile **211**.

4-(5-Phenyloxazol-2-yl)benzonitrile **211** was converted to the oxazole-amidine **195** through the formation of the amidoxime intermediate **212**. The reduction of the amidoxime **212** resulted in the formation of amidine **195** (Scheme 51). The structure of the amidine **195** was confirmed by ^1H NMR spectroscopy.



Scheme 51. Pathway for the synthesis of 4-(5-phenyloxazol-2-yl)benzamidinium acetate **195**; Reagents and conditions: i- $\text{NH}_2\text{OH}\cdot\text{HCl}$, $t\text{-BuOK}$, dry DMSO, $0\text{ }^\circ\text{C}$ - rt; ii- $\text{HCOO}^- \text{ } ^+\text{NH}_4$, Pd/C, AcOH, reflux.

5.2. Hypothesized correlation between compound structure and NQO2 inhibitory activity

The overall objective of the research is the synthesis of novel, potent and selective inhibitors of the NQO2 enzyme. Many isosteric replacements and structural modifications of the lead asymmetric furan-amidine **110** have been completed in the search for a potent NQO2 inhibitor with optimal drug-like properties.

5.2.1. Synthesis of an asymmetric 3,4-disubstituted furan-amidine

The best lead furan-amidine with the highest inhibition activity against the NQO2 enzyme was the symmetric 3,4-dimethyl-substituted furan-amidine **112** (Figure 64 and Table 10) with an IC₅₀ of 50 nM.⁸² As the symmetric furan-amidines are known to be DNA intercalators, an asymmetric 3,4-dimethylfuran-amidine **213** (Figure 64) may prove to be a potent and selective NQO2 inhibitor without off-target effects, e.g. DNA intercalation.

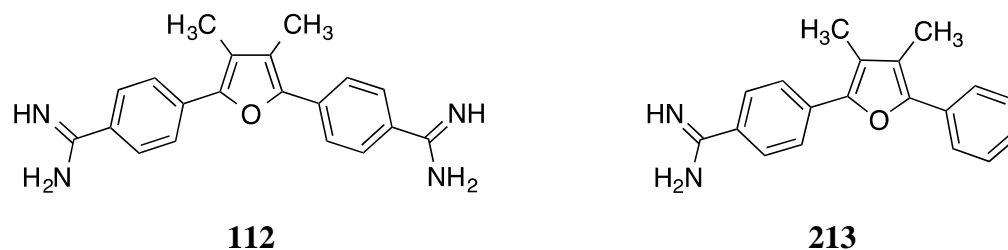
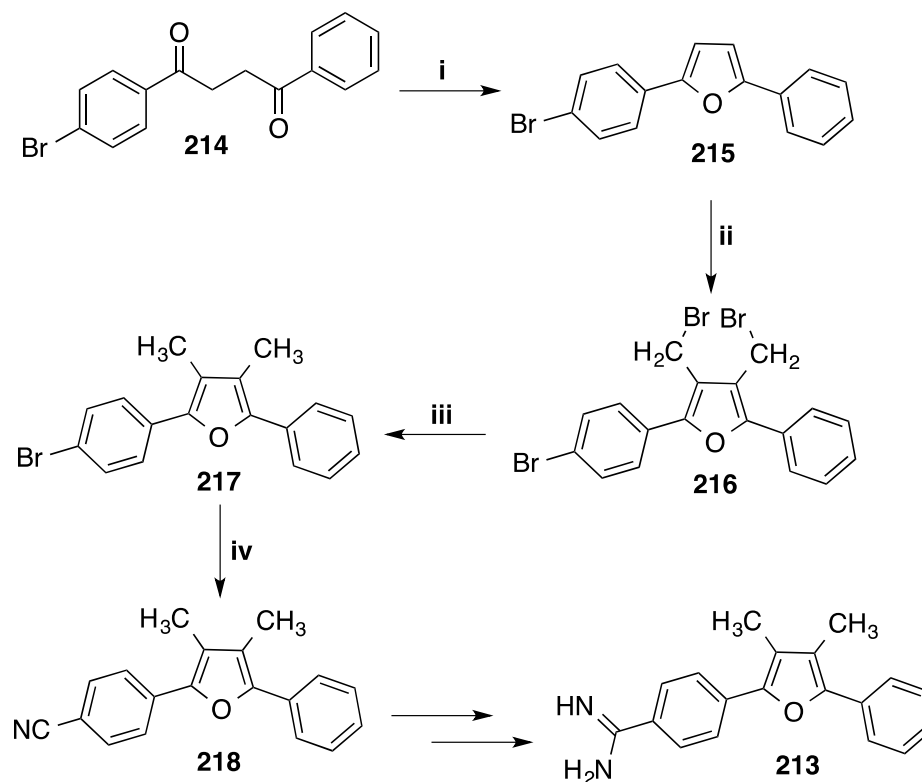


Figure 64. Structures of the symmetric furan-amidine **112** and the proposed asymmetric 3,4-dimethylfuran-amidine **213**.

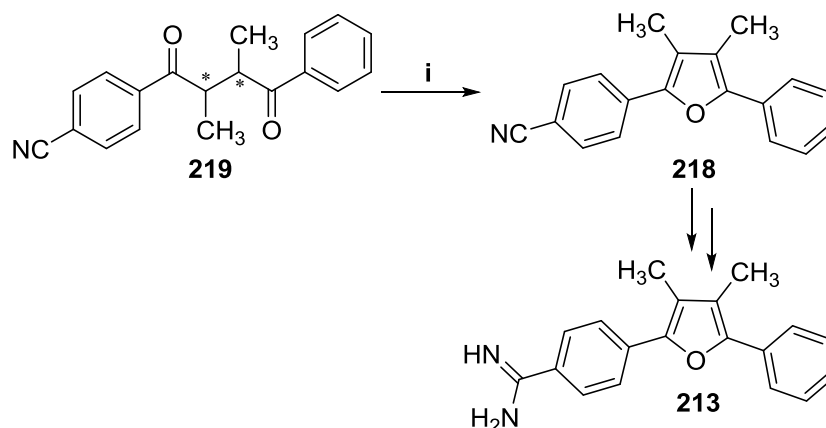
The synthesis of furan-amidine **213** utilises 2,5-diphenylfuran **215** as the starting material. Heating 2,5-diphenylfuran **215** at reflux with paraformaldehyde in 33% (wt) HBr in acetic acid solution gave 3,4-di(bromomethyl)furan **216**. The bromomethyl substituents on C-3 and C-4 of the furan ring **216** were reduced into methyl groups **217** using lithium aluminum hydride (LiAlH₄) to give **217**.¹⁰⁸ The methylation of C-3 and C-4 of the furan ring is not possible if the nitrile group is present in the compound as the reaction conditions are too harsh for the nitrile group. Consequently, the starting 1,4-diketone **214** in this synthetic pathway has a *para*-bromine atom, which is substituted by copper cyanide to give **218** (Scheme 52).



Scheme 52. Synthetic pathway for the preparation of 4-(3,4-dimethyl-5-phenylfuran-2-yl)benzamidine **213**; Reagents and conditions: i- Ac_2O , H_2SO_4 , reflux; ii- paraformaldehyde, 33% wt HBr in AcOH, reflux; iii- LiAlH_4 , dry THF, rt; iv- CuCN , quinoline, reflux.

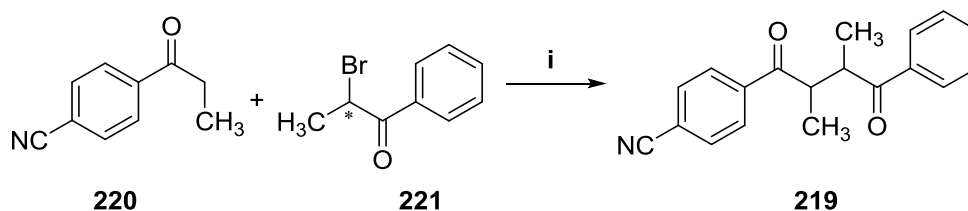
To avoid the use of the toxic copper cyanide, an alternative synthesis of the asymmetric furan-amidine **213** was proposed starting from the preparation of the key aryl-substituted 1,4-diketones intermediate **219**, which has a nitrile group as the amidine precursor (Scheme 53).

Chapter II. Results and Discussion/ Chemistry



Scheme 53. Proposed alternative synthetic pathway for the preparation of 4-(3,4-dimethyl-5-phenylfuran-2-yl)benzamidine **213**; Reagents and conditions: i- Ac_2O , H_2SO_4 , reflux .

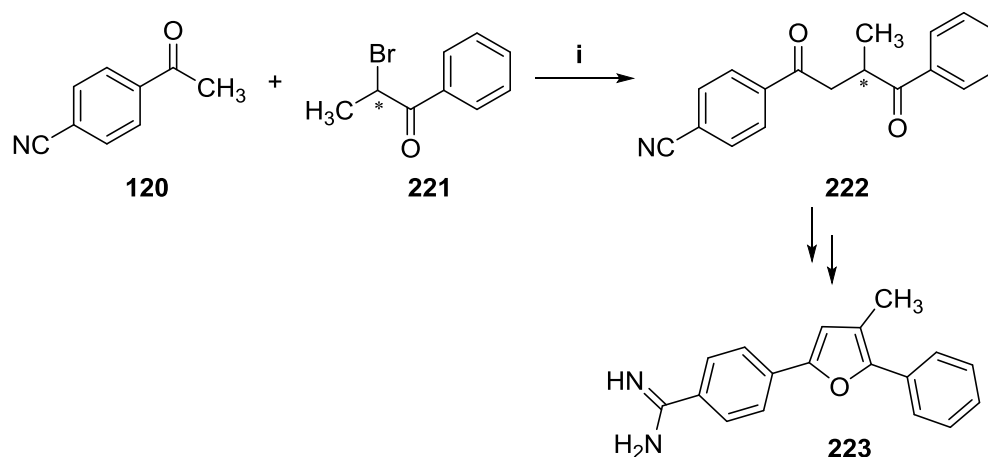
The synthesis of 1,4-diketone **219** was proposed from the coupling between ethyl aryl ketone **220** and the α -bromoethyl aryl ketone **221** using diethylamido magnesium bromide as condensation agent (Scheme 54). Diethylamido magnesium bromide is prepared *in situ* from the reaction between ethyl magnesium bromide and diethylamine.¹³⁵



Scheme 54. Synthetic pathway of the 1,4-diketone **219**; Reagents and condirions: i- EtMgBr , Et_2NH , dry THF, $0\text{ }^\circ\text{C}$ - rt.

The ethyl aryl ketone **220** is commercially available on a kilogram scale. The difficulty of purchasing smaller quantities of this reagent led to the proposal of the synthesis of aryl mono-substituted 1,4-diketone **222** to serve as an intermediate in the synthesis of the 4-methylfuran-amidine **223** (Scheme 55). The 1,4-diketone **222** was synthesized through the coupling between the methyl aryl ketone **120** and α -bromomethyl aryl ketone **221** using *in situ* prepared diethylamido magnesium bromide, followed by triethylamine.

Chapter II. Results and Discussion/ Chemistry



Scheme 55. Pathway for the synthesis of 4-(4-methyl-5-phenylfuran-2-yl)benzamide **223**; Reagents and conditions: i- EtMgBr, Et₂NH, dry THF, 0 °C - rt.

Unexpectedly, the condensation of the methyl aryl ketone **120** and α -bromomethyl aryl ketone **221** led to the formation of the furan 4-(4-methyl-5-phenylfuran-2-yl)benzamide **223** instead of the expected 1,4-diketone **222**. The structure of compound **223** was confirmed by ¹H (Figure 65) and ¹³C NMR spectroscopy.

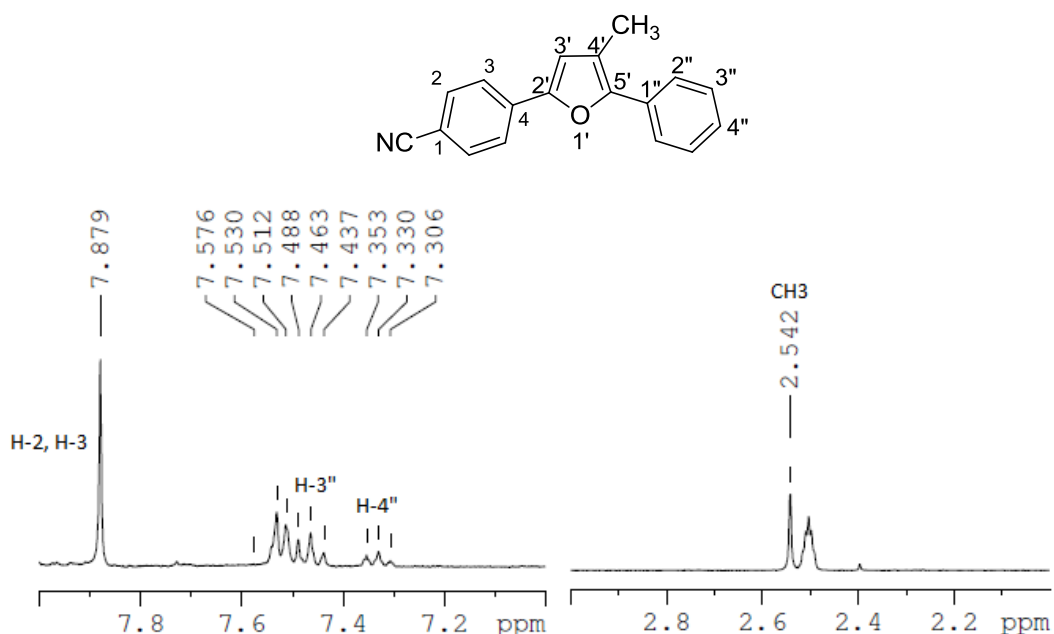


Figure 65. ¹H NMR (DMSO-d₆) spectrum for the furan compound 4-(4-methyl-5-phenylfuran-2-yl)benzamide **223**.

Chapter II. Results and Discussion/ Chemistry

The nitrile group of **224** was observed at 2224 cm^{-1} in the IR spectrum and no peaks were observed for ketone groups, which confirmed that cyclization to give the furan ring had occurred (Figure 66).

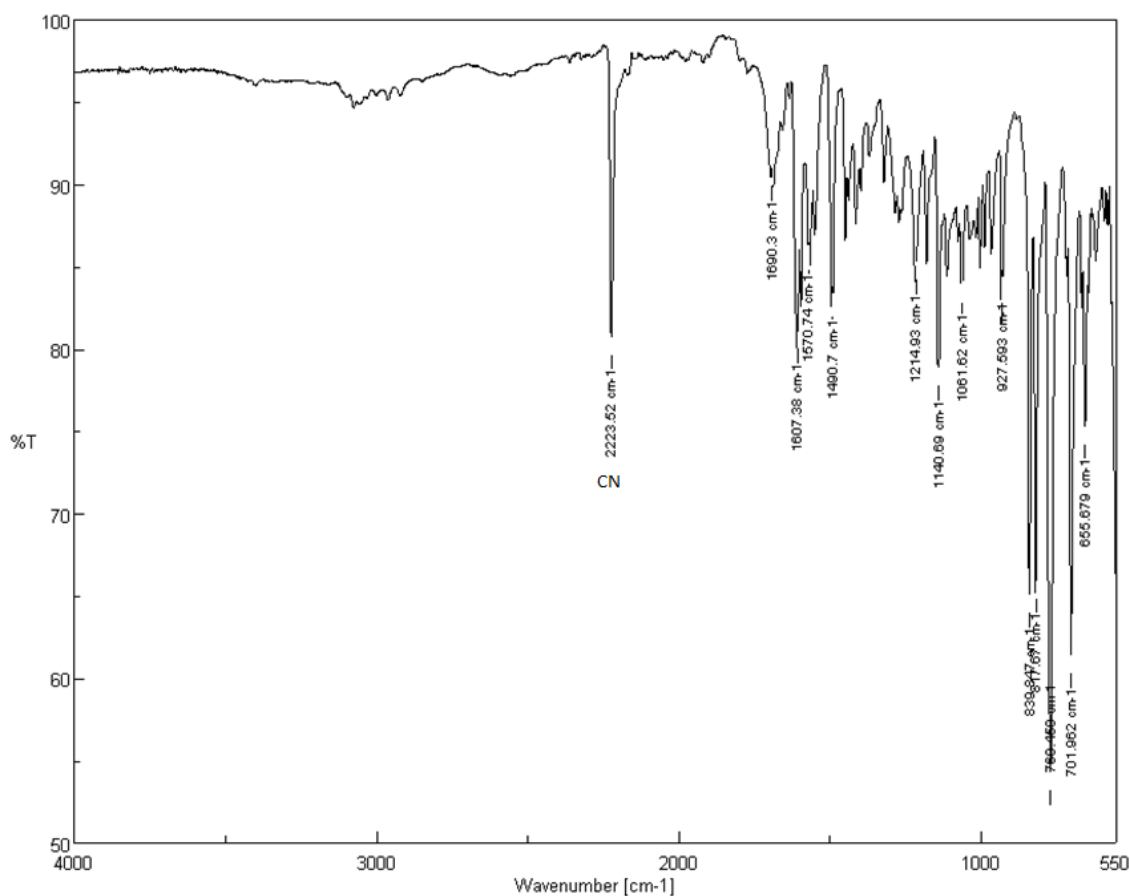
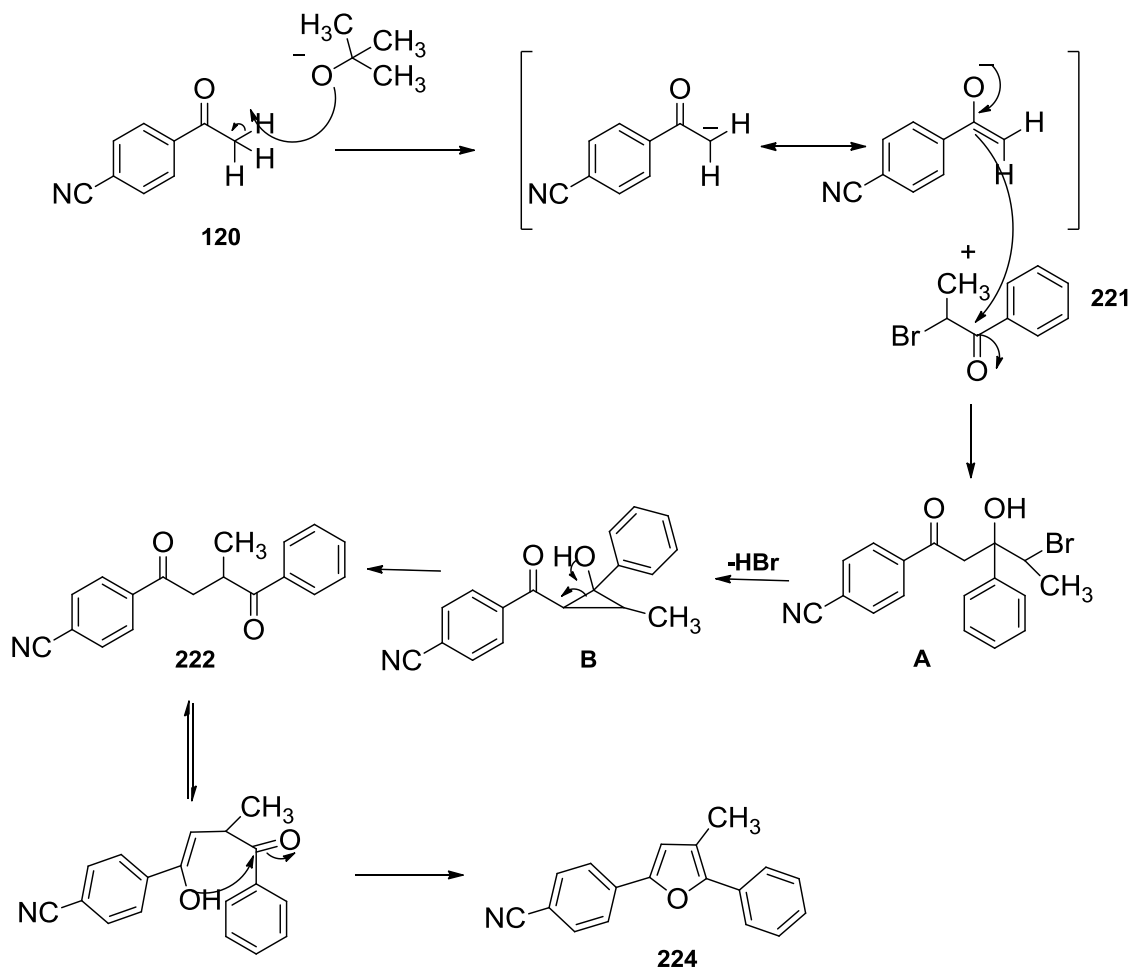


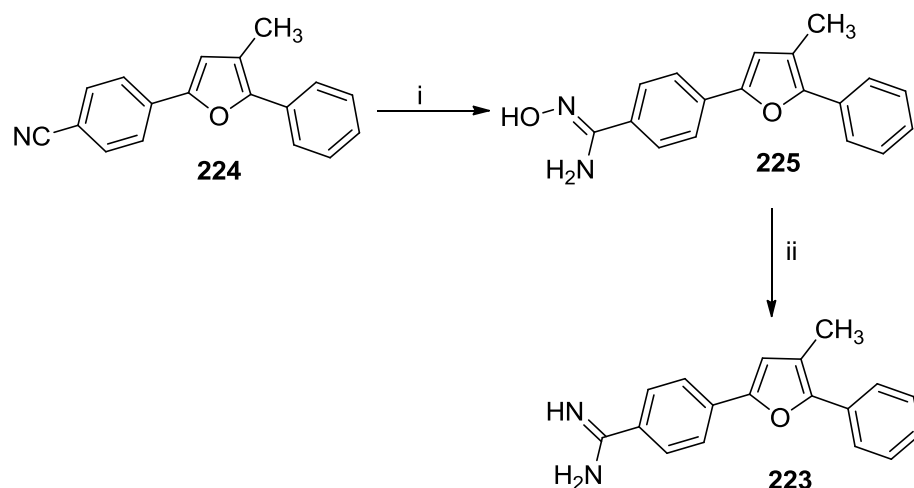
Figure 66. IR spectrum of 4-(4-methyl-5-phenylfuran-2-yl)benzonitrile **224**.

In the mechanism of the reaction to prepare the 1,4-diketone **222** the enolate anion of **120** attacks the carbonyl group of the α -bromoethyl aryl ketone **221** forming the 4-bromo-3-hydroxyketone intermediate **A**. The 4-bromo-3-hydroxyketone intermediate **A** converts to the 1,4-diketone **222** through the formation of the unstable cyclopropane intermediate **B**. Under the basic conditions the presence of the methyl group in **222** caused the diketone to cyclise to give the furan **224** (Scheme 56).



Scheme 56. Mechanism for the synthesis of 4-(4-methyl-5-phenylfuran-2-yl)benzonitrile **224**.

The nitrile group of **224** was converted into amidine **223** through the formation of the amidoxime **225** (Scheme 57). The use of amidoxime as an intermediate in the synthesis of amidine is fully discussed in section 5.1.2.



Scheme 57. Pathway for the synthesis of 4-(4-methyl-5-phenylfuran-2-yl)benzamidine **223** via amidoxime intermediate **225**; Reagents and conditions: i- Ac₂O, conc. H₂SO₄, reflux; ii- NH₂OH·HCl, *t*-BuOK, dry DMSO, 0 °C - rt.

5.2.2. Synthesis of the asymmetric 2,5-diarylthiophene-amidine **226**

The thiophene-amidine **226** (Figure 67), an analogue of the lead asymmetric furan-amidine **110**, is expected to be a potential inhibitor of NQO2 as the active site is highly hydrophobic in nature, leading to the preference of the hydrophobic inhibitors. Thiophene is a 5-membered ring heterocycle analogue of furan, which is more hydrophobic than the furan itself.

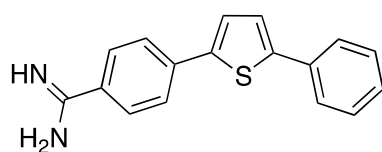
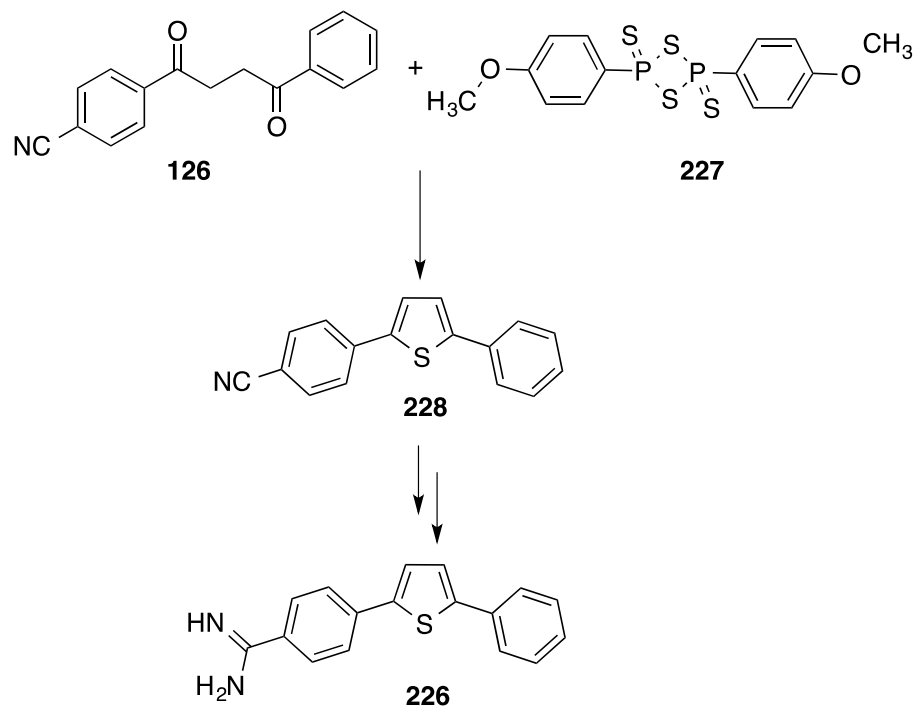


Figure 67. The structure of thiophene-amidine **226**.

The synthesis of the thiophene-amidine **226** first required the preparation of 2,5-diarylthiophene **228** from the reaction between the 1,4-diketone **126** and Lawesson's reagent **227** (Scheme 58).

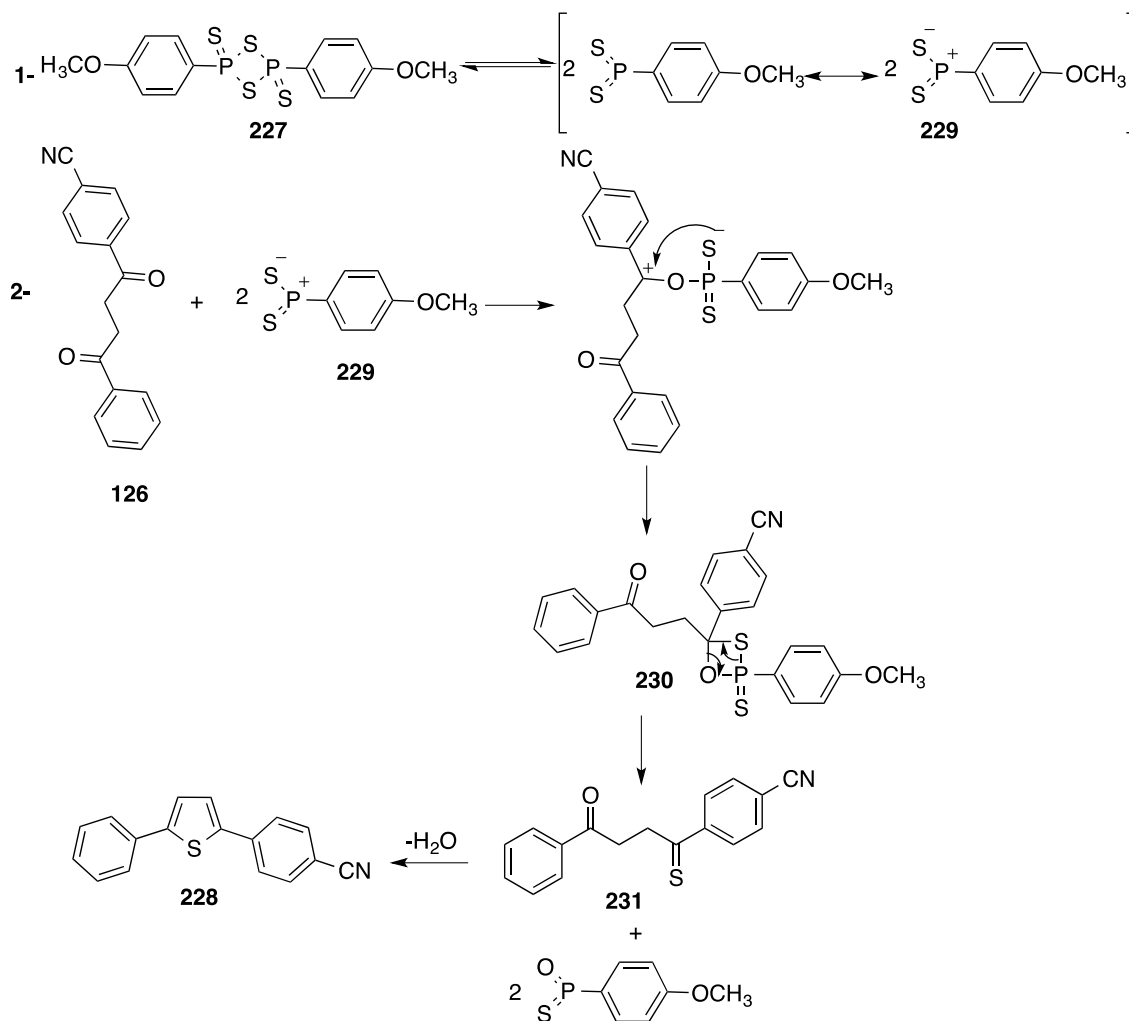


Scheme 58. Synthetic pathway for the preparation of the asymmetric 4-(5-phenylthiophen-2-yl)benzamidinium **226**.

In general, 2,5-diarylthiophenes, such as **228** are synthesized starting from 1,4-diketones using different thionation agents. Thionation agents can be either inorganic phosphorus compound such as sulfur pentasulfide (P_4S_{10}) or organophosphorus compounds, such as Lawesson's reagent (2,4-bis-(*p*-methoxyphenyl)-1,2,3,4-dithiaphosphetane disulfide) **227**. The use of phosphorus pentasulfide as a thionation agent for the cyclization of 1,4-diketones into 2,5-diarylthiophene has many limitations. These limitations include the need for a large excess of phosphorus pentasulfide, long reaction times, the formation of tarry by-products and variable low yields of 2,5-diarylthiophene are usually obtained.¹³⁶

The use of Lawesson's reagent is preferred because of the mild reaction conditions together with higher yields of pure 2,5-diarylthiophenes. In general, the heating of Lawesson's reagent **227** results in the formation of a highly reactive dithiophosphine ylide **229**, which is in equilibrium with **227**. The dithiophosphine ylide **229** reacts with the 1,4-diketones **126** forming a thioxaphosphetane intermediate **230**, which decomposes to the corresponding thioketone **231** (Scheme 59).^{136b} Finally, spontaneous dehydration of the thioketone **231** yields the 2,5-diarylthiophene **228**.¹³⁷

Chapter II. Results and Discussion/ Chemistry



Scheme 59. Mechanism for the synthesis of 2,5-diarylthiophene **228** using Lawesson's reagent **227**.

The structure of 4-(5-phenylthiophen-2-yl)benzonitrile **228** was confirmed by ^1H NMR and IR spectroscopy. The H-3' and H-4' protons of the thiophene ring were each observed as doublets downfield at 7.64 ppm (J 3.9 Hz) and 7.79 ppm (J 3.9 Hz). Surprisingly, the aryl protons H-2 and H-3 were observed as a singlet integrating to 4H at 7.90 ppm. On the other hand, the aryl protons H-2'', H-3'' and H-4'' were observed as a doublet at 7.74 ppm (J 7.5 Hz), a triplet at 7.47 ppm (J 7.5 Hz) and a triplet at 7.37 ppm (J 7.5 Hz), respectively.

Chapter II. Results and Discussion/ Chemistry

The IR spectrum of **228** showed the presence of the nitrile group at 2227 cm^{-1} , which means that the nitrile was not affected by the reaction conditions (Figure 68).

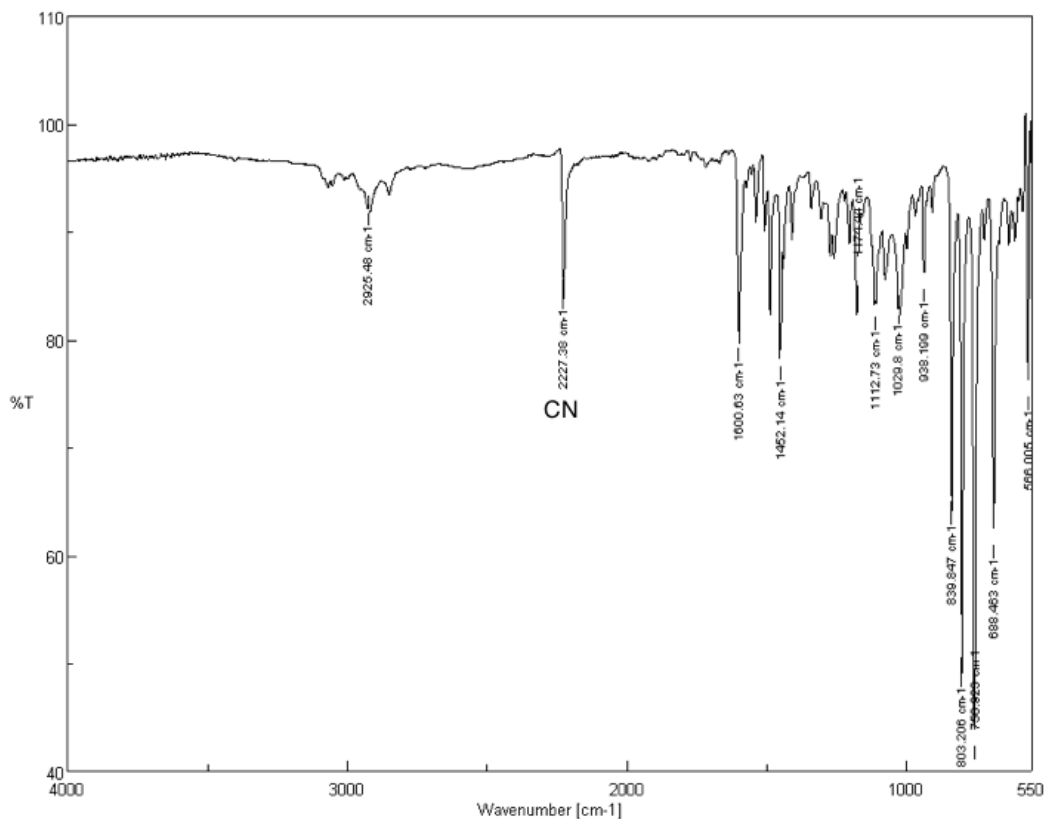
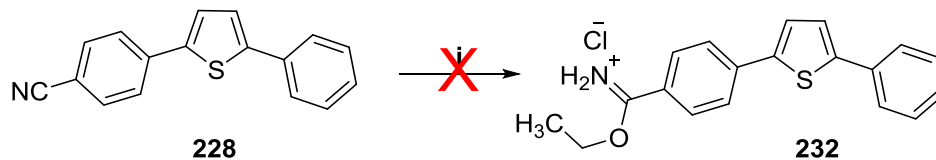


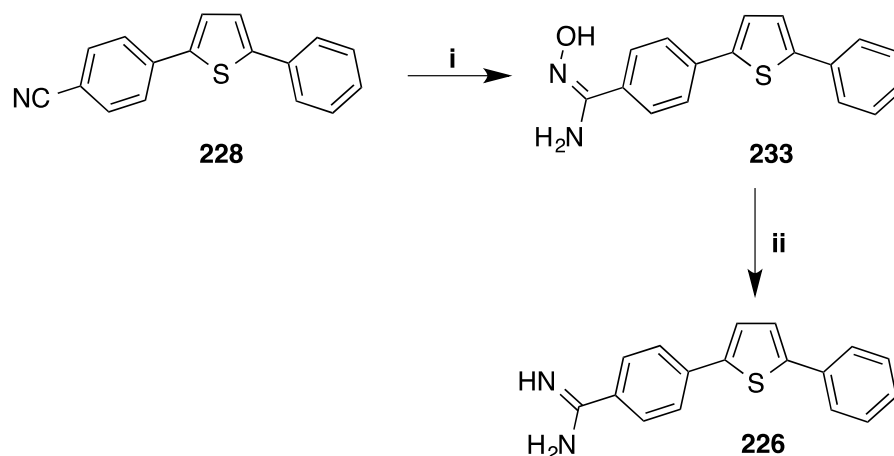
Figure 68. IR spectrum of 4-(5-phenylthiophen-2-yl)benzonitrile **228**.

To synthesize the thiophene-amidine **226**, the nitrile group in **228** must be transformed into the amidine. The use of Pinner synthetic method to prepare the amidine from nitrile through the formation of an imidate intermediate failed. The conversion of the nitrile group in **228** into ethyl imidate **232** using *in situ* generated hydrogen chloride gas and ethanol also did not work (Scheme 60).



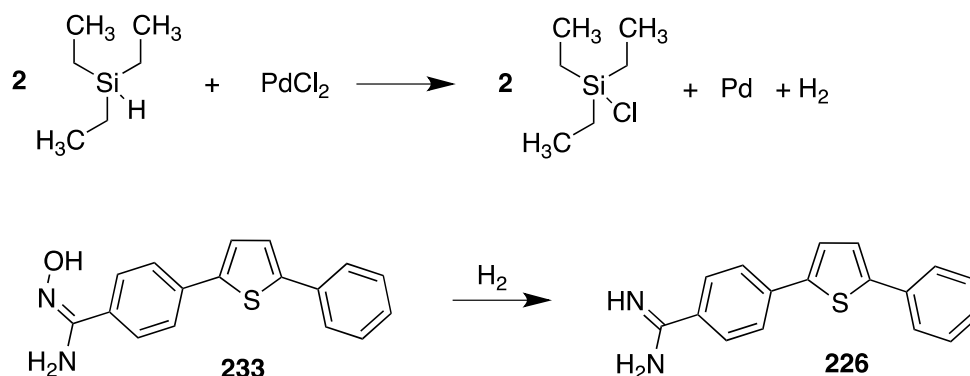
Scheme 60. Attempted synthesis of ethyl 4-(5-phenylthiophen-2-yl)benzimidate hydrochloride **232**; Reagents and conditions: *i*- $\text{HCl}_{(g)}$, EtOH, CHCl_3 , $0\text{ }^\circ\text{C}$ - rt.

The alternative synthetic pathway to prepare the thiophene-amidine **226** was through the preparation of amidoxime intermediate **233**, followed by reduction of the amidoxime intermediate into amidine (Scheme 61).



Scheme 61. The alternative synthetic pathway for 4-(5-phenylthiophen-2-yl)benzamidine **226**; Reagents and conditions: i- $\text{NH}_2\text{OH}\cdot\text{HCl}$, $t\text{-BuOK}$, dry DMSO, 0°C - rt; ii- $\text{HCOO}^- \text{NH}_4^+$, Pd/C, AcOH, reflux.

The structure of *N*-hydroxy 4-(5-phenylthiophen-2-yl)benzamidoxime **233** was confirmed by ^1H NMR spectroscopy. The reduction of the amidoxime group **233** into amidine **226** using ammonium formate as organic hydrogen donor did not work. The starting material **233** was recovered after heating at reflux in acetic acid in the presence of ammonium formate and palladium. This can be explained by poisoning of the palladium catalyst by thiophene. The reduction of **233** into **226** was achieved using triethylsilane as hydrogen donor and palladium (II) chloride as a catalyst (PdCl_2) (Scheme 62).¹³⁸



Scheme 62. The reduction of *N*-hydroxy 4-(5-phenylthiophen-2-yl)benzamidoxime **233** using catalytic transfer hydrogenation.

The reduction of *N*-hydroxy 4-(5-phenylthiophen-2-yl)benzamidoxime **233** into 4-(5-phenylthiophen-2-yl)benzamidine acetate **226** was confirmed by low resolution

Chapter II. Results and Discussion/ Chemistry

(ESIMS m/z 279.3 for the parent amidine compound) and high resolution mass spectrometry (Mass measured for the parent amidine compound was 279.0952).

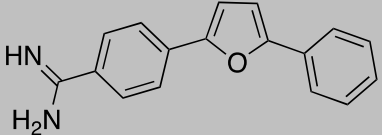
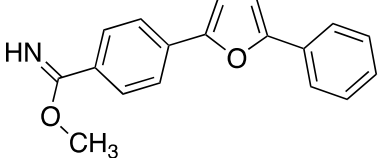
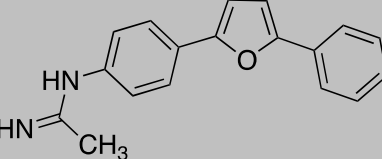
5.3. Amidine isosteres: Bioavailability optimization

Aryl amidine compounds are highly basic. The pK_a of the conjugate acid of benzamidine is 11.8, giving complete ionisation at pH 2.0 (pH of stomach) (Equation 1).

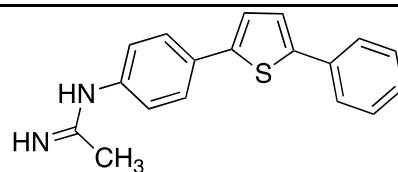
$$pH = pK_a + \text{Log}_{10} ([\text{PhC(=NH)NH}_2] / [\text{PhC(=NH}_2^+)\text{NH}_2]) \dots \dots \dots \text{Equation 1}$$

Drugs with the amidine group showed low oral bioavailability because of the high basicity of the amidine group.^{129, 139} The amidine group is protonated at a wide range of pH, which decreases its permeation through the phospholipid layers of the stomach. Several analogues of the asymmetric furan-amidine **110** were synthesized in which the amidine group was isosterically replaced with imidate **234**, *N*-aryl amidine (reversed amidine) **235** and **236**, *N*-aryl amide **237**, **238** and **239** and amidoxime **240** (Table 16). The amidine isosteres have lower pK_a values, which would be expected to enhance oral bioavailability of the compounds.

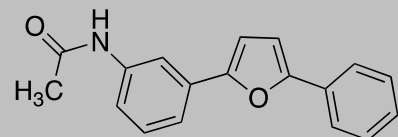
Table 16. The structures of the amidine-isosteres of **110**.

Compound ID	Structure
110	
234	
235	

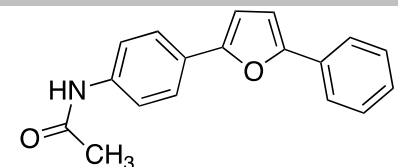
236



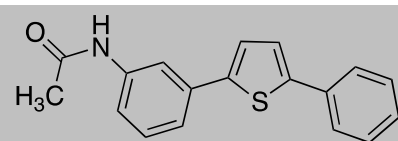
237



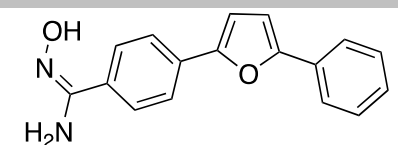
238



239

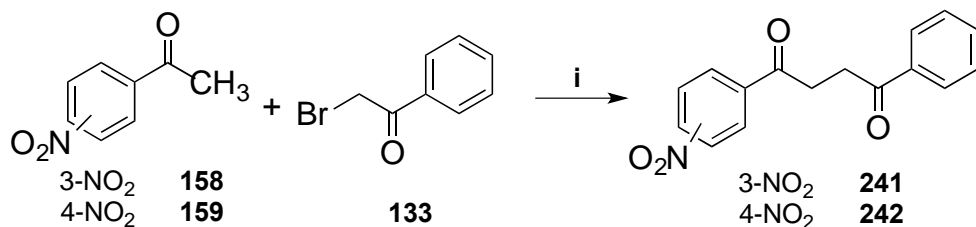


240



5.3.1. Amidines isosteres: Synthesis of 1,4-diketone substrates

The first step in the synthesis of the amidine analogues **234-240** was the preparation of the key 1,4-diketone intermediates **126** (synthesis reported in section 2.2), **241** and **242**. The 1,4-diketones **241** and **242** were synthesized through the coupling between the methyl aryl ketones **158** and **159** and the α -bromomethyl ketone **133** using zinc chloride, triethylamine and ethanol as the condensation agent (Scheme 63). The 1,4-diketones **241** and **242** were obtained in modest yields of 44% and 31%, respectively. The structures of the 1,4-diketones **241** and **242** were confirmed by ^1H NMR spectroscopy.



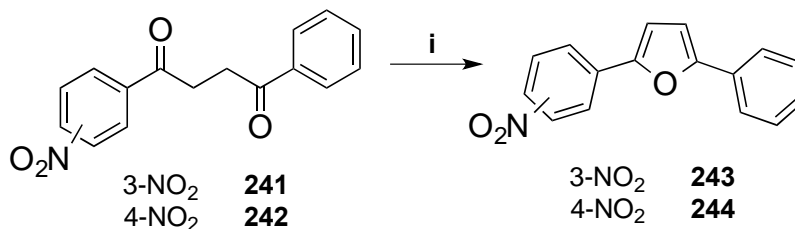
Scheme 63. Pathway for the synthesis of 1,4-diketones **241** and **242**; Reagents and conditions: i- ZnCl_2 , NEt_3 , EtOH, dry toluene, rt.

Chapter II. Results and Discussion/ Chemistry

The imidate **234** and amidoxime **240** were synthesized starting from the 1,4-diketones **126** as discussed in detail in sections 5.3.7 and 5.3.8, respectively.

5.3.2. Amidines isosteres: 2,5-Diarylfurans syntheses

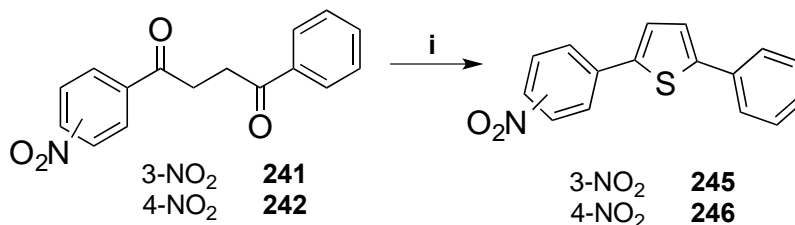
2-(3-Nitrophenyl)-5-phenylfuran **243** and 2-(4-nitrophenyl)-5-phenylfuran **244** were prepared from the reaction of the 1,4-diketones **241** and **242**, respectively, using dry hydrogen chloride gas to catalyse the cyclization to the furan ring (Scheme 64).



Scheme 64. Pathway for the synthesis of 2-(3-nitrophenyl)-5-phenylfuran **243** and 2-(4-nitrophenyl)-5-phenylfuran **244**; Reagents and conditions: i- HCl_(g), CHCl₃, 0 °C - rt.

5.3.3. Amidines isosteres: 2,5-diarylthiophenes syntheses

The thiophenes 2-(3-nitrophenyl)-5-phenylthiophene **245** and 2-(4-nitrophenyl)-5-phenylthiophene **246** were prepared from the reactions of the 1,4-diketones **241** and **242**, respectively, with Lawesson's reagent **227** (Scheme 65).



Scheme 65. Pathway for the synthesis of 2-(3-nitrophenyl)-5-phenylthiophene **245** and 2-(4-nitrophenyl)-5-phenylthiophene **246**; Reagents: i- Lawesson's reagent **227**, THF, 55 °C.

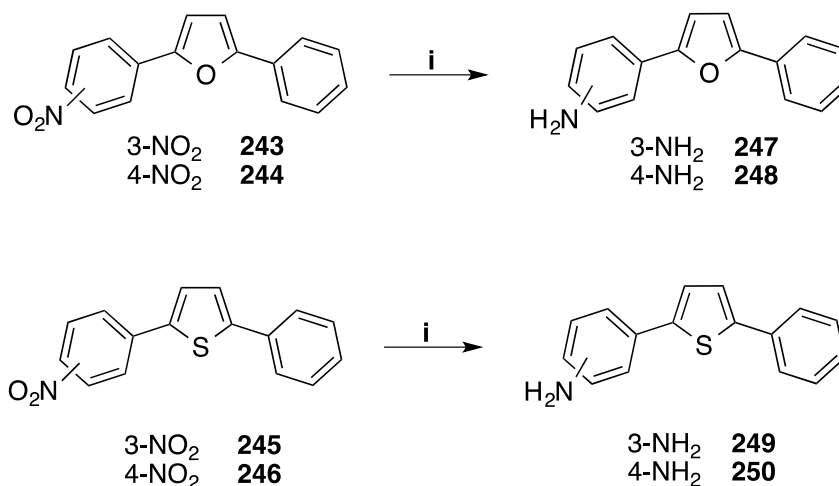
The structures of the thiophenes **245** and **246** were characterized by ¹H NMR spectroscopy, here discussed for **246**. The H-3 and H-4 protons of the thiophene ring in **246** were each observed as doublets at 7.66 ppm (*J* 3.9 Hz) and 7.84 ppm (*J* 3.6 Hz). The aryl H-2'', H-3'' and H-4'' protons were observed as a doublet at 7.75 ppm (*J* 7.5 Hz), a triplet at 7.47 ppm (*J* 7.2 Hz) and a triplet at 7.34 ppm (*J* 7.2 Hz). The aryl H-

Chapter II. Results and Discussion/ Chemistry

2' and H-3' protons were each observed as doublets at 7.97 ppm (J 8.4 Hz) and 8.27 ppm (J 8.4 Hz).

5.3.4. Amidines isosteres: Reduction of the nitro-groups into aromatic amines

The nitro-groups in the compounds **243-246** were reduced to amines **247-250** using sodium borohydride in the presence of a catalytic amount of copper sulfate (Scheme 66).¹⁴⁰



Scheme 66. Reduction of the nitro-group in compounds **243-246** to give amines **247-250**; Reagents and conditions: i- NaBH₄, CuSO₄, EtOH, 0 °C - rt.

The reduction of the nitro-groups into amines was confirmed by ¹H NMR spectroscopy. The key differences between the ¹H NMR spectra of 3-(5-phenylfuran-2-yl)aniline **247** (Figure 69A) and 2-(3-nitrophenyl)-5-phenylfuran **243** (Figure 69B) are discussed.

Chapter II. Results and Discussion/ Chemistry

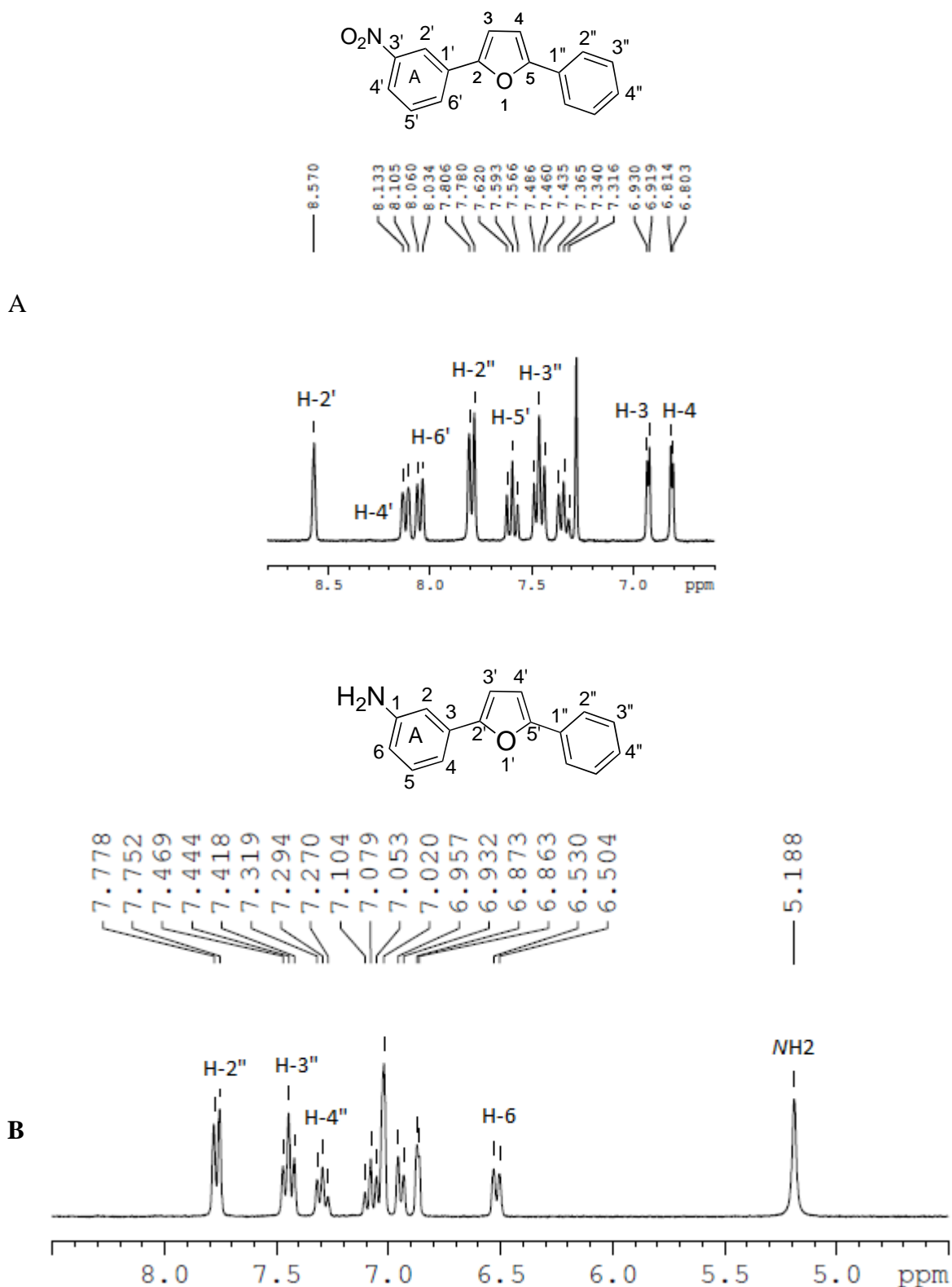


Figure 69. A- ^1H NMR (CDCl_3) spectrum of A- 2-(3-nitrophenyl)-5-phenylfuran **243**;
 B- ^1H NMR (DMSO-d_6) spectrum of 3-(5-phenylfuran-2-yl)aniline **247**.

Chapter II. Results and Discussion/ Chemistry

The aryl protons of the aromatic ring **A** in **243** were shifted up-field upon the reduction of the nitro-group into amine. The peaks of the H-2', H-4', H-5' and H-6' protons of **243** were shifted up-field from 8.57, 8.12, 7.59 and 8.05 ppm to 6.87, 6.52, 7.08 and 6.94 ppm in **247**, respectively. The up-field shift is attributed to the difference in the nature of the nitro-group when compared to the amino-group. The nitro-group is an electron-withdrawing group by resonance, which leads to a decrease in the electron density on the aryl ring **A**. In contrast, the amino-group is an electron-donating group through resonance, which leads to an increase in the electron density in the aryl ring **A** (Figure 70).

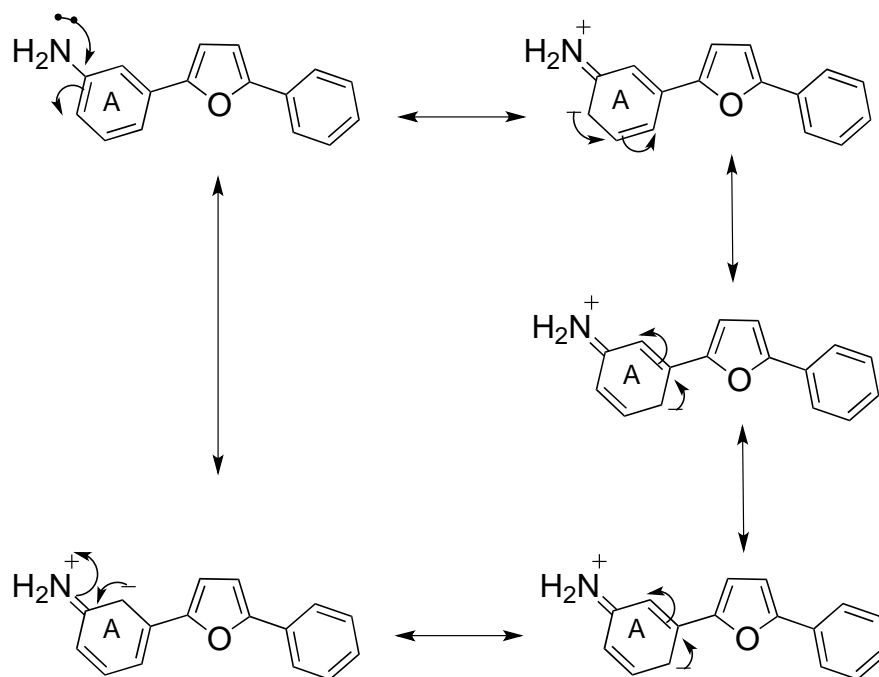
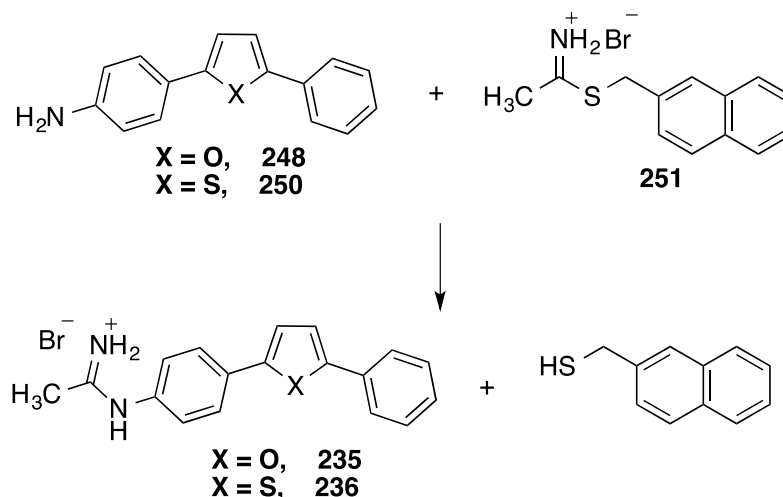


Figure 70. Resonance states of the aryl ring **A** in 3-(5-phenylfuran-2-yl)aniline **247**.

5.3.5. Amidines isosteres: *N*-Aryl amidines “reversed amidine” syntheses

Two *N*-aryl amidines, namely *N*-(4-(5-phenylfuran-2-yl)phenyl)acetamidine hydrobromide **235** and *N*-(4-(5-phenylthiophen-2-yl)phenyl)acetamidine hydrobromide **236** were synthesized from the reaction of the amines **248** and **250**, respectively, with *S*-2-naphthylmethyl thioacetimidate hydrobromide **251** (Scheme 67).¹⁴¹ The synthesis of reagent **251** is discussed in the next section 5.3.5.1.



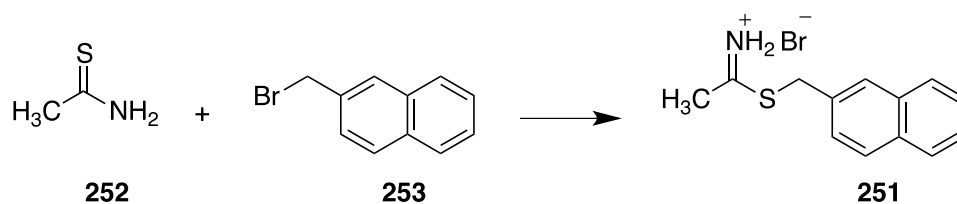
Scheme 67. Routes for the synthesis of *N*-(4-(5-phenylfuran-2-yl)phenyl)acetamidine hydrobromide **235**, X = O and *N*-(4-(5-phenylthiophen-2-yl)phenyl)acetamidine hydrobromide **236**, X = S.

The *N*-aryl amidine products **235** and **236** were characterized by ¹H and ¹³C NMR spectroscopy and the spectra for **235** are discussed here. In the ¹H NMR spectrum, the protons H-2, H-3, H-3', H-4', H-2'', H-3'' and H-4'' were observed as a doublet at 7.34 ppm (*J* 8.4 Hz), a doublet at 7.91 ppm (*J* 8.7 Hz), a doublet at 7.08 ppm (*J* 3.3 Hz), a doublet at 7.14 ppm (*J* 3.6 Hz), a doublet at 7.78 ppm (*J* 7.2 Hz), a triplet at 7.41 ppm (*J* 7.5 Hz) and a triplet at 7.28 ppm (*J* 7.2 Hz), respectively. The methyl protons were observed as a singlet at 2.28 ppm. The three non-equivalent *N*-H protons were observed as three singlet peaks at 8.58 ppm, 9.44 ppm and 11.14 ppm. The quaternary amidine carbon was observed at 164.3 in the ¹³C NMR spectrum, which was appropriately absent in the DEPT135 spectrum.

5.3.5.1. Synthesis of S-2-naphthylmethyl thioacetimidate hydrobromide **251**

S-2-Naphthylmethyl thioacetimidate hydrobromide **251** was required for use as a reagent in the synthesis of *N*-aryl amidines (reversed amidines) **235** and **236**. S-2-Naphthylmethyl thioacetimidate hydrobromide **251** was synthesized by the alkylation of thioacetamide **252** with 2-bromomethylnaphthalene **253** with heating at reflux in chloroform (Scheme 68).^{141c}

Chapter II. Results and Discussion/ Chemistry

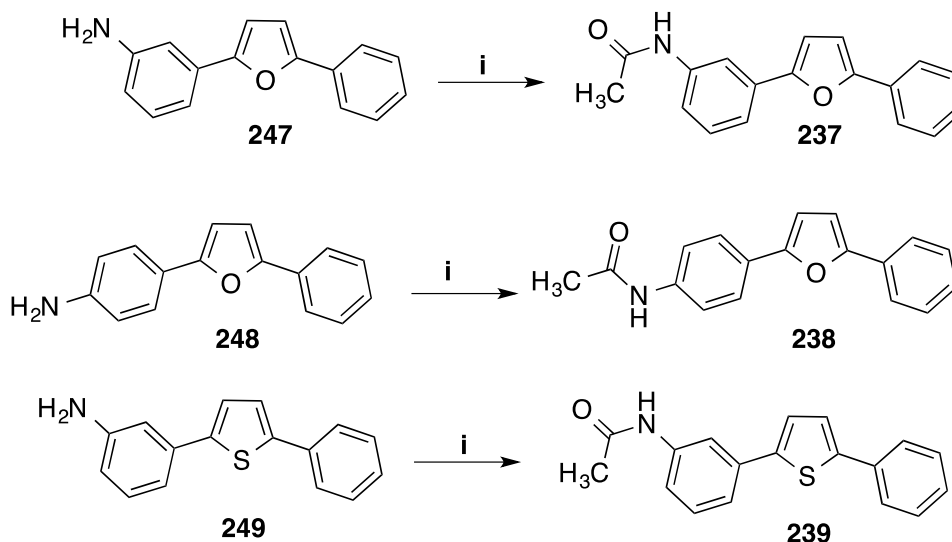


Scheme 68. Pathway for the synthesis of S-2-naphthylmethyl thioacetimidate hydrobromide **251**.

The structure of **251** was characterized by ^1H NMR spectroscopy. The methyl and methylene protons were observed as singlets at 2.64 ppm and 4.75 ppm, respectively. The aryl protons of the naphthalene ring were observed as multiplets at 7.54-7.56 ppm and 7.91-8.00 ppm.

5.3.6. Amidines isosteres: *N*-Aryl amide syntheses

Three *N*-aryl amides, namely *N*-(3-(5-phenylfuran-2-yl)phenyl)acetamide **237**, *N*-(4-(5-phenylfuran-2-yl)phenyl)acetamide **238** and *N*-(3-(5-phenylthiophen-2-yl)phenyl)acetamide **239** were synthesized from the reaction of the amines **247**, **248** and **249** with acetyl chloride, respectively (Scheme 69).



Scheme 69. Synthetic pathway of *N*-aryl amides **237-239**; Reagents and conditions: i- AcCl, dry CH_3CN , rt.

The structures of the *N*-aryl amides **237-239** were characterized by ^1H and ^{13}C NMR spectroscopy. The ^1H and ^{13}C NMR spectra for *N*-(4-(5-phenylfuran-2-yl)phenyl)acetamide **238** is discussed as an example. In the ^1H NMR spectrum of **238** the methyl group and *N*-H proton were observed as singlets at 2.06 ppm and 10.06 ppm,

Chapter II. Results and Discussion/ Chemistry

respectively. The aryl protons, H-2, H-3, H-3', H-4', H-2'', H-3'' and H-4'' were observed as a doublet at 7.66 ppm (J 8.1 Hz), a doublet at 7.74 ppm (J 8.4 Hz), a singlet at 6.95 ppm, a singlet at 7.05 ppm, a doublet at 7.79 ppm (J 7.5 Hz), a triplet at 7.44 ppm (J 7.8 Hz) and a triplet at 7.29 ppm (J 7.2 ppm), respectively (Figure 71). In the ^{13}C -NMR spectrum the amide carbon was observed at 168.3 ppm.

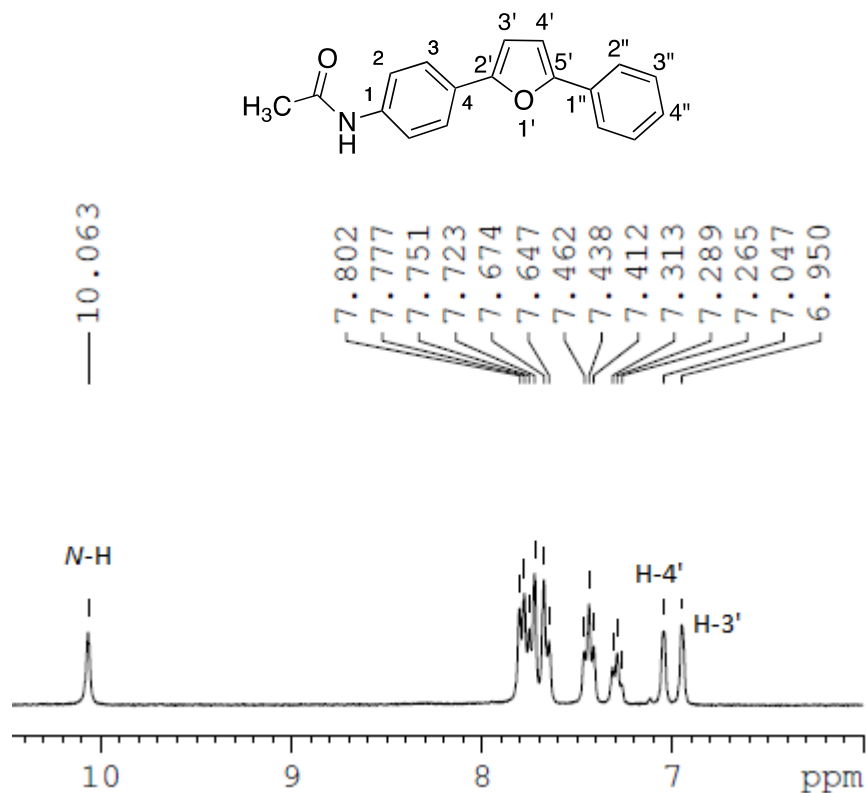
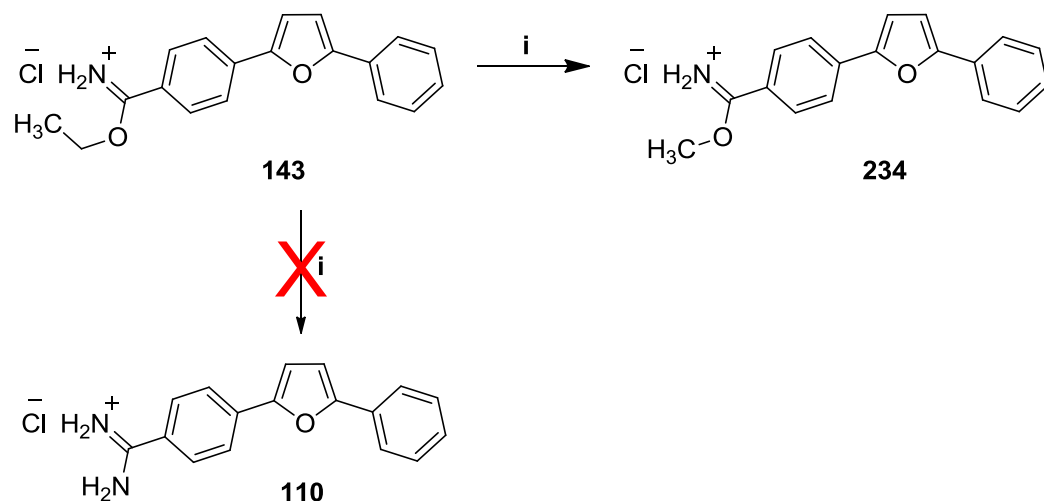


Figure 71. ^1H NMR (DMSO- d_6) spectrum of *N*-(4-(5-phenylfuran-2-yl)phenyl)acetamide **238**.

5.3.7. Amidines isosteres: Carboximidate synthesis

It was anticipated that the heating of ethyl benzimidate hydrochloride **143** at reflux with ammonium chloride salt into a mixture of methanol and water would give the furan-amidine **110**, however the isolated product was the methyl imidate **234** (Scheme 70).¹⁴²

Chapter II. Results and Discussion/ Chemistry



Scheme 70. Reaction of **143** gave methyl 4-(5-phenylfuran-2-yl)benzimidate hydrochloride **234** and not **110**; Reagents and conditions: i- NH₄Cl, MeOH/ H₂O, reflux.

Methanol attacked the carbon atom of benzimidate group in compound **143** to give methyl 4-(5-phenylfuran-2-yl)benzimidate hydrochloride **234**. This is an analogue of the asymmetric furan-amidine **110** and was therefore tested for inhibition of NQO2. The imidate group is considered as a much less basic isostere (pKa of conjugate acid 6.2)¹⁰⁷ than the highly basic amidine group, which has a pKa of 11.8.¹⁰¹

The structure of compound **234** was confirmed by ¹H NMR spectroscopy, with the methyl group present as a singlet at 3.94 ppm (Figure 72A). In the ¹³C NMR spectrum, the methyl group was observed at 52.1 ppm and the imidate carbon was observed at 166.8 ppm (Figure 72B).

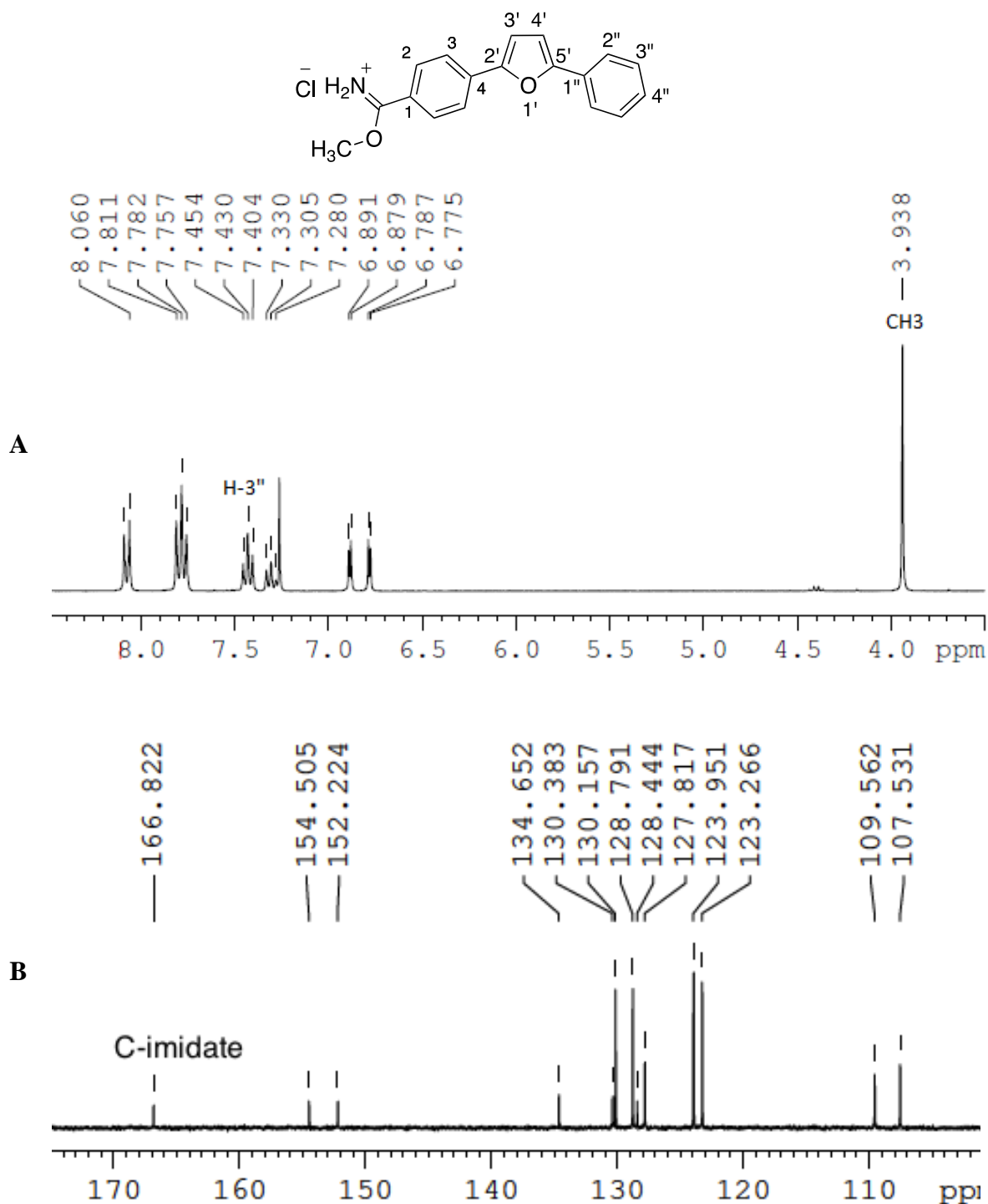


Figure 72. NMR (CDCl_3) spectra of methyl 4-(5-phenylfuran-2-yl)benzimidate hydrochloride **234**; A- ^1H NMR; B- ^{13}C NMR.

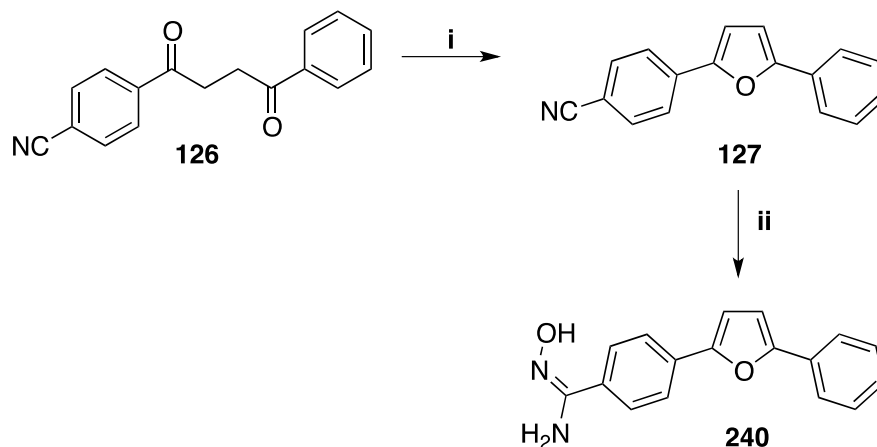
5.3.8. Amidines isosteres: Amidoxime synthesis

One compound with the amidoxime (*N*-hydroxyamidine) group **240** was synthesized as an isostere for the asymmetric furan-amidine **110**. The amidoxime is considered as a less basic isostere than the amidine as the pK_a value of the conjugate

Chapter II. Results and Discussion/ Chemistry

acid is approximately 5-6¹⁴³ compared with 5-12 for the amidine.¹⁰¹ In addition, amidoximes are considered as potential prodrugs for amidines and used as isosteres to optimize the oral bio-availability of amidine-containing drugs.^{129, 139} The amidoxime prodrugs are reduced into the parent amidine drugs in human liver microsomes.¹⁴⁴

N-Hydroxy-4-(5-phenylfuran-2-yl)benzamidine **240** was synthesized starting from the 1,4-diketone **126**. The 1,4-diketone **126** was cyclized into furan **127**, which reacted with hydroxylamine to give **240** (Scheme 71).



Scheme 71. Pathway for the synthesis of *N*-hydroxy-4-(5-phenylfuran-2-yl)benzamidine **240**; Reagents and conditions: i- Ac₂O, conc. H₂SO₄, reflux; ii- NH₂OH. HCl, *t*-BuOK, dry DMSO, 0 °C - rt.

The characterization of 4-(5-phenylfuran-2-yl)benzonitrile **127** was discussed in Section 3.3. The structure of *N*-hydroxy-4-(5-phenylfuran-2-yl)benzamidine **240** was characterized by ¹H NMR and IR-spectroscopies. The NH₂ and *N*-OH protons were observed as singlets at 5.85 ppm and 9.69 ppm, respectively (Figure 73). These exchangeable protons disappeared from the ¹H NMR spectrum after the addition of D₂O.

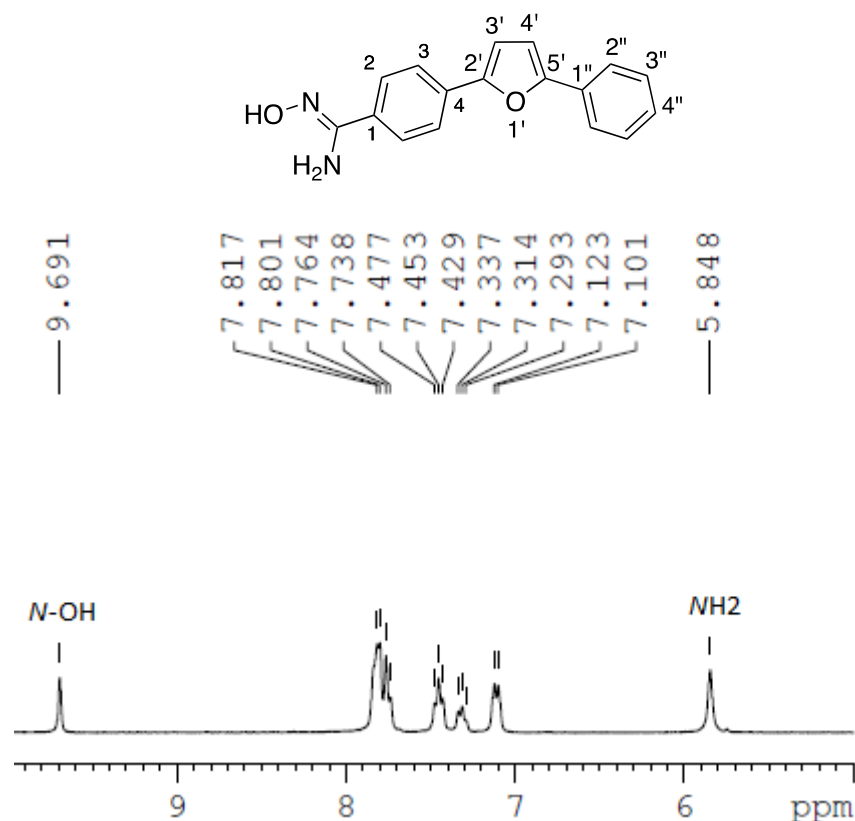


Figure 73. ^1H NMR (DMSO- d_6) spectrum of *N*-hydroxy-4-(5-phenylfuran-2-yl)benzamidinium **240**.

6. Furan analogue of resveratrol

Resveratrol **60** is a known inhibitor for NQO2 with an IC_{50} of 450 nM.⁸² Resveratrol has a planar conformation allowing its accommodation inside the deep cleft of the NQO2 active site.⁵⁵ Resveratrol has a *trans*-stilbene nucleus with hydroxyl substituents on both aromatic rings. The furan-analogue of resveratrol **250** (Figure 74) with a *cis*-geometry was proposed as a potential inhibitor of NQO2.

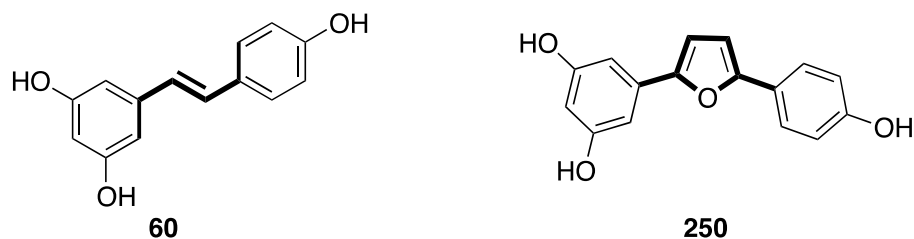
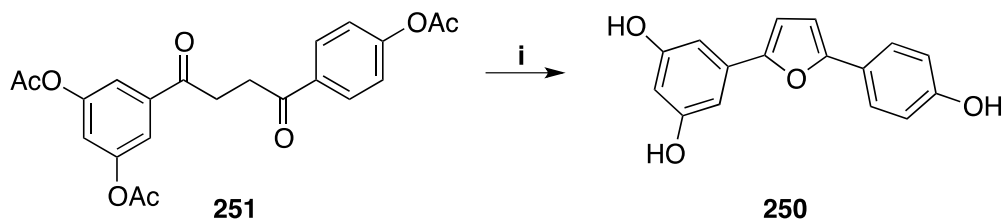


Figure 74. The structures of resveratrol (**60**) and the furan-analogue of resveratrol (**250**).

The synthetic pathway to prepare 5-(5-(4-hydroxyphenyl)furan-2-yl)benzene-1,3-diol **250** (Scheme 72) first requires the preparation of the starting 1,4-diketone **251**.

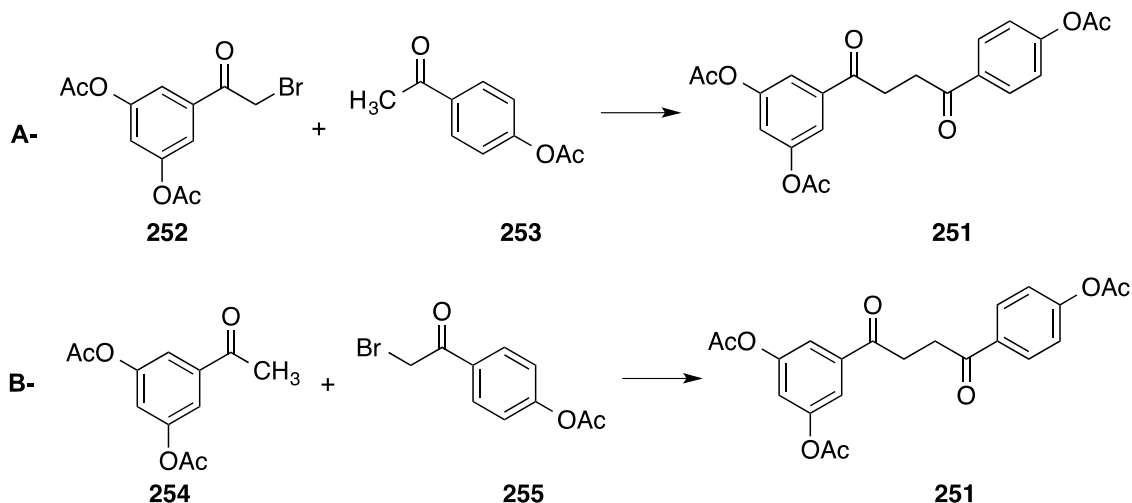
Chapter II. Results and Discussion/ Chemistry

As the hydroxyl groups can affect the synthetic pathway, they were protected with acetyl groups at the start of the synthesis.



Scheme 72. Pathway for the synthesis of 5(5-(4-hydroxyphenyl)furan-2-yl)benzene-1,3-diol **250**; Reagents and conditions: i- $\text{HCl}_{(g)}$, CHCl_3 , 0°C - rt.

Two synthetic pathways were proposed to prepare the 1,4-diketone **251** (Scheme 73) and both required the coupling between a methyl aryl ketone and an α -bromomethyl aryl ketone.



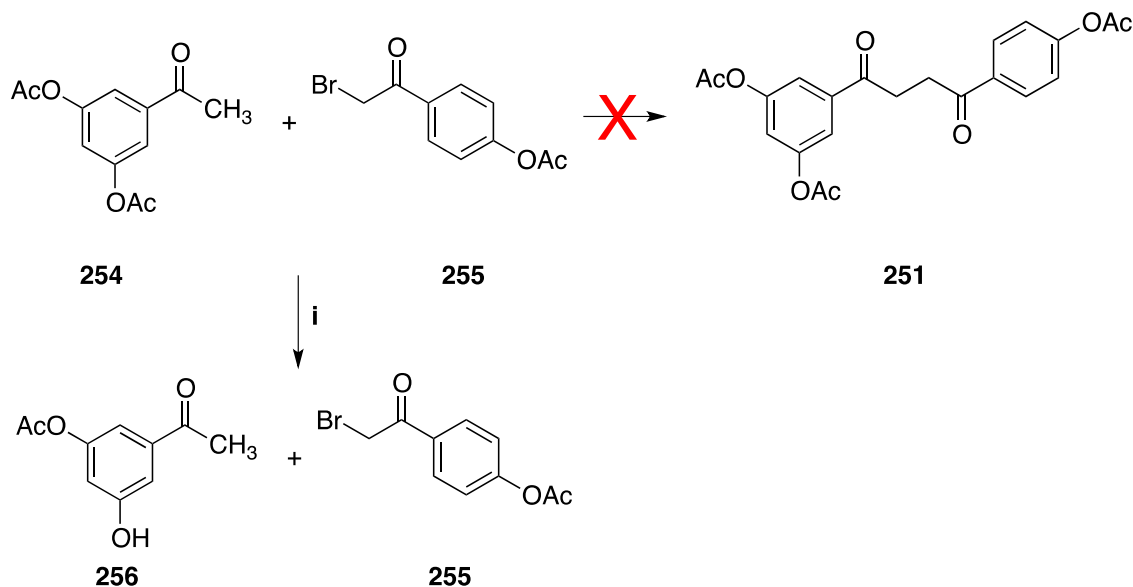
Scheme 73. Pathways for the synthesis of 1-(3,5-di(acetyloxy)phenyl)-4-(acetyloxyphenyl)-1,4-butanedione **251**.

The choice between the synthetic pathway A or B to prepare 1-(3,5-di(acetyloxy)phenyl)-4-(acetyloxyphenyl)-1,4-butanedione **251** depends on the ease of preparation of the methyl aryl ketones **253** or **254** and the α -bromomethyl aryl ketones **252** or **255**. As the methyl aryl ketone **254** and the α -bromomethyl aryl ketone **255** were easier to prepare, synthetic pathway B was preferred for the synthesis of 1,4-diketone **251**. The syntheses of the compounds **252-255** are discussed further in sections 6.1-6.4.

The coupling between 3',5'-di(acetyloxy)acetophenone **54** and 2-bromo-4'-(acetyloxy)acetophenone **255** was performed using two different coupling agents. With zinc chloride, triethylamine and ethanol as the condensation reaction conditions, no

Chapter II. Results and Discussion/ Chemistry

reaction was observed between **254** and **255** by t.l.c. The use of *t*-butoxymagnesium bromide as a condensation agent¹³⁵ resulted in the formation of **256** instead of the 1,4-diketone **251** without the consumption of **255** (Scheme 74). The reactivity of *t*-butoxymagnesium bromide led to the de-acetylation of compound **254** and no coupling occurred with compound **255**.



Scheme 74. Pathways attempted for the synthesis of 1-(3,5-di(acetyloxy)phenyl)-4-(acetyloxyphenyl)-1,4-butanedione **251**; Reagents and conditions: *i*- *t*-BuOMgBr, dry THF, 0 °C- rt.

The structure of compound **256** was characterized by ¹H-NMR spectroscopy. Two singlet peaks for two different methyl protons were observed at 2.39 ppm (ester) and 2.55 ppm (ketone). The OH proton was observed as a broad singlet at 7.76 ppm. The aryl protons H-2, H-4 and H-6 were observed as fine triplets (*meta*-coupling) at 7.29 ppm, 6.84 ppm and 7.20 ppm, respectively (Figure 75).

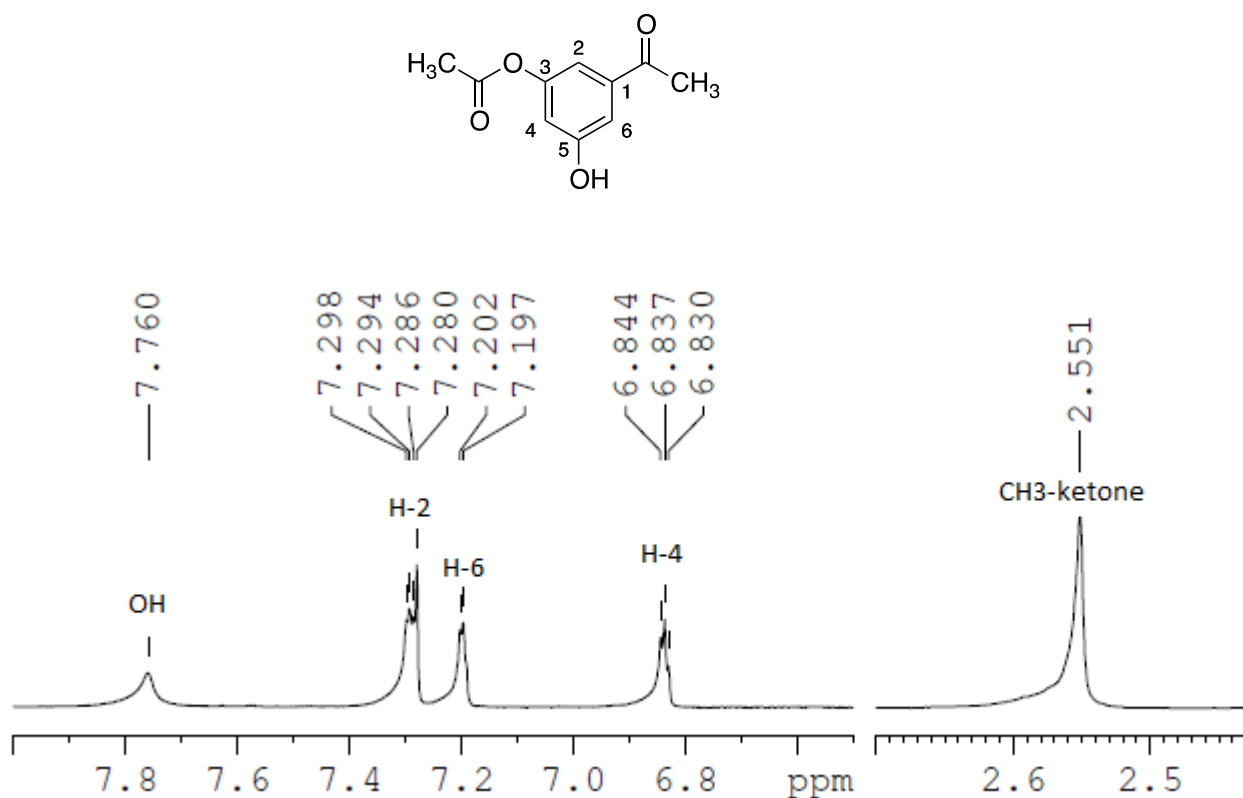
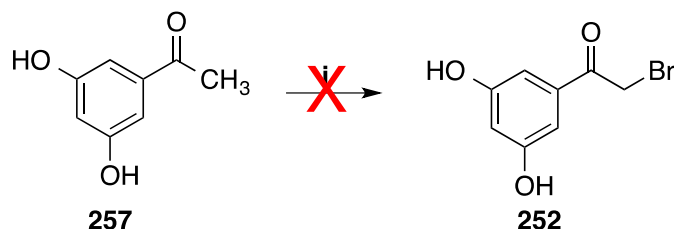


Figure 75. ¹H NMR (CDCl₃) spectrum of 3-(acetyloxy)-5-hydroxyacetophenone **256**.

6.1. Synthesis of 3',5'-dihydroxy-2-bromoacetophenone **252**

The synthesis of α -bromomethyl aryl ketone **252** was attempted by the α -bromination of 3',5'-dihydroxyacetophenone **257** using copper (II) bromide (Scheme 75).¹⁴⁵ The expected product was the α -bromo-compound **252**, but heating at reflux led to a mixture of products. From the ¹H NMR spectrum, there was evidence for electrophilic aromatic substitution, aryl oxidation and the formation of an α,α -dibromo compound.



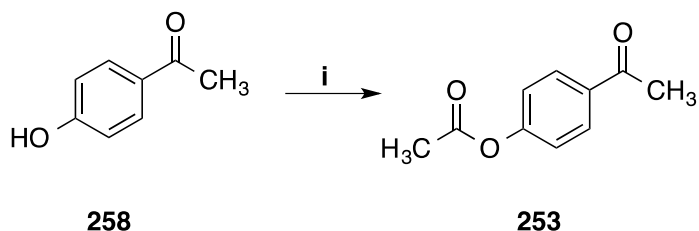
Scheme 75. Synthetic pathway for α -bromo-compound **252**; Reagents and conditions:

i- CuBr₂, EtOAc/DCM, reflux.

Chapter II. Results and Discussion/ Chemistry

6.2. Synthesis of 4'-(acetyloxy)acetophenone **253**

The acetylation of the hydroxyl group in 4'-hydroxyacetophenone **258** was performed by using acetic anhydride as the acetylating agent (Scheme 76). 4-(Dimethylamino)pyridine (DMAP) and triethylamine were used to increase the hydroxyl nucleophilicity to attack the carbonyl group of acetic anhydride.¹⁴⁶

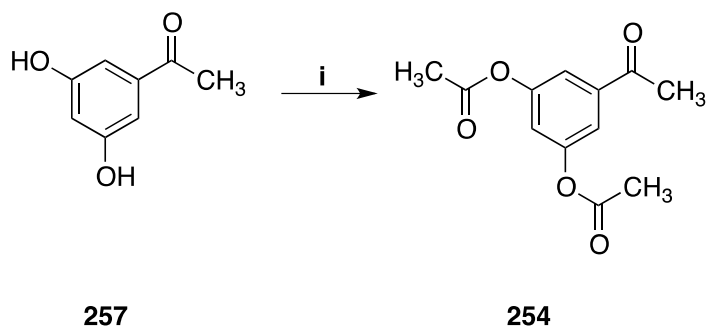


Scheme 76. Pathway for the synthesis of 4'-(acetyloxy)acetophenone **253**; Reagents: i- Ac₂O, DMAP, NEt₃, DCM, 0 °C - rt .

The structure of 4'-(acetyloxy)acetophenone **253** was characterized by ¹H-NMR spectroscopy. The methyl protons adjacent to the ester group were observed as a singlet at 2.30 ppm and the methyl protons adjacent to the ketone group were observed as a singlet at 2.57 ppm. H-2 and H-3 protons were observed as doublets at 7.97 ppm (*J* 8.7 Hz) and 7.17 ppm (*J* 8.7 Hz), respectively.

6.3. Synthesis of 3',5'-di(acetyloxy)acetophenone **254**

The acetylation of the hydroxyl groups in 3',5'-dihydroxyacetophenone **257** was performed by using acetic anhydride as the acetylating agent (Scheme 77).¹⁴⁷ The structure of 3',5'-di(acetyloxy)acetophenone **254** was characterized by ¹H-NMR spectroscopy.

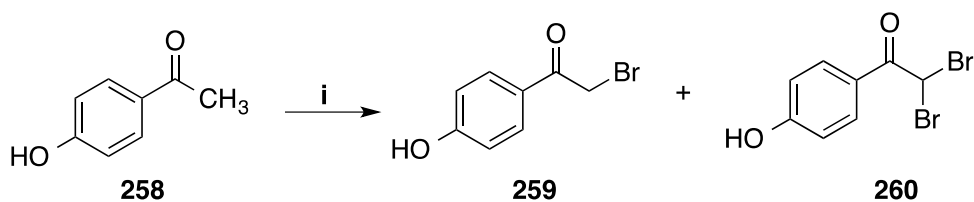


Scheme 77. Pathway for the synthesis of 3',5'-di(acetyloxy)acetophenone **254**;
Reagents: i- Ac₂O, DMAP, NEt₃, DCM, 0 °C - rt.

Chapter II. Results and Discussion/ Chemistry

6.4. Synthesis of 2-bromo-4'-(acetyloxy)acetophenone **255**

2-Bromo-4'-(acetyloxy)acetophenone **255** was synthesized using a two-step synthetic pathway. The first step involved the preparation of 2-bromo-4'-hydroxyacetophenone using a different brominating agent. Heating **258** at reflux with copper (II) bromide led to the formation of 2-bromo-4'-hydroxyacetophenone **259** and 2,2-dibromo-4'-hydroxyacetophenone **260** in a ratio of 80%: 20%, respectively (Scheme 78). It was not easy to separate the two products **260** and **261** as they have very close R_f values (mobile phase 1.0 % MeOH/ CHCl_3) of 0.41 and 0.49, respectively.

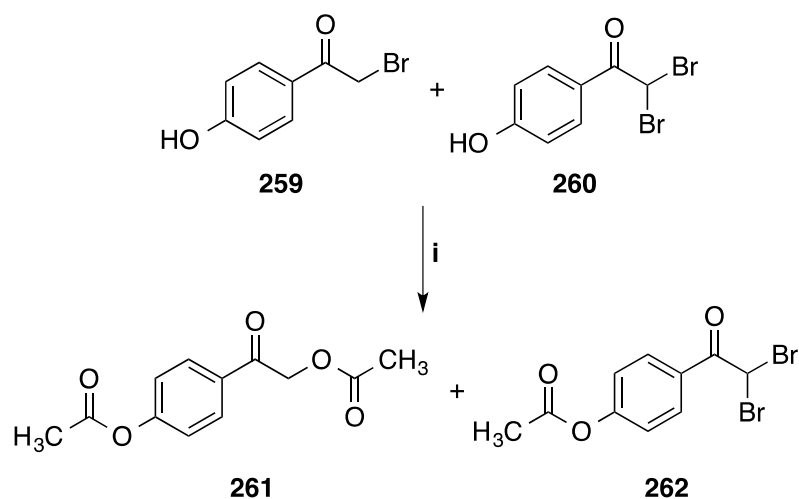


Scheme 78. α -Bromination of 4'-hydroxyacetophenone **258**; Reagents and conditions:
i- CuBr_2 , EtOAc/DCM, reflux.

The ^1H NMR spectrum of the reaction mixture showed the presence of the two compounds. The CH_2Br protons of **259** were observed as singlet at 4.43 ppm and the CHBr_2 protons of **260** was down-field giving a singlet at 6.70 ppm.

The reaction of bromine with **258** at room temperature also led to the formation of both 2-bromo-4'-hydroxyacetophenone **259** and 2,2-dibromo-4'-hydroxyacetophenone **260**. The mixture of **259** and **260** was reacted with acetic anhydride to prepare 2-bromo-4'-acetyloxyacetophenone **255**. The bromo-atom in 2-bromo-4'-hydroxyacetophenone **259** was replaced by the acetate group forming 2,4'-di(acetyloxy)acetophenone **261** (Scheme 79).

Chapter II. Results and Discussion/ Chemistry



Scheme 79. Pathway for the synthesis of 2,4'-di(acetyloxy)acetophenone **261** and 2,2-dibromo-4'-acetyloxyacetophenone **262**; Reagents: i- Ac₂O, DMAP, NEt₃, DCM, 0 °C - rt.

The structure of 2,4'-di(acetyloxy)acetophenone **261** was characterized by ¹H NMR spectroscopy. The methyl protons a and b were observed as singlets at 2.25 ppm and 2.35 ppm. The CH₂ protons were observed as a singlet at 5.33 ppm and the aryl protons H-2 and H-3 were observed as doublets at 7.25 ppm (*J* 8.7 Hz) and 7.98 ppm (*J* 8.7 Hz) (Figure 76).

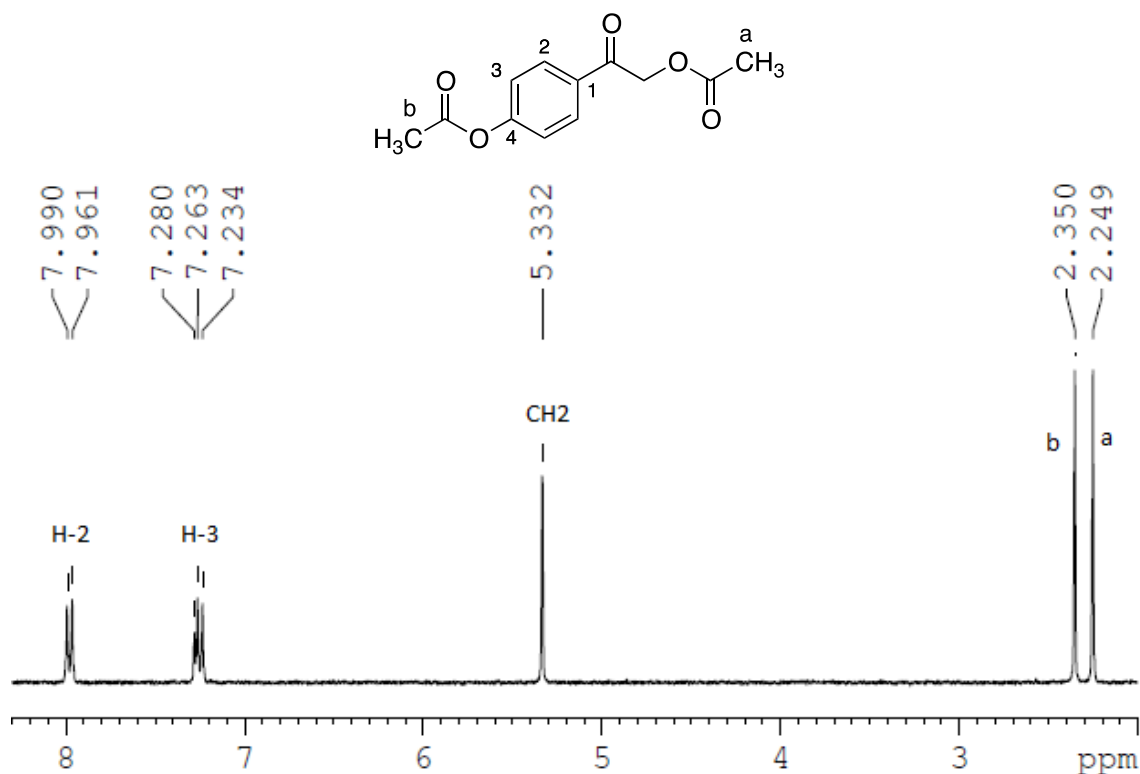
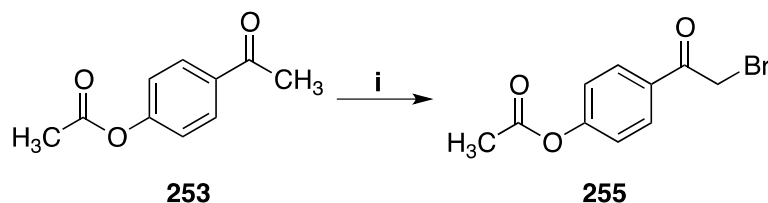


Figure 76. ^1H NMR (CDCl_3) spectrum of 2,4'-di(acetyloxy)acetophenone **261**.

In contrast, the hydroxyl group in 2,2-dibromo-4'-hydroxyacetophenone **260** was acetylated without acetate substitution of one of α -bromo atoms. The difference in R_f values between **261** and **262** was large enough to separate both compounds using column chromatography. The structure of 2,2-dibromo-4'-(acetyloxy)acetophenone **262** was characterized by ^1H NMR spectroscopy. The CH_3 and CHBr_2 protons were observed as singlet peaks at 2.28 ppm and 6.57 ppm, respectively.

Depending on these results, 2-bromo-4'-(acetyloxy)acetophenone **255** was synthesized by firstly preparing 4'-(acetyloxy)acetophenone **253**, followed by its α -bromination using bromine (Scheme 80).



Scheme 80. Pathway for the synthesis of 2-bromo-4'-(acetyloxy)acetophenone **255**;

Reagents and conditions: i- $\text{Br}_2/\text{AlCl}_3$, THF, 0°C - rt.

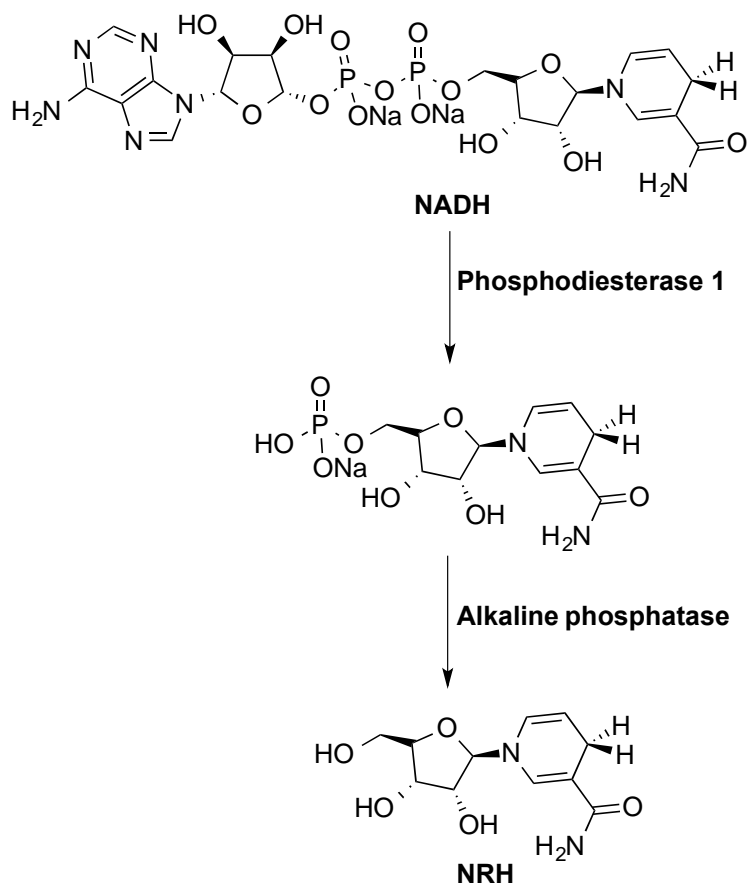
Chapter II. Results and Discussion/ Chemistry

The reaction of 4'-(acetyloxy)acetophenone **253** with bromine in the presence of a catalytic amount of aluminium chloride yielded 2-bromo-4'-(acetyloxy)acetophenone **255**.¹⁴⁸ No dibromo compound was detected from this reaction. The structure of 2-bromo-4'-(acetyloxy)acetophenone **255** was characterized by ¹H NMR spectroscopy. The CH₃ and CH₂Br protons were observed as singlet peaks at 2.35 ppm and 4.44 ppm, respectively. H-2 and H-3 protons were each observed as doublets at 7.25 ppm (*J* 8.7 Hz) and 8.05 ppm (*J* 8.7 Hz).

7. Synthesis of *N*-ribosyl dihydronicotinamide NRH

For the NQO2 enzyme studies, the synthesis of *N*-ribosyl dihydronicotinamide **NRH** was required. **NRH** was synthesized according to an enzymatic method reported by Long and coworkers⁶³ that utilizes NADH as the starting material. The hydrolysis of NADH to **NRH** is achieved in two steps (Scheme 81); the first step involves phosphodiesterase enzyme, which cleaves the phosphodiester bond leading to the formation of the phosphate ester of **NRH**. In the second step the alkaline phosphatase – which works optimally at basic pH-¹⁴⁹ removes the phosphate group¹⁵⁰ leading to the formation of NRH. NRH is a stable compound⁷² that will not be affected during the purification process. NRH was purified using preparative HPLC and the sample concentrated on a freeze-dryer.

Chapter II. Results and Discussion/ Chemistry

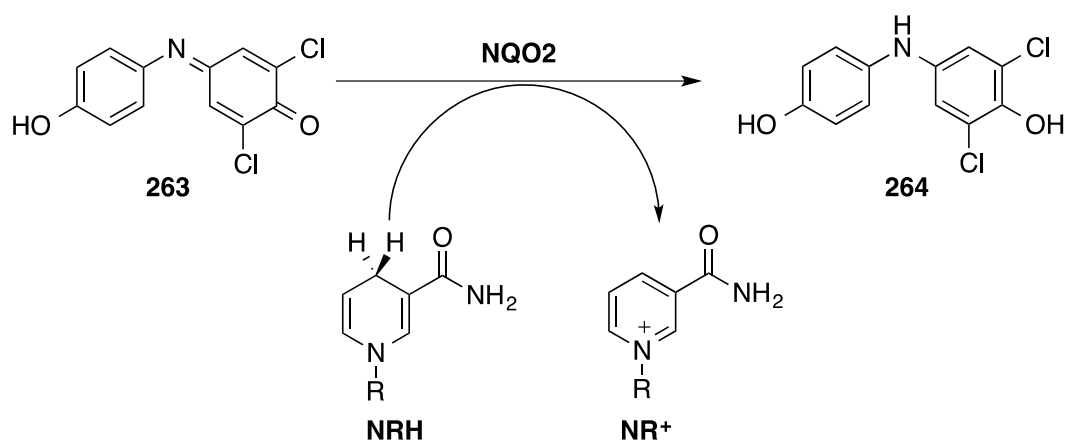


Scheme 81. Pathway for the enzymatic synthesis of the co-substrate *N*-riboseyl dihydronicotinamide **NRH**.

Chapter II. Results and Discussion/ NQO2 Inhibitory Activity

1. Inhibition of recombinant human NQO2 enzyme activity

The ability of the synthesized compounds to inhibit the NQO2 enzyme was determined by a spectrophotometric method using the redox dye 2,6-dichlorophenolindophenol (DCPIP) **263** in the presence of *N*-ribosyl dihydronicotinamide (NRH). DCPIP **263** is an iminoquinone compound with a blue colour, which is reduced by NQO2 into aminophenol **264**. The aminophenol **264** is a colourless compound compared to **263** because of the loss of conjugation with the second phenol ring (Scheme 82). In this method, the rate of DCPIP **263** colour change, which correlates to the rate of NQO2 activity, is monitored spectrophotometrically.



Scheme 82. Reduction of DCPIP **263** by NQO2 in the presence of NRH (R=ribose).

Resveratrol **60** was used as the positive control in this assay. The IC₅₀ values of resveratrol **60** and the synthesized compounds **110-154**, **191-195**, **226** and **234-240** were determined. The IC₅₀ value represents the concentration of a drug that is required for 50% inhibition compared with the control rate *in vitro*. Table 17 summarizes the IC₅₀ values of resveratrol and the synthesized compounds.

Chapter II. Results and Discussion/ NQO2 Inhibitory Activity

Table 17. The IC₅₀ values of resveratrol and the synthesized furan-amidine compounds (compounds **60**, **110**, **111**, **147**, **148** were tested by myself and all other compounds were tested by my colleague PhD student Elham Santana).

Compound ID	R	IC ₅₀ (nM) ± SE
Resveratrol 60	----	913.0 ± 2.3
110	H	68.0 ± 0.9
Symmetric furan-amidine 111	<i>para</i> -C(=N)NH ₂	35.0 ± 0.8
144	<i>meta</i> -F	98.0 ± 0.5
145	<i>para</i> -F	505.0 ± 1.2
146	<i>para</i> -Br	27.0 ± 0.5
147	<i>meta</i> -NO ₂	14.5 ± 2.3
148	<i>para</i> -NO ₂	15.2 ± 2.2
149	<i>para</i> -OCH ₃	107.0 ± 0.8
154	----	Inactive

The positive control resveratrol **60** showed an IC₅₀ value of 913.0 ± 2.3 nM. All of the synthesized asymmetric furan-amidines and their pyrrole and *N*-methylpyrrole analogues with a *para*-amidine showed superior inhibitory activity to resveratrol, with IC₅₀ values in the nano-molar range. The asymmetric furan-amidines with a *para*-amidine group and a substituent on the other phenyl group showed very good inhibitory activity in the < 100 nM range, the exception being **145**.

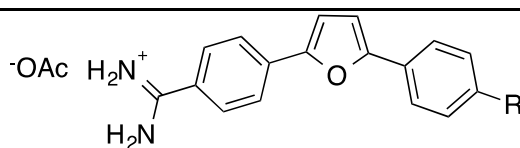
The best asymmetric furan-amidines inhibitors with *meta*- and *para*-NO₂ group **147** and **148**, respectively, both showed IC₅₀ values of ~15 nM. The low water solubility of the most potent NQO2 inhibitors **147** and **148** limited their further evaluation to be potential drugs for cancer.

The effect of length and branching of the alkyl groups on NQO2 inhibitory ability was studied by preparing asymmetric furan-amidine with homologous alkyl

Chapter II. Results and Discussion/ NQO2 Inhibitory Activity

substituents **150-153** (Table 18). Both asymmetric furan-amidines **110** (R = H) and **150** (R = Me) showed approximately similar IC₅₀ values of ~70 nM. An increase in the alkyl chain length to ethyl and *tert*-butyl led to the increase of the IC₅₀ values by 3 and 8 fold, respectively, when compared with **110**. This can be explained by the increase in the lipophilicity of the synthesized compounds with the increase in the alkyl chain length. Compound **152**, with the isopropyl group, could not be tested because of its low aqueous solubility.

Table 18. The IC₅₀ values of the asymmetric furan-amidine **110** and its alkyl-substituted analogues (tested by my colleague PhD student Elham Santina).



Compound ID	R	IC ₅₀ (nM) ± SE
110	H	68.0 ± 0.9
150	Me	72.0 ± 0.9
151	Et	202.0 ± 0.3
152	<i>i</i> Pr	Poor aqueous solubility
153	<i>t</i> -Bu	509.9 ± 0.3

The change of amidine from the *para*-position **110** to the *meta*-position **154** led to the loss of NQO2 inhibitory activity. The opposite effect was seen with the fluoro-substituent as the *meta*-fluoro compound **144** showed a five-fold enhanced inhibitory activity compared to the *para*-fluoro analogue **145**.

The isosteric replacement of furan ring **110** into pyrrole **191**, *N*-methylpyrrole **192**, imidazole **193**, *N*-methylimidazole **194** and thiophene **226** all led to an increase of the IC₅₀ values when compared with **110** (Table 19). This can be rationalized by the loss of the planar geometry, which is an essential property for NQO2 inhibitors in order to be accommodated into the deep active site cleft.⁵⁵

Chapter II. Results and Discussion/ NQO2 Inhibitory Activity

Table 19. The IC₅₀ values of the asymmetric furan-amidine **110** and its furan isosteric analogues (tested by my colleague PhD student Elham Santana).

Compound ID	IC ₅₀ (nM) ± SE
4-Methylfuran-amidine 224	Inactive
Furan-amidine 110	68.0 ± 0.9
Pyrrole-amidine 191	332.0 ± 1.2
N-Methylpyrrole-amidine 192	410.0 ± 1.1
Imidazole-amidine 193	1111.0 ± 0.5
N-Methylimidazole-amidine 194	Inactive
Oxazole-amidine 195	Inactive
Thiophene-amidine 226	773.1 ± 0.4

The isosteric replacement of amidine group **110** by ethyl imidate **234**, *N*-aryl amidine (reversed amidine) **235** and **236**, *N*-aryl amide **238** and *N*-hydroxy amidine (amidoxime) **240** all led to the loss of NQO2 inhibitory activity (Table 20). The *N*-aryl amides **237** and **239** showed mild NQO2 inhibitory effect with IC₅₀ values of approximately 1 and 2 μM, respectively. The amidine group is mainly protonated at physiological pH (the pH of the assay media) as the pK_a of the conjugate acid of the amidine group is 11.8.¹⁰¹ On the other hand, the protonated and neutral forms of the imidate group in compound **234** will be in equilibrium, with the preference for the neutral form as the pK_a of the conjugate acid of the imidate group is 6.2.¹⁰⁷

Chapter II. Results and Discussion/ NQO2 Inhibitory Activity

Table 20. The IC₅₀ values of the asymmetric furan-amidine **110** and its amidine isosteric analogues (tested by my colleague PhD student Elham Santana).

Compound ID	X	Y	IC ₅₀ (nM) ± SE
110	O	<i>para</i> -	68.0 ± 0.9
234	O	<i>para</i> -	Inactive
235	O	<i>para</i> -	Inactive
236	S	<i>para</i> -	Inactive
237	O	<i>meta</i> -	1145 (n =1)
238	O	<i>para</i> -	Inactive
239	S	<i>meta</i> -	2000 (n =1)
240	O	<i>para</i> -	Inactive

The loss of activity in the reversed amidines **235** and **236** may be explained by the steric effect of the methyl group, as the distance between the phenyl ring and methyl group in **235** and **236** is longer than the distance between the phenyl group and the amine group in **110** (Figure 77).

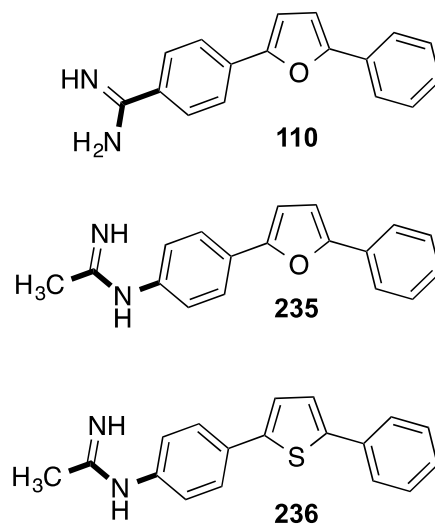


Figure 77. The structures of the furan-amidine **110** and its furan- and thiophene-reversed amidines **235** and **236**, respectively.

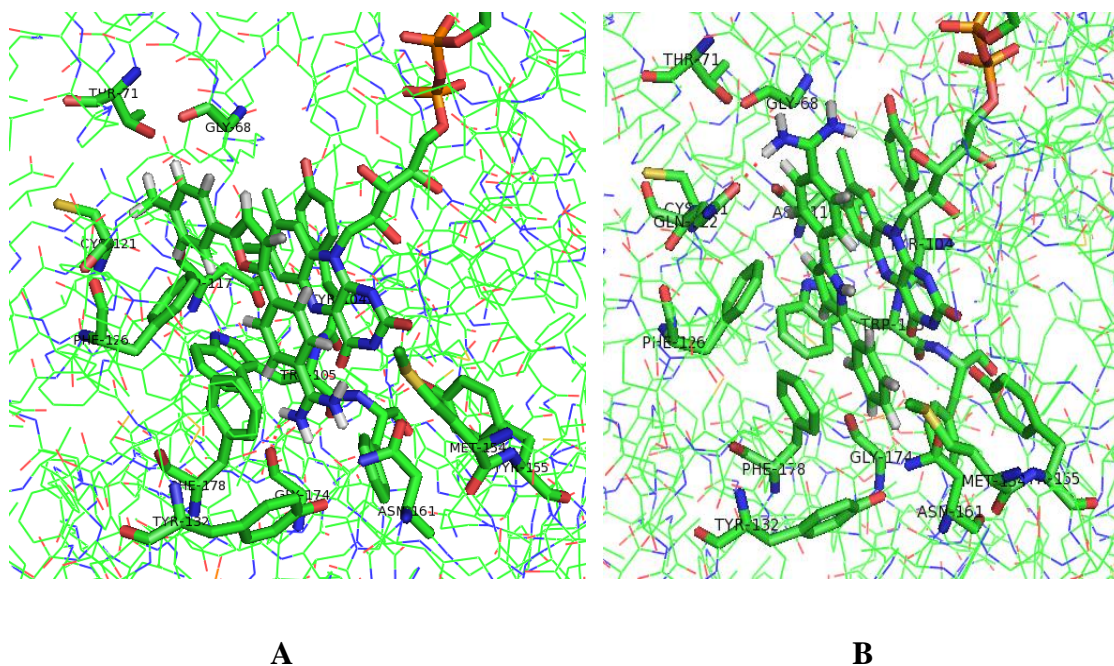
The *N*-hydroxy amidine **240** is a potential pro-drug for the asymmetric furan-amidine **110**. The pro-drug approach can provide a potential solution for the low water solubility of parent compounds, as all the isosteric modifications led to a decrease or total loss of the inhibitory activity.

Chapter II. Results and Discussion/ Docking

1. Docking: Correlation between the predicted and experimental NQO2 inhibitory activity of the synthesized compounds

The *in silico* study of the binding modes of the synthesized inhibitors in the active site of NQO2 aids the design of potential highly potent inhibitors. The synthesized NQO2 inhibitors were computationally docked in the NQO2 active site using the X-ray crystal structure of human NQO2 with bound FAD (PDB code 1QR2; Resolution at 2.10 Å).

The docking calculations predicted an energetically favourable binding mode for the asymmetric furan-, pyrrole-, *N*-methylpyrrole-, thiophene-, imidazole-, *N*-methylimidazole- and oxazole-amidines. All the inhibitors are positioned in the centre of the active site co-planar with the isoalloxazine ring of the FAD molecule. The inhibitors mainly make a hydrophobic interaction with the FAD molecule and the hydrophobic amino acids Trp¹⁰⁵, Phe¹⁷⁸, Phe¹²⁶, Met¹⁵⁴ and Cys¹²¹ through π - π stacking interactions. The amidine group forms hydrogen bonds with the side chain of the hydrophilic amino acid Glu-122 or the backbone of the simple amino acid Gly-174. Figure 78 shows that the asymmetric furan-amidine **150** (A), pyrrole-amidine **191** (B), *N*-methylpyrrole-amidine **192** (C) and thiophene-amidine **226** (D) adopt a flat conformation, which optimizes the hydrophobic interaction with the isoalloxazine ring of the FAD molecule.



Chapter II. Results and Discussion/ Docking

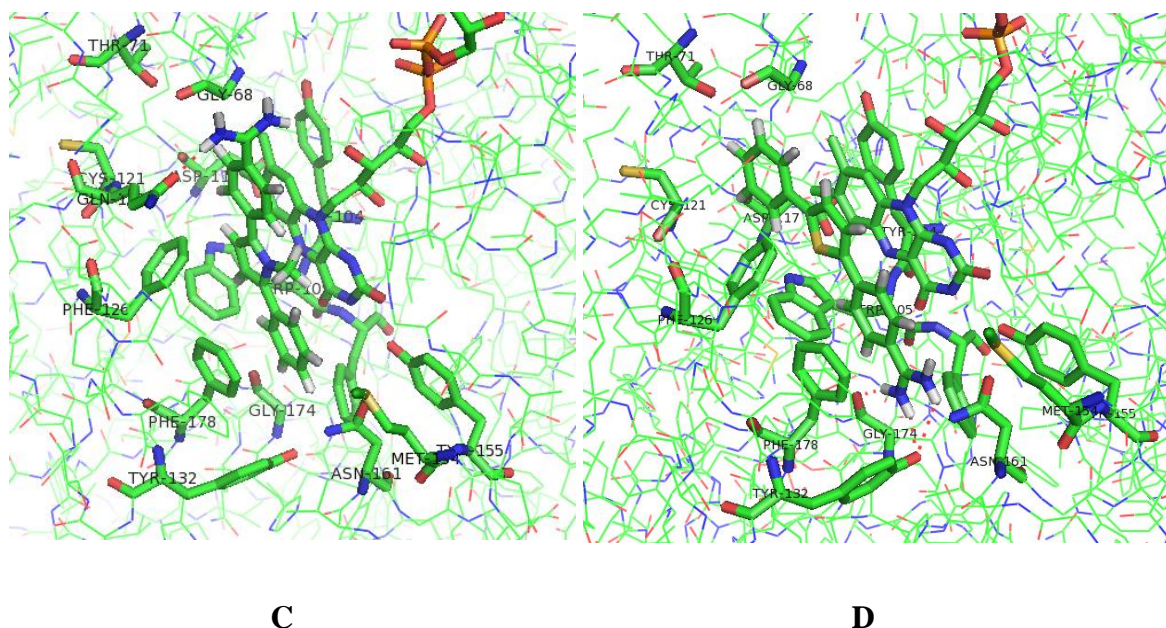


Figure 78. The most energetically favourable docking binding mode in the NQO2 active site (PDB code 1QR2; Resolution at 2.10 Å) for: A- Asymmetric furan-amidine **150**; B- Asymmetric pyrrole-amidine **191**; C- Asymmetric *N*-methylpyrrole-amidine **192**; D- Asymmetric thiophene-amidine **226**.

The binding affinities ΔG_{calc} of the synthesized inhibitors were calculated after their docking in the NQO2 active site (PDB code 1QR2; Resolution at 2.10 Å). The binding affinity is an indication of the strength of the non-covalent interaction between the protein receptor or enzyme active site and the ligand or inhibitor. The inhibitors' *in silico* binding affinities ΔG_{calc} (KJ/mol) were compared to the *in vitro* ΔG_{exp} (KJ/mol) binding affinities derived from the experimental IC_{50} values. The experimental binding affinities were calculated using the Cheng-Prusoff equation (Equation 2) from the IC_{50} values:^{96-97, 151}

$$\Delta G_{\text{exp}} (\text{J}) = -RT \ln (K_i) \dots \dots \dots \text{Equation 2}$$

R = ideal gas constant, which equals 8.31 J/mol.K

T = Temperature at which the IC_{50} was calculated, Kelvin

K_i = Inhibition constant, which is equal to IC_{50} (molar concentration).

Only a poor correlation (correlation coefficient $R^2 = 0.0366$) between the calculated and experimental binding affinities was observed (Figure 79).

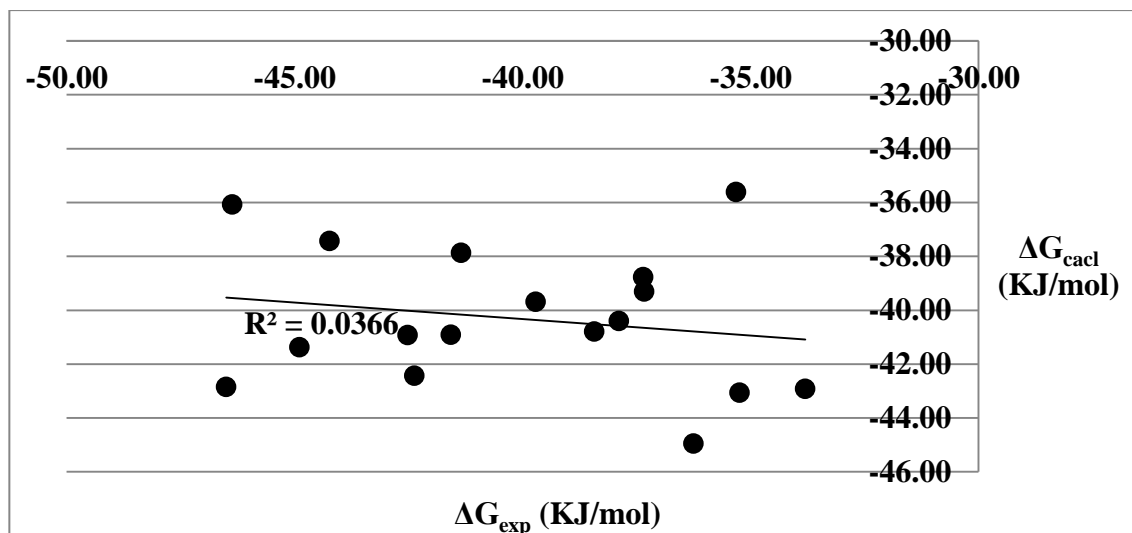
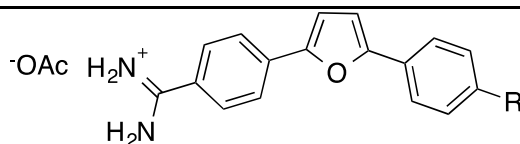


Figure 79. Experimental (ΔG_{exp} ; KJ/mol) and calculated (ΔG_{cal} ; KJ/mol) binding affinities for the synthesized inhibitors binding to NQO2.

The calculated binding affinities of the asymmetric furan-amidine **110** (R = H) and its alkyl-substituted analogues **150** (R = Me), **151** (R = Et) and **153** (R = *tert*-Bu) were consistent with the experimental binding affinities (Table 21). With the increase in the length and branching of the alkyl group, the possibility of the steric effect increases, which results in the overall decrease in the value of the calculated binding affinity. A very good correlation (correlation coefficient $R^2 = 0.725$) between the calculated and the experimental binding affinities was observed for these inhibitors (Figure 80)

Table 21. The experimental (ΔG_{exp} ; KJ/mol) and calculated (ΔG_{cal} ; KJ/mol) binding affinities of the asymmetric furan-amidine **110** and its alkyl-substituted analogues **150**, **151** and **153**.



Compound ID	R	ΔG_{cal} (KJ/mol)	ΔG_{exp} (KJ/mol)
110	H	-40.92	-42.52
150	Me	-42.44	-42.37
151	Et	-39.69	-39.71
153	<i>t</i> -Bu	-39.31	-37.33

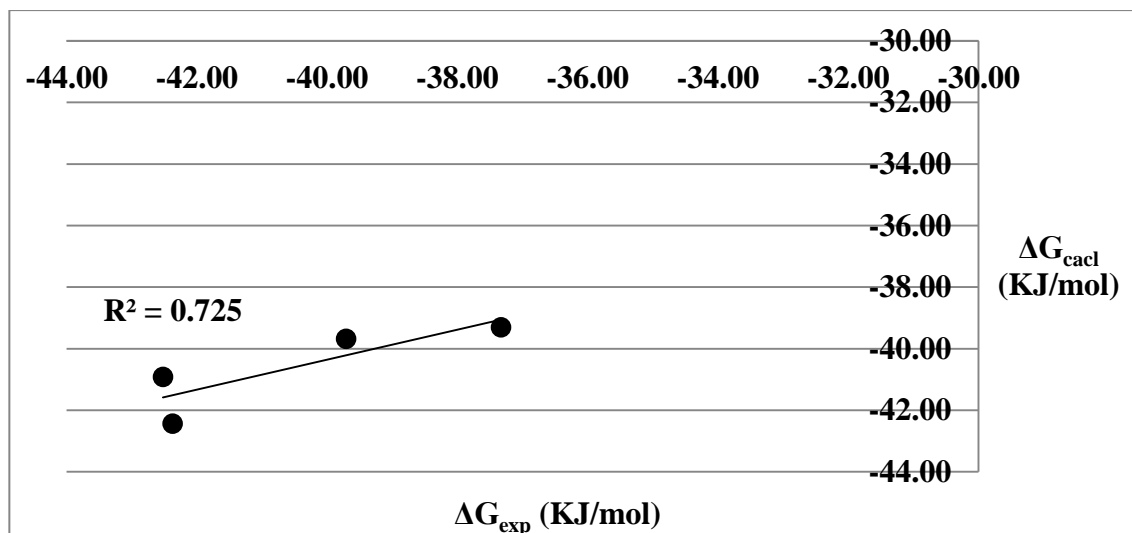


Figure 80. Experimental (ΔG_{exp} ; KJ/mol) and calculated (ΔG_{calcl} ; KJ/mol) binding affinities for the synthesized inhibitors **110**, **150**, **151** and **153** binding to NQO2.

Poor correlation (correlation coefficient $R^2 = 0.0397$) was observed when comparing the asymmetric furan-amidine **110** with its heterocyclic-containing analogues; pyrrole- **191**, *N*-methylpyrrole- **192**, imidazole- **193**, and thiophene- **226** (Figure 81).

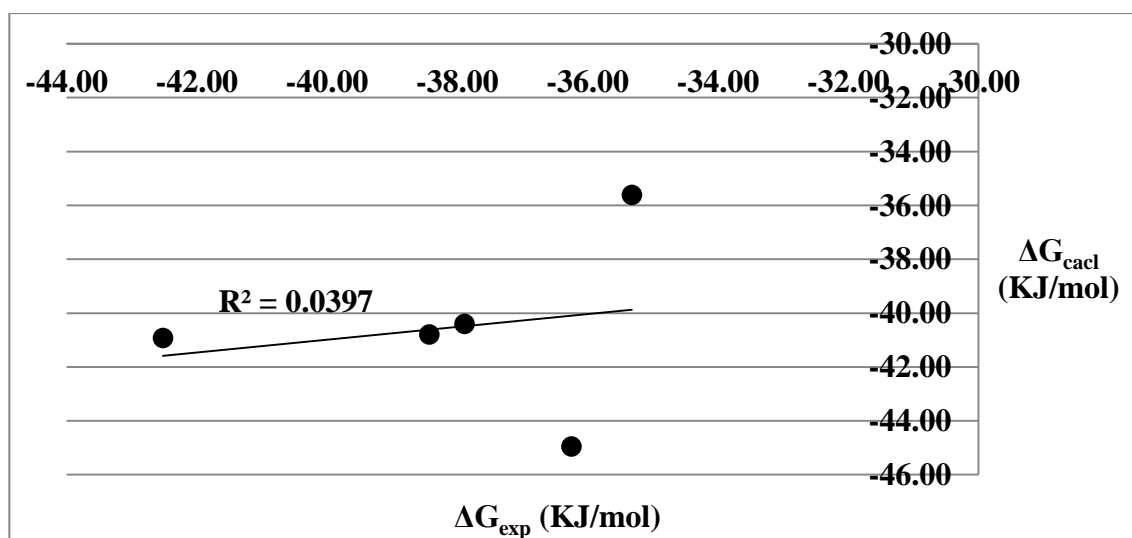


Figure 81. Experimental (ΔG_{exp} ; KJ/mol) and calculated (ΔG_{calcl} ; KJ/mol) binding affinities for the synthesized inhibitors **110**, **191**, **192**, **193** and **226** binding to NQO2.

In contrast, better correlation (correlation coefficient $R^2 = 0.583$) was observed when comparing the asymmetric furan-amidine **110** with its heterocyclic-containing analogues; pyrrole- **191**, *N*-methylpyrrole- **192** and imidazole-amidines **193**, except thiophene-amidine **226** (Figure 82). The calculated binding affinity for the thiophene-

Chapter II. Results and Discussion/ Docking

amidine **226** (-44.95 KJ/mol) was much higher than the experimental binding affinity (-36.25 KJ/mol). This large difference can be explained by the high lipophilicity of the thiophene heterocycle compared to the furan, pyrrole and imidazole heterocycles. As the NQO2 active site is highly hydrophobic in nature, it is expected that the thiophene-containing inhibitors form more hydrophobic interaction with the hydrophobic amino acids than the other inhibitors, leading to higher predicted binding affinity values. The same difference was observed between the calculated (-42.92 KJ/mol) and experimental (-35.24 KJ/mol) binding affinities with the thiophene-reversed amidine **239**.

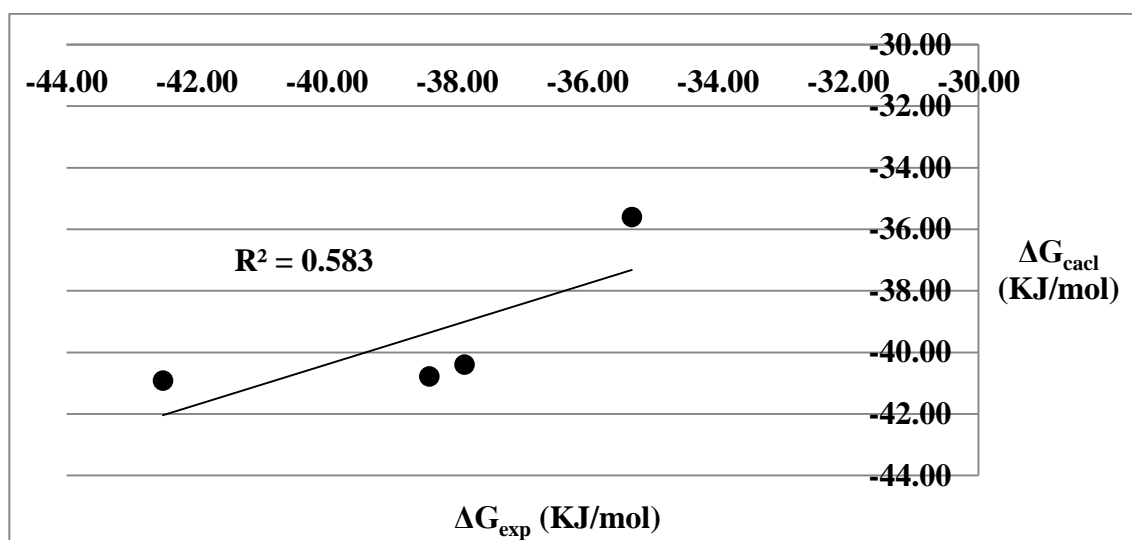


Figure 82. Experimental (ΔG_{exp} ; KJ/mol) and calculated (ΔG_{cal} ; KJ/mol) binding affinities for the synthesized inhibitors **110**, **191**, **192** and **193** binding to NQO2.

Although, the computational docking gives a prediction for the affinity of a ligand to bind to a protein receptor or enzyme active site, it can only be used as a guide to aid and direct the synthesis of novel NQO2 inhibitors.

Chapter II. Results and Discussion/ DNA Melting

1. Introduction

The stability of the secondary structure of DNA in aqueous solution depends on the interaction between the complementary bases through H-bonds and the interaction between neighbouring pairs through π - π stacking of the bases.¹⁵² The heating of DNA over a range of 25-98 °C leads to the breaking of H-bonds and the un-stacking of the base pairs. As a result a separation of the double strands occurs, which is known as DNA thermal denaturation or melting.¹⁵³ DNA has a characteristic UV absorption spectrum with a maximum near 260 nm and a minimum near 230 nm, and the un-stacking of DNA pairs can be readily monitored spectrophotometrically. The un-stacking of DNA pairs leads to a hyperchromic effect in which the absorbance increases by 30% as the un-stacked base pairs can absorb more light.¹⁵⁴ The plot of the DNA absorbance versus the temperature gives a sigmoidal curve. At the beginning of the experiment, double-stranded DNA is present. With the increase in the temperature, the bonds between the base pairs start to break and a hyperchromic shift is observed. At the end of the experiment, the DNA has melted and only DNA single strands are present (Figure 83).

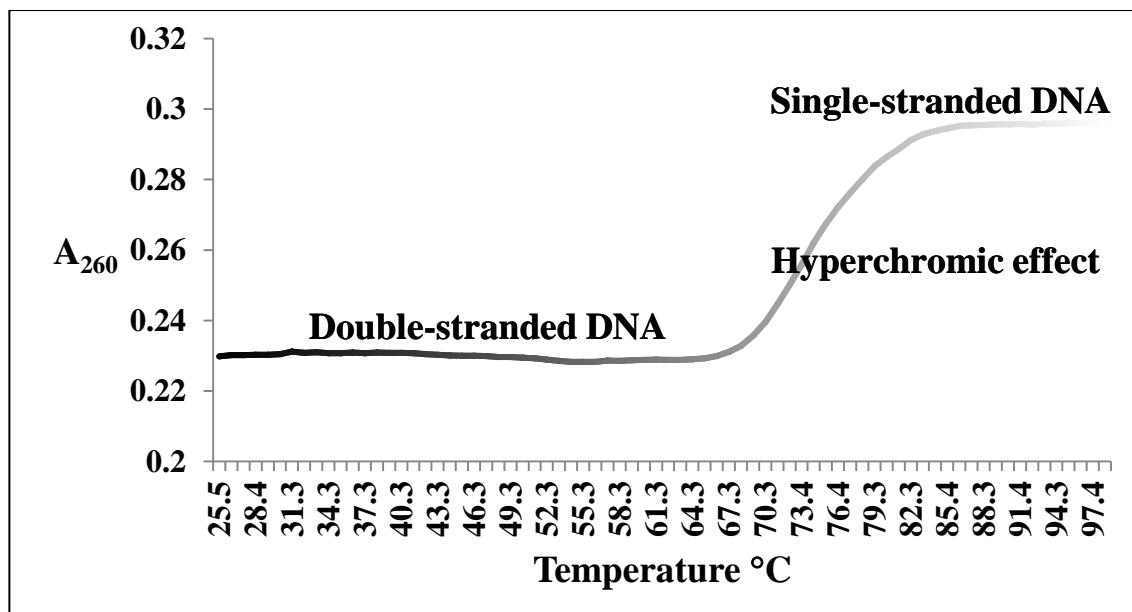


Figure 83. Thermal denaturation sigmoidal curve for DNA.

The temperature at which the DNA melts is known as the DNA melting temperature (T_m), which is defined as the temperature in degrees Celsius, at which 50% of DNA is hybridized into a double strand, and 50% is present as single strands (Figure 84).

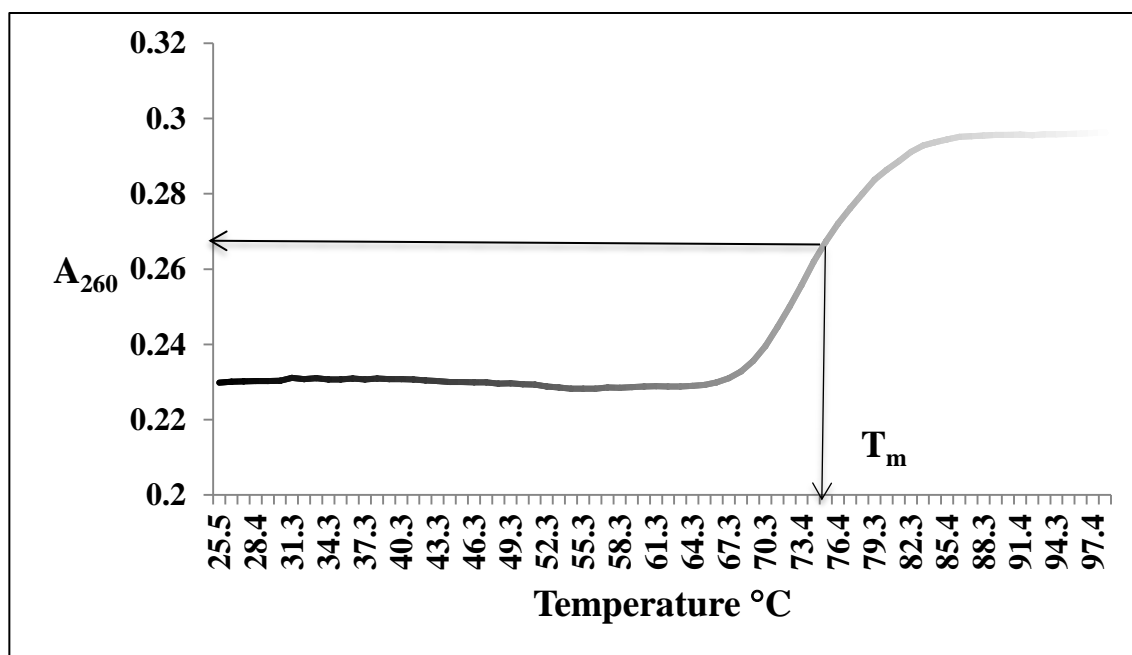


Figure 84. DNA melting temperature (T_m) measurement.

The binding of a ligand to DNA usually leads to an increase in the DNA T_m value as more energy is needed to overcome the interactions between the ligand and DNA.¹⁵³ The DNA thermal denaturation method can be used as an indicator for the binding of the drugs to DNA.

2. DNA binding: Is it an off-target effect for the synthesized asymmetric furan-and *N*-methylpyrrole-amidines?

Symmetric furan-amidines are known to be DNA minor grooves binder and they bind strongly in the minor groove of the AT sequence.¹⁵⁵ To ensure the selectivity of the synthesized asymmetric amidine-compounds towards the inhibition of NQO2 without DNA off-target effects, the T_m values of double-stranded DNA in the presence of the synthesized asymmetric furans- **110**, **144-146** and **149-150** and *N*-methylpyrrole-amidines **192** were measured. Two positive controls were used in this experiment, which were doxorubicin **20** and the symmetric furan-amidine **111**, both known to intercalate into DNA. The melting of DNA in the presence of doxorubicin **20**, symmetric furan-amidine **111**, furan- **110**, **144-146** and **149-150** and *N*-methylpyrrole-amidines **192** were monitored spectrophotometrically over a range of 25-98 °C in low salt solution. To get the DNA melting temperature in a more accurate way than the sigmoidal curve, the first derivative of the DNA sigmoidal was calculated. The first derivative curve is the plot of $-(dA/dT)$ versus temperature (Figure 85).

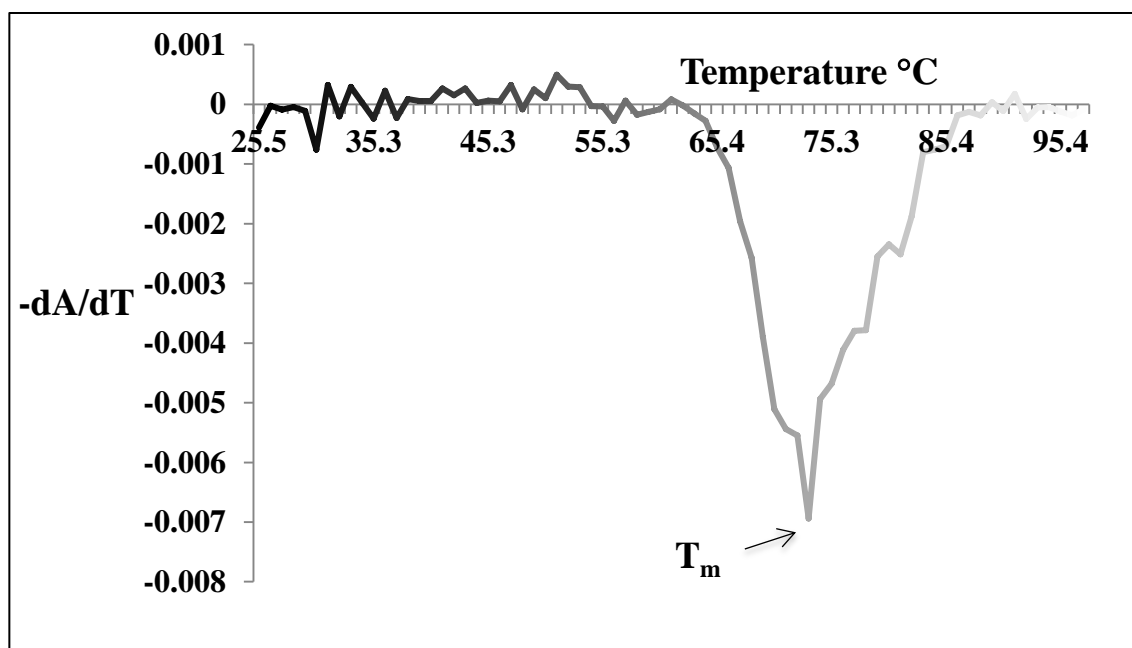


Figure 85. DNA thermal denaturation first derivative curve, asymmetric furan-amidine 144.

The melting point temperatures of doxorubicin **20**, **111**, **110**, **144-146**, **149-150** and **192** are summarized in Table 22. Table 22 showed also the difference in DNA melting temperatures in the absence and presence of the compound ($\Delta T_m = T_m^{\text{compound-DNA complex}} - T_m^{\text{DNA alone}}$).

Table 22. DNA melting temperatures of doxorubicin, symmetric and asymmetric furan-amidines and asymmetric *N*-methylpyrrole-amidine in low salt solution.

Compound ID	T_m (°C)	ΔT_m (°C)
DNA	70.8 ± 1.5	0
Doxorubicin 20	91.2 ± 1.0	20.5
Symmetric furan-amidine 111	90.8 ± 0.6	20.0
Asymmetric furan-amidine 110	72.3 ± 0.4	1.9
Asymmetric furan-amidine 144	74.0 ± 0.5	3.2
Asymmetric furan-amidine 145	74.0 ± 0.6	3.2
Asymmetric furan-amidine 146	75.2 ± 1.4	4.4
Asymmetric furan-amidine 149	72.7 ± 0.6	2.0
Asymmetric furan-amidine 150	73.6 ± 0.5	2.8
Asymmetric <i>N</i> -methylpyrrole-amidine 192	71.7 ± 0.6	0.9

Chapter II. Results and Discussion/ DNA Melting

Doxorubicin and the symmetric furan-amidine **111** showed high affinity for binding of approximately 20 °C. The amidine groups of the symmetric furan-amidine **111** form H-bonding with thymine keto-groups forming the floor of DNA minor grooves. In addition, the furan ring is pushed slightly away from the floor of DNA minor groove, but it fits well between the walls of the groove, which consists of deoxyribose groups.¹²⁴

In contrast, all of the asymmetric furan-amidines **110**, **144-146**, **149-150** showed low affinity for DNA. Their weaker interactions comparing to the symmetric furan-amidine **111** led to a slight increase in DNA melting temperature approximately 2-4.4 °C. This can be explained by the presence of one amidine group, which is capable of making H-bonding with the thymine keto-group inside the minor groove of DNA.

The *N*-methylpyrrole-amidine **192** showed the lowest binding affinity for DNA with an increase of only 0.9°C in DNA melting temperature. *N*-Methylpyrrole-amidine **192** is forced from being a planar compound by the methyl group attached to the nitrogen atom, which decreases the ability of this compound to bind in the minor groove of DNA.

The plot of relative absorbance ($A/A_{25\text{ °C}}$) versus the temperature (°C) showed the effect of a compound with a high DNA binding affinity on the T_m when comparing to a compound with low DNA binding affinity. Figure 86 shows the effect of doxorubicin **20**, the symmetric furan-amidine **111** and the asymmetric furan-amidine **144** on DNA melting temperatures.

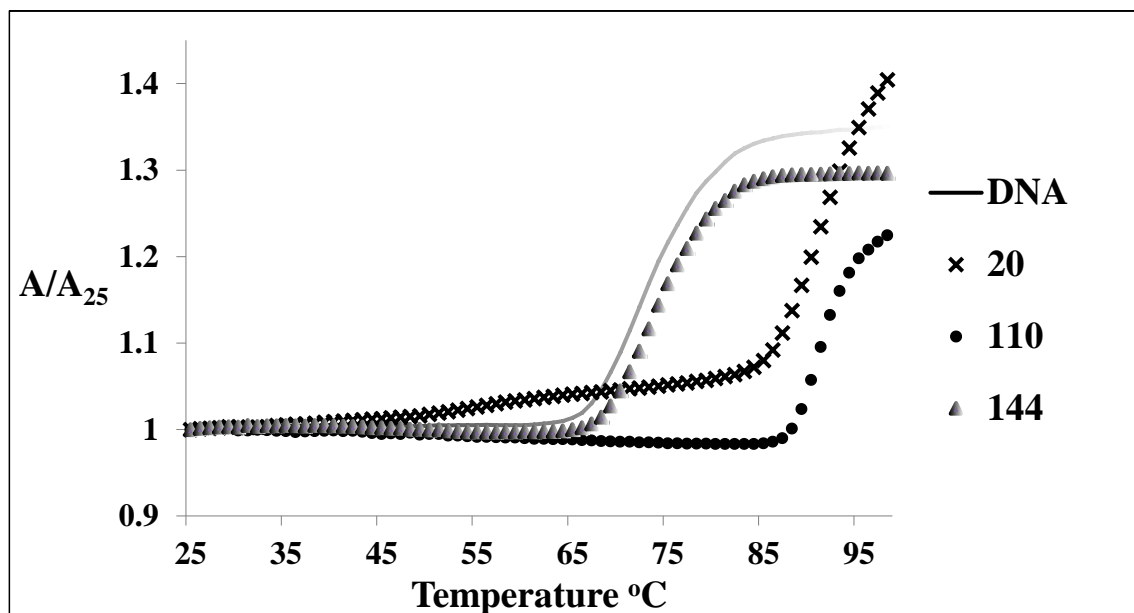


Figure 86. DNA melting temperature: The plot of relative absorbance *versus* temperature.

In addition, the melting temperatures of DNA in the presence of doxorubicin **20**, **111**, **110**, **144-146**, **149-150** and **192** were measured in high salt solutions (Table 23). The T_m melting temperature of DNA increases with increasing salt concentration as the DNA is more stable and the cations in the solution form ionic interactions with the negatively charged phosphate groups.¹⁵⁶ The T_m value of DNA alone in high salt solution is 88.1 °C compared to 70.8 °C in low salt solution. The same pattern of binding affinities was observed for the compounds in high salt solution, with only small ΔT_m .

Chapter II. Results and Discussion/ DNA Melting

Table 23. DNA melting temperatures of doxorubicin, symmetric and asymmetric furan-amidines and asymmetric *N*-methylpyrrole-amidine in high salt solution.

Compound ID	T _m (°C)	Δ T _m (°C)
DNA	88.1 ± 1.0	0
Doxorubicin 20	92.9 ± 0.6	4.8
111	90.6 ± 0.6	2.5
110	87.7 ± 0.7	-0.4
144	87.5 ± 0.1	-0.7
145	88.2 ± 0.4	0.1
146	88.7 ± 1.2	0.6
149	88.3 ± 0.0	0.2
150	87.8 ± 1.1	-0.3
192	88.5 ± 0.1	0.4

3. DNA binding: Reversed amidines and DNA binding affinities

Unsymmetrical reversed amidines **235** and **236** were designed as potential NQO2 inhibitors with low DNA binding affinities. Aryl reversed amidine has a larger amidine-phenyl dihedral angle than aryl amidine, making aryl reversed amidines possess 10-fold lower DNA binding affinity than aryl amidine.¹²⁴ The amidine-phenyl dihedral angle in the reversed amidine is 90° compared with 40-45° in aryl amidine, which leads to unfavourable interactions of the reversed amidine inside the minor groove of DNA.¹²⁴

As the reversed amidines **235** and **236** did not show any inhibitory activity against NQO2; their DNA binding affinities and DNA melting temperatures have not been measured.

Chapter II. Results and Discussion/ Conclusion

1. Conclusion on synthesis and evaluation of novel NQO2 inhibitors

An efficient total synthesis of the lead asymmetric furan-amidine **110** and a series of asymmetric furan-, pyrrole-, *N*-methylpyrrole-, thiophene-, imidazole, *N*-methylimidazole- and oxazole-amidines have been successfully carried out using multi-step synthetic pathways. The synthesis of the target compounds started from the preparation of different substituted 1,4-diketone intermediates. The 1,4-diketone intermediates were cyclized to different 5-membered heterocycles using a variety of reagent. The nitrile and nitro groups served as the precursor for amidine and *N*-aryl amidine (reversed amidine) and amide groups, respectively.

The substitution of the phenyl ring in the case of furan-amidines, specifically with a nitro-group resulted in the most active inhibitors **147** and **148** (Figure 87) of NQO2 activity. In contrast, structural modification of the amidine group in the parent asymmetric furan-amidine **110** resulted in loss of the NQO2 inhibitory activity.

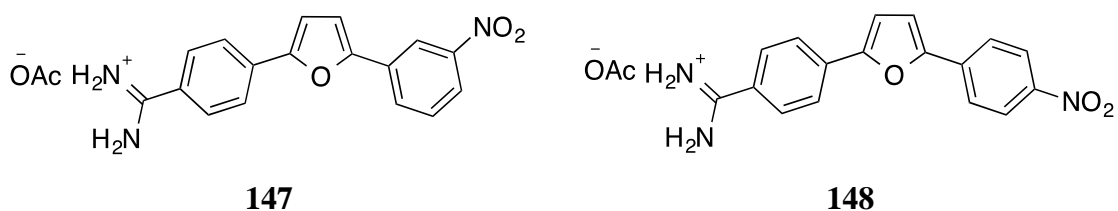


Figure 87. Structures of the most active asymmetric furan-amidines **147** and **148**.

The isosteric replacement of the furan ring into more water-soluble 5-membered heterocycles, namely, pyrrole **191**, *N*-methylpyrrole **192**, imidazole **193**, *N*-methylimidazole **194** and oxazole **195**, led to the decrease in the NQO2 inhibitory activities when compared to the lead asymmetric furan-amidine **110** (Figure 88).

Chapter II. Results and Discussion/ Conclusion

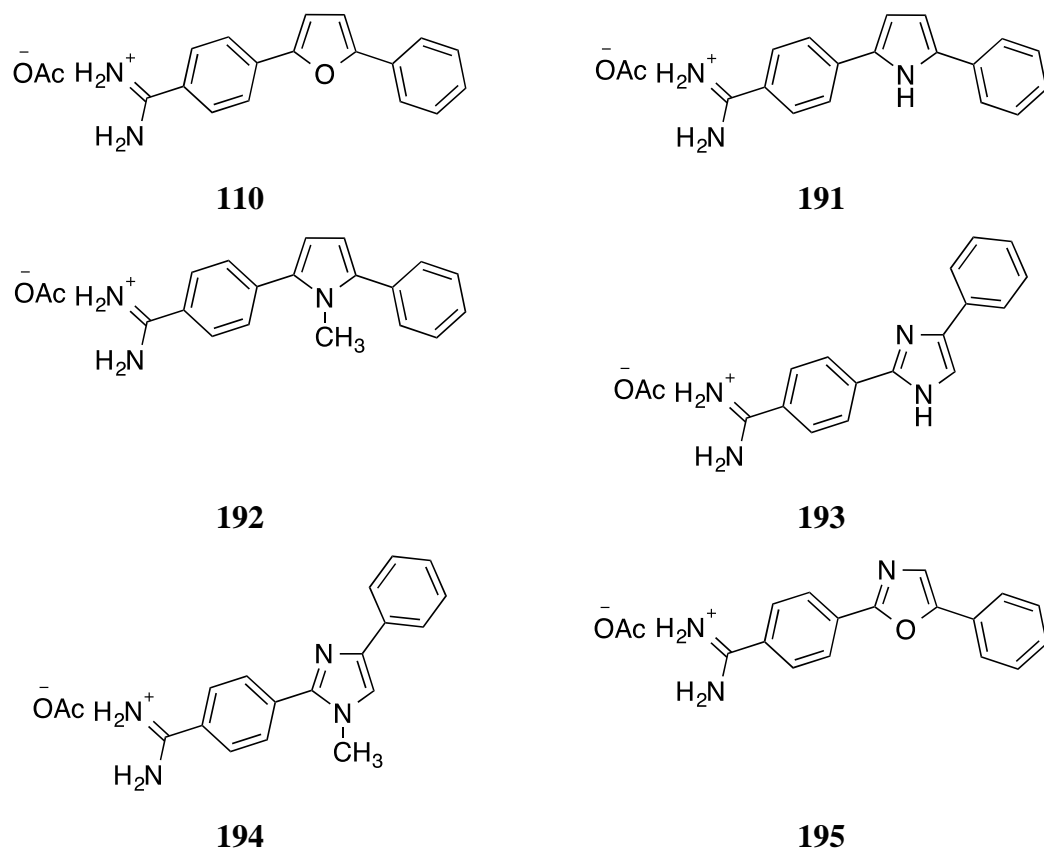


Figure 88. Structures of the asymmetric furan-amidine **110** and its 5-membered heterocycle analogues.

One compound with the *N*-hydroxy amidine group **240** was synthesized (Figure 89), which is considered as a potential pro-drug for the asymmetric furan-amidine **110**. The pro-drug approach can provide a solution for the low water solubility as all the isosteric modifications led to a decrease or total loss of the inhibitory activity.

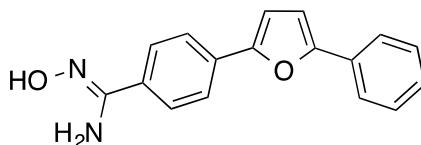


Figure 89. Structure of the potential prodrug **240** of the asymmetric furan-amidine **110**.

The asymmetric furan-amidines showed no binding affinity towards DNA when compared to the symmetric furan-amidines, which are known as DNA intercalators. This improves the selectivity of the asymmetric furan-amidines towards NQO2.

In conclusion, the synthesis of potent selective NQO2 inhibitors with the asymmetric furan-amidine scaffold has been achieved. They can be further investigated as potential drugs in chemotherapy and chemoprevention.

Chapter II. Results and Discussion/ Future Work

1. Isosteric replacement of the basic amidine group with the acidic carboxylic acid

A targeted compound with a carboxylic acid **265** as an isostere of the amidine group **110** is proposed for synthesis (Figure 90). The presence of a highly acidic group can give an indication if the basicity of amidine group was an important reason for the high NQO2 inhibition activity of the furan-amidines.

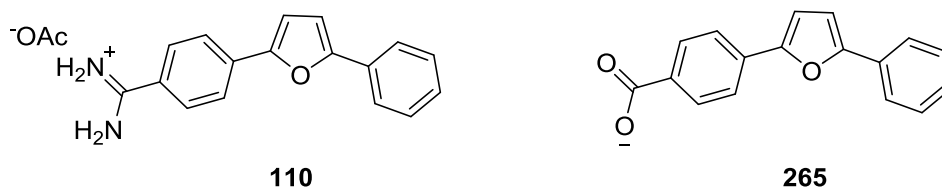


Figure 90. Structure of asymmetric furan-amidine **110** and its carboxylic acid isostere **265**.

2. Synthesis of 3-fluoro diarylimidazole-amidine

In general, the synthesized furan-amidines showed poor water solubility. An imidazole-amidine **193** (Figure 88) was synthesized as an analogue for the asymmetric furan-amidine **110** (calculated log *P* value of 2.8) with expected improved water solubility (calculated log *P* value of 1.8 for **193**). The imidazole-amidine **193** inhibited the NQO2 enzyme with an IC₅₀ value of approximately 1.0 μM compared to a value of 68.0 nM for the furan-amidine **110**.

As the fluoro-substitution on the *meta*-position **144** (Figure 91) of the phenyl ring of the asymmetric furan-amidine **110** led to the conservation of the inhibition activity, an-imidazole-amidine with *meta*-fluoro substituent **266** (Figure 91) is proposed to be synthesized.

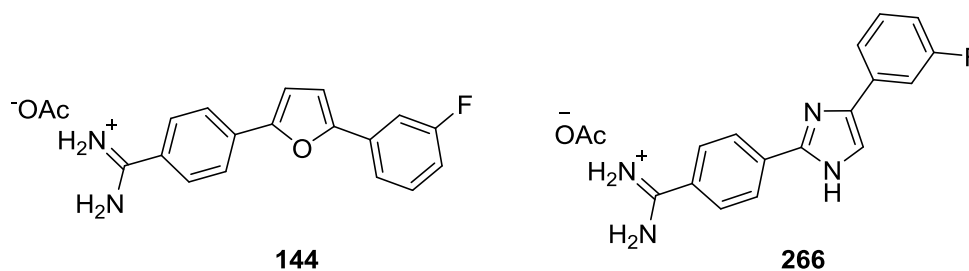


Figure 91. Structure of asymmetric furan-amidine **144** and 3-fluoro diarylimidazole-amidine **266**.

3. Positron Emission Tomography (PET): study of NQO2 biological role and the consequence of its inhibition in tumour cells

Positron emission tomography (PET) is a non-invasive technology that is used

Chapter II. Results and Discussion/ Conclusion

to monitor the biological systems at the molecular level by using a camera that can image high-energy gamma rays emitted from inside the subject. The technology depends on labelling natural biological molecules or drugs with isotopes capable of producing two gamma-rays through the emission of a positron from their nuclei. The isotopes that are frequently used in this technology are ^{11}C , ^{15}O , ^{13}N or ^{18}F .¹⁵⁷

PET technology can be used to monitor the changes in cancer cells at the molecular level during the pharmacological and radiation therapy to get more information that aids the drug design focused on chemoprevention or chemotherapy.¹⁵⁷

The limitation of the use of this technology is the short half-lives of the isotopes used; for example, the half-life of ^{18}F is 110 m. In order to benefit from this technology, the rapid and efficient synthesis of the labelled molecules first and their safe administration to the subject are essential.¹⁵⁷

PET technology can be used to study the biological role of NQO2 and the consequences of its inhibition in tumour cells by introducing labelled drugs that selectively and potently inhibit the enzyme. The asymmetric furan-amidines **144** and **149** (Figure 92) were chosen as the target compounds to be used. The aim is the label of **144** and **149** with the isotopes ^{18}F and ^{11}C , respectively, then the administration of these drugs *in vivo*. As, the isotopes ^{18}F and ^{11}C are radioactive isotopes; the handling and synthesis must be done in a special purpose laboratory.

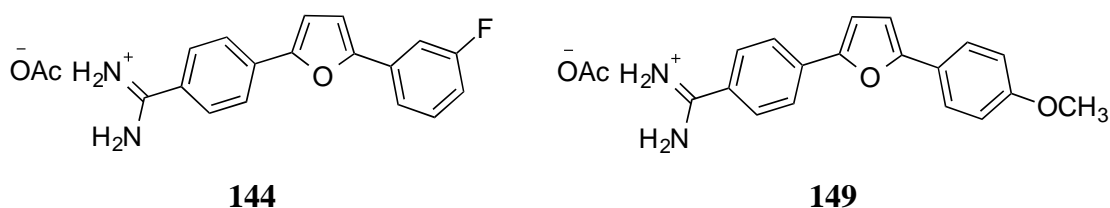


Figure 92. Structures of PET candidate compounds **144** and **149**.

Chapter III. Experimental/ Chemistry

1. Chemicals and materials

Chemicals were purchased from Sigma-Aldrich, solvents were purchased from Fisher Scientific, and deuterated solvents were purchased from Goss. Melting points were measured using a Stuart Scientific melting point apparatus SAMP10. Infrared spectra were recorded in the solid state using a J.A.S.C.O fourier transform infrared spectrophotometer. A Bruker Avance 300 and 400 MHz spectrometer was used to record ^1H and ^{13}C NMR spectra. Chemical shifts are quoted in parts per million (ppm) and referenced to tetramethylsilane ($\delta = 0$). Mass spectrometry was carried out in the School of Chemistry, University of Manchester using a Micromass Platform II instrument. Molecular ions peaks are reported as mass/charge (m/z) ratios. Solvents were evaporated on a Buchi rotavapor R-200 equipped with a Buchi heating bath B-490. Thin layer chromatography (TLC) was performed using silica gel 60 on aluminum sheets with F254. The spots were visualized using a UV Mineralight lamp (254/365) UVGL-58. Column chromatography was performed using silica gel particle size 40-63 microns. A BECKMAN DU 7400 spectrophotometer was used to determine enzyme activity. A Grant JB series water bath was used to heat the buffer to 37 °C.

2. Synthesis

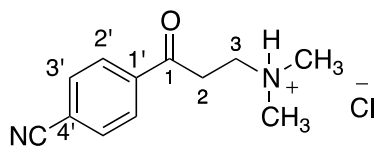
The detailed syntheses of the compounds mentioned in the results and discussion chapter are discussed in the following sections.

2.1. Mannich bases **121** and **125**

Concentrated hydrochloric acid in ethanol (20 drops of 10.0 % (w/v)) was added to a mixture of 4-acetylbenzointrile **120** (Mannich base **121** synthesis) or acetophenone **124** (Mannich base **125** synthesis) (1.0 mmol), paraformaldehyde (1.5 mmol) and dimethylammonium hydrochloride (1.5 mmol) in absolute ethanol (20 ml). The mixture was heated at reflux for 3 h and monitored by TLC (10.0 % MeOH/ CHCl_3). The workup was as described for each Mannich base compound.

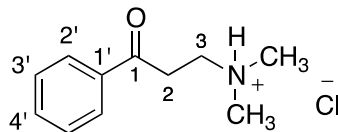
Chapter III. Experimental/ Chemistry

2.1.1. *N,N*-Dimethyl 1-(4-cyanophenyl)-1-oxopropan-3-ammonium chloride **121**



Compound **121** was crystallized from ethanol by adding 20 ml acetone. Colourless crystals were collected by filtration and rinsed with acetone to yield 0.96 g (58.0 %) of **121**: IR (cm⁻¹): 3405 (N-H), 2380, 2227 (CN), 1686 (C=O), 1408, 1332, 1220, 962, 858, 786; ¹H NMR (300 MHz; DMSO-d₆): 2.79 (6H, s, 2 × CH₃), 3.40 (2H, t, *J* = 7.5 Hz, CH₂, H-2), 3.67 (2H, t, *J* = 7.2 Hz, CH₂, H-3), 8.07 (2H, d, *J* = 8.1 Hz, 2 × CH, H-2'), 8.16 (2H, d, *J* = 8.1 Hz, 2 × CH, H-3'); ¹³C NMR (75 MHz; DMSO-d₆) (assignments made using DEPT-135): 33.6 (CH₃), 33.9 (CH₃), 42.1 (CH₂, C-2), 51.4 (CH₂, C-3), 115.5 (C, C-4'), 118.1 (CN), 128.6 (2 × CH, C-2'), 132.8 (2 × CH, C-3'), 139.0 (C, C-1'), 196.1 (C=O).

2.1.2 *N,N*-Dimethyl 1-oxo-1-phenylpropan-3-ammonium chloride **125**



Compound **125** was crystallized from ethanol by adding 20 ml acetone. Colourless crystals were collected by filtration and rinsed with acetone to yield 4.20 g (47.0 %): mp 145 °C (Lit. mp 152-153 °C)¹⁵⁸; IR (cm⁻¹): 3486, 3411 (NH), 2662, 1674 (C=O), 1334, 1223, 958, 689; ¹H NMR (300 MHz; DMSO-d₆): 2.79 (6H, s, 2 × CH₃), 3.63 (2H, t, *J* = 7.2 Hz, CH₂, H-2), 3.39, (2H, t, *J* = 7.4 Hz, CH₂, H-3), 7.57 (2H, t, *J* = 7.5 Hz, 2 × CH, H-3'), 7.69 (1H, t, *J* = 7.2 Hz, CH, H-4'), 8.02 (2H, d, *J* = 7.5 Hz, 2 × CH, H-2'); ¹³C NMR (75 MHz; DMSO-d₆) (assignments made using DEPT-135): 33.1 (CH₃), 34.1 (CH₃), 42.3 (CH₂, C-2), 51.8 (CH₂, C-3), 128.0 (2 × CH, C-3'), 128.8 (2 × CH, C-2'), 133.7 (CH, C-4'), 135.8 (C, C-1'), 196.8 (C=O).

2.2. Aryl 1,4-diketones **123** and **126**

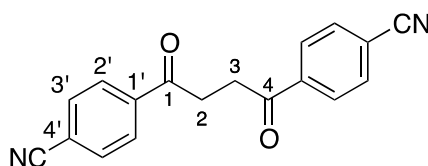
The aryl 1,4-diketones, named 1,4-bis(4-cyanophenyl)-1,4-butadione **123** and 1-(4-cyanophenyl)-4-phenyl-1,4-butadione **126** were synthesized using two synthetic pathways. The two compounds were synthesized under Stetter reaction conditions starting from the Mannich bases or through the coupling between methyl aryl ketones and α -bromomethyl aryl ketones.

Chapter III. Experimental/ Chemistry

2.2.1. General procedure for Stetter reaction

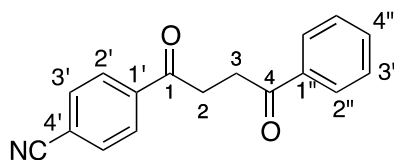
Triethylamine (2.0 mmol) was added to a suspension of Mannich base (1.0 mmol), 4-formylbenzonitrile **122** (1.0 mmol) and **19** (0.2 mmol) in dry THF (20.0 ml). The mixture was heated at reflux under an atmosphere of N₂ conditions for 48 h and monitored by TLC (20.0% EtOAc/Hexane). After the reaction mixture was cooled to room temperature, triethylammonium chloride (the identity was confirmed by ¹H NMR spectroscopy) was filtered off and THF was evaporated. Aryl 1,4-diketones **123** and **126** were purified from the crude reaction mixture by flash column chromatography using EtOAc–hexane (1:9) as the mobile phase.

2.2.1.1. 1,4-Bis(4-cyanophenyl)-1,4-butadione **123**



Light yellow fine solid; 257 mg (21.2 %): mp 247-249 °C (lit. mp 260-265 °C)¹¹⁰; IR (cm⁻¹): 2227 (CN), 1682 (C=O), 1404, 1321, 1195, 1011, 860, 785; ¹H NMR (300 MHz; DMSO-d₆): 3.48 (4H, s, 2 × CH₂, H-2, H-3), 8.04 (4H, d, *J* = 8.1 Hz, 4 × CH, H-2'), 8.16 (4H, d, *J* = 8.4 Hz, 4 × CH, H-3'); ¹³C NMR (75 MHz; DMSO-d₆) (assignments made using DEPT-135): 32.7 (2 × CH₂, C-2, C-3), 115.2 (2 × C, C-4'), 118.1 (CN), 128.5 (4 × CH, C-2'), 132.8 (4 × CH, C-3'), 139.5 (2 × C, C-1'), 198.1 (2 × C=O). The spectroscopic data (IR, ¹H and ¹³C NMR) were identical to the reported in the literature.¹¹⁰

2.2.1.2. 1-(4-Cyanophenyl)-4-phenyl-1,4-butadione **126**

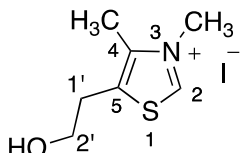


Light yellow fine solid; 88.0 mg (36.0 %): mp 126-128 °C; IR (cm⁻¹): 2225 (CN), 1673 (C=O), 1334, 1223, 959, 753; ¹H NMR (300 MHz; CDCl₃): 3.44 (2H, t, *J* = 5.4 Hz, CH₂, H-3), 3.51 (2H, t, *J* = 5.4 Hz, CH₂, H-2), 7.49 (2H, t, *J* = 7.2 Hz, 2 × CH, H-3''), 7.60 (1H, t, *J* = 7.5 Hz, CH, H-4''); 7.80 (4H, d, *J* = 8.1 Hz, 2 × CH, H-2''), 8.03 (2H, d, *J* = 7.5 Hz, 2 × CH, H-2''), 8.20 (2H, d, *J* = 8.1 Hz, 2 × CH), ¹³C NMR (75 MHz, CDCl₃) (assignments made using DEPT-135): 32.6 (CH₂, C-3), 32.8 (CH₂, C-2),

Chapter III. Experimental/ Chemistry

116.4 (C, C-4'), 118.0 (CN), 128.1 (2 × CH), 128.6 (2 × CH), 128.7 (2 × CH), 132.5 (2 × CH), 133.4 (CH, H-4'), 136.5 (C), 139.8 (C), 197.5 (C=O), 198.2 (C=O); -ESIMS m/z (relative intensity): 262 (100%, [M - H]⁻); +ESIMS m/z (relative intensity): 286 (100%, [M + Na]⁺); found by +ESIMS 286.0844, C₁₇H₁₃NO₂Na [M + Na]⁺, requires 286.0839, error 1.8 ppm.

2.2.1.3. 5-(2-Hydroxyethyl)-3,4-dimethyl-1,3-thiazolium iodide catalyst **128**



To a solution of 5-(2-hydroxyethyl)-4-methylthiazole **127** (5.00 g, 35.0 mmol) in dry acetonitrile (6.0 ml) was added iodomethane (7.45 g, 53.0 mmol). The mixture was heated at reflux for 24 h. The reaction mixture was cooled at room temperature. Acetonitrile was evaporated and the crude residue was mixed with ethyl acetate (50.0 ml) at room temperature for 6 h. A tan solid 9.77 g (98.0 %) was collected by filtration and rinsed with ethyl acetate. The catalyst was used in the synthesis of 1,4-diketone compounds without further purification: IR (cm⁻¹): 3283 (O-H), 3023, 2360, 2341, 1056, 812; ¹H NMR (300 MHz; DMSO-d₆): 2.44 (3H, s, CH₃), 3.03 (1H, t, *J* = 5.4 Hz, CH, H-1'), 3.64 (1H, q, *J* = 5.4 Hz, CH, H-2'), 4.09 (3H, s, NCH₃), 5.15 (1H, t, *J* = 4.8, OH), 9.96 (1H, s, CH, H-2); ¹³C NMR (75 MHz; DMSO-d₆) (assignments made using DEPT-135): 11.3 (C-1'), 29.4 (CH₃), 40.2 (CH₂, C-2'), 59.7 (NCH₃), 134.7 (C), 142.1 (C), 156.4 (CH, C-2).

2.2.2. General procedure for the coupling between methyl aryl ketones and α-bromomethyl aryl ketones

Zinc chloride (2.0 mmol) was added to dry toluene (5.0 ml), absolute ethanol (1.5 mmol) and triethylamine (1.5 mmol). The mixture was stirred at room temperature for 1-2 h. 4-Cyanoacetophenone **120** (1.5 mmol) and 2-bromo-4'-cyanobenzonitrile **136** (aryl 1,4-diketones **123** synthesis) or 2-bromo-acetophenone **133** (aryl 1,4-diketones **126** synthesis) (1.0 mmol) were added and the mixture was stirred at room temperature for 3-4 days and monitored by TLC (20.0 % EtOAc/ hexane). The workup was as described for each 1,4-diketone compound.

Chapter III. Experimental/ Chemistry

2.2.2.1. 1,4-Bis(4-cyanophenyl)-1,4-butadione 123

Toluene was decanted and the pale yellow residue gum was dissolved in DMF (~80 °C, 50.0 ml). Compound **6** was crystallized from DMF as a pale yellow solid by the addition of methanol (10.0 ml), filtered under vacuum and washed with cold methanol to yield 0.81 g (61.0 %). The ¹H NMR spectrum was identical to that reported in the previous synthesis of **123** (section 2.2.1.1).

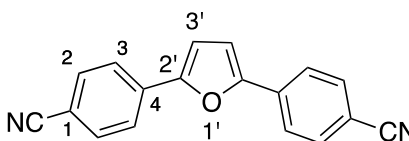
2.2.2.2. 1-(4-Cyanophenyl)-4-phenyl-1,4-butadione 126

The reaction mixture was quenched with cold 10.0% (v/v) aqueous sulfuric acid (10.0 ml). The organic layer was extracted with brine (10.0 ml), dried over magnesium sulfate and concentrated. Compound **126** was crystallized from methanol to give 1.51 g (39.0%) as light-yellow crystals. The ¹H NMR spectrum was identical to that reported in the previous synthesis of **126** (section 2.2.1.2).

2.3. General procedure for the synthesis of 2,5-diarylfurans 118 and 127

A solution of 1,4-bis(4-cyanophenyl)-1,4-butadione **123**, (2,5-diarylfuran **118** synthesis) or 1-(4-cyanophenyl)-4-phenyl-1,4-butadione **126** (2,5-diarylfuran **127** synthesis) in acetic anhydride was heated at reflux. A few drops of concentrated sulfuric acid in acetic anhydride (1.0 ml) was added to the solution. The solution became dark in colour, was removed from heating and allowed to cool to room temperature.

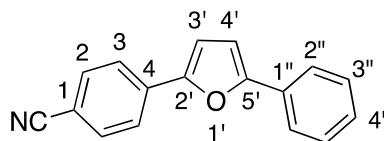
2.3.1. 4,4'-(Furan-2,5-diyl)benzotrile 118



The yellow crystals of 4,4'-(furan-2,5-diyl)benzotrile **118** were filtered off under vacuum and washed with hexane: ¹H NMR (300 MHz; DMSO-d₆): 7.44 (2H, s, 2 × CH, H-3'), 7.92 (4H, d, *J* = 8.1 Hz, 4 × CH, H-3), 8.06 (4H, d, *J* = 8.4 Hz, 4 × CH, H-2); ¹³C NMR (75 MHz; CDCl₃) (assignments made using DEPT-135): 109.8 (C), 111.9 (2 × CH, C-3'), 118.8 (CN), 124.3 (4 × CH, C-3), 132.9 (4 × CH, C-2), 133.4 (2 × C, C-4), 152.2 (2 × C, C-2'); the spectroscopic data (IR, ¹H- and ¹³C-NMR) were identical to those reported in the literature.¹¹⁰

Chapter III. Experimental/ Chemistry

2.3.2. 4-(5-Phenylfuran-2-yl)benzonitrile **127**

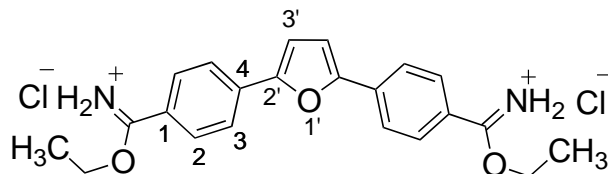


The reaction mixture was poured into iced water (75.0 ml) and the yellow precipitate was collected and re-crystallized from methanol to give 0.61 g of a light yellow fine solid (78.0%): mp 122-124 °C; IR (cm⁻¹): 2224 (CN), 1738, 1606 (furan C=C), 1023 (C-O), 795; ¹H NMR (300 MHz; CDCl₃): 6.81 (1H, d, *J* = 3.6 Hz, furan-CH), 6.93 (1H, d, *J* = 3.3 Hz, furan-CH), 7.34 (1H, t, *J* = 7.5 Hz, CH, H-4''), 7.45 (2H, t, *J* = 7.8 Hz, 2 x CH, H-3''), 7.70 (2H, d, *J* = 8.4, 2 x CH), 7.78 (2H, d, *J* = 7.2 Hz, 2 x CH, H-2''), 7.83 (2H, d, *J* = 8.4, 2 x CH); ¹³C NMR (100 MHz; CDCl₃) (assignments made using DEPT-135): 107.7 (CH), 110.1 (C), 110.5 (CH), 119.1 (C, CN), 123.8 (CH), 124.1 (CH), 128.1 (CH), 128.9 (CH), 130.1 (C), 132.7 (CH), 134.5 (C), 151.2 (C), 155.1 (C); +APCI *m/z* (relative intensity): 246.2 (100%, [M + H]⁺).

2.4. General procedure for the synthesis of furan-imidates **119** and **143**

Acetyl chloride (24.0 mmol for **119** or 16.0 mmol for **143** syntheses) was added dropwise to a suspension of **123** or **124** (1.0 mmol) in absolute ethanol (48.0 mmol for **119** or 24.0 mmol for **143** syntheses) in dry chloroform at 0 °C. The reaction was allowed to warm up to room temperature and stirring was continued for 1-3 days. The precipitated product was filtered off under vacuum and rinsed with hexane or diethyl ether.

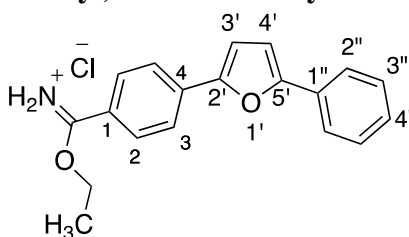
2.4.1. Diethyl 4,4'-(furan-2,5-diyl)dibenzimidate dihydrochloride **119**



The orange precipitate was filtered off under vacuum and rinsed with hexane. The precipitate was added to boiling ethanol and filtered while it was hot to give 0.84 g (42.0%) of **119**: ¹H NMR (300 MHz; DMSO-d₆): 1.52 (6H, t, *J* = 6.9 Hz, CH₃), 4.66 (4H, q, *J* = 6.9 Hz, CH₂), 7.54 (2H, s, 2 x CH, H-3'), 8.15 (4H, d, *J* = 8.1 Hz, 4 x CH), 8.25 (4H, d, *J* = 8.4 Hz, 4 x CH).

Chapter III. Experimental/ Chemistry

2.4.2. Ethyl 4-(5-phenylfuran-2-yl)benzimidate hydrochloride **143**

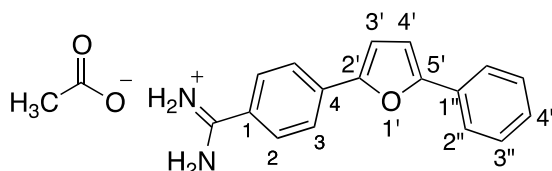


The yellow-coloured precipitate was filtered off under vacuum and rinsed with hexane. The precipitate was added to boiling ethyl acetate and filtered while it was hot to give 0.47 g (76.0%) of **143**: mp 233-235 °C; IR (cm⁻¹): 2777, 1628, 1606, 1435 (Ar C=C), 1069 (C-O), 781, 751, 601; ¹H-NMR (300 MHz; DMSO-d₆): 1.52 (3H, t, *J* = 6.9 Hz, CH₃), 4.63 (2H, q, *J* = 6.9 Hz, CH₂), 7.22 (1H, d, *J* = 3.3 Hz, furan-CH), 7.37 (1H, t, *J* = 7.5 Hz, CH, H-4''), 7.45 (1H, d, *J* = 3.6 Hz, furan-CH), 7.49 (2H, t, *J* = 7.8 Hz, 2 x CH, H-3''), 7.90 (2H, d, *J* = 7.8 Hz, 2 x CH, H-2''), 8.08 (2H, d, *J* = 8.7 Hz, 2 x CH), 8.17 (2H, d, *J* = 8.4 Hz, 2 x CH); ¹³C NMR (75 MHz, DMSO-d₆) (assignments made using DEPT-135): 13.5 (CH₃), 69.5 (OCH₂), 108.4 (CH), 109.8 (CH), 123.6 (CH), 123.8 (C-4''), 127.8 (CH), 128.2 (CH), 128.9 (CH), 129.8 (C), 132.4 (C), 132.7 (C), 151.8 (C), 153.3 (C), 167.3 (C=N); +ESIMS *m/z* (relative intensity): 292.3 (100%, [M + H]⁺); found by +ESIMS 292.1331, C₁₉H₁₈NO₂ [M + H]⁺, requires 292.1338, error 2.2 ppm.

2.5. General procedure for the synthesis of furan-amidines **110** and **111**

Ammonium acetate (4.0 mmol for **110** and 8.0 mmol for **111** syntheses) was added to a stirred suspension of furan-imidates **143** or **119** (1.0 mmol) in anhydrous ethanol. The mixture was stirred at room temperature for 1- 3 days. The workup was as described for each furan-amidine compound.

2.5.1. 4-(5-Phenylfuran-2-yl)benzamidine acetate **110**

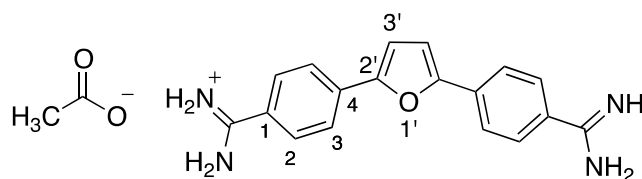


4-(5-Phenylfuran-2-yl)benzamidine acetate **110** was collected by filtration and rinsed with ethanol to give 0.28 g (62.0 %) of **110** as a fine pale yellow solid: mp 234-237 °C; IR (cm⁻¹): 2924 (C-H), 1613, 1487, 1440, 796; ¹H NMR (300 MHz; DMSO-d₆): 1.74 (3H, s, CH₃), 7.17 (1H, d, *J* = 3.6 Hz, furan-CH), 7.34 -7.38 (2H, m, 2 x CH

Chapter III. Experimental/ Chemistry

including furan-CH), 7.48 (2H, t, $J = 7.8$ Hz, 2 x CH, H-3''), 7.87 – 7.90 (4H, m, 4 x CH), 8.01 (2H, d, $J = 8.4$ Hz, 2 x CH); ^{13}C NMR (75 MHz; DMSO- d_6) (assignments made using DEPT-135): 22.3 (CH₃), 108.6 (CH), 111.3 (CH), 123.4 (CH), 123.8 (CH), 126.2 (C), 128.1(CH), 128.7 (CH), 129.0 (CH), 129.6 (C), 134.5 (C), 151.0 (C), 154.0 (C), 164.9 (C, C-amidine), 173.9 (C=O); ESIMS m/z (relative intensity): 263 (100%, [M + H]⁺).

2.5.2. 4,4'-(Furan-2,5-diyl)dibenzamidine acetate **111**



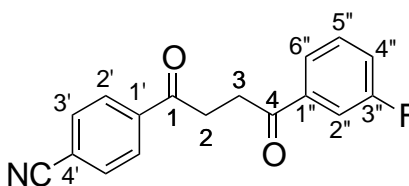
4,4'-(Furan-2,5-diyl)dibenzamidine acetate **111** was collected by filtration, added to boiling ethanol and filtered whilst hot to yield 0.37 g (46%) of an olive-green solid; IR (cm⁻¹): 3030 (Ar C-H), 2360, 2341, 1668, 1606 (C-O), 1488; ^1H NMR (300 MHz; DMSO- d_6): 1.80 (3H, s, CH₃), 7.46 (2H, s, 2 x CH, H-3'), 7.95 (4H, d, $J = 8.4$ Hz, 4 x CH), 8.11 (4H, d, $J = 8.4$ Hz, 4 x CH); ^{13}C NMR (75 MHz; DMSO- d_6) (assignments made using DEPT-135): 22.6 (CH₃), 111.6 (2 x CH, C-3'), 123.8 (4 x CH), 126.8 (C), 128.8 (4 x CH), 134.1 (C), 152.4 (C), 164.8 (C, C-amidine), (C, C=O) was not observed; ESIMS m/z (relative intensity): 305 (50.0 %, [M + H]⁺).

2.6. General procedure for the synthesis of the asymmetric aryl 1,4-diketones **165-174**

Zinc chloride (9.0 mmol) was added to dry toluene or dry THF (5.0 ml), absolute ethanol (6.8 mmol) and triethylamine (6.8 mmol). The mixture was stirred at room temperature for 1-2 h. Methyl aryl ketone (6.8 mmol) and 2-bromo-4'-cyanobenzonitrile **136** (4.5 mmol) were added and the mixture was stirred at room temperature for 3-7 days and monitored by TLC (20.0 % EtOAc/ hexane). The workup was as described for each 1,4-diketone compound.

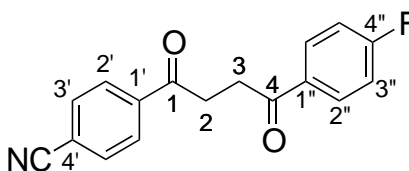
Chapter III. Experimental/ Chemistry

2.6.1. 1-(4-Cyanophenyl)-4-(3-fluorophenyl)-1,4-butadione **165**



Toluene was evaporated leaving an oily residue. Compound **165** was crystallized from methanol as pale yellow solid to give 0.59 g (16.0 %): mp: 143-147 °C; IR (cm⁻¹): 2220 (CN), 1679 (C=O), 1317, 1201 (C-F), 1006, 781 (C-F), 677; ¹H NMR (300 MHz; CDCl₃): 3.47 (4H, s, 2 × CH₂, H-2, H-3), 7.33 (1H, t, ³J_{HF} = J_{HH} = 8.4 Hz, CH, H-4''), 7.50 (1H, ddd~q, ⁴J_{HF} = J_{HH} = 6.0 Hz, CH, H-5''), 7.71 (1H, d, ³J_{HF} = 9.6 Hz, CH, H-2''), 7.81-7.85 (3H, m, 3 × CH, H-6''), 8.14 (2H, d, J = 8.4 Hz, 2 × CH); ¹³C NMR (100 MHz, CDCl₃) (assignments made using DEPT-135): 32.68 (CH₂), 32.7 (CH₂), 114.9 (d, ²J_{CF} = 22.0 Hz, CH, C-4''), 116.5 (C, C-4'), 118.0 (CN), 120.4 (d, ²J_{CF} = 21.0 Hz, CH, C-2''), 123.9 (d, ⁴J_{CF} = 3.0 Hz, C-6''), 128.8 (CH), 130.4 (d, ³J_{CF} = 8.0 Hz, C-5''), 132.61 (C), 138.5 (d, ³J_{CF} = 6.0 Hz, C-1''), 139.6 (C), 162.9 (d, ¹J_{CF} = 247.0 Hz, C-3''), 197.0 (C=O), 197.3 (C=O); ¹⁹F-NMR (376.5 MHz, CDCl₃): -111.7; -ESIMS m/z (relative intensity): 280 (100%, [M - H]⁻); found by -ESIMS 280.0789, C₁₇H₁₁NO₂F [M - H]⁻, requires 280.0779, error 3.6 ppm.

2.6.2. 1-(4-Cyanophenyl)-4-(4-fluorophenyl)-1,4-butadione **166**

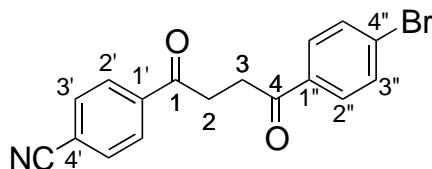


The reaction mixture was diluted by the addition of ethyl acetate (10 ml). Ethyl acetate and toluene were decanted and evaporated to give a yellow solid. Compound **166** was re-crystallized from methanol to give 0.34 g (26.0 %) of a bright yellow crystals: mp 162-164 °C; IR (cm⁻¹): 2222 (CN), 1677 (C=O), 1593, 1405, 1295, 1186, 1001 (C-F), 854, 708 (C-F), 590; ¹H NMR (300 MHz; CDCl₃): 3.35-3.44 (4H, m, 2 × CH₂, H-2, H-3), 7.09 (2H, dd~t, ³J_{HF} = J_{HH} = 8.4 Hz, 2 × CH, H-3''), 7.73 (2H, d, J = 8.4 Hz, 2 × CH), 7.98 (2H, dd ~ t, ⁴J_{HF} = J_{HH} = 7.8 Hz, 2 × CH, H-2''), 8.06 (2H, d, J = 8.4 Hz, 2 × CH); ¹³C NMR (75 MHz; CDCl₃) (assignments made using DEPT-135): 32.4 (CH₂), 32.8 (CH₂), 115.8 (d, ²J_{CF} = 22.0, 2 × CH, C-3''), 116.5 (C, C-4'), 118.0 (CN), 128.6 (2 × CH), 130.8 (d, ³J_{CF} = 9.0 Hz, 2 × CH, C-2''), 132.6 (2 × CH), 132.9 (d, ⁴J_{CF} = 3.0 Hz, C-1''), 139.7 (C), 165.9 (d, ¹J_{CF} = 253.0 Hz, C-4''), 196.6 (C=O), 197.4

Chapter III. Experimental/ Chemistry

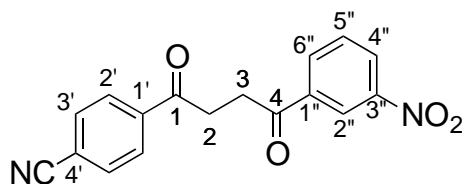
(C=O); ^{19}F -NMR (376.5 MHz, CDCl_3): -104.7; +ESIMS m/z (relative intensity): 320 (100%, $[\text{M} + \text{K}]^+$), -ESIMS m/z (relative intensity): 280 (100%, $[\text{M} - \text{H}]^-$); found by -ESIMS 280.07829, $\text{C}_{17}\text{H}_{11}\text{NO}_2\text{F}$ $[\text{M} - \text{H}]^-$, requires 280.0779, error 1.1 ppm.

2.6.3. 1-(4-Cyanophenyl)-4-(4-bromophenyl)-1,4-butadione 167



The reaction was diluted by the addition of hexane (20 ml). Hexane was decanted and compound **167** was re-crystallized from $\text{MeOH}/\text{CHCl}_3$ to give 1.38 g (56.0 %) of colourless crystals: mp 158-160 °C; IR (cm^{-1}): 2227 (CN), 1678 (C=O), 1583, 995, 780 (C-Br); ^1H NMR (300 MHz; CDCl_3): 3.45 (4H, s, $2 \times \text{CH}_2$), 7.64 (2H, d, $J = 8.1$ Hz, $2 \times \text{CH}$), 7.80 (2H, d, $J = 8.1$ Hz, $2 \times \text{CH}$), 7.89 (2H, d, $J = 8.4$ Hz, $2 \times \text{CH}$), 8.12 (2H, d, $J = 8.4$ Hz, $2 \times \text{CH}$); ^{13}C NMR (75 MHz; CDCl_3) (assignments made using DEPT-135): 32.5 (CH_2), 32.7 (CH_2), 116.5 (C, C-4'), 118.0 (CN), 128.6 ($2 \times \text{CH}$), 129.6 ($2 \times \text{CH}$), 131.6 (C), 132.0 ($2 \times \text{CH}$), 132.6 ($2 \times \text{CH}$), 135.2 (C), 139.7 (C), 197.2 (C=O), 197.3 (C=O); -ESIMS m/z (relative intensity): 340 (90%, ^{79}Br , $[\text{M} - \text{H}]^-$), 342 (100%, ^{81}Br); found by -ESIMS 339.9977, $\text{C}_{17}\text{H}_{11}\text{NO}_2\text{Br}$ $[\text{M} - \text{H}]^-$, requires 339.9978, error 0.3 ppm.

2.6.4. 1-(4-Cyanophenyl)-4-(3-nitrophenyl)-1,4-butadione 168

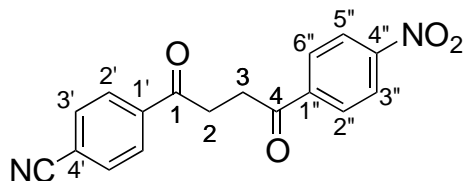


Toluene was decanted from the reaction mixture and the pale yellow residue gum was dissolved in DMF (~80 °C, 50.0 ml). Compound **168** was crystallized from DMF as pale yellow crystals by the addition of methanol (10.0 ml), filtered under vacuum and washed with cold methanol to yield 0.66 g (47.0 %): mp 174-176 °C; IR (cm^{-1}): 2229 (CN), 1680 (C=O), 1655, 1527 (NO_2), 1348, 1313 (NO_2), 1302, 1192, 793, 736, 671; ^1H NMR (300 MHz; CDCl_3): 3.52 (4H, s, $2 \times \text{CH}_2$, H-2, H-3), 7.73 (1H, t, $J = 8.1$ Hz, CH, H-5''), 7.82 (2H, d, $J = 8.4$ Hz, $2 \times \text{CH}$), 8.13 (2H, d, $J = 8.4$ Hz, $2 \times \text{CH}$), 8.36 (1H, d, $J = 7.8$ Hz, CH, H-6''), 8.46 (1H, d, $J = 8.2$ Hz, CH, H-4''), 8.87 (1H, s, CH, H-2''); ^{13}C NMR (75 MHz; CDCl_3) (assignments made using DEPT-135): 32.7

Chapter III. Experimental/ Chemistry

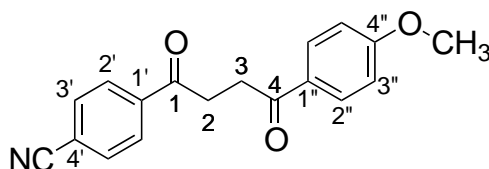
(CH₂), 32.8 (CH₂), 116.7 (C, C-4'), 117.9 (CN), 123.1 (CH), 127.6 (CH), 128.6 (2 × CH), 130.0 (C, C-4''), 132.6 (2 × CH), 133.6 (C, C-2''), 137.8 (C), 139.5 (C), 148.5 (C, C-3''), 196.2 (C=O), 197.0 (C=O); +ESIMS m/z (relative intensity): 347 (100%, [M + K]⁺); -ESIMS m/z (relative intensity): 307 (100%, [M - H]⁻); found by -ESIMS 307.0722, C₁₇H₁₁NO₄[M - H]⁻, requires 307.0710, error 0.6 ppm.

2.6.5. 1-(4-Cyanophenyl)-4-(4-nitrophenyl)-1,4-butadione **169**



The reaction mixture was quenched with 10.0 % (v/v) aqueous H₂SO₄ solution (10 ml) and extracted with ethyl acetate (20 ml). The organic layer was washed with brine (10.0 ml), dried over MgSO₄ and concentrated. Compound **169** was crystallized from methanol to give 0.71 g (51.0%) of a fine orange solid: mp 173-175 °C; IR (cm⁻¹): 2226 (CN), 1683 (C=O), 1521 (NO₂), 1316 (NO₂), 1310, 1291, 1184, 1002, 860, 794, 741; ¹H NMR (300 MHz; CDCl₃): 3.52 (4H, s, 2 × CH₂), 7.83 (2H, d, *J* = 8.1 Hz, 2 × CH), 8.14 (2H, d, *J* = 8.4 Hz, 2 × CH), 8.20 (2H, d, *J* = 8.7 Hz, 2 × CH, H-2''), 8.36 (2H, d, *J* = 8.7 Hz, 2 × CH, H-3''); ¹³C NMR (75 MHz; CDCl₃) (assignments made using DEPT-135): 44.8 (2 × CH₂, C-2, C-3), 109.5 (C), 115.3 (C), 118.1 (C, C-4'), 118.9 (C≡N), 128.8 (2 × CH), 131.1 (2 × CH), 132.0 (2 × CH, C-2''), 132.8 (2 × CH, C-3''), 139.5 (C, C-1''), 140.6 (C, C-4''), 196.3 (2 × C=O); -ESIMS m/z (relative intensity): 307 (100%, [M - H]⁻); found by -ESIMS 307.0727, C₁₇H₁₁NO₄ [M - H]⁻, requires 307.0724, error 1.0 ppm.

2.6.6. 1-(4-Cyanophenyl)-4-(4-methoxyphenyl)-1,4-butadione **170**

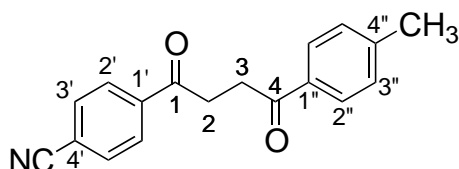


The reaction was quenched by the addition of 10.0 % (v/v) aqueous sulfuric acid solution and extracted with ethyl acetate (20 ml). The organic layer was washed with brine (10 ml), dried over dry MgSO₄ and evaporated. The crude reaction mixture was purified by column chromatography using EtOAc-hexane (1:9) as a mobile phase to

Chapter III. Experimental/ Chemistry

give 0.35 g (27.0 %) of **170** as a colourless solid: mp 120-122 °C; IR (cm⁻¹): 3041, 2231, 1676 (C=O), 1606, 1356, 1226, 991, 823; ¹H NMR (300 MHz; CDCl₃): 3.42-3.49 (4H, m, 2 × CH₂, H-2, H-3), 3.90 (3H, s, OCH₃), 6.84 (2H, d, *J* = 8.7 Hz, 2 × CH, H-3''), 7.81 (2H, d, *J* = 8.4 Hz, 2 × CH), 8.03 (2H, d, *J* = 8.7 Hz, 2 × CH), 8.15 (2H, d, *J* = 8.4 Hz, 2 × CH); ¹³C NMR (75 MHz; CDCl₃) (assignments made using DEPT-135): 32.3 (CH₂), 32.8 (CH₂), 55.5 (OCH₃), 113.8 (CH), 116.4 (C, C-4'), 118.0 (CN), 128.6 (2 × CH, C-3''), 129.6 (C), 130.4 (2 × CH), 132.5 (2 × CH), 139.9 (C), 163.7 (C), 197.6 (C=O), 197.7 (C=O); +ESIMS *m/z* (relative intensity): 316 (100%, [M + Na]⁺); found by +ESIMS 316.0938, C₁₈H₁₅NO₃Na [M + Na]⁺, requires 316.0944, error 1.9 ppm.

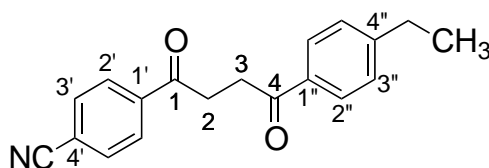
2.6.7. 1-(4-Cyanophenyl)-4-(4-methylphenyl)-1,4-butadione **171**



The reaction mixture was diluted by the addition of ethyl acetate (10 ml), washed with 0.1 N HCl (10 ml) and water (10 ml). The organic layer was dried over dry MgSO₄ and concentrated. Compound **171** was re-crystallized from methanol to give 0.12 g (9.0 %) of colourless crystals: mp 134-136 °C; IR (cm⁻¹): 2227 (CN), 1680 (C=O), 1676 (C=O), 1356, 1226, 991, 840, 822, 565; ¹H NMR (300 MHz; CDCl₃): 2.45 (3H, s, CH₃), 3.45-3.50 (4H, m, 2 × CH₂, H-2, H-3), 7.31 (2H, d, *J* = 8.7 Hz, 2 × CH, H-3''), 7.82 (2H, d, *J* = 8.1 Hz, 2 × CH), 7.95 (2H, d, *J* = 8.1 Hz, 2 × CH, H-2''), 8.15 (2H, d, *J* = 8.4 Hz, 2 × CH); ¹³C NMR (75 MHz; CDCl₃) (assignments made using DEPT-135): 21.7 (CH₃), 32.5 (CH₂), 32.8 (CH₂), 116.4 (C, C-4'), 118.0 (CN), 128.2 (2 × CH, C-3''), 128.6 (2 × CH), 129.4 (2 × CH, C-2''), 132.5 (2 × CH), 134.0 (C), 139.8 (C), 144.2 (C), 197.6 (C=O), 197.8 (C=O); +ESIMS *m/z* (relative intensity): 316 (100%, [M + K]⁺), -ESIMS *m/z* 276 (100%, [M - H]⁻); found by +ESIMS 300.0997, C₁₈H₁₅NO₂Na [M + Na]⁺, requires 300.0995, error 0.5 ppm.

Chapter III. Experimental/ Chemistry

2.6.8. 1-(4-Cyanophenyl)-4-(4-ethylphenyl)-1,4-butadione **172**

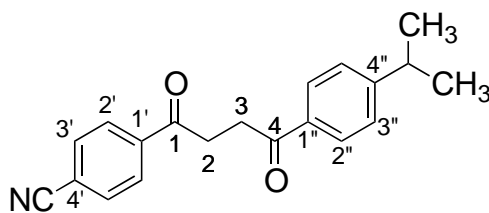


The reaction was quenched by the addition of 10.0 % (v/v) aqueous sulfuric acid solution and extracted with ethyl acetate (20 ml). The organic layer was washed with brine (10.0 ml), dried over dry MgSO_4 and concentrated. Compound **172** was crystallized from methanol to give 0.19 g (15.0 %) of colourless crystals: mp 126-128 °C; IR (cm^{-1}): 2222 (CN), 1671 (C=O), 1224, 992, 801, 568; ^1H NMR (300 MHz; CDCl_3): 1.20 (3H, t, $J = 7.5$ Hz, CH_3), 2.65 (2H, q, $J = 7.5$ Hz, CH_2), 3.36-3.41 (4H, m, $2 \times \text{CH}_2$, H-2, H-3), 7.24 (2H, d, $J = 7.8$ Hz, $2 \times \text{CH}$, H-3''), 7.73 (2H, d, $J = 7.8$ Hz, $2 \times \text{CH}$), 7.88 (2H, d, $J = 7.8$ Hz, $2 \times \text{CH}$), 8.06 (2H, d, $J = 7.8$ Hz, $2 \times \text{CH}$); ^{13}C NMR (100 MHz; CDCl_3) (assignments made using DEPT-135): 15.2 (CH_3), 29.0 (CH_3CH_2), 32.5 (CH_2), 32.8 (CH_2), 116.4 (C, C-4'), 118.0 (CN), 128.2 ($2 \times \text{CH}$, C-3''), 128.4 ($2 \times \text{CH}$), 128.6 ($2 \times \text{CH}$), 132.5 ($2 \times \text{CH}$), 134.2 (C), 139.9 (C), 150.4 (C), 197.7 (C=O), 197.9 (C=O); +ESIMS m/z (relative intensity): 292.3 (100%, $[\text{M} + \text{H}]^+$), -ESIMS m/z 290.4 (100%, $[\text{M} - \text{H}]^-$); found by +ESIMS 292.1331, $\text{C}_{19}\text{H}_{18}\text{NO}_2$ $[\text{M} + \text{H}]^+$, requires 292.1332, error 0.4 ppm.

Compound **172** was also synthesized using an alternative synthetic pathway starting from 4-acetylbenzotrile **120** and 2-bromo-1-(4-ethylphenyl)ethanone **175**. The procedure for this synthetic pathway: triethylamine (0.6 ml, 4.1 mmol) was added to a suspension of zinc chloride (0.74 g, 5.4 mmol) in dry toluene (5.0 ml) and absolute ethanol (0.2 ml, 4.1 mmol). The reaction mixture was stirred at room temperature for 1-2 h. 4-Acetylbenzotrile **120** (0.61 g, 2.7 mmol) and 2-bromo-1-(4-ethylphenyl)ethanone **175** (0.60 g, 4.1 mmol) were added and the reaction mixture was stirred at room temperature for 7 days and monitored by TLC (20.0 % EtOAc/ hexane). The reaction was quenched by the addition of 10.0 % (v/v) aqueous sulfuric acid solution and extracted with ethyl acetate (20 ml). The organic layer was washed with brine (10 ml), dried over anhydrous MgSO_4 and evaporated. The crude reaction mixture was purified by column chromatography using EtOAc-hexane (1:9) as the mobile phase to give 0.14 g (18.0 %) of **172** as a colourless solid.

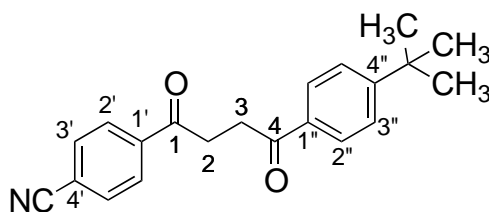
Chapter III. Experimental/ Chemistry

2.6.9. 1-(4-Cyanophenyl)-4-(4-isopropylphenyl)-1,4-butadione 173



The reaction was quenched by the addition of 10.0 % (v/v) aqueous sulfuric acid solution and extracted with ethyl acetate (20 ml). The organic layer was rinsed with brine (10.0 ml), dried over anhydrous MgSO_4 and evaporated. The crude reaction mixture was purified by column chromatography using EtOAc-hexane (1:9) as the mobile phase to give 0.28 g (11.0 %) of **173** as a colourless solid: mp 92-93 °C; IR (cm^{-1}): 2222 (CN), 1675 (C=O), 1001, 788, 582; ^1H NMR (300 MHz; CDCl_3): 1.28 (6H, d, $J = 6.9$ Hz, $2 \times \text{CH}_3$), 2.98 (1H, septet, $J = 6.9$ Hz, CH), 3.43-3.48 (4H, m, $2 \times \text{CH}_2$, H-2, H-3), 7.34 (2H, d, $J = 7.8$ Hz, $2 \times \text{CH}$, H-3''), 7.79 (2H, d, $J = 8.1$ Hz, $2 \times \text{CH}$), 7.96 (2H, d, $J = 8.1$ Hz, $2 \times \text{CH}$); ^{13}C NMR (100 MHz; CDCl_3) (assignments made using DEPT-135): 23.7 ($2 \times \text{CH}_3$), 31.1 (CH), 32.5 (CH_2), 32.8 (CH_2), 116.3 (C, C4'), 118.0 (CN), 125.6 ($2 \times \text{CH}$), 126.8 ($2 \times \text{CH}$), 128.4 ($2 \times \text{CH}$), 132.5 ($2 \times \text{CH}$), 139.8 (C), 155.0 (C), 157.2 (C), 197.6 (C=O), 197.8 (C=O); +ESIMS m/z (relative intensity): 328 (100%, $[\text{M} + \text{H}]^+$); found by +ESIMS 328.1300, $\text{C}_{20}\text{H}_{19}\text{NO}_2\text{Na}$ $[\text{M} + \text{Na}]^+$, requires 328.1308, error 2.4 ppm.

2.6.10. 1-(4-Cyanophenyl)-4-(4-tert-butylphenyl)-1,4-butadione 174

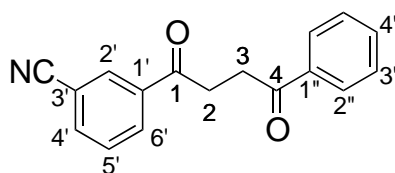


The reaction was quenched by the addition of 10.0 % (v/v) aqueous sulfuric acid solution and extracted with ethyl acetate (20 ml). The organic layer was washed with brine (10 ml), dried over anhydrous MgSO_4 and concentrated. The crude reaction mixture was purified by column chromatography using EtOAc-hexane (1:9) as the mobile phase to give 0.13 g (9.0 %) of **174** as a white solid: mp 133-135 °C; IR (cm^{-1}): 2222 (CN), 1671 (C=O), 1320, 1006, 855, 701, 569; ^1H NMR (300 MHz; CDCl_3): 1.35 (9H, s, $3 \times \text{CH}_3$), 3.43-3.48 (4H, m, $2 \times \text{CH}_2$, H-2, H-3), 7.50 (2H, d, $J = 8.4$ Hz, $2 \times \text{CH}$, H-3''), 7.79 (2H, d, $J = 8.4$ Hz, $2 \times \text{CH}$), 7.97 (2H, d, $J = 8.1$ Hz, $2 \times \text{CH}$), 8.13

Chapter III. Experimental/ Chemistry

(2H, d, $J = 8.1$ Hz, $2 \times CH$); ^{13}C NMR (100 MHz; $CDCl_3$) (assignments made using DEPT-135): 23.7 ($3 \times CH_3$), 32.5 ($2 \times CH_2$, C-2, C-3), 35.2 (C), 116.4 (C, C-4'), 118.0 (CN), 125.6 ($2 \times CH$, C-3''), 126.8 ($2 \times CH$), 128.4 ($2 \times CH$), 132.5 ($2 \times CH$), 134.3 (C), 139.8 (C), 155.0 (C), 197.6 (C=O), 197.8 (C=O); +ESIMS m/z (relative intensity): 342 (100%, $[M + Na]^+$); found by +ESIMS 320.1648, $C_{21}H_{22}NO_2$ $[M + H]^+$, requires 320.1645, error 0.9 ppm.

2.7. 1-(3-Cyanophenyl)-4-phenyl-1,4-butadione **179**



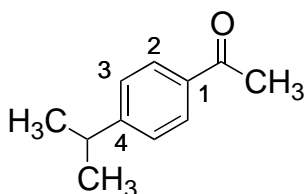
Zinc chloride (1.40 g, 10 mmol) was added to dry toluene (5.0 ml), absolute ethanol (0.4 ml, 7.5 mmol) and triethylamine (1.0 ml, 7.5 mmol). The mixture was stirred at room temperature for 1-2 h. 3-Acetylbenzonitrile **178** (1.10 g, 7.5 mmol) and 2-bromoacetophenone **133** (1.00 g, 5.0 mmol) were added and the mixture was stirred at room temperature for 4 days and monitored by TLC (20.0 % EtOAc/ hexane). The reaction was quenched by the addition of 10.0 % (v/v) aqueous sulfuric acid solution and extracted with ethyl acetate (20 ml). The organic layer was washed with brine (10 ml), dried over anhydrous $MgSO_4$ and evaporated. The crude reaction mixture was purified by column chromatography using EtOAc-hexane (1:9) as the mobile phase to give 0.20 g (15.2%) of **179** as a colourless solid: mp 102-104 °C; IR (cm^{-1}): 2222 (CN), 1670 (C=O), 750, 680; 1H NMR (300 MHz; $CDCl_3$): 3.45 (2H, t, $J = 5.7$ Hz, CH_2), 3.53 (2H, t, $J = 6.0$ Hz, CH_2), 7.51 (2H, t, $J = 7.5$ Hz, $2 \times CH$, H-3''), 7.60 (1H, d, $J = 7.5$ Hz, CH); 7.63 (1H, t, $J = 7.8$ Hz, CH), 7.88 (1H, d, $J = 7.8$ Hz, CH), 8.05 (2H, d, $J = 7.5$ Hz, $2 \times CH$, H-2''), 8.28 (1H, d, $J = 7.8$ Hz, CH), 8.35 (1H, s, CH , H-2'); ^{13}C NMR (75 MHz, $CDCl_3$) (assignments made using DEPT-135): 31.50 (CH_2), 31.52 (CH_2), 112.2 (C, C-3'), 117.0 (CN), 127.1 (CH), 127.7 (CH), 128.7 (CH), 130.9 (CH), 131.1 (CH), 132.4 (CH), 135.0 (CH), 135.4 (C), 136.5 (C), 195.8 (C=O), 197.2 (C=O); +ESIMS m/z 264 (50%, $[M + H]^+$), 286 (100%, $[M + Na]^+$), 302 (32%, $[M + K]^+$); found by +ESIMS 264.1018, $C_{17}H_{13}NO_2$ $[M + H]^+$, requires 264.1019, error 0.4 ppm.

Chapter III. Experimental/ Chemistry

2.8. General procedure for the synthesis of methyl aryl ketones 163 and 164

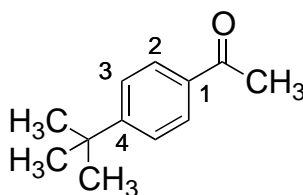
Acetyl chloride (1.8 mmol) was added dropwise to a suspension of AlCl_3 (1.8 mmol) in dry dichloromethane (20.0 ml) at 0°C . After 10-15 m stirring at 0°C the alkylbenzene was added dropwise. The reaction mixture was stirred at room temperature for 30 m and monitored by TLC using 20 % EtOAc in hexane as a mobile phase. The reaction mixture was cooled to 0°C and water (60.0 ml) was added slowly. The organic layer was washed with saturated NaCl solution (30 ml), dried over dry MgSO_4 and evaporated to give the product as an oil.

2.8.1. 4-Isopropylacetophenone 163



Yellow oil (1.22 g, 90.0%); ^1H NMR (300 MHz; CDCl_3): 1.28 (6H, d, $J = 6.9$ Hz, $2 \times \text{CH}_3$), 2.58 (3H, s, CH_3), 2.97 (1H, septet, $J = 6.9$ Hz, CH), 7.32 (2H, d, $J = 8.1$ Hz, $2 \times \text{CH}$, H-3), 7.91 (2H, d, $J = 7.8$ Hz, $2 \times \text{CH}$, H-2); ^{13}C NMR (100 MHz; CDCl_3) (assignments made using DEPT-135): 23.7 ($2 \times \text{CH}_3$), 26.6 (CH_3), 34.3 (CH), 127.7 (C, C-4), 128.6 ($2 \times \text{CH}$, C-3), 135.1 ($2 \times \text{CH}$, C-2), 154.6 (C, C-1), 197.8 (C=O); +ESIMS m/z 163 (100%, $[\text{M} + \text{H}]^+$), 185 (800%, $[\text{M} + \text{Na}]^+$).

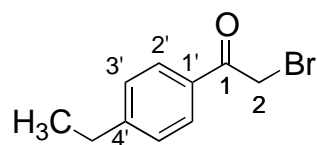
2.8.2. 4-tert-Butylacetophenone 164



Yellow oil (1.30 g, 98.0%); ^1H NMR (300 MHz; CDCl_3): 1.34 (9H, s, $3 \times \text{CH}_3$), 2.58 (3H, s, CH_3), 7.48 (2H, d, $J = 8.4$ Hz, $2 \times \text{CH}$, H-3), 7.91 (2H, d, $J = 8.4$ Hz, $2 \times \text{CH}$, H-2); ^{13}C NMR (100 MHz; CDCl_3) (assignments made using DEPT-135): 26.6 ($3 \times \text{CH}_3$), 31.1 (CH_3), 35.1 (C), 124.9 ($2 \times \text{CH}$, C-3), 128.0 ($2 \times \text{CH}$, C-2), 139.4 (C, C-4), 156.8 (C, C-1), 198.3 (C=O).

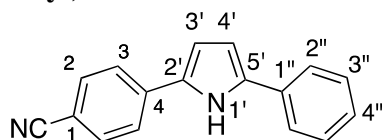
Chapter III. Experimental/ Chemistry

2.9. 2-Bromo-1-(4-ethylphenyl)ethanone **175**



4-Ethylacetophenone **162** (1.00 g, 6.7 mmol) and *N*-bromosuccinimide (1.20 g, 6.7 mmol) were dissolved in acetonitrile (10.0 ml). *para*-Toluenesulfonic acid (1.90 g, 10.1 mmol) was added slowly to the reaction mixture and the reaction mixture was heated at reflux and monitored by TLC (10.0 % EtOAc/ hexane). Acetonitrile was evaporated and the oily residue was dissolved in dichloromethane, washed with water and dried over anhydrous MgSO₄. The organic layer was evaporated to give 1.06 g (69.7 %) of **175** as a light yellow oil, which was used in the further step without any further purification: ¹H NMR (300 MHz; CDCl₃): 1.26 (3H, t, *J* = 6.6 Hz, CH₃), 2.71 (2H, q, *J* = 6.6 Hz, CH₃CH₂), 4.43 (2H, s, CH₂, H-2), 7.30 (2H, d, *J* = 6.9 Hz, 2 x CH, H-3'), 7.90 (2H, d, *J* = 6.9 Hz, 2 x CH, H-2'); +ESIMS *m/z* (relative intensity): 227 (30%, ⁷⁹Br, [M - H]⁻), 229 (28 %, ⁸¹Br). ¹H NMR data for compound **175** are identical to those reported in literature.¹⁵⁹

2.10. 4-(5-Phenyl-1*H*-pyrrol-2-yl)benzonitrile **198**

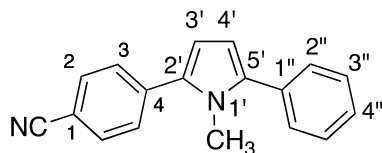


Ammonium acetate (0.31 g, 4.0 mmol) was added to a stirred solution of **126** (0.20 g, 0.8 mmol) in absolute ethanol (7.0 ml) and chloroform (10.0 ml). The reaction mixture was stirred at room temperature and monitored by TLC (10 % EtOAc/ hexane) for the consumption of the starting material. The reaction mixture was concentrated and kept in the fridge overnight. Compound **198** was collected by filtration and rinsed with hexane to give 0.06 g (32.0 %) of yellow needle crystals; mp 158-161 °C; IR (cm⁻¹): 3400 (NH), 2220 (CN), 725; ¹H NMR (300 MHz; DMSO-d₆/ D₂O): 6.65 (1H, d, *J* = 3.9 Hz, pyrrole-CH), 6.81 (1H, d, *J* = 3.6 Hz, pyrrole-CH), 7.23 (1H, t, *J* = 7.2 Hz, CH, H-4''), 7.39 (2H, t, *J* = 7.8 Hz, 2 x CH, H-3''), 7.56-7.62 (4H, m, 4 x CH), 7.89 (2H, d, *J* = 8.4 Hz, 2 x CH); ¹³C NMR (100 MHz; DMSO-d₆) (assignments made using DEPT-135): 107.0 (C, C-1), 108.4 (CH), 110.7 (CH), 119.3 (CN), 123.9 (2 x CH), 124.3 (2 x CH), 126.4 (CH), 128.6 (2 x CH), 131.1 (C), 131.9 (C), 132.6 (2 x CH), 135.1 (C),

Chapter III. Experimental/ Chemistry

136.6 (C); m/z (-ES) 243 (100, [M - H]⁻); found by -ES 243.0929, C₁₇H₁₁N₂ [M - H]⁻, requires 243.0927, error 0.7 ppm.

2.11. 4-(1-Methyl-5-phenyl-1H-pyrrol-2-yl)benzonitrile **199**



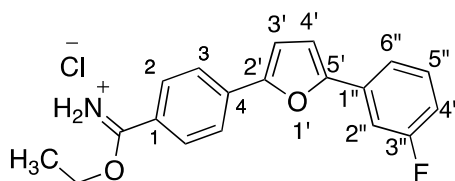
Methylamine (0.35 ml g, 4.0 mmol) and 15 drops glacial acetic acid were added to a solution of **126** (0.27 g, 1.0 mmol) in chloroform (12.0 ml) and absolute ethanol (8.0 ml). The reaction mixture was stirred at 50 °C and monitored by TLC (10 % MeOH-CHCl₃). After 24 h of heating, the reaction was cooled to room temperature, concentrated on a rotary evaporator and kept in the fridge overnight. The pale yellow crystals were collected by filtration and washed with hexane to give 0.20 g (78.0 %): mp 173-175 °C; IR (cm⁻¹): 2231 (CN), 1461, 755; ¹H NMR (300 MHz; DMSO-d₆): 3.63 (3H, s, NCH₃), 6.35 (1H, d, *J* = 3.6 Hz, pyrrole-CH), 6.51 (1H, d, *J* = 3.6 Hz, pyrrole-CH), 7.36 (1H, t, *J* = 7.2 Hz, CH, H-4''), 7.45-7.54 (4H, m, 4 × CH, H-2'', H-3''), 7.72 (2H, d, *J* = 8.1 Hz, 2 × CH), 7.90 (2H, d, *J* = 8.4 Hz, 2 × CH); ¹³C NMR (75 MHz; DMSO-d₆) (assignments made using DEPT-135): 34.5 (NCH₃), 108.2 (C, C-1), 109.2 (CH), 110.9 (CH), 119.1 (CN), 127.2 (CH, C-4''), 128.0 (2 × CH), 128.2 (2 × CH), 128.7 (2 × CH), 132.3 (2 × CH), 132.5 (C), 134.5 (C), 137.2 (C), 138.4 (C); m/z (-ES) 243 (100, [M - CH₄]⁻).

2.12. General procedure for the synthesis of ethyl furan- **180-190**, pyrrole- **200** and *N*-methylpyrrole-imidate hydrochloride **201** intermediates

Acetyl chloride (16.0 mmol for compounds **165-174** and **179** and 8.0 mmol for compounds **200-201**) was added dropwise to a suspension of **165-174**, **179** or **200-201** (1.0 mmol) in absolute ethanol (24 mmol for compounds **165-174** and **179** and 12.0 mmol for **200-201**) in dry chloroform (10 ml) at 0 °C. The reaction was allowed to warm up to room temperature and stirring was continued for 1-3 days.

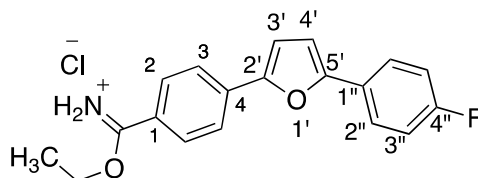
Chapter III. Experimental/ Chemistry

2.12.1. Ethyl 4-(5-(3-fluorophenyl)furan-2-yl)benzimidate hydrochloride 180



The yellow precipitate was filtered off under vacuum and rinsed with hexane to give 0.36 g (61.0 %): mp 236-238 °C; IR (cm⁻¹): 2814, 1606, 1433, 1060 (C-F), 846, 752, 686; ¹H NMR (300 MHz; DMSO-d₆): 1.51 (3H, t, *J* = 6.6 Hz, CH₃), 4.63 (2H, q, *J* = 6.9 Hz, CH₂), 7.16 (1H, dd~t, ³*J*_{HF} = *J*_{HH} = 8.7 Hz, CH, H-4''), 7.31 (1H, d, *J* = 3.3 Hz, furan-CH), 7.45 (1H, d, *J* = 3.3 Hz, furan-CH), 7.52 (1H, dt~q, ⁴*J*_{HF} = *J*_{HH} = 8.1 Hz, CH, H-5''), 7.73-7.78 (2H, m, 2 x CH, H-2'', H-6''), 8.10 (2H, d, *J* = 8.7 Hz, 2 x CH), 8.18 (2H, d, *J* = 8.4 Hz, 2 x CH), 12.0 (1H, s, *N*-H); ¹³C NMR (75 MHz; DMSO-d₆): 18.8 (CH₃), 60.7 (CH₂), 109.8 (CH), 110.1 (CH), 114.4 (d, ²*J*_{CF} = 21.2 Hz), 119.7, 123.2, 128.2, 129.8, 131.0 (d, ³*J*_{CF} = 8.6 Hz), 132.1 (d, ³*J*_{CF} = 8.8 Hz), 132.2, 132.9, 151.95, 151.99, 162.6 (d, ¹*J*_{CF} = 241.5 Hz, C-3''), 167.3 (C-imidate); +ESIMS *m/z* (relative intensity): 310 (100%, [M + H]⁺); found by +ESIMS 310.1238, C₁₉H₁₇NO₂F [M + H]⁺, requires 310.1238, error 0.0 ppm.

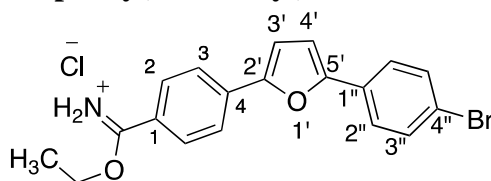
2.12.2. Ethyl 4-(5-(4-fluorophenyl)furan-2-yl)benzimidate hydrochloride 181



The yellow precipitate was filtered off under vacuum and rinsed with hexane to give 0.22 g (89.0 %): mp 190-192 °C (decomposed); IR (cm⁻¹): 2910, 1606, 1408, 1229 (C-F), 829, 807, 750 (C-F); ¹H NMR (300 MHz; DMSO-d₆): 1.51 (3H, t, *J* = 6.9 Hz, CH₃), 4.60 (2H, q, *J* = 6.9 Hz, CH₂), 7.19 (1H, d, *J* = 3.6 Hz, furan-CH), 7.34 (2H, t, ³*J*_{HF} = *J*_{HH} = 8.4 Hz, 2 x CH, H-3''), 7.43 (1H, d, *J* = 3.0 Hz, furan-CH), 7.95 (2H, dd~t, ⁴*J*_{HF} = *J*_{HH} = 7.2 Hz, 2 x CH, H-2''), 8.07 (2H, d, *J* = 8.4 Hz, 2 x CH), 8.12 (2H, d, *J* = 8.4 Hz, 2 x CH); +ESIMS *m/z* (relative intensity): 310.6 (100%, [M + H]⁺); found by +ESIMS 310.1252, C₁₉H₁₇NO₂F [M + H]⁺, requires 310.1243, error 2.8 ppm.

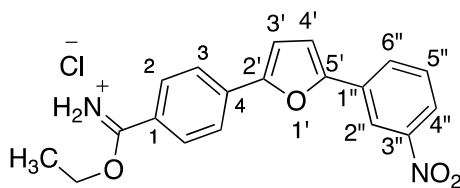
Chapter III. Experimental/ Chemistry

2.12.3. Ethyl 4-(5-(4-bromophenyl)furan-2-yl)benzimidate hydrochloride **182**



The orange precipitate was filtered off under vacuum and rinsed with hexane. Compound **182** was re-crystallized from methanol to give 0.73 g (64.0 %) of a bright yellow solid: mp 144-145 °C; IR (cm⁻¹): 2360, 1607, 752; ¹H NMR (300 MHz; DMSO-d₆): 1.52 (3H, t, *J* = 6.9 Hz, CH₃), 4.62 (2H, q, *J* = 6.9 Hz, CH₂), 7.28 (1H, d, *J* = 3.5 Hz, furan-CH), 7.45 (1H, d, *J* = 3.5 Hz, furan-CH), 7.68 (2H, d, *J* = 8.4 Hz, 2 x CH), 7.85 (2H, d, *J* = 8.4 Hz, 2 x CH), 8.08 (2H, d, *J* = 8.6 Hz, 2 x CH), 8.15 (2H, d, *J* = 8.6 Hz, 2x CH); +ESIMS *m/z* (relative intensity): 370 (100%, ⁷⁹Br, [M + H]⁺), 372 (98%, ⁸¹Br); found by +ESIMS 370.0438, C₁₉H₁₇NO₂Br [M + H]⁺, requires 370.0443, error 1.3 ppm.

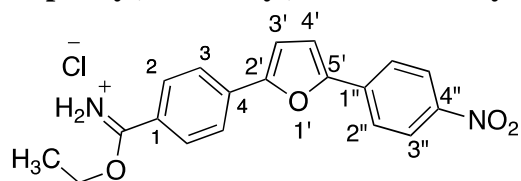
2.12.4. Ethyl 4-(5-(3-nitrophenyl)furan-2-yl)benzimidate hydrochloride **183**



The precipitate was filtered under vacuum and rinsed with chloroform to give 0.65 g (97%) of a fine bright yellow solid: mp 200-203 °C; IR (cm⁻¹): 2981, 1677 (C=N), 1606 (furan C=C), 1527, 1342; ¹H NMR (400 MHz; DMSO-d₆): 1.35 (3H, t, *J* = 8.0 Hz, CH₃), 4.34 (2H, q, *J* = 8.0 Hz, CH₂), 7.37 (1H, d, *J* = 3.6 Hz, furan-CH), 7.47 (1H, d, *J* = 3.0 Hz, furan-CH), 7.77 (1H, t, *J* = 8.0 Hz, CH, H-5''), 8.00 (2H, d, *J* = 8.8 Hz, 2 x CH), 8.04 (2H, d, *J* = 8.8 Hz, 2 x CH), 8.17 (1H, d, *J* = 8.0 Hz, CH, H-6''), 8.31 (1H, d, *J* = 7.6 Hz, CH, H-4''), 8.59 (1H, s, CH, H-2''); ¹³C NMR (100 MHz; DMSO-d₆) (assignments made using DEPT-135): 14.2 (CH₃), 60.8 (CH₂), 111.0 (CH), 111.1 (CH), 117.8 (CH), 122.2 (CH), 123.7 (2 x CH), 128.6 (CH), 129.8 (CH), 129.9 (2 x CH), 130.7 (CH), 131.2 (C), 133.6 (C), 148.5 (C, C-3''), 151.4 (C), 152.6 (C), 165.3 (C, C-imidate); +ESIMS *m/z* (relative intensity): 337.4 (100%, [M + H]⁺); found by +ESIMS 337.1200, C₁₉H₁₇NO₄ [M + H]⁺, requires 337.1188, error 3.5 ppm.

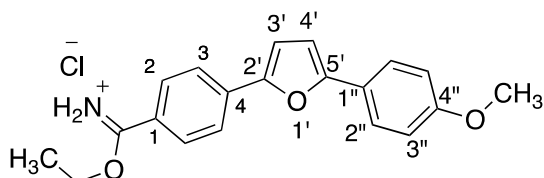
Chapter III. Experimental/ Chemistry

2.12.5. Ethyl 4-(5-(4-nitrophenyl)furan-2-yl)benzimidate hydrochloride **184**



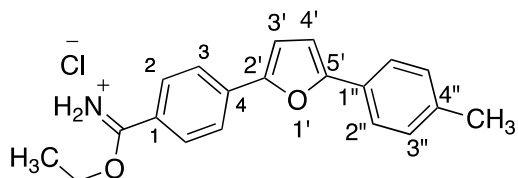
The orange precipitate was filtered under vacuum and rinsed with hexane. Compound **184** was re-crystallized from DMF/H₂O to give 0.32 g (53.3 %): mp 250-252°C; IR (cm⁻¹): 2981, 1677 (C=N), 1606, 1527, 1342; ¹H NMR (300 MHz; DMSO-d₆): 1.34 (3H, t, *J* = 7.2 Hz, CH₃), 4.33 (2H, q, *J* = 7.2 Hz, CH₂), 7.41 (1H, d, *J* = 3.6 Hz, furan-CH), 7.51 (1H, d, *J* = 3.6 Hz, furan-CH), 8.00-8.03 (4H, m, 4 x CH), 8.11 (2H, d, *J* = 8.7 Hz, 2 x CH), 8.31 (2H, d, *J* = 8.7 Hz, 2 x CH).

2.12.6. Ethyl 4-(5-(4-methoxyphenyl)furan-2-yl)benzimidate hydrochloride **185**



The reaction mixture was diluted with hexane and the yellow-coloured precipitate was collected and rinsed with hexane to give 0.014 g (57.0 %) of **185**: ¹H NMR (300 MHz; DMSO-d₆): 1.51 (3H, t, *J* = 6.6 Hz, CH₃), 3.81 (3H, s, OCH₃), 4.60 (2H, q, *J* = 6.6 Hz, CH₂), 7.04-7.06 (3H, m, 3 x CH, including H-3' and H-4'), 7.39 (1H, s, CH), 7.82 (2H, d, *J* = 8.1 Hz, 2 x CH, H-2''), 8.03 (2H, d, *J* = 7.8 Hz, 2 x CH), 8.11 (2H, d, *J* = 7.8 Hz, 2 x CH); ¹³C NMR (75 MHz; DMSO-d₆): 14.2, 55.2, 60.7, 106.9, 110.9, 114.2, 114.4, 123.0, 125.3, 127.9, 129.8, 150.6, 159.1, 165.4.

2.12.7. Ethyl 4-(5-(4-methylphenyl)furan-2-yl)benzimidate hydrochloride **186**

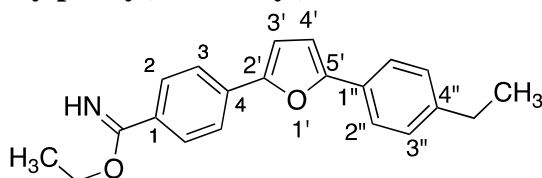


The yellow precipitate was filtered off under vacuum and rinsed with hexane to give 0.8 g (65.0 %) of **186**: ¹H NMR (300 MHz; DMSO-d₆): 1.50 (3H, t, *J* = 7.2 Hz, CH₂CH₃), 2.35 (3H, s, CH₃), 4.53 (2H, q, *J* = 6.4 Hz, OCH₂), 7.13 (1H, d, *J* = 3.6 Hz, furan-CH), 7.30 (2H, d, *J* = 7.8 Hz, 2 x CH, H-3''), 7.40 (1H, d, *J* = 3.3 Hz, furan-CH), 7.78 (2H, d, *J* = 8.1 Hz, 2 x CH, H-2''), 8.04 (2H, d, *J* = 9.0 Hz, 2 x CH), 8.09 (2H, d, *J*

Chapter III. Experimental/ Chemistry

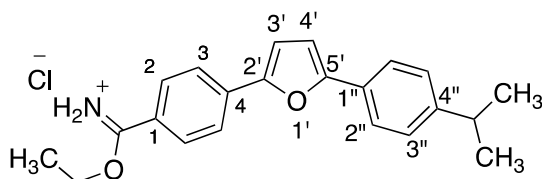
= 8.7 Hz, 2 x *CH*); ^{13}C NMR (75 MHz; DMSO- d_6) (assignments made using DEPT-135): 14.2 (CH_3), 20.9 (OCH_2CH_3), 60.0 (OCH_2), 109.8 (*CH*), 110.8 (*C*), 122.9 (*CH*), 123.2 (*CH*), 123.6 (*CH*), 123.7 (*CH*), 128.2 (*C*), 129.5 (*CH*), 129.8 (*C*), 132.5 (*C*), 151.4 (*C*), 153.5 (*C*), 167.6 (*C*, C-imidate).

2.12.8. Ethyl 4-(5-(4-ethylphenyl)furan-2-yl)benzimidate **187**



The reaction was cooled to 0 °C and saturated solution of sodium bicarbonate was added dropwise until the gas evolution ceased. The organic layer was extracted, washed with water, dried over anhydrous MgSO_4 and evaporated to give 0.10 g (89.0 %) of **187** as a yellow solid: mp 250-252 °C; IR (cm^{-1}): 3438 (*NH*), 2891, 1606 (furan $\text{C}=\text{C}$), 1441, 1384, 1060, 675; ^1H NMR (300 MHz; DMSO- d_6): 1.21 (3H, t, $J = 7.5$ Hz, CH_2CH_3), 1.51 (3H, t, $J = 7.2$ Hz, OCH_2CH_3), 2.65 (2H, q, $J = 7.5$ Hz, CH_2CH_3), 4.64 (2H, q, $J = 6.9$ Hz, OCH_2), 7.14 (1H, d, $J = 3.6$ Hz, furan-*CH*), 7.32 (2H, d, $J = 8.1$ Hz, 2 x *CH*, H-4''), 7.42 (1H, d, $J = 3.6$ Hz, furan-*CH*), 7.80 (2H, d, $J = 8.1$ Hz, 2 x *CH*), 8.05 (2H, d, $J = 8.4$ Hz, 2 x *CH*), 8.20 (2H, d, $J = 7.8$ Hz, 2 x *CH*), 11.75 (1H, s, *N-H*); +ESIMS m/z (relative intensity): 320.6 (100%, $[\text{M} + \text{H}]^+$); found by +ESIMS 320.1644, $\text{C}_{21}\text{H}_{22}\text{NO}_2$ $[\text{M} + \text{H}]^+$, requires 320.1651, error 2.0 ppm.

2.12.9. Ethyl 4-(5-(4-isopropylphenyl)furan-2-yl)benzimidate hydrochloride **188**

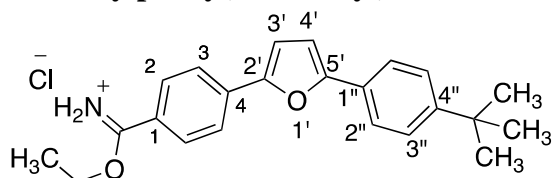


The reaction mixture was diluted with diethyl ether and the precipitate was filtered off under vacuum, rinsed with diethyl ether and re-crystallized from ethanol to give 0.11 g (32.4 %) of **188**: mp 231-233 °C; IR (cm^{-1}): 3136, 3049, 1606, 1408, 795, 750, 677; ^1H NMR (300 MHz; DMSO- d_6): 1.24 (6H, d, $J = 6.9$ Hz, 2 x CH_3), 1.51 (3H, t, $J = 6.9$ Hz, CH_3), 2.88-2.94 (1H, septet, $J = \text{Hz}$, *CH*), 4.61 (2H, q, $J = 6.9$ Hz, CH_2), 7.14 (1H, d, $J = 3.9$ Hz, furan-*CH*), 7.36 (2H, d, $J = 8.4$ Hz, 2 x *CH*, H-3''), 7.42 (1H, d, $J = 3.6$ Hz, furan-*CH*), 7.81 (2H, d, $J = 8.1$ Hz, 2 x *CH*), 8.06 (2H, d, $J = 8.7$ Hz, 2 x *CH*), 8.15 (2H, d, $J = 8.4$ Hz, 2 x *CH*); ^{13}C NMR (75 MHz; DMSO- d_6): 14.2, 23.7, 33.2,

Chapter III. Experimental/ Chemistry

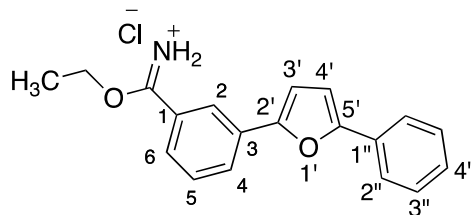
60.7, 107.7, 109.8, 122.9, 123.7, 126.8, 128.2, 129.8, 132.46, 132.52, 148.2, 151.5, 153.5, 167.3; +ESIMS m/z (relative intensity): 334.6 (100%, $[M + H]^+$); found by +ESIMS 334.1800, $C_{22}H_{24}NO_2$ $[M + H]^+$, requires 334.1802, error 0.5 ppm.

2.12.10. Ethyl 4-(5-(4-*tert*-butylphenyl)furan-2-yl)benzimidate hydrochloride **189**



The reaction mixture was diluted with diethyl ether; The precipitate was filtered off under vacuum and rinsed with diethyl ether. Compound **189** was re-crystallized from ethanol to give 0.08 g (19.0 %): mp; IR (cm^{-1}): 3128, 2965, 1604, 1407, 1071, 807, 750; 1H NMR (300 MHz; DMSO- d_6): 1.32 (9H, s, 3 x CH_3), 1.51 (3H, t, $J = 6.9$ Hz, CH_3CH_2), 4.62 (2H, q, $J = 6.9$ Hz, OCH_2), 7.14 (1H, d, $J = 3.3$ Hz, furan- CH), 7.43 (1H, d, $J = 3.6$ Hz, furan- CH), 7.50 (2H, d, $J = 8.4$ Hz, 2 x CH , H-3''), 7.81 (2H, d, $J = 8.4$ Hz, 2 x CH , H-2''), 8.05 (2H, d, $J = 8.7$ Hz, 2 x CH), 8.17 (2H, d, $J = 8.4$ Hz, 2 x CH); ^{13}C NMR (75 MHz; DMSO- d_6): 18.5, 31.0, 34.4, 60.7, 109.8, 110.9, 122.9, 123.2, 123.6, 125.7, 128.0, 128.2, 129.8, 134.1, 153.5, 154.0, 167.3; +ESIMS m/z (relative intensity): 348.8 (100%, $[M + H]^+$); found by +ESIMS 348.1960, $C_{23}H_{24}NO_2$ $[M + H]^+$, requires 348.1964, error 1.0 ppm.

2.12.11. Ethyl 3-(5-phenylfuran-2-yl)benzimidate hydrochloride **190**

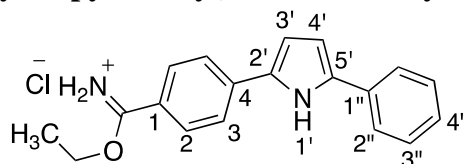


The green-yellow precipitate was filtered off under vacuum and rinsed with diethyl ether to give 0.22 g (88.0 %) of **190**: mp 174 °C; IR (cm^{-1}): 2827, 2362, 1738, 1635 ($C=N$), 1464, 1353, 1077, 782, 677; 1H NMR (300 MHz; DMSO- d_6): 1.52 (3H, t, $J = 6.9$ Hz, CH_3), 4.66 (2H, q, $J = 6.9$ Hz, CH_2), 7.16 (1H, d, $J = 3.3$ Hz, furan- CH), 7.32-7.37 (2H, m, 2 x CH including furan- CH), 7.47 (2H, t, $J = 7.5$ Hz, 2 x CH , H-3''), 7.71 (1H, t, $J = 7.8$ Hz, CH , H-5), 7.89 (2H, d, $J = 7.5$ Hz, 2 x CH , H-2''), 7.96 (1H, d, $J = 7.8$ Hz, CH), 8.22 (1H, d, $J = 7.8$ Hz, CH), 8.64 (1H, s, CH , H-2), 11.97 (s, NH); ^{13}C NMR (100 MHz; DMSO- d_6) (assignments made using DEPT-135): 14.2 (CH_3), 61.0 (OCH_2), 108.4 (CH), 108.8 (CH), 122.3 (CH), 123.5 (CH), 126.0 (CH), 126.5 (CH),

Chapter III. Experimental/ Chemistry

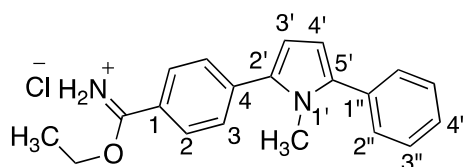
126.9 (C), 127.7 (CH), 127.9 (CH), 128.9 (CH), 129.5 (C), 130.5 (C), 151.4 (C), 152.9 (C), 167.4 (C, C-imidate); +ESIMS m/z (relative intensity): 292 (100%, $[M + H]^+$); found by +ESIMS 292.1324, $C_{19}H_{18}NO_2 [M + H]^+$, requires 292.1332, error 2.8 ppm.

2.12.12. Ethyl 4-(5-phenyl-*H*-pyrrol-2-yl)benzimidate hydrochloride **200**



The precipitate was filtered off under vacuum and rinsed with hexane. Compound **200** was re-crystallized from MeOH/ $CHCl_3$ to give 0.16 g (30.8 %) of a brown solid: mp 232-235 °C; IR (cm^{-1}): 3343 (NH), 3172, 3002, 1601, 1383, 744; 1H NMR (300 MHz; DMSO- d_6): 1.51 (3H, t, $J = 6.9$ Hz, CH_3), 4.62 (2H, q, $J = 6.6$ Hz, CH_2), 6.72 (1H, s, pyrrole- CH), 6.97 (1H, s, pyrrole- CH), 7.25 (1H, t, $J = 6.9$ Hz, CH , H-4''), 7.42 (2H, t, $J = 7.5$ Hz, 2 x CH , H-3''), 7.84 (2H, d, $J = 7.5$ Hz, 2 x CH , H-2''), 8.06 (2H, d, $J = 8.4$ Hz, 2 x CH), 8.13 (2H, d, $J = 8.1$ Hz, 2 x CH), 11.62 (1H, s, $N-H$); +ESIMS m/z (relative intensity): 291.7 (100%, $[M + H]^+$); found by +ESIMS 291.1488, $C_{19}H_{19}N_2O [M + H]^+$, requires 291.1497, error 3.2 ppm.

2.12.13. Ethyl 4-(1-methyl-5-phenyl-*H*-pyrrol-2-yl)benzimidate hydrochloride **201**



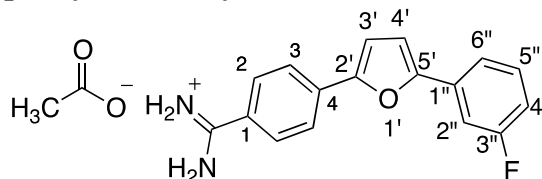
The reaction mixture was concentrated and kept in the fridge overnight. The yellow-green precipitate was filtered off under vacuum and rinsed with diethyl ether to give 0.10 g (58.8 %) of **201**; IR (cm^{-1}): 2842, 1647, 1604, 1460, 1078, 700; 1H NMR (300 MHz; DMSO- d_6): 1.51 (3H, t, $J = 6.9$ Hz, CH_3), 3.67 (3H, s, NCH_3), 4.64 (2H, q, $J = 6.9$ Hz, CH_2), 6.38 (1H, d, $J = 3.9$ Hz, pyrrole- CH), 6.60 (1H, d, $J = 3.9$ Hz, pyrrole- CH), 7.38 (1H, t, $J = 6.9$ Hz, CH , H-4''), 7.46-7.55 (4H, m, 4 x CH , H-2'', H-3''), 7.81 (2H, d, $J = 8.1$ Hz, 2 x CH), 8.17 (2H, d, $J = 8.4$ Hz, 2 x CH); +ESIMS m/z (relative intensity): 305.7 (100%, $[M + H]^+$); found by +ESIMS 305.1649, $C_{20}H_{21}N_2O [M + H]^+$, requires 305.1648, error 0.2 ppm.

Chapter III. Experimental/ Chemistry

2.13. General procedure for the synthesis of furan- 144-154, pyrrole- 191 and *N*-methylpyrrole-amidine acetates 192

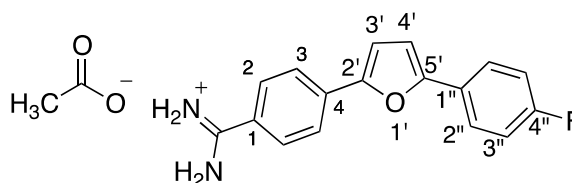
Ammonium acetate (4.0 mmol) was added to a stirred suspension of furan- **180-190**, pyrrole **200** and *N*-methylpyrrole-imidates **201** (1.0 mmol) in anhydrous ethanol. The mixture was stirred at room temperature for 1- 3 days.

2.13.1. 4-(5-(3-Fluorophenyl)furan-2-yl)benzamidine acetate **144**



The light yellow fine solid was filtered off under vacuum and rinsed with ethanol to give 0.21 g (64.0 %) of **144**: mp 234-236 °C; IR (cm⁻¹): 2965, 1738, 1610 (furan C=C), 1403, 844, 750, 688; ¹H NMR (300 MHz; DMSO-d₆): 1.73 (3H, s, CH₃), 7.17 (1H, t, ³J_{HF} = J_{HH} = 8.1 Hz, CH, H-4''), 7.26 (1H, d, J = 3.0 Hz, furan-CH), 7.34 (1H, d, J = 3.0 Hz, furan-CH), 7.51 (1H, ddd~q, ⁴J_{HF} = J_{HH} = 7.8 Hz, CH, H-5''), 7.71-7.75 (2H, m, 2 x CH, H-2'', H-6''), 7.88 (2H, d, J = 8.4 Hz, 2 x CH), 8.03 (2H, d, J = 8.4 Hz, 2 x CH); ¹³C NMR (75 MHz; DMSO-d₆): 22.9, 109.9, 111.3, 114.7 (d, ²J_{CF} = 22.0 Hz, 2 x CH), 119.8, 123.6, 126.7, 128.7, 131.3, 131.7 (d, ³J_{CF} = 8.6 Hz), 134.2, 151.5, 152.6, 162.6 (d, ¹J_{CF} = 241.5 Hz, C-3''), 165.1 (C-amidine), 174.5 (C=O); ¹⁹F-NMR (377 MHz; DMSO-d₆): -112.4; -ESIMS m/z (relative intensity): 279 (90 %, [M - H]⁻); +ESIMS m/z (relative intensity): 281 (100 %, [M + H]⁺); found by +ESIMS 281.1080, C₁₇H₁₄NO₂F [M + H]⁺, requires 281.1085, error 1.7 ppm.

2.13.2. 4-(5-(4-Fluorophenyl)furan-2-yl)benzamidine acetate **145**

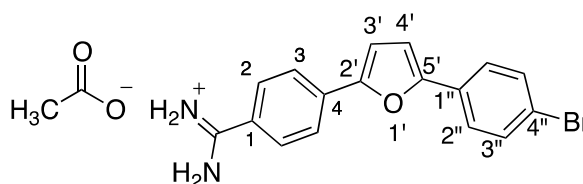


The white precipitate was filtered off under vacuum and rinsed with hexane. Compound **145** was re-crystallized from ethanol to give 0.05 g (47.0 %): mp 219-222 °C; IR (cm⁻¹): 2970, 1614 (furan C=C), 1401, 1209 (C-F), 1156, 844, 781, 675, 603; ¹H NMR (300 MHz; DMSO-d₆): 1.74 (3H, s, CH₃), 7.15 (1H, d, J = 2.7 Hz, furan-CH), 7.30-7.35 (3H, m, 3 x CH, including furan-CH), 7.87-8.01 (6H, m, 6 x CH, H-2, H-3, H-2''); ¹³C NMR (75 MHz; DMSO-d₆) (assignments made using DEPT-135): 24.2

Chapter III. Experimental/ Chemistry

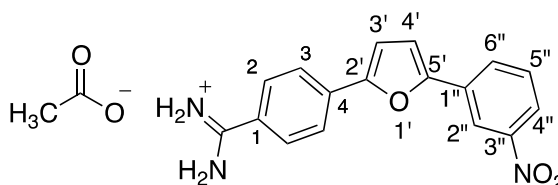
(CH₃), 108.4 (CH), 110.9 (CH), 116.0 (d, ²J_{CF} = 21.9 Hz, 2 × CH, C-3''), 123.3 (CH), 125.9 (d, ³J_{CF} = 8.1 Hz, 2 × CH, C-2''), 126.4 (C), 128.1 (C), 128.2 (CH), 133.8 (C), 152.4 (C), 152.6 (C), (C-4''), C-amidine and C=O were not observed in the ¹³C NMR spectrum); ¹⁹F NMR (377 MHz; DMSO-d₆): -113.1; +ESIMS m/z (relative intensity): 281 (100 %, [M + H]⁺); found by +ESIMS 281.1094, C₁₇H₁₄NO₂F [M + H]⁺, requires 281.1085, error 3.1 ppm

2.13.3. 4-(5-(4-Bromophenyl)furan-2-yl)benzamidinium acetate **146**



The light yellow-coloured precipitate was filtered off under vacuum and rinsed with hexane. Compound **146** was re-crystallized from ethanol to give 0.05 g (18.2 %) of **146**: IR (cm⁻¹): 2915, 1395, 995, 780; ¹H NMR (300 MHz; DMSO-d₆): 1.80 (3H, s, CH₃), 7.20 (1H, d, *J* = 3.3 Hz, furan-CH), 7.24 (1H, d, *J* = 3.4 Hz, furan-CH), 7.67 (2H, d, *J* = 8.3 Hz, 2 x CH), 7.84 (2H, d, *J* = 8.3 Hz, 2 x CH), 7.90 (2H, d, *J* = 8.2 Hz, 2 x CH), 8.04 (2H, d, *J* = 8.2 Hz, 2 x CH); ¹³C NMR (75 MHz, DMSO-d₆) (assignments made using DEPT-135): 14.2 (CH₃), 109.3 (CH), 109.9 (CH), 120.7 (C), 123.3 (CH), 125.5 (CH), 127.4 (CH), 128.9 (C), 129.0 (C), 131.7 (C), 131.9 (CH), 152.2 (C), 164.5 (C-amidine), (C=O and one quaternary C were not observed in the ¹³C NMR spectrum); +ESIMS m/z (relative intensity): 341 (85 %, ⁷⁹Br, [M + H]⁺), 343 (100 %, ⁸¹Br); found by +ESIMS 341.0287, C₁₇H₁₄N₂OBr [M + H]⁺, requires 341.0284, error 0.7 ppm.

2.13.4. 4-(5-(3-Nitrophenyl)furan-2-yl)benzamidinium acetate **147**

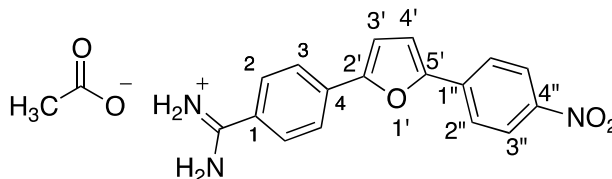


The bright yellow precipitate was filtered under vacuum and rinsed with hexane. Compound **147** was added to boiling ethanol and filtered while it is hot to give 0.33 g (58.0 %): mp 253-255°C; IR (cm⁻¹): 2978, 2362, 1613, 1518, 1487, 1347, 733; ¹H NMR (400 MHz; DMSO-d₆): 1.75 (3H, s, CH₃), 7.40 (1H, d, *J* = 3.6 Hz, furan-CH), 7.48 (1H, d, *J* = 3.6 Hz, furan-CH), 7.77 (1H, t, *J* = 8.1 Hz, CH, H-5''), 7.90 (2H, d, *J* = 8.4 Hz, 2

Chapter III. Experimental/ Chemistry

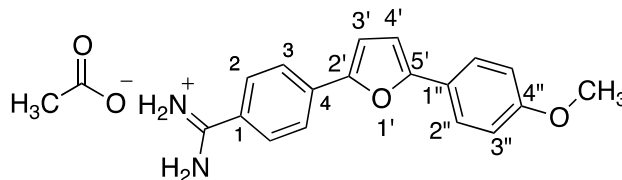
x CH), 8.06 (2H, d, $J = 8.4$ Hz, 2 x CH), 8.17 (1H, d, $J = 9.0$ Hz, CH, H-6''), 8.34 (1H, d, $J = 7.8$ Hz, CH, H-4''), 8.62 (s, CH, H-2''); The poor solubility of compound **147** in DMSO- d_6 meant that a good ^{13}C NMR spectrum could not be recorded; +ESIMS m/z (relative intensity): 308 (100%, $[\text{M} + \text{H}]^+$); found by +ESIMS 308.1038, $\text{C}_{17}\text{H}_{14}\text{N}_3\text{O}_3$ $[\text{M} + \text{H}]^+$, requires 308.1030, error 2.5 ppm.

2.13.5. 4-(5-(4-Nitrophenyl)furan-2-yl)benzamidinium acetate **148**



The dark yellow-coloured precipitate was filtered under vacuum and rinsed with hexane. Compound **148** was added to boiling ethanol and filtered while was hot to give 0.45 g (68.0 %): mp 257-260 °C; IR (cm^{-1}): 2933, 1598, 1509, 1408, 1325, 851, 751; ^1H NMR (300 MHz; DMSO- d_6): 1.75 (3H, s, CH_3), 7.44 (1H, d, $J = 3.3$ Hz, furan-CH), 7.52 (1H, d, $J = 3.0$, furan-CH), 7.91 (2H, d, $J = 8.1$, 2 x CH), 8.07 (2H, d, $J = 8.1$ Hz, 2 x CH), 8.14 (2H, d, $J = 8.7$ Hz, 2 x CH), 8.32 (2H, d, $J = 8.4$ Hz, 2 x CH); ^{13}C NMR (75 MHz; DMSO- d_6) (assignments made using DEPT-135): 111.4 (CH), 112.9 (CH), 123.9 (2 x CH), 124.3 (2 x CH), 124.5 (2 x CH), 128.6 (C), 129.9 (2 x CH), 133.5 (C), 135.4 (C), 146.1 (C, C-4''), 151.6 (C), 153.4 (C), 165.8 (C-amidinium). The carbons of the acetate groups were not observed in the ^{13}C NMR spectrum, but the methyl group was observed in the ^1H NMR spectrum; +ESIMS m/z (relative intensity): 308 (100%, $[\text{M} + \text{H}]^+$); found by +ESIMS 308.1023, $\text{C}_{17}\text{H}_{14}\text{N}_3\text{O}_3$ $[\text{M} + \text{H}]^+$, requires 308.1030, error 2.3 ppm.

2.13.6. 4-(5-(4-Methoxyphenyl)furan-2-yl)benzamidinium acetate **149**

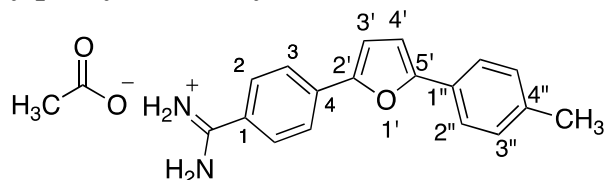


The reaction mixture was diluted with hexane and the yellow precipitate was collected and rinsed with hexane to give 0.014 g (57.0 %) of **149**: mp 215-218 °C; IR (cm^{-1}): 2928, 1610, 1491, 1409, 1022, 789, 746; the spectroscopic data (^1H and ^{13}C NMR) were identical to the reported in the literature.^{106a} +ESIMS m/z (relative

Chapter III. Experimental/ Chemistry

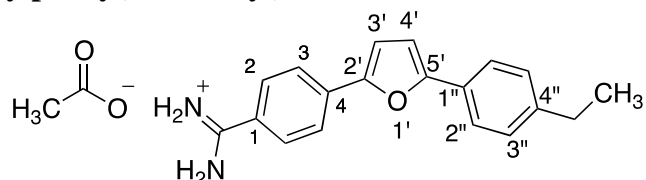
intensity): 293 (100%, $[M + H]^+$); found by +ESIMS 293.1284, $C_{18}H_{17}N_2O_2$ $[M + H]^+$, requires 293.1285, error 0.4 ppm.

2.13.7. 4-(5-(4-Methylphenyl)furan-2-yl)benzamidinium acetate **150**



The white-coloured precipitate was filtered off under vacuum and rinsed with hexane. Compound **150** was re-crystallized from ethanol to give 0.04 g (51.2 %): mp 233-235 °C; IR (cm^{-1}): 3125, 3023, 2969, 1614, 1495, 1409, 790; 1H NMR (300 MHz; DMSO- d_6): 1.78 (3H, s, $OOCCH_3$), 2.35 (3H, s, CH_3), 7.08 (1H, d, $J = 3.6$ Hz, furan- CH), 7.28-7.30 (3H, m, 3 x CH including furan- CH), 7.76 (2H, d, $J = 8.1$ Hz, 2 x CH , H-2''), 7.87 (2H, d, $J = 8.1$ Hz, 2 x CH), 7.96 (2H, d, $J = 8.4$ Hz, 2 x CH); ^{13}C NMR (75 MHz, DMSO- d_6): 20.9 (CH_3), 23.5 ($OCOCH_3$), 107.8, 111.0, 123.2, 123.7, 127.1, 128.4, 129.5, 137.6, 150.8, 154.1, Four carbon were not observed in the spectrum; +ESIMS m/z (relative intensity): 277 (100%, $[M + H]^+$); found by +ESIMS 277.1348, $C_{18}H_{17}N_2O$ $[M + H]^+$, requires 277.1336, error 4.4 ppm.

2.13.8. 4-(5-(4-Ethylphenyl)furan-2-yl)benzamidinium acetate **151**

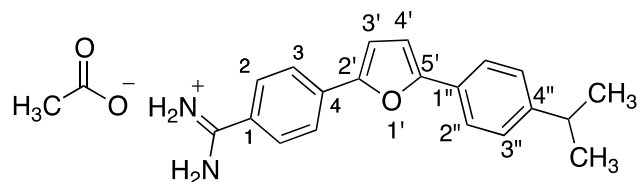


The light yellow precipitate was filtered off under vacuum and rinsed with hexane to give 0.04 g (73.0 %) of **151**: mp 249-252 °C; IR (cm^{-1}): 2969, 2359, 1610 (furan $C=C$), 1495, 1411, 1200, 790; 1H NMR (300 MHz; DMSO- d_6): 1.20 (3H, t, $J = 7.2$ Hz, CH_2CH_3), 1.74 (3H, s, CH_3), 2.64 (2H, q, $J = 7.2$ Hz, CH_2CH_3), 7.09 (1H, d, $J = 3.3$ Hz, furan- CH), 7.30-7.32 (3H, m, 3 x CH including furan- CH), 7.78 (2H, d, $J = 7.8$ Hz, 2 x CH , H-2''), 7.87 (2H, d, $J = 8.1$ Hz, 2 x CH), 7.98 (2H, d, $J = 8.4$ Hz, 2 x CH); ^{13}C NMR (75 MHz, DMSO- d_6) (assignments made using DEPT-135): 15.7 (CH_3), 22.4 ($OOCCH_3$), 27.9 (CH_2), 123.3 (CH), 123.7 (CH), 126.9 (CH), 127.3 (CH), 128.3 (CH), 128.6 (C), 134.3 (CH), 143.9 (C), 150.7 (C), 154.2 (C), 165.0 (C-amidinium), 173.6 (C, $C=O$), two carbons (C) were not observed or were overlapping in the ^{13}C NMR

Chapter III. Experimental/ Chemistry

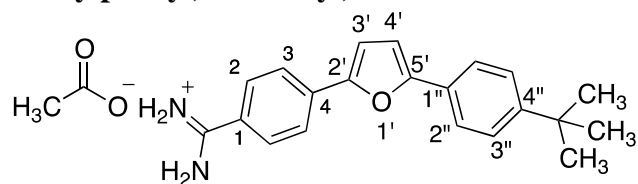
spectrum; +ESIMS m/z (relative intensity): 291.3 (100 %, $[M + H]^+$); found by +ESIMS 291.1493, $C_{19}H_{19}ON_2 [M + H]^+$, requires 291.1492, error 0.4 ppm.

2.13.9. 4-(5-(4-Isopropylphenyl)furan-2-yl)benzamidinium acetate **152**



The white precipitate was filtered off under vacuum and rinsed with hexane to give 0.07 g (95.7 %) of **152**: mp 235-238 °C (decomposed); IR (cm^{-1}): 2961, 1610 (furan C=C), 1495, 1488, 840, 788; 1H NMR (300 MHz; DMSO- d_6): 1.25 (6H, d, $J = 6.9$ Hz, 2 x CH_3), 1.83 (3H, s, $OCCH_3$), 2.94 (1H, septet, $J = 6.9$ Hz, $CH(CH_3)_2$), 7.11 (1H, d, $J = 3.6$ Hz, furan- CH), 7.34-7.37 (3H, m, 3 x CH including furan- CH), 7.80 (2H, d, $J = 8.1$ Hz, 2 x CH , H-2''), 7.91 (2H, d, $J = 8.7$ Hz, 2 x CH), 8.02 (2H, d, $J = 8.4$ Hz, 2 x CH); ^{13}C NMR (75 MHz, DMSO- d_6) (assignments made using DEPT-135): 21.0 (2 x CH_3), 23.7 ($OCOCH_3$), 33.2 (CH), 108.0 (CH), 111.5 (CH), 123.3 (CH), 123.9 (CH), 125.8 (C), 126.9 (CH), 127.4 (C), 128.9 (CH), 134.7 (C), 148.6 (C), 150.6 (C), 154.3 (C), 164.8 (C , C-amidinium), 172.0 (C , C=O); +ESIMS m/z (relative intensity): 305.6 (100%, $[M + H]^+$); found by +ESIMS 305.1648, $C_{20}H_{21}N_2O [M + H]^+$, requires 305.1648, error 0.0 ppm.

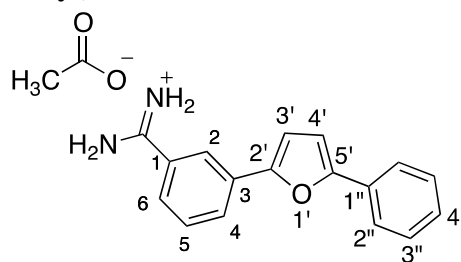
2.13.10. 4-(5-(4-*tert*-Butylphenyl)furan-2-yl)benzamidinium acetate **153**



The white precipitate was filtered off under vacuum and rinsed with hexane. Compound **153** was re-crystallized from ethanol to give 0.04 g (97.4 %): mp 272-274 °C; IR (cm^{-1}): 2969, 1738, 1614, 1487, 1407, 1058, 781; 1H NMR (300 MHz; DMSO- d_6): 1.32 (9H, s, 3 x CH_3), 1.74 (3H, s, $OCCH_3$), 7.09 (1H, d, $J = 3.3$ Hz, furan- CH), 7.31 (1H, d, $J = 3.6$ Hz, furan- CH), 7.49 (2H, d, $J = 8.4$ Hz, 2 x CH , H-3''), 7.79 (2H, d, $J = 8.1$ Hz, 2 x CH , H-2''), 7.88 (2H, d, $J = 8.4$ Hz, 2 x CH), 7.98 (2H, d, $J = 8.4$ Hz, 2 x CH); +ESIMS m/z (relative intensity): 319.7 (100%, $[M + H]^+$); found by +ESIMS 319.1805, $C_{21}H_{23}N_2O [M + H]^+$, requires 319.1805, error 0.0 ppm.

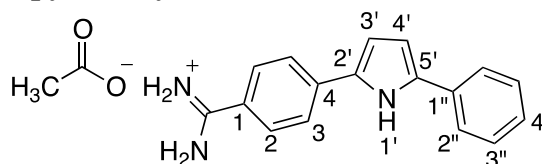
Chapter III. Experimental/ Chemistry

2.13.11. 3-(5-Phenylfuran-2-yl)benzamidinium acetate **154**



The white precipitate was filtered off under vacuum and rinsed with hexane to give 0.08 g (84.6 %) of **154**: mp 190-192 °C; IR (cm⁻¹): 3136, 3037, 2838, 1407, 758, 681; ¹H NMR (300 MHz; DMSO-d₆): 1.80 (3H, s, CH₃), 7.15 (1H, d, *J* = 3.3 Hz, furan-CH), 7.25 (1H, d, *J* = 3.3 Hz, furan-CH), 7.34 (1H, t, *J* = 7.2 Hz, CH, H-4''), 7.47 (2H, t, *J* = 7.5 Hz, 2 x CH, H-3''), 7.64-7.73 (2H, m, 2 x CH), 7.88 (2H, d, *J* = 7.8 Hz, 2 x CH), 8.12 (1H, d, *J* = 7.2 Hz, CH, H-6), 8.24 (1H, s, CH, H-2); ¹³C NMR (100 MHz; DMSO-d₆) (assignments made using DEPT-135): 23.1 (CH₃), 108.4 (CH), 109.8 (CH), 122.5 (CH), 123.6 (CH), 126.5 (CH), 127.8 (CH), 127.9 (CH), 128.9 (CH), 129.6 (CH), 129.7 (C), 129.8 (C), 130.6 (C), 151.1 (C), 153.3 (C), 165.6 (C-amidinium), (C, C=O) was not observed in the spectrum; +ESIMS *m/z* (relative intensity): 263 (100%, [M + H]⁺); found by +ESIMS 263.1167, C₁₇H₁₅N₂O [M + H]⁺, requires 263.1179, error 4.5 ppm.

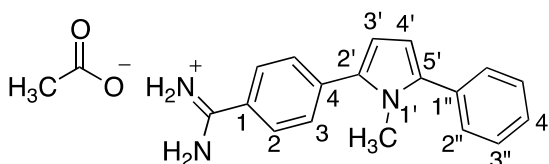
2.13.12. 4-(5-Phenyl-*H*-pyrrol-2-yl)benzamidinium acetate **191**



The yellow precipitate was filtered off under vacuum and rinsed with hexane to give 0.03 g (67.0 %) of **191**: mp > 300 °C (decomposed); IR (cm⁻¹): 3444 (NH), 3128, 3043, 1601, 1408, 747; ¹H NMR (300 MHz; DMSO-d₆): 1.83 (3H, s, CH₃), 6.68 (1H, d, *J* = 3.6 Hz, pyrrole-CH), 6.89 (1H, d, *J* = 3.6 Hz, pyrrole-CH), 7.24 (1H, t, *J* = 7.5 Hz, CH, H-4''), 7.41 (2H, t, *J* = 7.8 Hz, 2 x CH, H-3''), 7.80-7.86 (4H, m, 4 x CH), 8.01 (2H, d, *J* = 8.4 Hz, 2 x CH), 11.50 (1H, s, NH); +ESIMS *m/z* (relative intensity): 262 (100%, [M + H]⁺), -ESIMS *m/z* (relative intensity): 260 (98%, [M - H]⁻); found by 262.1338, C₁₇H₁₆N₃ [M + H]⁺, requires 262.1339, error 0.3 ppm.

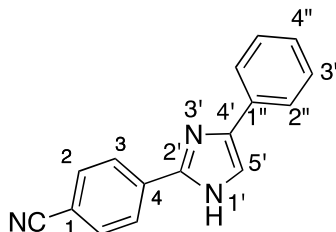
Chapter III. Experimental/ Chemistry

2.13.13. 4-(1-Methyl-5-phenyl-*H*-pyrrol-2-yl)benzamidinium acetate **192**



The light yellow precipitate was filtered off under vacuum and rinsed with hexane to give 0.04 g (60.0 %) of **192**: mp 226-228 °C; IR (cm⁻¹): 2842, 1647, 1604, 1460, 1078, 700; ¹H NMR (300 MHz; DMSO-d₆): 1.73 (3H, s, CH₃), 3.64 (3H, s, NCH₃), 6.34 (1H, d, *J* = 3.9 Hz, pyrrole-CH), 6.47 (1H, d, *J* = 3.6 Hz, pyrrole-CH), 7.36 (1H, t, *J* = 7.2 Hz, CH, H-4''), 7.45-7.54 (4H, m, 4 x CH), 7.71 (2H, d, *J* = 8.1 Hz, 2 x CH), 7.88 (2H, d, *J* = 8.4 Hz, 2 x CH); ¹³C NMR (75 MHz; DMSO-d₆) (assignments made using DEPT-135): 24.6 (CH₃), 34.5 (NCH₃), 109.0 (CH), 110.3 (CH), 127.1 (CH, C-4''), 127.5 (C), 127.7 (2 x CH, C-3''), 127.8 (2 x CH), 128.3 (2 x CH), 128.6 (2 x CH), 132.6 (C), 134.9 (C), 137.1 (C), 137.8 (C), 165.2 (C, C-amidinium), 176.1 (C=O); -ESIMS *m/z* (relative intensity): 279 (90 %, [M - H]⁻); +ESIMS *m/z* (relative intensity): 276 (100 %, [M + H]⁺); found by +ESIMS 276.1492, C₁₈H₁₈N₃ [M + H]⁺, requires 276.1496, error 1.3 ppm.

2.14. 4-(4-Phenyl-1*H*-imidazol-2-yl)benzonitrile **203**

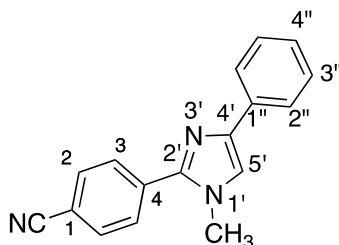


Phenylglyoxal monohydrate **202** (2.31 g, 15.2 mmol) was dissolved in methanol (30.0 ml) and was added dropwise to a suspension of 4-cyanobenzaldehyde **122** (2.0 g, 15.2 mmol) and ammonium acetate (14.50 g, 76.0 mmol) in methanol (30.0 ml). The reaction mixture was stirred at room temperature for 3 days and was monitored by TLC (20 % EtOAc/ hexane). The reaction mixture was concentrated, kept in the fridge overnight and the precipitate was filtered off under vacuum and rinsed with hexane. Compound **203** was re-crystallized from ethanol to give 2.25 g (66.8 %) of yellow-orange-coloured precipitate: mp 126-129 °C; IR (cm⁻¹): 3500 (NH), 3039, 2228 (CN), 1591, 1495, 1182, 851, 759, 697; ¹H NMR (300 MHz; DMSO-d₆ + D₂O): 7.25 (1H, t, *J* = 7.2 Hz, CH, H-4''), 7.41 (2H, t, *J* = 7.8 Hz, 2 x CH, H-3''), 7.84-7.94 (5H, m, 5 x CH

Chapter III. Experimental/ Chemistry

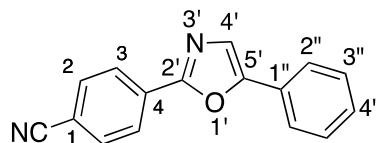
including H-5'), 8.17 (2H, d, $J = 8.4$ Hz, 2 x CH); +ESIMS m/z (relative intensity): 246.5 (100 %, $[M + H]^+$); found by +ESIMS 246.1023, $C_{16}H_{12}N_3$ $[M + H]^+$, requires 246.1026, error 1.1 pm.

2.15. 4-(1-Methyl-4-phenyl-1H-imidazol-2-yl)benzonitrile 205A



Ground potassium hydroxide (1.20 g, 20.5 mmol) was added to a solution of 4-(4-phenyl-1H-imidazol-2-yl)benzonitrile **203** (1.0 g, 4.1 mmol) in acetone (50.0 ml) and stirred at room temperature for a few minutes. Iodomethane (0.64 g, 4.5 mmol) was added and the reaction mixture was stirred vigorously for 30 m and monitored by TLC (20 % EtOAc/ Hex). The reaction was quenched with water and diluted with ethyl acetate, washed with brine, dried over dry $MgSO_4$ and evaporated to give 0.81 g (80.2 %) of a yellow-orange-coloured solid: mp 142-143 °C; IR (cm^{-1}): 2225 (CN), 1606, 1485, 947, 839, 755, 600; 1H NMR (300 MHz; DMSO- d_6): 3.86 (3H, s, NCH_3), 7.23 (1H, t, $J = 7.2$ Hz, CH, H-4''), 7.39 (2H, t, $J = 7.8$ Hz, 2 x CH, H-3''), 7.81 (2H, d, $J = 7.2$ Hz, 2 x CH, H-2''), 7.86 (1H, s, CH, H-5'), 7.97 (2H, d, $J = 8.7$ Hz, 2 x CH), 8.00 (2H, d, $J = 8.7$ Hz, 2 x CH); +ESIMS m/z (relative intensity): 260.4 (100%, $[M + H]^+$); found by +ESIMS 260.1180, $C_{17}H_{14}N_3$ $[M + H]^+$, requires 260.1182, error 0.9 ppm.

2.16.1. 4-(5-Phenylloxazol-2-yl)benzonitrile 211

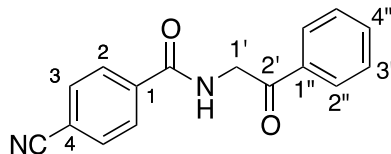


To a solution of 4-cyano-*N*-(2-oxo-2-phenylethyl)benzamide **209** (1.00 g, 3.8 mmol) in acetic anhydride (25.0 ml) was added concentrated sulfuric acid (8 drops) and the reaction mixture was stirred at room temperature for 10 m. The white precipitate was filtered off and rinsed with hexane to give 0.80 g (85.1 %): mp 174-176 °C (Lit. mp 173-175 °C)¹⁶⁰; IR (cm^{-1}): 2227 (CN), 1642, 1163, 1017, 842, 770, 689; 1H NMR (300 MHz; DMSO- d_6): 7.43 (1H, t, $J = 7.5$ Hz, CH, H-4''), 7.53 (2H, t, $J = 7.5$ Hz, 2 x CH, H-3''), 7.90 (2H, d, $J = 7.2$ Hz, 2 x CH, H-2''), 7.97 (1H, s, CH, H-4'), 8.04 (2H, d, $J =$

Chapter III. Experimental/ Chemistry

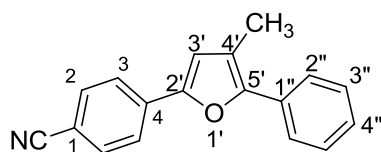
8.7 Hz, 2 x *CH*), 8.26 (2H, 8.4, $J = 8.4$ Hz, 2 x *CH*); +ESIMS m/z (relative intensity): 247 (100 %, $[M + H]^+$).

2.16.2. 4-Cyano-*N*-(2-oxo-2-phenylethyl)benzamide **209**



Saturated sodium bicarbonate solution (25.0 ml) and dichloromethane (10.5 ml) were stirred vigorously and cooled to 0 °C. 4-Cyanobenzoyl chloride **207** (1.0 g, 6.0 mmol) and 2-amino-1-phenylethanone hydrochloride **208** (0.69 g, 4.0 mmol) were added and the reaction mixture was stirred at room temperature for 2 h. The organic layer was extracted, dried over dry $MgSO_4$ and evaporated. Compound **209** was re-crystallized from DMF/ H_2O to give white solid 1.40 g (88.0 %): mp 169-173 °C; IR (cm^{-1}): 3361 (*NH*), 2227 (*CN*), 1680 (*C=O*), 1643 (*NHC=O*), 1524, 1487, 1360, 1222, 859, 680, 597; 1H NMR (300 MHz; $DMSO-d_6$): 4.83 (2H, d, $J = 5.7$ Hz, CH_2 , H-1'), 7.58 (2H, t, $J = 7.8$ Hz, 2 x *CH*, H-3''), 7.70 (1H, t, $J = 7.2$ Hz, *CH*, H-4''), 7.99-8.08 (6H, m, 6 x *CH*), 9.16 (1H, t, $J = 5.7$ Hz, *NH*); +ESIMS m/z (relative intensity): 288 (100 %, $[M + Na]^+$).

2.17. 4-(Methyl-5-phenylfuran-2-yl)benzonitrile **224**

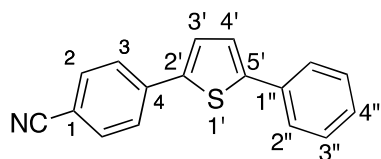


Diethylamine (0.52 g, 7.1 mmol) in dry THF (5 ml) was added dropwise to a solution of ethyl magnesium bromide (1.0 M in THF, 7.1 mmol) at 0 °C. The reaction was allowed to warm to 35 °C and stirred at that temperature for 1 h. The reaction mixture was cooled to 0 °C and a solution of 4-acetylbenzonitrile **120** (1.0 g, 7.1 mmol) and 2-bromopropiophenone **221** (0.7 ml, 4.7 mmol) in THF (5 ml) was added. The reaction was kept at 0 °C for 1 h then stirred at room temperature for 24 h and monitored by TLC (20 % EtOAc/ hexane). The reaction mixture was quenched with cold 5% v/v aqueous sulfuric acid solution, extracted with ethyl acetate, dried over dry $MgSO_4$ and evaporated. Compound **224** was purified from the crude by column chromatography using ethyl acetate-hexane (2:8) as a mobile phase. Compound **224** was re-crystallized from methanol to give 0.41 g (33.6 %) of a yellow solid: mp 149-

Chapter III. Experimental/ Chemistry

153 °C; IR (cm⁻¹): 2224 (CN), 1607, 1491, 1141, 840, 760, 702; ¹H NMR (300 MHz; DMSO-d₆): 2.54 (3H, s, CH₃), 7.33 (1H, t, *J* = 7.3 Hz, CH, H-4''), 7.46 (2H, t, *J* = 7.8 Hz, 2 x CH, H-3''), 7.52 (3H, d, 3 x CH, H-3, H-2''), 7.88 (4H, s, 4 x CH, H-2, H-3); ¹³C NMR (100 MHz; CDCl₃): 13.3 (CH₃), 109.7 (CH, H-3'), 109.8 (C, C-4'), 119.1 (C, CN), 123.5 (CH), 123.9 (C), 126.9 (CH), 127.5 (CH), 128.8 (CH), 132.6 (CH), 133.3 (C), 134.6 (C), 149.6 (C), 149.7 (C).

2.18. 4-(5-Phenylthiophen-2-yl)benzonitrile **228**



Lawesson's reagent (0.77 g, 1.9 mmol) was added portionwise to a solution of 1-(4-cyanophenyl)-4-phenyl-1,4-butadione **126** (0.25 g, 1.0 mmol) in tetrahydrofuran (10.0 ml). The reaction mixture was heated at 50 °C for 2 days and was monitored by TLC (20 % EtOAc/Hex). The crude product was purified by column chromatography using EtOAc-Hex (1:9) as a mobile phase to give 0.14 g (56.0 %) as a yellow solid: mp 165-166 °C; IR (cm⁻¹): 2225 (CN), 1600, 1453, 839, 803, 755, 688, 576; ¹H NMR (300 MHz; DMSO-d₆): 7.37 (1H, t, *J* = 7.5 Hz, CH, H-4''), 7.47 (2H, t, *J* = 8.1 Hz, 2 x CH, H-3''), 7.64 (1H, d, *J* = 3.9 Hz, thiophene-CH), 7.73 (2H, d, *J* = 7.5 Hz, 2 x CH, H-2''), 7.79 (1H, d, *J* = 3.9 Hz, thiophene-CH), 7.90 (4H, s, 4 x CH, H-2, H-3); ¹³C NMR (100 MHz; DMSO-d₆) (assignments made using DEPT-135): 109.6 (C, C-4), 118.8 (C, CN), 125.38 (CH), 125.4 (CH), 125.6 (CH), 127.6 (CH), 128.3 (CH), 129.2 (CH), 133.0 (C), 133.1 (CH), 137.8 (C), 140.2 (C), 144.9 (C); +APCIMS *m/z* (relative intensity): 262 (100 %, [M + H]⁺).

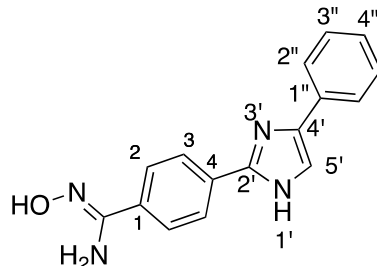
2.19. General procedure for the synthesis of *N*-hydroxy amidines (amidoximes) **204**, **206**, **212**, **225**, **233** and **240**

Hydroxylamine hydrochloride (10.0 mmol) was suspended in dry DMSO and the mixture was cooled to 0 °C. Potassium *tert*-butoxide (10.0 mmol) was added portionwise to the reaction mixture under an argon atmosphere and the reaction mixture was stirred at room temperature for 1 h. Diarylimidazole- **203**, diaryl *N*-methylimidazole- **205A**, diaryloxazole- **211**, diarylthiophene- **228** or diarylfuran-nitrile-

Chapter III. Experimental/ Chemistry

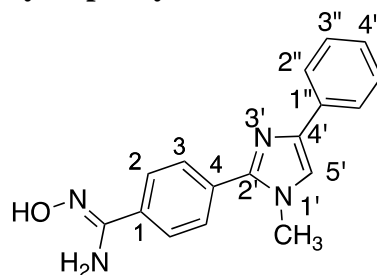
127 (1.0 mmol) was added and the reaction mixture was stirred at room temperature for 1-3 days and monitored by TLC (10.0 % MeOH/ CHCl₃).

2.19.1. *N*-Hydroxy-4-(4-phenyl-1*H*-imidazol-2-yl)benzamidine **204**



The reaction mixture was poured into iced water and the yellow precipitate was filtered off under vacuum, rinsed with hexane and re-crystallized from ethanol to give 0.37 g (66.1 %) of yellow-coloured solid: mp 150-151 °C (decomposed); IR (cm⁻¹): 3179, 3114, 2798, 1637, 1386, 1022, 939, 846, 804; ¹H NMR (300 MHz; DMSO-d₆): 5.87 (2H, s, NH₂), 7.22 (1H, t, *J* = 7.2 Hz, CH, H-4''), 7.38 (2H, t, *J* = 7.2 Hz, 2 x CH, H-3''), 7.77-7.80 (3H, m, 3 x CH, H-5', H-2''), 7.88 (2H, d, *J* = 7.8 Hz, 2 x CH), 8.00 (2H, d, *J* = 7.8 Hz, 2 x CH), 9.72 (1H, s, NOH); ¹³C NMR (100 MHz; DMSO-d₆) (assignments made using DEPT-135): 114.4 (CH), 124.4 (CH), 124.5 (CH), 125.7 (CH), 126.3 (CH), 128.5 (CH), 130.7 (C), 132.6 (C), 134.4 (C), 141.2 (C), 145.3 (C), 150.3 (C, C-amidoxime); +ESIMS *m/z* (relative intensity): 279.6 (100 %, [M + H]⁺); found by +ESIMS 279.0952, C₁₇H₁₅N₂S [M + H]⁺, requires 279.0950, error 0.6 ppm.

2.19.2. *N*-Hydroxy-4-(1-methyl-4-phenyl-1*H*-imidazol-2-yl)benzamidine **206**

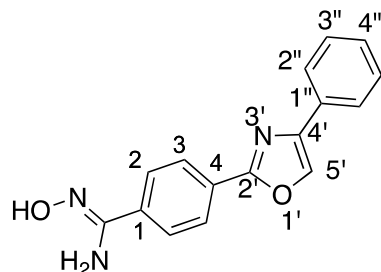


The reaction mixture was poured into iced water and the white precipitate was filtered off under vacuum, rinsed with hexane and re-crystallized from ethanol to give 0.40 g (71.4 %) of **206**: mp 186-189 °C; IR (cm⁻¹): 3502 (*N*-H), 3384 (*N*-H), 3060, 2928, 1664, 1456, 1391, 940, 852, 754, 691; ¹H NMR (300 MHz; DMSO-d₆): 3.82 (3H, s, NCH₃), 5.91 (2H, s, *N*-H₂), 7.21 (1H, t, *J* = 7.2 Hz, CH, H-4''), 7.38 (2H, t, *J* = 7.5 Hz, 2 x CH, H-3''), 7.77-7.83 (7H, m, 7 x CH, H-2, H-3, H-5', H-2''), 9.76 (1H, s, NOH); ¹³C NMR (75 MHz; DMSO-d₆): 33.7 (CH₃), 124.8, 126.0, 127.3, 127.7, 128.5,

Chapter III. Experimental/ Chemistry

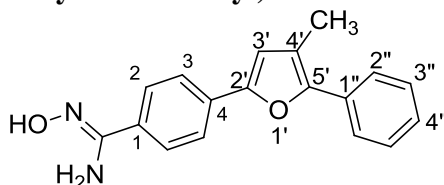
129.4, 130.7, 132.9, 134.1, 139.5, 146.4, 150.3 (C, C-amidoxime); +ESIMS m/z (relative intensity): 293.4 (100%, $[M + H]^+$); found by +ESIMS 293.1405, $C_{17}H_{17}N_4O$ $[M + H]^+$, requires 293.1397, error 2.8 ppm.

2.19.3. *N*-Hydroxy-4-(4-phenyloxazol-2-yl)benzamidine **212**



The reaction mixture was poured into iced water and the precipitate was filtered off under vacuum, rinsed with hexane, added to boiling ethanol and filtered while it was hot to give 0.45 g (53.6 %) of **212**: mp 196-198 °C; IR (cm^{-1}): 3368 (*N*-H and OH), 3165, 1621, 1412, 1400, 1139, 855, 790, 753, 676, 601; 1H NMR (300 MHz; DMSO- d_6): 5.95 (2H, s, NH_2), 7.40 (1H, t, $J = 7.2$ Hz, CH, H-4''), 7.51 (2H, t, $J = 7.8$ Hz, 2 x CH, H-3''), 7.85-7.89 (5H, m, 5 x CH including H-5'), 8.09 (2H, d, $J = 8.4$ Hz, 2 x CH), 9.87 (1H, s, *N*-OH).

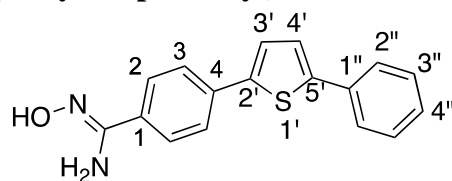
2.19.4. *N*-Hydroxy-4-(4-methyl-5-furan-2-yl)benzamidine **225**



The reaction mixture was poured into iced water and the precipitate was filtered off under vacuum, rinsed with hexane and re-crystallized from ethanol to give 0.16 g (42.1 %) of **225**: mp 163-166 °C; IR (cm^{-1}): 3448 (*N*-H), 3357 (*N*-H), 3326, 1644, 1388, 1117, 1062, 926, 761, 670; 1H NMR (300 MHz; DMSO- d_6): 2.52 (3H, s, CH_3), 5.89 (2H, s, NH_2), 7.28 (1H, s, CH, H-3'), 7.31 (1H, t, $J = 7.2$ Hz, CH, H-4''), 7.45 (2H, t, $J = 8.1$ Hz, 2 x CH, H-3''), 7.52 (2H, d, $J = 6.9$ Hz, 2 x CH, H-2''), 7.70 (2H, d, $J = 9.0$ Hz, 2 x CH), 7.74 (2H, d, $J = 9.0$ Hz, 2 x CH), 9.71 (1H, s, *N*-OH); ^{13}C NMR (75 MHz; DMSO- d_6): 13.2 (CH_3), 108.0 (CH), 122.6 (CH), 125.2 (C), 125.8 (CH), 126.4 (CH), 127.0 (CH), 128.7 (CH), 130.4 (C), 131.8 (C), 133.1 (C), 147.6(C), 150.4 (C), one quaternary carbon has not been observed; +ESIMS m/z (relative intensity): 293.2 (100%, $[M + H]^+$); found by +ESIMS 293.1277, $C_{18}H_{17}N_2O_2$ $[M + H]^+$, requires 293.1290, error 4.4 ppm.

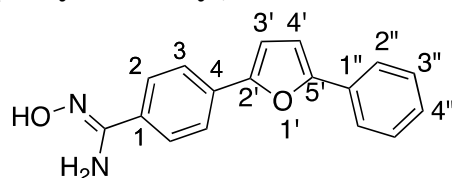
Chapter III. Experimental/ Chemistry

2.19.5. *N*-Hydroxy-4-(5-phenylthiophen-2-yl)benzamidine **233**



The reaction mixture was poured into iced water and the precipitate was filtered off under vacuum, rinsed with hexane, added to boiling ethanol and filtered while it was hot to give 0.37 g (78.7 %) of white precipitate of **233**: mp 217-219 °C (decomposed); IR (cm⁻¹): 3438 (*N*-H), 3348 (*N*-H), 3060, 1655, 1592, 1393, 938, 837, 735; ¹H NMR (300 MHz; DMSO-d₆): 5.87 (2H, s, *N*-H₂), 7.33 (1H, t, *J* = 7.2 Hz, *CH*, H-4''), 7.45 (2H, t, *J* = 7.5 Hz, 2 x *CH*, H-3''), 7.57 (1H, d, *J* = 3.6 Hz, thiophene-*CH*), 7.61 (1H, d, *J* = 3.3 Hz, thiophene-*CH*), 7.70-7.76 (6H, m, 6 x *CH*, H-2, H-3, H-2''), 9.72 (1H, s, *NOH*), ¹³C NMR (100 MHz; DMSO-d₆) (assignments made using DEPT-135): 124.8 (CH), 125.1 (CH), 125.2 (CH), 125.3 (CH), 126.0 (CH), 127.8 (CH), 129.2 (CH), 132.4 (C), 133.4 (C), 133.8 (C), 142.0 (C), 142.8 (C), 150.3 (C); +ESIMS *m/z* (relative intensity): 279 (100 %, [M + H]⁺); found by +ESIMS 295.0900, C₁₇H₁₅N₂OS [M + H]⁺, requires 295.0900, error 0.1 ppm.

2.19.6. *N*-Hydroxy-4-(5-phenylfuran-2-yl)benzamidine **240**



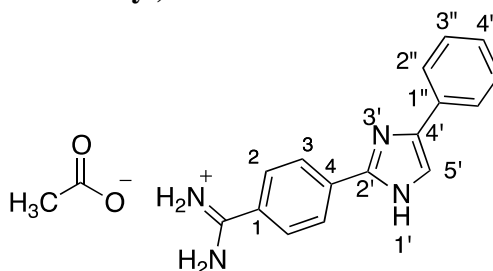
The reaction mixture was poured into iced water and compound **240** was extracted with dichloromethane, washed with water, dried over MgSO₄ and evaporated to give 0.02 g (87.0 %) of **240** as a yellow solid: mp 179-181 °C (decomposed); IR (cm⁻¹): 3492(*N*-H), 33548 (*N*-H), 2362, 1664, 1388, 1022, 927, 791, 754, 680, 670; ¹H NMR (300 MHz; DMSO-d₆): 5.85 (2H, s, *N*-H₂), 7.11 (2H, d, *J* = 6.6 Hz, 2 x *CH*, H-3', H-4'), 7.31 (1H, t, *J* = 6.9 Hz, *CH*, H-4''), 7.45 (2H, t, *J* = 7.2 Hz, 2 x *CH*, H-3''), 7.74-7.82 (6H, m, 6 x *CH*, H-2, H-3, H-2''), 9.69 (1H, s, *NOH*), ¹³C NMR (100 MHz; DMSO-d₆) (assignments made using DEPT-135): 108.3 (CH), 108.8 (CH), 123.1 (CH), 123.5 (CH), 125.8 (CH), 127.7 (CH), 129.0 (CH), 129.9 (C), 130.3 (C), 132.0 (C), 150.3 (C), 152.2 (C), 152.8 (C); -ESIMS *m/z* (relative intensity): 277 (100 %, [M - H]⁻); +ESIMS *m/z* (relative intensity): 279 (100 %, [M + H]⁺); found by +ESIMS 279.1129, C₁₇H₁₅O₂N₂ [M + H]⁺, requires 279.1128, error 0.3 ppm.

Chapter III. Experimental/ Chemistry

2.20. General procedure for the synthesis of amidines **193-195** and **223**

Ammonium formate (5.0 mmol) and Pd/C (10.0 % g/ml) were added slowly to a solution of the amidoxime (1.0 mmol) in glacial acetic acid. The reaction mixture was heated at reflux and monitored with TLC (1.0 % MeOH/ CHCl₃). Upon the consumption of the starting amidoxime, the reaction mixture was cooled to room temperature, filtered through Celite 521 and rinsed with glacial acetic acid. The reaction mixture was quenched with 1.0 M NaOH until pH became around 7 and stirred at room temperature for 1 h.

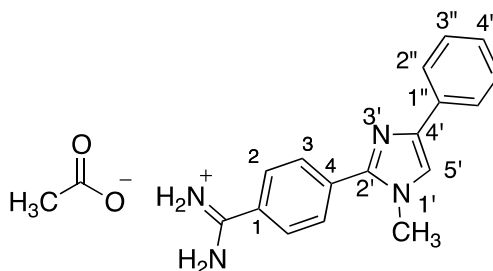
2.20.1. 4-(Phenyl-1*H*-imidazol-2-yl)benzamidinium acetate **193**



The precipitate was filtered off under vacuum, rinsed with H₂O and re-crystallized from ethanol to give 0.18 g (27.7 %) of **193** as an orange solid: mp 228-231 °C; IR (cm⁻¹): 2920, 1557, 1409, 1157, 823, 740; ¹H NMR (300 MHz; DMSO-d₆): 1.72 (3H, s, CH₃), 7.24 (1H, t, *J* = 7.5 Hz, CH, H-4''), 7.40 (2H, t, *J* = 7.5 Hz, 2 x CH, H-3''), 7.81 (1H, s, CH, H-5'), 7.87-7.92 (4H, m, 4 x CH), 8.20 (2H, d, *J* = 8.4 Hz, 2 x CH), 8.32 (1H, s, *N*-H); ¹³C NMR (100 MHz; DMSO-d₆) (assignments made using DEPT-135): 24.7 (CH₃), 124.5 (CH), 124.8 (CH), 126.5 (CH), 128.1 (CH), 128.46 (C), 128.5 (CH), 134.6 (C), 144.8 (C), 165.4 (C, C-amidinium), 176 (C=O), two quaternary carbons have not been observed and one CH carbon is overlapping; +ESIMS *m/z* (relative intensity): 263.4 (100 %, [M + H]⁺); found by +ESIMS 263.1293, C₁₆H₁₅N₄ [M + H]⁺, requires 263.1291, error 0.7 ppm.

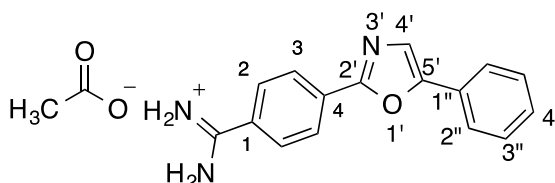
Chapter III. Experimental/ Chemistry

2.20.2. 4-(1-Methyl-4-phenyl-1*H*-imidazol-2-yl)benzamidinium acetate **194**



The precipitate was filtered off under vacuum, rinsed with H₂O and re-crystallized from ethanol to give 0.21 g (21.0 %) of creamy solid; IR (cm⁻¹): 3179, 2965, 1690, 1606, 1556, 1511, 1483, 1108, 753, 640; ¹H NMR (300 MHz; DMSO-d₆): 1.70 (3H, s, OCOCH₃), 3.85 (3H, s, NCH₃), 7.23 (1H, t, *J* = 7.5 Hz, CH, H-4''), 7.38 (2H, t, *J* = 7.8 Hz, 2 x CH, H-3''), 7.81 (2H, d, *J* = 7.2 Hz, 2 x CH, H-2''), 7.84 (1H, s, CH, H-5'), 7.92 (2H, d, *J* = 8.4 Hz, 2 x CH), 7.97 (2H, d, *J* = 9.3 Hz, 2 x CH); ¹³C NMR (75 MHz; DMSO-d₆) (assignments made using DEPT-135): 24.7 (OCOCH₃), 35.3 (NCH₃), 120.8 (CH), 124.2 (CH), 126.5 (CH), 127.8 (CH), 128.2 (CH), 128.6 (CH), 134.1 (C), 134.3 (C), 139.8 (C), 145.5 (C), 165.2 (C, C-amidinium), 175.7 (C, C=O); +ESIMS *m/z* (relative intensity): 277.4 (100 %, [M + H]⁺); found by +ESIMS 277.1449, C₁₇H₁₇N₄ [M + H]⁺, requires 277.1453, error 1.5 ppm.

2.20.3. 4-(4-Phenyloxazol-2-yl)benzamidinium acetate **195**

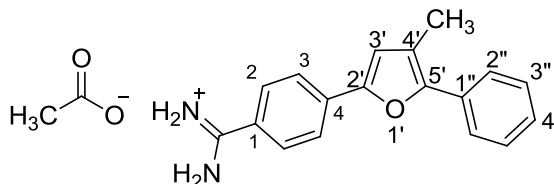


The grey-coloured precipitate was filtered off under vacuum, rinsed with H₂O and re-crystallized from ethanol to give 0.06 g (23.6 %) of **195**: mp 240-243 °C; IR (cm⁻¹): 2921, 1556, 1486, 1409, 848, 766, 707, 688; ¹H NMR (300 MHz; DMSO-d₆): 1.76 (3H, s, CH₃), 7.42 (1H, t, *J* = 7.2 Hz, CH, H-4''), 7.53 (2H, t, *J* = 7.8 Hz, 2 x CH, H-3''), 7.90 (2H, d, *J* = 7.5 Hz, 2 x CH, H-2''), 7.93 (1H, s, CH, H-4'), 7.97 (2H, d, *J* = 8.4 Hz, 2 x CH), 8.22 (2H, d, *J* = 8.4 Hz, 2 x CH); ¹³C NMR (75 MHz; DMSO-d₆) (assignments made using DEPT-135): 23.7 (CH₃), 123.8 (C), 124.2 (CH), 124.7 (CH), 125.1 (C), 126.1 (CH), 127.1 (C), 128.0 (C), 128.4 (CH), 128.8 (CH), 130.0 (CH), 159.2 (C), 164.7 (C, C-amidinium), C=O was not observed; +ESIMS *m/z* (relative intensity): 264.5

Chapter III. Experimental/ Chemistry

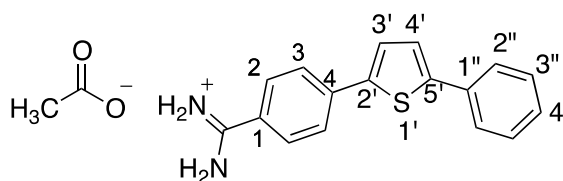
(100 %, $[M + H]^+$); found by +ESIMS 264.1147, $C_{16}H_{14}ON_3$ $[M + H]^+$, requires 264.1137, error 3.8 ppm.

2.20.4. 4-(4-Methyl-5-phenylfuran-2-yl)benzamidinium acetate 223



The precipitate was filtered off under vacuum, rinsed with H_2O and recrystallized from EtOH to give 0.1 g (21%): mp 224 °C (decomposed); IR (cm^{-1}): 3354 (*N*-H), 3205, 1571, 1415, 932, 844, 761, 697; NMR (300 MHz; DMSO- d_6): 1.68 (3H, s CH_3 of acetate), 2.54 (3H, s, CH_3), 7.32 (1H, t, $J = 7.2$ Hz, *CH*, H-4''), 7.43-7.54 (5H, m, 5 x *CH*, H-3', H-2'', H-3''), 7.86 (4H, s, 4 x *CH*, H-2, H-3); +ESIMS m/z (relative intensity): 277.0 (100 %, $[M + H]^+$).

2.21. 4-(5-Phenylthiophen-2-yl)benzamidinium acetate 226

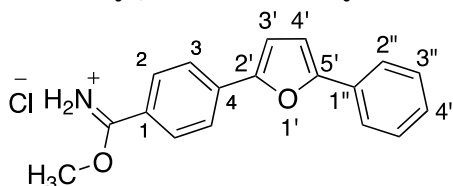


N-Hydroxy-4-(5-phenylthiophen-2-yl)benzamidinium 233 (0.11 g, 0.4 mmol) was dissolved in glacial acetic acid (2.0 ml) and acetic anhydride (0.04 g, 0.4 mmol) and the reaction mixture was stirred at room temperature for 30 m. Triethylsilane (0.06 g, 0.5 mmol) and $PdCl_2$ (10.0 %) were added and the reaction mixture was refluxed for 12 h and monitored by TLC (1.0 MeOH/ $CHCl_3$). Upon the consumption of the starting amidoxime, the reaction was cooled to room temperature, filtered through Celite 521 and neutralized with saturated sodium bicarbonate solution. The precipitate was filtered off under vacuum, rinsed with acetone, added to boiling ethanol and filtered while it was hot to give 0.06 g (42.6 %): mp > 300 °C; IR (cm^{-1}): 2973, 1487, 1409, 1077, 1012, 808, 750, 691, 670; 1H NMR (300 MHz; DMSO- d_6): 1.60 (3H, s, CH_3), 7.35 (1H, t, $J = 7.2$ Hz, *CH*, H-4''), 7.46 (2H, t, $J = 7.5$ Hz, 2 x *CH*, H-3''), 7.60 (1H, d, $J = 3.9$ Hz, thiophene-*CH*), 7.68 (1H, d, $J = 3.9$ Hz, thiophene-*CH*), 7.72 (2H, d, $J = 7.2$ Hz, 2 x *CH*, H-2''), 7.78 (2H, d, $J = 8.1$ Hz, 2 x *CH*), 7.85 (2H, d, $J = 7.2$ Hz, 2 x *CH*); ^{13}C NMR (100 MHz; DMSO- d_6) (assignments made using DEPT-135): 25.9 (CH_3), 125.3

Chapter III. Experimental/ Chemistry

(CH), 125.7 (CH), 125.8 (CH), 126.7 (CH), 128.3 (CH), 128.5 (CH), 129.7 (CH), 133.8 (C), 136.5 (C), 141.8 (C), 144.1 (C), 175.3 (C), C-amidine and another quaternary carbon have not been observed; +ESIMS m/z (relative intensity): 279.3 (100 %, $[M + H]^+$); found by +ESIMS 279.0952, $C_{17}H_{15}N_2S$ $[M + H]^+$, requires 279.0950, error 0.6 ppm.

2.22. Methyl 4-(5-phenylfuran-2-yl)benzimidate hydrochloride **234**



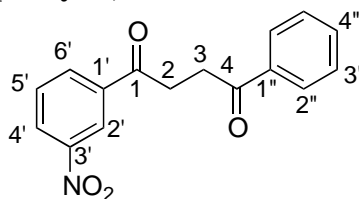
Ammonium chloride (0.04 g, 0.8 mmol) was added to a solution of ethyl 4-(5-phenylfuran-2-yl)benzimidate hydrochloride **143** (0.20 g, 0.7 mmol) in methanol (15.0 ml) and water (2.0 ml). The reaction mixture was heated at reflux for 3 h. The yellow precipitate was filtered off and rinsed with hexane: 1H NMR (DMSO- d_6): 3.90 (3H, s, CH_3), 7.16 (1H, d, $J = 3.6$ Hz, furan- CH), 7.31 (1H, d, $J = 3.6$ Hz, furan- CH), 7.36 (1H, t, $J = 7.2$ Hz, CH , H-4''), 7.48 (2H, t, $J = 7.8$ Hz, 2 x CH , H-3''), 7.86 (2H, d, $J = 7.5$ Hz, 2 x CH , H-2''), 7.96 (2H, d, $J = 8.1$ Hz, 2 x CH), 8.03 (2H, d, $J = 8.4$ Hz, 2 x CH); ^{13}C NMR (75 MHz; DMSO- d_6) (assignments made using DEPT-135): 52.1 (CH_3), 107.5 (CH), 109.6 (CH), 123.3 (CH), 124.0 (CH), 127.8 (CH), 128.4 (C), 128.8 (CH), 130.2 (CH), 130.4 (C), 134.7 (C), 152.2 (C), 154.5 (C), 166.8 (C, C-imidate).

2.23. General procedure for the synthesis of the aryl 1,4-diketones **241** and **242**

Triethylamine (1.5 mmol) was added to a suspension of zinc chloride (2.0 mmol) in dry toluene and absolute ethanol (1.5 mmol). The reaction mixture was stirred at room temperature for 1-2 h. Methyl aryl ketone (1.5 mmol) and α -bromomethyl aryl ketone (1.0 mmol) were added and the mixture was stirred at room temperature for 3-7 days and monitored by TLC (20.0 % EtOAc/ hexane). The workup was as described for each 1,4-diketone.

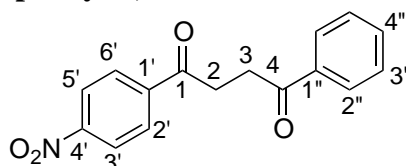
Chapter III. Experimental/ Chemistry

2.23.1. 1-(3-Nitrophenyl)-4-phenyl-1,4-butandione **241**



The reaction was quenched by the addition of 10.0 % (v/v) aqueous sulfuric acid solution. The organic layer was washed with brine, dried over MgSO_4 and concentrated. Compound **241** was crystallized from methanol to give 0.87 g (61.3 %) of colourless crystals: mp 93-94 °C (Lit mp 92 °C)¹¹²; IR (cm^{-1}): 1676 (C=O), 1527 (NO_2), 1310 (NO_2), 1191, 756, 730, 692; ^1H NMR (300 MHz; CDCl_3): 3.49-3.55 (4H, m, $2 \times \text{CH}_2$, H-2, H-3), 7.51 (2H, t, $J = 7.5$ Hz, $2 \times \text{CH}$, H-3''), 7.62 (2H, t, $J = 7.5$ Hz, CH, H-4''), 7.72 (1H, t, $J = 8.1$ Hz, CH, H-5'), 8.06 (2H, d, $J = 7.5$ Hz, $2 \times \text{CH}$, H-2''), 8.39 (1H, d, $J = 7.8$ Hz, CH, H-6'), 8.47 (1H, d, $J = 8.1$ Hz, CH, H-4'), 8.90 (1H, s, CH, H-2'); ^{13}C NMR (100 MHz; CDCl_3) (assignments made using DEPT-135): 32.6 (CH_2 , C-3), 32.7 (CH_2 , C-2), 123.1 (CH), 127.5 (CH), 128.2 (CH), 128.7 (CH), 129.9 (CH), 133.4 (CH), 133.7 (CH), 136.5 (C, C-1''), 138.1 (C, C-1'), 196.7 (C=O), 198.2 (C=O), C-3' (C) was not observed in the ^{13}C NMR spectrum; +ESIMS m/z 306 (100%, $[\text{M} + \text{Na}]^+$).

2.23.2. 1-(4-Nitrophenyl)-4-phenyl-1,4-butandione **242**



The reaction was quenched by the addition of 10.0 % (v/v) aqueous sulfuric acid solution. The organic layer was washed with brine, dried over MgSO_4 and concentrated. Compound **242** was crystallized from methanol to give 0.44 g (31.0 %) of light orange crystals: mp 145-146 °C (Lit mp 140-142 °C)¹¹²; IR (cm^{-1}): 1670 (C=O), 1515 (NO_2), 1318 (NO_2), 701; ^1H NMR (300 MHz; CDCl_3): 3.48-3.54 (4H, m, $2 \times \text{CH}_2$, H-2, H-3), 7.51 (2H, t, $J = 7.5$ Hz, $2 \times \text{CH}$, H-3''), 7.62 (1H, t, $J = 7.5$ Hz, CH, H-4''), 8.05 (2H, d, $J = 7.5$ Hz, $2 \times \text{CH}$, H-2''), 8.21 (2H, d, $J = 8.7$ Hz, $2 \times \text{CH}$, H-2'), 8.36 (2H, d, $J = 8.7$ Hz, $2 \times \text{CH}$, H-3'); ^{13}C NMR (100 MHz; CDCl_3) (assignments made using DEPT-135): 32.6 (CH_2 , C-3), 33.0 (CH_2 , C-2), 123.9 ($2 \times \text{CH}$, C-3''), 128.1 (CH, C-4''), 128.7 ($2 \times \text{CH}$, C-2''), 129.2 ($2 \times \text{CH}$, C-2'), 133.4 ($2 \times \text{CH}$, C-3'), 136.4 (C, C-1''), 141.3 (C, C-1'), 150.4 (C, C-4'), 197.4 (C=O), 198.2 (C=O); +ESIMS m/z 306 (100%, $[\text{M} + \text{Na}]^+$).

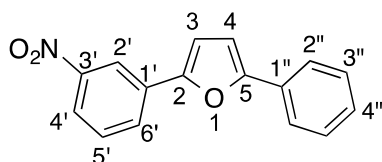
Chapter III. Experimental/ Chemistry

284 (70%, $[M + H]^+$); found by +ESIMS 284.0917, $C_{16}H_{14}O_4N$ $[M + H]^+$, requires 284.0917, error 0.1 ppm.

2.24. General procedure for the synthesis of 2,5-diarylfurans **243** and **244**

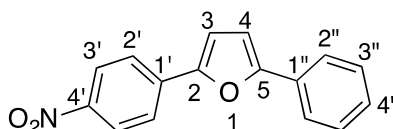
Acetyl chloride (8.0 mmol) was added dropwise to a solution of 1,4-diarylfurans **241** or **242** (1.0 mmol) in chloroform and ethanol (12.0 mmol) at 0 °C. The reaction was stirred at room temperature for 1 day and monitored by TLC (20 % EtOAc/ hexane).

2.24.1. 2-(3-Nitrophenyl)-5-phenylfuran **243**



The reaction mixture was cooled to 0 °C and saturated sodium bicarbonate solution was added dropwise until the gas evolution ceased. The organic layer was extracted, washed with water, dried over $MgSO_4$ and evaporated to give 0.79 g (87.8 %) of an orange solid: mp 111-113 °C; IR (cm^{-1}): 1590, 1501 (NO_2), 1327 (NO_2), 844, 794, 688; 1H NMR (300 MHz; $CDCl_3$): 6.81 (1H, d, $J = 3.3$ Hz, CH, H-4), 6.92 (1H, d, $J = 3.3$ Hz, CH, H-3), 7.34 (1H, t, $J = 7.5$ Hz, CH, H-4''), 7.46 (2H, t, $J = 7.5$ Hz, 2 x CH, H-3''), 7.59 (1H, t, $J = 8.1$ Hz, CH, H-5'), 7.79 (2H, d, $J = 7.8$ Hz, 2 x CH, H-2''), 8.05 (1H, d, $J = 7.8$ Hz, CH, H-6'), 8.12 (1H, d, $J = 8.4$ Hz, CH, H-4'), 8.57 (1H, s, CH, H-2'); ^{13}C NMR (100 MHz; $CDCl_3$) (assignments made using DEPT-135): 107.5 (CH, C-4'), 109.6 (CH, C-3'), 118.3 (CH), 121.6 (CH), 124.0 (CH), 128.0 (CH), 128.8 (CH), 129.1 (CH), 129.8 (CH), 130.1 (C), 132.3 (C), 148.8 (C), 150.8 (C), 154.7 (C); +ESIMS m/z 288 (100%, $[M + Na]^+$).

2.24.2. 2-(4-Nitrophenyl)-5-phenylfuran **244**



The reaction mixture was cooled to 0 °C and saturated sodium bicarbonate solution was added dropwise until the gas evolution ceased. The organic layer was extracted, washed with water, dried over $MgSO_4$ and evaporated to give 0.70 g (88.6 %)

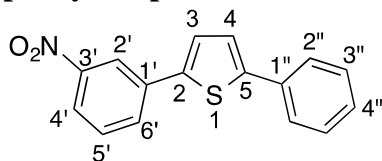
Chapter III. Experimental/ Chemistry

of an orange solid: mp 136-138 °C (Lit mp 132 °C)¹⁶¹; IR (cm⁻¹): 1590, 1501 (NO₂), 1327 (NO₂), 844, 794, 688; ¹H NMR (300 MHz; CDCl₃): 6.84 (1H, d, *J* = 3.6 Hz, CH, H-4), 7.00 (1H, d, *J* = 3.6 Hz, CH, H-3), 7.36 (1H, t, *J* = 7.5 Hz, CH, H-4''), 7.47 (2H, t, *J* = 7.8 Hz, 2 x CH, H-3''), 7.79 (2H, d, *J* = 7.5 Hz, 2 x CH, H-2''), 7.87 (2H, d, *J* = 9.0 Hz, 2 x CH, H-2'), 8.29 (2H, d, *J* = 9.0 Hz, 2 x CH, H-3'); ¹³C NMR (100 MHz; CDCl₃) (assignments made using DEPT-135): 107.9 (CH, C-4), 111.4 (CH, C-3), 123.7 (CH), 124.2 (CH), 124.4 (CH), 128.3 (CH), 128.9 (CH), 130.0 (C), 136.3 (C), 146.3 (C), 151.0 (C), 155.6 (C). The spectral data (¹H, ¹³C NMR and IR) were identical to those reported in the literature.¹⁶¹

2.25. General procedure for the synthesis of 2,5-diarylthiophenes **245** and **246**

Lawesson's reagent (1.1 mmol) was added portionwise to a solution of aryl 1,4-diketones **241** or **242** (1.0 mmol) in tetrahydrofuran. The reaction mixture was heated at 55 °C for 1-2 days and was monitored by TLC (20 % EtOAc/ hexane).

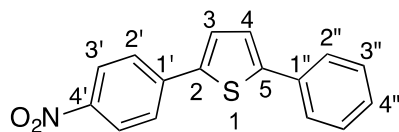
2.25.1. 2-(3-Nitrophenyl)-5-phenylthiophene **245**



The reaction mixture was concentrated, diluted with hexane and diethyl ether and the yellow precipitate was filtered off under vacuum to give 1.13 g (36.5 %) of **245**: mp °C; IR (cm⁻¹): 1516 (NO₂), 1344 (NO₂), 798, 757, 734, 687; ¹H NMR (300 MHz; CDCl₃): 7.32-7.46 (5H, m, 5 x CH, H-3, H-4, H-3'', H-4''), 7.58 (1H, t, *J* = 7.8 Hz, CH, H-5'), 7.66 (2H, d, *J* = 7.5 Hz, 2 x CH, H-2''), 7.94 (1H, d, *J* = 7.8 Hz, CH, H-6'), 8.14 (1H, d, *J* = 8.1 Hz, CH, H-4'), 8.49 (1H, s, CH, H-2'); ¹³C NMR (100 MHz; DMSO-d₆) (assignments made using DEPT-135): 119.2 (CH), 122.1 (CH), 125.3 (CH), 125.4 (CH), 127.1 (CH), 128.2 (CH), 129.2 (CH), 130.8 (CH), 131.4 (CH), 133.1 (C), 135.1 (C), 139.6 (C), 144.3 (C), 148.5 (C).

Chapter III. Experimental/ Chemistry

2.25.2. 2-(4-Nitrophenyl)-5-phenylthiophene **246**

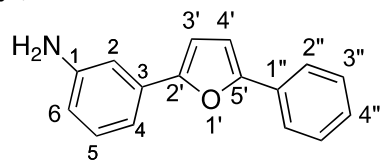


Compound **246** was purified by column chromatography using ethyl acetate/hexane (1:9) as the mobile phase to give 0.14 g (56.0 %) of **246** as a yellow solid: mp 176-178 °C; IR (cm^{-1}): 1592, 1505 (NO_2), 1335 (NO_2), 844, 804, 790, 740, 691, 564; ^1H NMR (300 MHz; DMSO-d_6): 7.37 (1H, t, $J = 7.2$ Hz, CH, H-4''), 7.47 (2H, t, $J = 7.2$ Hz, 2 x CH, H-3''), 7.66 (1H, d, $J = 3.9$ Hz, CH, H-4), 7.75 (2H, d, $J = 7.5$ Hz, 2 x CH, H-2''), 7.84 (1H, d, $J = 3.6$ Hz, CH, H-3), 7.97 (2H, d, $J = 8.4$ Hz, 2 x CH, H-2'), 8.27 (2H, d, $J = 8.4$ Hz, 2 x CH, H-3'); ^{13}C NMR (100 MHz; DMSO-d_6) (assignments made using DEPT-135): 124.6 (CH), 125.4 (CH), 125.6 (CH), 125.8 (CH), 128.3 (CH), 128.4 (CH), 129.3 (CH), 132.9 (C), 139.7 (C), 145.7 (C), 146.0 (C), one quaternary carbon was not observed in the spectrum; +ESIMS m/z (relative intensity): 304 (100 %, $[\text{M} + \text{Na}]^+$).

2.26. General procedure for the synthesis of amines **247-250**

Copper (II) sulfate (2 M solution in H_2O , 0.1 mmol) was added to a solution of a nitro-compound **243-246** (1.0 mmol) in ethanol. The reaction mixture was cooled to 0 °C and sodium borohydride (5.0 mmol) was added portionwise. The reaction mixture was stirred at room temperature for 1 h and monitored with TLC (20 % EtOAc/hexane). Upon consumption of the starting material, the reaction was diluted with ethyl acetate, washed with water, dried over MgSO_4 and evaporated.

2.26.1. 3-(5-Phenylfuran-2-yl)aniline **247**

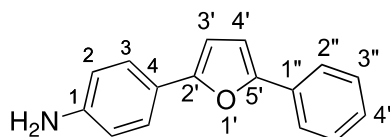


White solid 0.50 g (66.7 %): mp 139-141 °C; IR (cm^{-1}): 3455 (N-H), 3376 (N-H), 3339 (N-H), 1608, 1487, 1022, 778, 759, 690; ^1H NMR (300 MHz; DMSO-d_6): 5.19 (2H, s, NH_2), 6.52 (1H, d, $J = 7.8$ Hz, CH, H-6), 6.87 (1H, s, CH, H-2), 6.94 (1H, d, $J = 7.5$ Hz, CH, H-4), 7.02 (2H, s, 2 x CH, H-3', H-4'), 7.08 (1H, t, $J = 7.8$ Hz, CH, H-4''), 7.29 (1H, t, $J = 7.5$ Hz, CH, H-5), 7.44 (2H, t, $J = 7.8$ Hz, 2 x CH, H-3''), 7.77 (2H, d, $J = 7.8$ Hz, 2 x CH, H-2''); ^{13}C NMR (100 MHz; DMSO-d_6) (assignments made using

Chapter III. Experimental/ Chemistry

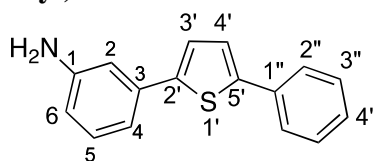
DEPT-135): 107.3 (CH), 108.0 (CH), 108.5 (CH), 111.5 (CH), 113.5 (CH), 123.2 (CH), 127.4 (CH), 128.9 (CH), 129.4 (CH), 130.2 (C), 130.5 (C), 149.0 (C), 151.9 (C), 153.4 (C); +ESIMS m/z (relative intensity): 236 (100 %, $[M + H]^+$); found by +ESIMS 236.1073, $C_{16}H_{14}ON$ $[M + H]^+$, requires 236.1070, error 1.1 ppm.

2.26.2. 4-(5-Phenylfuran-2-yl)aniline 248



White solid 0.19 g (35.0 %): mp 129-133 °C (decomposed); IR (cm^{-1}): 3463 (*N*-H), 3372 (*N*-H), 1620, 1498, 1295, 1020, 823, 795, 694; 1H NMR (300 MHz; DMSO- d_6): 5.36 (2H, s, NH_2), 6.62 (2H, d, $J = 8.1$ Hz, 2 x CH, H-2), 6.67 (1H, s, CH, H-3'), 6.96 (1H, s, CH, H-4'), 7.24 (1H, t, $J = 7.5$ Hz, CH, H-4''), 7.41 (2H, t, $J = 7.2$ Hz, 2 x CH, H-3''), 7.47 (2H, d, $J = 8.1$ Hz, 2 x CH, H-2), 7.73 (2H, d, $J = 7.8$ Hz, 2 x CH, H-3), 7.77 (2H, d, $J = 7.8$ Hz, 2 x CH, H-2''); ^{13}C NMR (100 MHz; DMSO- d_6) (assignments made using DEPT-135): 104.0 (CH), 108.0 (CH), 113.9 (CH), 122.9 (CH), 124.8 (CH), 126.8 (CH), 128.8 (CH), 130.5 (C), 148.5 (C), 150.6 (C), 154.1 (C) one quaternary carbon was not observed in the spectrum; +ESIMS m/z (relative intensity): 236.2 (100 %, $[M + H]^+$); found by +ESIMS 236.1071, $C_{16}H_{14}ON$ $[M + H]^+$, requires 236.1070, error 0.5 ppm.

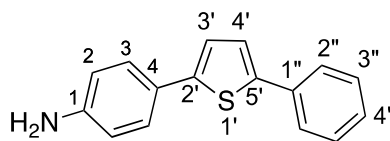
2.26.3. 3-(5-Phenylthiophen-2-yl)aniline 249



Grey solid 0.20 g (32.0 %): IR (cm^{-1}): 3430 (*N*-H), 3346 (*N*-H), 3205, 1596, 1581, 1483, 1454, 808, 775, 756, 288; 1H NMR (300 MHz; DMSO- d_6): 5.22 (2H, s, NH_2), 6.52 (1H, s, CH, H-2), 6.82-6.86 (2H, m, 2 x CH, H-3', H-4'), 7.06 (1H, t, $J = 7.5$ Hz, CH), 7.30-7.48 (5H, m, 5 x CH), 7.66 (2H, d, $J = 7.2$ Hz, 2 x CH, H-2'').

Chapter III. Experimental/ Chemistry

2.26.4. 4-(5-Phenylthiophen-2-yl)aniline **250**

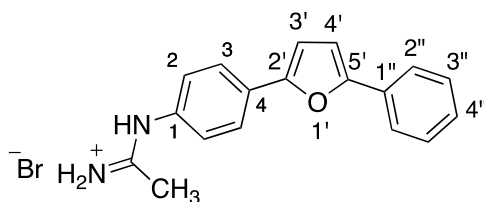


Orange solid 0.08 g (64.0 %): IR (cm^{-1}): 3392 (*N*-H), 3306 (*N*-H), 1609, 1516, 1489, 1263, 830, 801, 751; ^1H NMR (300 MHz; DMSO- d_6): 5.37 (2H, s, NH_2), 6.59 (2H, d, $J = 8.4$ Hz, 2 x *CH*, H-2), 7.21-7.44 (7H, m, 7 x *CH*, H-3', H-4', H-2'', H-3'', H-4''), 7.63 (d, $J = 7.5$ Hz, 2 x *CH*, H-3); ^{13}C NMR (100 MHz; DMSO- d_6) (assignments made using DEPT-135): 115.3 (*CH*), 122.1 (*CH*), 123.9 (*CH*), 125.1 (*C*), 125.5 (*CH*), 126.9 (*CH*), 127.2 (*C*), 128.9 (*CH*), 134.6 (*C*), 144.4 (*C*), 146.1 (*C*), one primary carbon (*CH*) was not observed in the spectrum.

2.27. General procedure for the synthesis of *N*-aryl amidines (reversed amidines) **235** and **236**

Glacial acetic acid (2.0 mmol) and *S*-2-naphthylmethylthioacetimidate hydrobromide **251** (1.0 mmol) were added to a solution of amines, **248** or **250** (1.0 mmol) in chloroform. The reaction was stirred at room temperature overnight and monitored by TLC (20 % EtOAc/ hexane).

2.27.1. *N*-(4-(5-Phenylfuran-2-yl)phenyl)acetimidate hydrobromide **235**

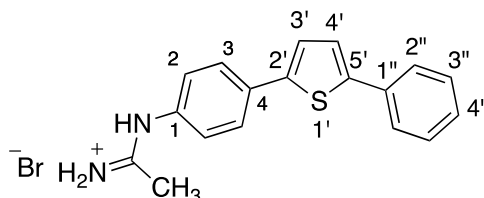


The brown precipitate was filtered off under vacuum and rinsed with diethyl ether to give 0.10 g (88.8 %) of **235**: mp 99 -100 °C (decomposed); IR (cm^{-1}): 3023, 2362, 1738, 1672, 1625, 1367, 1215, 768, 685; ^1H NMR (300 MHz; DMSO- d_6): 2.28 (3H, s, CH_3), 7.08 (1H, d, $J = 3.3$ Hz, furan-*CH*), 7.14 (1H, d, $J = 3.6$ Hz, furan-*CH*), 7.28 (1H, t, $J = 7.2$ Hz, *CH*, H-4''), 7.34 (2H, d, $J = 8.4$ Hz, 2 x *CH*), 7.41 (2H, t, $J = 7.8$ Hz, 2 x *CH*, H-3''), 7.78 (2H, d, $J = 7.2$ Hz, 2 x *CH*, H-2''), 7.91 (2H, d, $J = 8.7$ Hz, 2 x *CH*), 8.58 (1H, s, *N*-H), 9.44 (1H, s, *N*-H), 11.14 (1H, s, *N*-H); ^{13}C NMR (100 MHz; DMSO- d_6) (assignments made using DEPT-135): 19.0 (CH_3), 108.4 (*CH*), 109.2 (*CH*), 123.5 (*CH*), 124.9 (*CH*), 125.8 (*CH*), 127.8 (*CH*), 129.0 (*CH*), 129.8 (*C*), 129.9 (*C*), 133.0 (*C*), 151.6 (*C*), 153.1 (*C*), 164.3 (*C*, *C*-amidine); -ESIMS m/z (relative intensity):

Chapter III. Experimental/ Chemistry

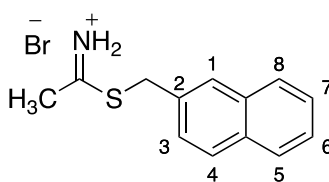
275 (60 %, [M - H]⁻); +ESIMS m/z (relative intensity): 277 (100 %, [M + H]⁺); found by +ESIMS 277.1335, C₁₈H₁₇ON₂ [M + H]⁺, requires 277.1335, error 0.1 ppm.

2.27.2. N-(4-(5-Phenylthiophen-2-yl)phenyl)acetimidate hydrobromide **236**



The precipitate was filtered off under vacuum and rinsed with diethyl ether to give 0.09 g (90.0 %) of **236**: mp 207-209 °C (decomposed); IR (cm⁻¹): 3031, 2362, 1670, 1625, 1203, 804, 1203, 804, 751, 695; ¹H NMR (300 MHz; DMSO-d₆): 2.33 (3H, s, CH₃), 7.32-7.39 (3H, m, 3 x CH), 7.49 (2H, t, *J* = 7.2 Hz, 2 x CH, H-3''), 7.59 (1H, d, *J* = 3.6 Hz, thiophene-CH), 7.63 (1H, d, *J* = 3.6 Hz, thiophene-CH), 7.71 (2H, d, *J* = 7.5 Hz, 2 x CH), 7.85 (2H, d, *J* = 8.1 Hz, 2 x CH), 8.65 (1H, s, N-H), 8.75 (1H, s, N-H), 9.48 (1H, s, N-H); ¹³C NMR (100 MHz; DMSO-d₆): 19.0 (CH₃), 125.18 (CH), 125.22 (CH), 125.8 (CH), 126.0 (CH), 126.6 (CH), 128.0 (CH), 129.2 (CH), 133.26 (C), 133.33 (C), 141.2 (C), 143.3 (C), 164.4 (C, C-amidine), one quaternary carbon has not been observed; +ESIMS m/z (relative intensity): 293 (100 %, [M + H]⁺); found by +ESIMS 293.1113, C₁₈H₁₇N₂ [M + H]⁺, requires 293.1107, error 1.9 ppm.

2.27.3. S-2-Naphthylmethylthioacetimidate hydrobromide **251**



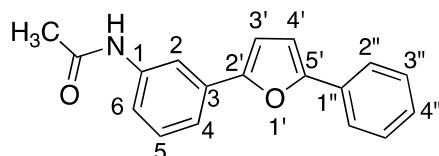
The solution of thioacetamide (0.34 g, 4.5 mmol) and 2-(bromomethyl)naphthalene (1.0 g, 4.5 mmol) in chloroform (10.0 ml) was heated at reflux for 1.5 h. S-2-Naphthylmethylthioacetimidate hydrobromide **251** precipitated from the reaction mixture, which was filtered off under vacuum and rinsed with hexane to give 1.10 g (82.7 %) of a white solid; IR (cm⁻¹): 2849, 1734, 1598, 845, 756, 694; ¹H NMR (300 MHz; DMSO-d₆): 2.64 (3H, s, CH₃), 4.75 (2H, s, CH₂), 7.54-7.56 (3H, m, 3 x CH), 7.91-8.00 (4H, m, 4 x CH), 11.90 (1H, s, N-H); ¹H NMR data were identical to those reported in the literature.^{141c}

Chapter III. Experimental/ Chemistry

2.28. General procedure for the synthesis of *N*-aryl amides 237-239

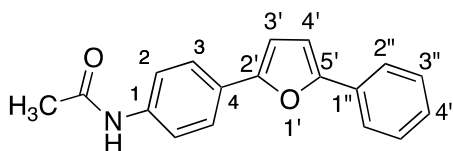
Acetyl chloride (1.0 mmol) was added dropwise at 0 °C to a solution of amine **247**, **248** or **249** (0.01 mmol) in acetonitrile (1.0 mmol) and ethanol (1.0 mmol). The reaction mixture was heated at reflux for 12 h and monitored by TLC with 20 % (EtOAc/ hexane).

2.28.1. *N*-(3-(5-Phenylfuran-2-yl)phenyl)acetamide **237**



The reaction mixture was concentrated, kept in a fridge overnight and the white crystals were filtered off under vacuum and rinsed with hexane. Compound **237** was recrystallized from DMF/ H₂O: mp 164-165 °C; IR (cm⁻¹): 3310 (*N*-H), 1665 (HNC=O), 1606, 1415, 1316, 1026, 762, 689; ¹H NMR (400 MHz; DMSO-d₆): 2.08 (3H, s, CH₃), 7.01 (1H, d, *J* = 3.6 Hz, furan-CH), 7.10 (1H, d, *J* = 3.6 Hz, furan-CH), 7.33-7.39 (2H, m, 2 x CH), 7.46-7.50 (3H, m, 3 x CH), 7.55 (1H, d, *J* = 7.8 Hz, CH), 7.80 (2H, d, *J* = 7.8 Hz, 2 x CH), 8.02 (1H, s, CH, H-2), 10.10 (1H, s, *N*-H); ¹³C NMR (100 MHz; DMSO-d₆) (assignments made using DEPT-135): 24.0 (CH₃), 108.2 (furan-CH, 2 x CH, one of the furan CH was observed overlapping with the second furan CH), 113.7 (CH), 118.2 (CH), 118.4 (CH), 123.3 (CH), 127.6 (CH), 128.9 (CH), 129.3 (CH), 130.0 (C), 133.4 (C), 139.9 (C), 152.45 (C), 152.5 (C), 168.5 (C, C-amide); -ESIMS *m/z* (relative intensity): 277 (100 %, [M - H]⁻).

2.28.2. *N*-(4-(5-Phenylfuran-2-yl)phenyl)acetamide **238**

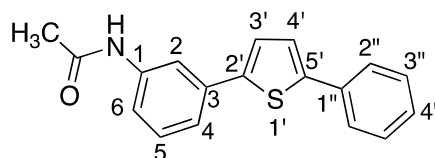


The reaction mixture was concentrated, kept in a fridge overnight and the white crystals were filtered off under vacuum and rinsed with hexane. Compound **238** was recrystallized from DMF/ H₂O to give 0.023 g (37.0 %): IR (cm⁻¹): 3274 (*N*-H), 1656 (HNC=O), 1530, 1369, 1023, 830, 782, 755, 573; ¹H NMR (300 MHz; DMSO-d₆): 2.06 (3H, s, CH₃), 6.95 (1H, s, furan-CH), 7.05 (1H, s, furan-CH), 7.29 (1H, t, *J* = 7.2 Hz, CH, H-4''), 7.44 (2H, t, *J* = 7.8 Hz, 2 x CH, H-3''), 7.65-7.80 (6H, m, 6 x CH, H-2, H-3,

Chapter III. Experimental/ Chemistry

H-2^{''}), 10.06 (1H, s, N-H); ¹³C NMR (100 MHz; DMSO-d₆) (assignments made using DEPT-135): 24.0 (CH₃), 107.0 (CH), 108.2 (CH), 119.1 (CH), 123.3 (CH), 124.0 (CH), 124.9 (C), 127.3 (CH), 128.9 (CH), 130.1 (C), 138.8 (C), 152.0 (C), 152.7 (C), 168.3 (C, C-amide); +ESIMS m/z (relative intensity): 277 (100 %, [M + H]⁺).

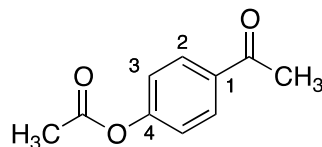
2.28.3. N-(3-(5-Phenylthiophen-2-yl)phenyl)acetamide **239**



The reaction mixture was diluted with dichloromethane, extracted and washed with saturated sodium bicarbonate solution and water. The organic extracted, dried over dry MgSO₄ and evaporated. The crude product was purified by column chromatography using ethyl acetate and hexane (2:8) as the mobile phase to give 0.026 g (23.0 %) of **239** as a yellow solid: mp 166-167 °C; IR (cm⁻¹): 1661, 1606, 1482, 1374, 1327, 779, 755; ¹H NMR (400 MHz; DMSO-d₆): 2.06 (3H, s, CH₃), 7.32-7.54 (8H, m, 8 x CH including H-3' and H-4'), 7.69 (1H, d, *J* = 7.2 Hz, CH), 7.95 (1H, s, CH, H-2), 10.06 (1H, s, N-H); ¹³C NMR (75 MHz; DMSO-d₆): 24.0 (CH₃), 115.5, 118.3, 119.9, 124.8, 124.9, 125.1, 127.8, 129.2, 129.5, 133.4, 133.8, 140.0, 142.46, 142.54, 186.7 (HNC=O); +ESIMS m/z (relative intensity): 316 (100 %, [M + Na]⁺).

2.29. Furan analogue of resveratrol

2.29.1. 4'-(Acetyloxy)acetophenone **253**

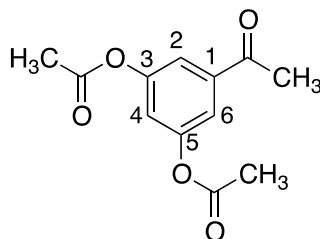


Triethylamine (0.6 g, 5.6 mmol) and 4-(dimethylamino)pyridine (0.01 g, 0.04 mmol) were added to a solution of 4'-hydroxyacetophenone **259** (0.5 g, 3.7 mmol) in dichloromethane (20.0 ml). The reaction mixture was cooled to 0 °C and acetic anhydride (0.40 g, 3.7 mmol) was added dropwise. The reaction mixture was stirred at room temperature for 1.5 h and monitored by TLC (10.0 % MeOH/ CHCl₃). Upon the consumption of the starting material **259**, the reaction was quenched with water and the organic layer was washed with saturated solution of sodium bicarbonate, dried over anhydrous MgSO₄ and evaporated to give 0.34 g (53.1 %) of a colourless oil: ¹H NMR

Chapter III. Experimental/ Chemistry

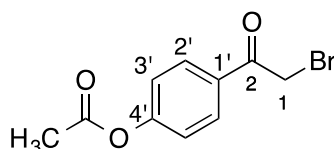
(300 MHz; CDCl_3): 2.30 (3H, s, OCOCH_3), 2.57 (3H, s, COCH_3), 7.17 (2H, d, $J = 8.7$ Hz, 2 x CH , H-3), 7.97 (2H, d, $J = 8.7$ Hz, 2 x CH , H-2); ^{13}C NMR (100 MHz; CDCl_3) (assignments made using DEPT-135): 21.1 (OCOCH_3), 28.3 (COCH_3), 122.0 (2 x CH , C-3), 129.6 (C, C-4), 134.7 (2 x CH , C-2), 168.9 (C, C-1), 174.3 ($\text{OC}=\text{O}$), 197.0 ($\text{C}=\text{O}$); ^1H -NMR data were identical to those reported in the literature.¹⁴⁷

2.29.2. 3',5'-Di(acetyloxy)acetophenone 254



Triethylamine (1.0 g, 9.96 mmol) and 4-(dimethylamino)pyridine (0.01 g, 0.07 mmol) were added to a solution of 3',5'-dihydroxyacetophenone **257** (1.00 g, 6.6 mmol) in dichloromethane (20.0 ml). The reaction mixture was cooled to 0 °C and acetic anhydride (2.70 g, 24.6 mmol) was added dropwise. The reaction mixture was stirred at room temperature for 1.5 h and monitored with TLC (10.0 % MeOH/ CHCl_3). Upon the consumption of the starting material **257**, the reaction was quenched with water and the organic layer was extracted, dried over anhydrous MgSO_4 and evaporated to give 1.10 g (66.0 %) of a white solid: IR (cm^{-1}): 2362, 1763 ($\text{OC}=\text{O}$), 1683 ($\text{C}=\text{O}$), 1363, 1201, 1123, 1018, 677; ^1H NMR (300 MHz; CDCl_3): 2.33 (6H, s, 2 x OCOCH_3), 2.59 (2H, s, COCH_3), 7.16 (1H, s, CH , H-4), 7.57 (2H, s, 2 x CH , H-2, H-6); ^{13}C NMR (100 MHz; CDCl_3) (assignments made using DEPT-135): 21.1 (OCOCH_3), 26.7 (COCH_3), 119.0 (CH , C-4), 120.2 (2 x CH , C-2, C-6), 138.9 (C), 151.2 (C), 168.8 ($\text{OC}=\text{O}$), 195.9 ($\text{C}=\text{O}$).

2.29.3. 2-Bromo-4'-(acetyloxy)acetophenone 255

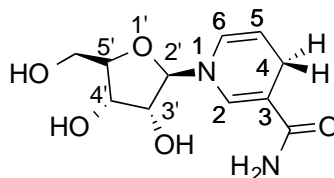


Bromine (1.20 g, 7.5 mmol) in tetrahydrofuran (10.0 ml) was added dropwise at 0 °C to a solution of 4'-hydroxyacetophenone acetate **253** (1.0 g, 5.8 mmol) and aluminium chloride (5.00 mg) in tetrahydrofuran (5.0 ml). The reaction mixture was stirred at room temperature for 2 h and monitored with TLC (1.0 % MeOH/ CHCl_3).

Chapter III. Experimental/ Chemistry

Upon the consumption of the starting material **253**, tetrahydrofuran was evaporated and the residue dissolved in ethyl acetate, washed with water and brine, and dried over anhydrous MgSO_4 . The crude was purified by column chromatography using ethyl acetate and hexane (1:9) as a mobile phase to give 0.25 g (17.0 %) of a white solid: mp 73-76 °C; IR (cm^{-1}): 3315, 1661 (OC=O), 1597, 1568, 1279, 1173, 851, 763, 710, 593; ^1H NMR (300 MHz; CDCl_3): 2.35 (3H, s, CH_3), 4.44 (2H, s, CH_2), 7.25 (2H, d, $J = 7.8$ Hz, 2 x CH , H-3'), 8.04 (2H, d, $J = 8.7$ Hz, 2 x CH , H-2'); ^{13}C NMR (100 MHz; CDCl_3) (assignments made using DEPT-135): 21.2 (OCOCH₃), 30.7 (CH_2), 122.2 (2 x CH , C-3), 130.5 (2 x CH , C-2), 131.6 (C), 154.9 (C), 168.8 (C, OC=O), 190.1 (C, C=O).

2.30. *N*-Ribosyl dihydronicotinamide NRH



NADH (0.50 g, 0.69 mmol) was dissolved in 20.0 ml of 0.4 M sodium carbonate/bicarbonate buffer, pH 10.0, and incubated at 37°C for 16 h with 0.1 unit of phosphodiesterase 1 type IV (phosphodiesterase I from *Crotalus atrox* western diamondback rattlesnake) and 500 units of alkaline phosphatase type VII-S. After complete digestion of NADH, the mixture was freeze dried. The dried powder was extracted with methanol (5 × 6 ml), and this methanol extract was dried by rotary evaporation and dissolved in 5.0 ml of water. The NRH was then purified by preparative HPLC performed on a microsorb C18 column (21.2 X 250 mm), eluted with 10 % methanol in water over 15 m at a flow rate of 15.0 ml/m, using a 1.0 ml injection size. The NRH peak was detected at a wavelength of 350 nm. This peak from each injection was collected, freeze-dried and stored at 4°C. ^1H NMR (300 MHz; D_2O): 2.95 (s, CH , H-4) 3.53-3.65 (m, OCH_2), 3.84-3.85 (m, CH), 3.91-4.01 (m, CH), 4.08 (t, $J = 6.0$ Hz, CH , H-3'), 4.75 (d, $J = 6.9$ Hz, CH , H-2'), 4.85-4.87 (m, CH , H-4') 5.98 (d, $J = 8.1$ Hz, CH , H-6), 7.03 (s, CH , H-2); ^{13}C -NMR (75 MHz; D_2O): 21.9, 61.4, 70.1, 70.9, 83.5, 94.8, 100.9, 105.1, 125.2, 137.8, 172.9 (C, C-amide).

Chapter III. Experimental/ NQO2 Inhibitory Activity

1. Materials and methods

BECKMAN DU 7400 spectrophotometer was used to determine enzyme activity. Water bath Grant JB series was used to heat the buffer to 37 °C. **NRH** used was synthesized according to the procedure described in Section 2.30.

2. General procedure⁸²

The rates of the NQO2 enzyme were determined spectrophotometrically by recording the rates of DCPIP colour change over 1 m at 37 °C in cuvettes of 1.0 cm width containing a final volume of 1.0 ml: 940 µl phosphate buffer (50.0 mM, pH 7.4), 10 µl NQO2 (5×10^{-3} mg/ml), 20.0 µl **NRH** (10.0 mM), 20.0 µl DCPIP (2.0 mM), 10.0 µl DMSO (in the control sample), and 10.0 µl inhibitor (5 samples of different concentration).

All the experiments were performed in triplicates, three independent times. In each independent experiment fresh solutions of **NRH** (10.0 mM), DCPIP (2.0 mM) and NQO2 (5×10^{-3} mg/ml) were prepared. **NRH** and NQO2 were dissolved in 50 mM phosphate buffer (50 mM, pH 7.4) and kept at 0 °C. DCPIP was dissolved in deionized water. The inhibitor stock solution was prepared by dissolving the inhibitor in DMSO. A 10-fold serial dilution was completed using DMSO to end up with five different concentrations of the inhibitor.

IC₅₀ values were determined by the Prism program. The curve was obtained from plotting enzyme activity as a percent of the control versus the final concentration of the inhibitor used. IC₅₀ values were determined as 50% reduction in the enzyme activity compared to control (100%).

Chapter III. Experimental/ Docking

1. Materials and methods

The X-ray crystal structure of human NQO2 (PDB code 1QR2, resolution 2 Å) was obtained from the Protein Bank database (PDB).¹⁶² The inhibitors were drawn using MOE 2011.10 software and the docking was performed using GOLD suite 5.1 software.⁹⁶

2. General procedure

Firstly the hydrogen atoms were added to the structure, which included the protein and FAD molecules. The binding affinities of the docked inhibitors were calculated using ChemScore scoring function. NQO2 protein was prepared for docking by determining the active site area. The active site was defined as being any volume within 15 Å of N5 of the FAD cofactor.⁸² The hydrophilic amino acid Asn¹⁶¹ was allowed to be flexible to maximize the ability of the prediction of hydrogen bonding with the amidine group of the docked inhibitors. The top 10 solutions for each ligand were retained and analyzed for favorable interactions within the active site of NQO2, including low protein ligand clash, lipophilic contacts, and hydrogen bonding interactions.

All figures of NQO2 enzyme and docking images were manipulated using Pymol software (for education use only) and the correlation charts and the regression analyses were done using the Excel program.

Chapter III. Experimental/ DNA Melting

1. Materials and methods

Calf thymus DNA was purchased from Sigma-Aldrich Company. The melting temperatures were measured using Thermal software on a Varian spectrophotometer.

2. Calf thymus DNA preparation

Calf thymus DNA lyophilized powder (1.0 mg) was dissolved in deionized water (1.0 ml) and kept at 2-8 °C overnight. 10.0 µl aliquot of calf thymus DNA solution (1.0 mg/ ml) was diluted with 990.0 µl buffer.

2. General procedure for DNA melting temperatures measurement⁹⁸

The melting temperatures of calf thymus DNA were determined spectrophotometrically by recording the absorbance of DNA at 260 nm over a range of 25-98 °C in cuvettes of 1.0 cm width containing a final volume of 1.0 ml: 980 µl low-salt phosphate buffer (7.5 mM NaH₂PO₄, 1 mM EDTA, pH 7.4) or high-salt buffer (7.5 mM NaH₂PO₄, 150.0 mM NaCl, 15.0 mM sodium citrate, pH 7.0), 10 µl calf thymus DNA (10 µg/ml), and 10.0 µl inhibitor (1.0 mM). All the experiments were performed in triplicates, three independent times. DNA melting temperatures (T_m) were determined using Excel program. The curve was obtained from plotting DNA absorbance at 260 nm versus the temperature. T_m values were from the first-derivative curves.

Chapter IV. References

1. References

1. Steward, W. P.; Brown, K., Cancer chemoprevention: a rapid evolving field. *Brit J Cancer* **2013**, *109*, 1-7.
2. Sherr, C. J., Cancer cell cycles. *Science* **1996**, *274*, 1672-7.
3. Poulsen, H. E.; Loft, S., Early biochemical markers of effects: enzyme induction, oncogene activation and markers of oxidative damage. *Toxicology* **1995**, *101* (1-2), 55-64.
4. Al-Hajj, M.; Clarke, M. F., Self-renewal and solid tumour stem cells. *Oncogene* **2004**, *23* (43), 7274-82.
5. Poste, G.; Fidler, I. J., The pathogenesis of cancer metastasis. *Nature* **1980**, *283* (5743), 139-46.
6. Gavhane, Y. N., Solid tumors: facts, challenges and solutions. *Int J Pharm Sci Res* **2011**, *2* (1), 1-12.
7. Chabner, B. A.; Roberts, T. G., Chemotherapy and the war on cancer. *Nat Rev Cancer* **2005**, *5* (1), 65-72.
8. Lemke, T. L.; Williams, D. A., *Foy's principles of Medicinal Chemistry*. Lippincott Williams and Wilkins: USA, 2008.
9. Bertino, J. R., The mechanism of action of folate antagonists in man. *Cancer Res* **1963**, *23* (7), 1282-06.
10. Gorlick, R.; Goker, E.; Trippett, T.; Waltham, M.; Banerjee, D.; Bertino, J. R., Intrinsic and acquired resistance to methotrexate in acute Leukaemia. *New Eng J Med* **1996**, *335* (14), 1041-8.
11. Kaye, S. B., New antimetabolites in cancer chemotherapy and their clinical impact. *Brit J Cancer* **1998**, *78* (Suppl 3), 1-7.
12. Perigaud, C.; Gosselin, G.; Imbach, J. L., Nucleoside analogues as a chemotherapeutic agents: a review. *Nucleos Nucleot* **1992**, *11* (2-4), 903-45.
13. Galmarini, C. M.; Mackey, J. R.; Dumontet, C., Nucleoside analogues and nucleobases in cancer treatment. *Lancet* **2002**, *3* (7), 415-24.
14. Longley, D. B.; Harkin, D. P.; Johnston, P. G., 5-Fluorouracil: mechanisms of action and clinical strategies. *Nat Rev Cancer* **2003**, *3* (5), 330-9.
15. Burchenal, J. H.; Murphy, M. L.; Ellison, R. R.; Sykes, M. P.; Tan, T. C.; Leone, L. A.; Karnof-Sky, D. A.; Craver, L. F.; Dargeon, H. W.; Rhoads, C. P., Clinical evaluation of a new antimetabolite, 6-mercaptopurine, in the treatment of leukaemia and allied diseases. *Blood* **1953**, *8* (11), 965-99.
16. Bignold, L. P., Alkylating agents and DNA polymerase. *Anticancer Res* **2006**, *26* (2B), 1327-36.
17. Warwick, G. P., The mechanism of action of alkylating agents. *Cancer Res* **1963**, *23* (8 part 1), 1315-33.
18. Colvin, D. M., Alkylating agents and platinum antitumour compounds. 5th ed.; BC Decker: Holland-Frei Cancer Medicine, 2000.
19. Lodish, H.; Berk, A.; L., Z. S.; Matsudaira, P.; Baltimore, D.; Darnell, J., *Molecular Cell Biology*. 4th ed.; W. H. Freeman 2000.
20. Pommier, Y., Topoisomerase I inhibitors: camptothecins and beyond. *Nat Rev Cancer* **2006**, *6* (10), 789-802.
21. Thakur, D. S., Topoisomerase II inhibitors in cancer treatment. *Int J Pharm Sci Nano* **2011**, *3* (4), 1173-81.
22. Williams, L. D.; Egli, M.; Rich, A., DNA Intercalation: helix unwinding and neighbour-exclusion. *Structure and Function* **1992**, *Volume 1: Nucleic acids*, 107-25.
23. Demeunynck, M., Antitumour acridines. *Expert Opin Ther Pat* **2004**, *14* (1), 55-70.

Chapter IV. References

24. Minotti, G.; Menna, P.; Salvatorelli, E.; Cairo, G.; Gianni, L., Anthracyclines: molecular advances and pharmacologic developments in antitumor activity and cardiotoxicity. *Pharmacol Rev* **2004**, *56* (2), 185-229.
25. Arcamone, F.; Cassinelli, G.; Faktini, G.; Grein, A.; Orezzi, P.; Pol, C.; Spalla, C., Adriamycin, 14-hydroxydaunomycin, a new antitumor antibiotic from *S. peucetius* var. *caesius* *Biotechnol Bioeng* **1969**, *11* (6), 1101-10.
26. (a) Zhou, J.; Giannakakou, P., Targeting microtubules for cancer chemotherapy. *Curr Med Chem: Anti-Cancer Agents* **2005**, *5* (1), 65-71; (b) Jordan, M. A.; Wilson, L., Microtubules as a targeting for cancer drugs. *Nat Rev Cancer* **2004**, *4* (4), 253-65.
27. Vermeulen, K.; Bockstaele, D. V.; Berneman, Z. N., The cell cycle: a review of regulation, deregulation and therapeutic targets in cancer. *Cell Proliferat* **2003**, *36* (3), 131-49.
28. Schwartz, G. K.; Shah, M. A., Targeting the cell cycle: a new approach to cancer therapy. *J Clin Bio* **2005**, *23* (36), 9408-21.
29. Akhdar, H.; Legendre, C.; Aninat, C.; More, F., Anticancer drug metabolism: chemotherapy resistance and new therapeutic approaches. In *Topics on drug metabolism*, Paxton, J., Ed. InTech: 2012.
30. (a) Sporn, M. B.; Suh, N., Chemoprevention of cancer. *Carcinogenesis* **2000**, *21* (3), 525-30; (b) Sporn, M. B.; Suh, N., Chemoprevention: an essential approach to controlling cancer. *Nat Rev Cancer* **2002**, *2* (7), 537-43.
31. Stoner, G. D.; Morse, M. A., Cancer chemoprevention: principles and prospects. *Carcinogenesis* **1993**, *14* (9), 1737-46.
32. Wu, X.; Patterson, S.; Hawk, E., Chemoprevention-history and general principles. *Best Pract res Cl Ga* **2011**, *25*, 445-59.
33. Nayfield, S. G.; Karp, J. E.; Ford, L. G.; Dorr, F. A.; Kramer, B. S., Potential role of tamoxifen in prevention of breast cancer. *J Natl Cancer Inst* **1991**, *83* (20), 1450-9.
34. Thomsen, A.; Kolesar, J. M., Chemoprevention of breast cancer. *Am J Health Syst Pharm* **2008**, *65* (23), 2221-8.
35. William Jr, W. N.; Heymach, J. V.; Kim, E. S.; Lippman, S. M., Molecular targets for cancer chemoprevention. *Nat Rev Drug Discov* **2009**, *8*, 213-25.
36. Gravitz, L., Chemoprevention: first line of defence. *Nature* **2011**, *471* (7339), S5-S7.
37. Nishiyama, T.; Izawa, T.; Usami, M.; Ohnuma, T.; Ogura, K.; Hiratsuka, A., Cooperation of NAD(P)H: quinone oxidoreductase 1 and UDP-glucuronosyltransferases reduce menadione cytotoxicity in HEK293 cells. *Biochem Bioph Res Co* **2010**, *394* (3), 459-63.
38. Deller, S.; Macheroux, P.; Sollner, S., Flavon-dependent quinone reductases. *Cell Mol Life Sci* **2008**, *65* (1), 141-60.
39. Brunmark, A.; Cadenas, E., Redox and addition chemistry of quinoid compounds and its biological implications. *Free Radical Bio Med* **1989**, *7* (4), 435-77.
40. Halliwell, B., Oxidative stress and cancer: have we moved forward? *Biochem J* **2007**, *401* (1), 1-11.
41. Celli, C. M.; Tran, N.; Knox, R.; Jaiswal, A. K., NRH: quinone oxidoreductase 2 (NQO2) catalyzes metabolic activation of quinone and anti-tumour drugs. *Biochem Pharmacol* **2006**, *72* (3), 366-76.
42. Ernster, L.; Danielson, L.; Ljunggren, M., DT Diaphorase: purification from the soluble fraction of rat-liver cytoplasm and properties. *Biochimica Et biophysica Acta* **1962**, *58*, 171-88.
43. (a) Lind, C.; Cadenas, E.; Hochstein, P.; Ernster, L., DT-Diaphorase: purification, properties and function. *Method Enzymol* **1990**, *186* (287-301); (b)

Chapter IV. References

- Edwards, Y. H.; Potter, J.; Hopkinson, D. A., Human FDA-dependent NAD(P)H diaphorase. *Biochem J* **1980**, *187* (429-36); (c) Ernster, L., DT Diaphorase. *Method Enzymol* **1967**, *10*, 309-17.
44. Ross, D.; Kepa, J. K.; Winski, S. L.; Beall, H. D.; Anwar, A.; Siegel, D., NAD(P)H: Quinone oxidoreductase 1 (NQO1): chemoprotection, bioactivation, gene regulation and genetic polymorphisms. *Chem-Biol Interact* **2000**, *129* (1-2), 77-97.
45. Huang, X.; Dong, Y.; Bey, E. A.; Kilgore, J. A.; Bair, J. S.; Li, L.; Patel, M.; Parkinson, E. I.; Wang, Y.; Williams, N. S.; Gao, J.; Hergenrother, P. J.; Boothman, D. A., An NQO1 substrate with potent antitumour activity that selectively kills by PARP1-induced programmed necrosis. *Cancer Res* **2012**, *72* (12), 3038-47.
46. Riley, R. J.; Workman, P., DT-Diaphorase and cancer chemotherapy. *Biochem Pharmacol* **1992**, *43* (8), 1657-69.
47. Asher, G.; Dym, O.; Tsvetkov, P.; Adler, J.; Shaul, Y., The crystal structure of NAD(P)H quinone oxidoreductase 1 in complex with its potent inhibitor dicumarol. *Biochemistry* **2006**, *45* (20), 6372-8.
48. Li, R.; Bianchet, M. A.; Talalay, P.; Amzel, L. M., The three-dimensional structure of NAD(P)H: quinone reductase, a flavoprotein involved in cancer chemoprotection and chemotherapy: mechanism of the two-electron reduction. *P Natl Acad Sci USA* **1995**, *92* (19), 8846-50.
49. Rauschnot, J. C.; Yang, C.; Yang, V.; Bhattacharyya, S., Theoretical determination of the redox potentials of NRH: quinone oxidoreductase 2 using quantum mechanical/molecular mechanical simulations. *J Phys Chem-US* **2009**, *113* (23), 8149-57.
50. Kwiek, J. J.; Haystead, T. A., Kinetic mechanism of quinone oxidoreductase 2 and its inhibition by the antimalarial quinolines. *Biochemistry* **2004**, *43*, 4538-47.
51. Liao, S.; Williams-Ashman, H. G., Enzymatic oxidation of some non-phosphorylated derivatives of dihydronicotinamide. *Biochem Bioph Res Co* **1961**, *4* (3), 208-13.
52. Jaiswal, A. K., Human NAD(P)H: quinone oxidoreductase 2, gene structure, activity and tissue expression *J Biol Chem* **1994**, *269*, 14502-8.
53. Jaiswal, A. K.; Burnett, P.; Adesnik, M.; McBride, O. W., Nucleotide and deduced amino acid sequence of human cDNA (NQO2) corresponding to a second member of the NAD(P)H: quinone oxidoreductase gene family. Extensive polymorphism at the NQO2 gene locus on chromosome 6 *Biochemistry* **1990**, *29* (7), 1899-906.
54. Foster, C. E.; Bianchet, M. A.; Talalay, P.; Zhou, Q.; Amzel, L. M., Crystal structure of human quinone reductase type 2, a metalloflavoprotein. *Biochemistry* **1999**, *38* (31), 9881-6.
55. Buryanovskyy, L.; Fu, Y.; Boyd, M.; Ma, Y.; Hsieh, T.; Wu, J. M.; Zhang, Z., Crystal structure of quinone reductase 2 in complex with resveratrol. *Biochemistry* **2004**, *43* (36), 11417-26.
56. Maiti, A.; reddy, P. V. N.; Sturdy, M.; Marler, L.; Pegan, S. D.; Mesecar, A. D.; Pezzuto, J. M.; Cushman, M., Synthesis of casimiroin and optimization of its quinone reductase 2 and aromatase inhibitory activities. *J Med Chem* **2009**, *52* (7), 1873-84.
57. Zhao, Q.; Yang, X. L.; Holtzclaw, W. D.; Talalay, P., Unexpected genetic and structural relationships of a long-forgotten flavoenzyme to NAD(P)H: quinone reductase (DT-diaphorase *P Natl Acad Sci USA* **1997**, *94* (5), 1669-74.
58. Hsieh, T.; Yang, C.; Linn, C.; Lee, Y.; Wu, J. M., Control of stability of cyclin D1 by quinone reductase 2 in CWR22Rv1 prostate cancer cells. *Carcinogenesis* **2012**, *33* (3), 670-7.

Chapter IV. References

59. Liao, S.; Dulaney, J. T.; Williams-Ashman, H. G., Purification of a flavoprotein catalyzing the oxidation of reduced ribosyl nicotinamide. *J Biol Chem* **1962**, *237*, 2981-7.
60. Boutin, J. A.; Chatelain-Egger, F.; Vella, F.; Delagrangé, P.; Ferry, G., Quinone reductase 2 substrate specificity and inhibition pharmacology. *Chem-Biol Interact* **2005**, *151* (3), 213-28.
61. Fu, Y.; Buryanovskyy, L.; Zhang, Z., Quinone reductase 2 is a catechol quinone reductase. *J Biol Chem* **2008**, *283*, 23829-35.
62. Gaikwad, N. W.; Yang, L.; Rogan, E. G.; Cavalieri, E. L., Evidence for NQO2-mediated reduction of the carcinogenic estrogen *ortho*-quinones. *Free Radical Bio Med* **2009**, *46* (2), 253-62.
63. Long II, D. J.; Iskander, K.; Gaikwad, A.; Arin, M.; Roop, D. R.; Knox, R.; Roberto, B.; Jaiswal, A. K., Disruption of dihydronicotinamide riboside: quinone oxidoreductase 2 (NQO2) leads to myeloid hyperplasia of bone marrow and decreased sensitivity to menadione toxicity. *J Biol Chem* **2002**, *277* (48), 46131-9.
64. (a) Lorentzen, R. J.; Ts'o, P. O., Benzo[a]pyrenedione/benzo[a]pyrenediol oxidation-reduction couples and the generation of reactive reduced molecular oxygen. *Biochemistry* **1977**, *16* (7), 1467-73; (b) Lorentzen, R. J.; Lesko, S. A.; McDonald, K.; Ts'o, P. O., Toxicity of metabolic benzo[a]pyrenediones to cultured cells and the dependence upon molecular oxygen. *Cancer Res* **1979**, *39* (8), 3194-8.
65. Chesis, P. L.; Levin, D. E.; Smith, M. T.; Ernster, L.; Ames, B. N., Mutagenicity of quinones: pathways of metabolic activation and detoxification. *P Natl Acad Sci USA* **1984**, *81* (6), 1696-700.
66. (a) Hosoda, S.; Nakamura, W.; Hayashi, K., Properties and reaction mechanism of DT diaphorase from rat liver. *J Biol Chem* **1974**, *249* (20), 6416-23; (b) Wu, K.; Knox, R.; Sun, X. Z.; Joseph, P.; Jaiswal, A. K.; Zhang, D.; Deng, P.; Chen, S., Catalytic properties of NAD(P)H: quinone oxidoreductase-2 (NQO2), a dihydronicotinamide riboside dependent oxidoreductase *Arch Biochem Biophys* **1997**, *347* (2), 221-8.
67. Chen, S.; Wu, K.; Knox, R., Structure-function studies of DT-diaphorase (NQO1) and NRH: quinone oxidoreductase (NQO2). *Free Radical Bio Med* **2000**, *29* (3-4), 276-84.
68. Gong, X.; Kole, L.; Iskander, K.; Jaiswal, A. K., NRH: Quinone oxidoreductase 2 and NAD(P)H: quinone oxidoreductase 1 protect tumour suppressor p53 against 20S proteasomal degradation leading to stabilization and activation of p53 *Cancer Res* **2007**, *67* (11), 5380-8.
69. Pietsch, E. C.; Humbey, O.; Murphy, M. E., Polymorphisms in the p53 pathway. *Oncogene* **2006**, *25* (11), 1602-11.
70. Rooseboom, M.; Commandeur, J.; Vermeulen, N., Enzyme-catalyzed activation of anticancer prodrugs. *Pharmacol Rev* **2004**, *56* (1), 53-102.
71. Schlager, J. J.; Powis, G., Cytosolic NAD(P)H-(quinone-acceptor) oxidoreductase in human normal and tumour tissue: effects of cigarette smoking and alcohol. *Int J Cancer* **1990**, *45*, 403-9.
72. Knox, R. J.; Jenkins, T. C.; Hobbs, S. M.; Chen, S.; Melton, R. G.; Burke, P. J., Bioactivation of 5-(Aziridin-1-yl)-2,4-dinitrobenzamide (CB 1954) by human NAD(P)H quinone oxidoreductase 2: a novel co-substrate-mediated antitumour prodrug therapy *Cancer Res* **2000**, *60* (15), 4179-86.
73. Seville, S.; Phillips, R. M.; Shnyder, S. D.; Wright, C. W., Synthesis of cryptolepine analogues as potential bioreducible anticancer agents. *Bioorgan Med Chem* **2007**, *15* (19), 6353-60.

Chapter IV. References

74. (a) Iyer, V. N.; Szybalski, W., Molecular mechanism of mitomycin action: linking of complementary DNA strands. *Microbiology* **1963**, *50*, 355-62; (b) Jamieson, D.; Tung, A. T.; Knox, R. J.; Boddy, A. V., Reduction of mitomycin C is catalyzed by human recombinant NRH: quinone oxidoreductase 2 using reduced nicotinamide adenine dinucleotide as an electron donating co-factor. *Brit J Cancer* **2006**, *95* (9), 1229-33.
75. Siegel, D.; Howard, B.; Senekowitsch, C.; Kasai, M.; Arai, H.; Gibson, N. W.; Ross, D., Bioreductive activation of mitomycin by DT-diaphorase. *Biochemistry* **1992**, *13* (34), 7879-85.
76. Siegel, D.; Beall, H.; Kasai, M.; Arai, H.; Gibson, N. W.; Ross, D., PH-dependent inactivation of DT-diaphorase by mitomycin C and proflomycin. *Mol Pharmacol* **1993**, *44* (6), 1128-34.
77. Phillips, R. M., Bioreductive activation of a series of analogues of 5-aziridinyl-3-hydroxymethyl-1-methyl-2-[1H-indole-4,7-dione]prop- β -en- α -ol (EO9) by human DT-diaphorase. *Biochem Pharmacol* **1996**, *52* (1711-8).
78. Ahn, K. S.; Gong, X.; Sethi, G.; Chaturvedi, M. M.; Jaiswal, A. K.; Aggarwal, B. B., Deficiency of NRH: quinone oxidoreductase 2 differentially regulates TNF signalling in keratinocytes: up-regulation of apoptosis correlates with down-regulation of cell survival kinases *Cancer Res* **2007**, *67* (20), 10004-11.
79. Aggarwal, B. B., Signalling pathways of the TNF superfamily: a double-edged sword. *Nat Rev Immunol* **2003**, *3* (9), 745-56.
80. Wang, C.; Mayo, M. W.; Baldwin, A. S., TNF- and cancer therapy-induced apoptosis: potentiation by inhibition of NF- κ B. *Science* **1996**, *274* (5288), 784-7.
81. Winger, J. A.; Hantschel, O.; Superti-Furga, G.; Kuriyan, J., The structure of the leukaemia drug imatinib bound to human quinone reductase 2 (NQO2). *BMC Structural Biology* **2009**, *9* (7).
82. Nolan, K. A.; Dunstan, M. S.; Caraher, M. C.; Scott, K. A.; Leys, D.; Stratford, I. J., *In silico* screening reveals structurally diverse, nanomolar inhibitors of NQO2 that are functionally active in cells and can modulate NF- κ B signaling. *Mol Cancer Ther* **2012**, *11* (1), 194-203.
83. Yamamoto, Y.; Gaynor, R. B., Therapeutic potential of inhibition of the NF- κ B pathway in the treatment of inflammation and cancer. *J Clin Invest* **2001**, *107* (135-41).
84. He, H.; Wang, X.; Zheng, X.; Sun, H.; Shi, X.; Zhong, Y.; Huang, B.; Yang, L.; Li, J.; Liao, L.; Zhang, L.; Hu, L.; Lin, Y., Concurrent blockade of the NF- κ B and Akt pathways potently sensitizes cancer cells to chemotherapeutic-induced cytotoxicity. *Cancer Lett* **2010**, *295* (1), 38-43.
85. Harada, S.; Fujii, C.; Hayashi, A.; Ohkoshi, N., An association between idiopathic parkinson's disease and polymorphisms of phase II detoxification enzymes: glutathione S-transferase M1 and quinone oxidoreductase 1 and 2. *Biochem Bioph Res Co* **2001**, *288* (4), 887-92.
86. Harada, S.; Tachikawa, H.; Kawanishi, Y., A possible association between an insertion/deletion polymorphism of the NQO2 gene and schizophrenia. *Psychiatr Genet* **2003**, *13*, 205-9.
87. Hashimoto, T.; Nakai, M., Increased hippocampal quinone reductase 2 in Alzheimer's disease. *Neuroscience Lett* **2011**, *502* (1), 10-12.
88. Graves, P. R.; Kwiek, J. J.; Fadden, P.; Ray, R.; Hardeman, K.; Coley, A. M.; Foley, M.; Haystead, T. A., Discovery of novel targets of quinoline drugs in the human purine binding proteome. *Mol Pharmacol* **2002**, *62* (6), 1364-72.
89. Jang, M.; Cai, L.; Udeani, G. O.; Slowing, K. V.; Thomas, C. F.; Beecher, C. W.; Fong, H. H.; Farnsworth, N. R.; Kinghorn, A. D.; Mehta, R. G.; Moon, R. C.;

Chapter IV. References

- Pezzuto, J. M., Cancer chemopreventive activity of resveratrol, a natural product derived from grapes. *Science* **1997**, 275 (5297), 218-20.
90. Leung, K.; Shilton, B., Chloroquine binding reveals flavin redox switch function of quinone reductase 2. *J Biol Chem* **2013**, 288 (16).
91. Nosjean, O.; Ferro, M.; Coge, F.; Beauverger, P.; Henlin, J.; Lefoulon, F.; Fauchere, J.; Delagrangé, P.; Canet, E.; Boutin, J. A., Identification of the melatonin-binding site MT3 as the quinone reductase 2. *J Biol Chem* **2000**, 275 (40), 31311-7.
92. Calamini, B.; Santarsiero, B. D.; Boutin, J. A.; Mesecar, A. D., Kinetic, thermodynamic and x-ray structural insights into the interaction of melatonin and analogues with quinone reductase 2. *Biochem J* **2008**, 413 (1), 81-91.
93. Ferry, G.; Delagrangé, P.; Boutin, J. A.; Mesecar, A. D., X-Ray structural studies of quinone reductase 2 nanomolar range inhibitors. *Protein Sci* **2011**, 20 (7), 1182-95.
94. Ferry, G.; Hecht, S.; Berger, S.; Moulharat, N.; Coge, F.; Gerald, G.; Leclerc, V.; Yous, S.; Delagrangé, P.; Boutin, J. A., Old and new inhibitors of quinone reductase 2. *Chem-Biol Interact* **2010**, 186 (2), 103-9.
95. Michaelis, S.; Marais, A.; Schrey, A. K.; Graebner, O. Y.; Schaudt, C.; Sefkow, M.; Kroll, F.; Dreger, M.; Glinski, M.; Koester, H.; Metternich, R.; Fischer, J. J., Dabigatran and dabigatran ethyl ester: potent inhibitors of ribosyldihydronicotinamide dehydrogenase (NQO2). *J Med Chem* **2012**, 55 (8), 3934-44.
96. Nolan, K. A.; Humphries, M. P.; Barnes, J.; Doncaster, J. R.; Caraher, M. C.; Tirelli, N.; Bryce, R. A.; Whitehead, R. C.; Stratford, I. J., Triazoloacridin-6-ones as novel inhibitors of the quinone oxidoreductases NQO1 and NQO2. *Bioorgan Med Chem* **2010**, 18 (2), 696-706.
97. Nolan, K. A.; Humphries, M. P.; Bryce, R. A.; Stratford, I. J., Imidazoacridin-6-ones as novel inhibitors of the quinone oxidoreductase NQO2. *Bioorg Med Chem Lett* **2010**, 20 (9), 2832-6.
98. Dunstan, M. S.; Barnes, J.; Humphries, M.; Whitehead, R. C.; Bryce, R. A.; Leys, D.; Stratford, I. J.; Nolan, K. A., Novel inhibitors of NRH: quinone oxidoreductase 2 (NQO2): crystal structures, biochemical activity, and intracellular effects of imidazoloacridin-6-ones. *J Med Chem* **2011**, 54 (19), 6597-611.
99. Dufour, M.; Yan, C.; Siegel, D.; Colucci, M. A.; Jenner, M.; Oldham, N. J.; Gomez, J.; Reigan, P.; Li, Y.; De Matteis, C. I.; Ross, D.; Moody, C. J., Mechanism-based inhibition of quinone reductase 2 (NQO2): selectivity for NQO2 over NQO1 and structural basis for flavoprotein inhibition. *Chembiochem* **2011**, 12 (8), 1203-8.
100. Reddy, P. V. N.; Jensen, K. C.; Mesecar, A. D.; Fanwick, P. E.; Cushman, M., Design, synthesis and biological evaluation of potent quinoline and pyrroloquinoline ammosamide analogues as inhibitors of quinone reductase 2. *J Med Chem* **2011**, 55 (1), 367-77.
101. Aly, A. A.; Nour-El-Din, A. M., Functionality of amidines and amidrazones. *ARKIVOC* **2008**, 1, 153-94.
102. Ishikawa, T., *Superbases for organic synthesis: guanidines, amidines, phosphazenes and related organocatalysts*. 1st ed.; John Wiley and Sons: 2009.
103. Shriner, R. L.; Neumann, F. W., The chemistry of the amidines. *Chem Rev* **1944**, 35 (3), 351-425.
104. Alig, L.; Edenhofer, A.; Hadvary, P.; Hurzeler, M.; Knopp, D.; Muller, M.; Steiner, B.; Trzeciak, A.; Weller, T., Low molecular weight, non-peptide fibrinogen receptor antagonists. *J Med Chem* **1992**, 35 (23), 4393-407.
105. Nagahara, T.; Yokoyama, Y.; Inamura, K.; Katakura, S.; Komoriya, S.; Yamaguchi, H.; Hara, T.; Iwamoto, M., Dibasic (amidinoaryl)propionic acid derivatives as novel blood coagulation factor Xa inhibitors. *J Med Chem* **1994**, 37 (8), 1200-7.

Chapter IV. References

106. (a) Lansiaux, A.; Dassonneville, L.; Facompre, M.; Kumar, A.; Stephens, C. E.; Bajic, M.; Tanious, F.; Wilson, W. D.; Boykin, D. W.; Bailly, C., Distribution of furamide analogues in tumour cells: influence of the number of positive charges. *J Med Chem* **2002**, *45* (10), 1994-2002; (b) Rahimian, M.; Kumar, A.; Say, M.; Bakunov, S. A.; Boykin, D. W.; Tidwell, R. R.; Wilson, W. D., Minor groove binding compounds that jump a GC base pair and bind to adjacent AT base pair sites. *Biochemistry* **2009**, *48* (7), 1573-83.
107. Streuli, C. A., Titration characteristics of organic bases in nitromethane. *Anal Chem* **1959**, *31* (10), 1652-4.
108. Das, B. P.; Boykin, D. W., Synthesis of antiprotozoal activity of 2,5-bis(4-guanylphenyl)furans. *J Med Chem* **1977**, *20* (4), 531-6.
109. Jacobs, W. A.; Heidelberger, M., An improved hydrogen chloride generator. *J Am Chem Soc* **1917**, *39* (10), 2186-8.
110. Suthiwangcharoen, N.; Stephens, C. E., A new synthesis of 2,5-bis(4-cyanophenyl)furan. *ARKIVOC* **2006**, *2006* (16), 122-7.
111. Stetter, H., Catalyzed addition of aldehydes to activated double bonds- a new synthetic approach. *Ange Chem Int Ed* **1976**, *15* (11), 639-712.
112. Nevar, N. M.; Kelin, A. V.; Kulinkovich, O. G., One step preparation of 1,4-diketones from methyl ketones and α -bromomethyl ketones in the presence of ZnCl₂.t-BuOH.Et₂NR as a condensation agent. *Synthesis* **2000**, *9*, 1259-62.
113. Amarnath, V.; Amarnath, K., Intermediates in the Paal-Knorr synthesis of furans. *J Org Chem* **1995**, *60*, 301-7.
114. Schaefer, F. C.; Peters, G. A., Base-catalyzed reaction of nitriles with alcohols. A convenient route to imidates and amidine salts. *J Org Chem* **1961**, *26* (2), 412-8.
115. Roger, R.; Neilson, D. G., The chemistry of imidates. *Chem Rev* **1961**, *61* (2), 179-211.
116. Yadav, V. K.; Babu, K. G., A remarkably efficient Mrkovnikov hydrogenation of olefins and transformation of nitriles into imidates by use of AcCl and an alcohol. *Eur J Org Chem* **2005**, (2), 452-6.
117. Zablocki, J. A.; Miyano, M.; Garland, R. B.; Pireh, D.; Schretzman, L.; Rao, S. N.; Lindmark, R. L.; Panzer-Knodle, S. G.; Nicholson, N. S.; Taite, B. B.; Salyers, A. K.; King, L. W.; Campion, J. G.; Feigen, L. P., Potent *in vitro* and *in vivo* inhibitors of platelet aggregation based upon the Arg-Gly-Asp-Phe sequence of fibrinogen. A proposal on the nature of the binding interaction between the Arg-guanidine of RGD_X mimetics and the platelet GP IIb-IIIa receptor. *J Med Chem* **1993**, *36*, 1811-9.
118. Schaefer, F. C.; Krapcho, A. P., Preparation of amidine salts by reaction of nitriles with ammonium salts in the presence of ammonia. *J Org Chem* **1962**, *27* (4), 1255-8.
119. Garigipati, R. S., An efficient conversion of nitriles to amidines. *Tetrahedron Lett* **1990**, *31* (14), 1969-72.
120. Rousselet, G.; Capdevielle, P.; Maumy, M., Copper(I)-induced addition of amines to unactivated nitriles: the first general one-step synthesis of alkyl amidines. *Tetrahedron Lett* **1993**, *34* (40), 6395-8.
121. Anderluh, P. S.; Anderluh, M.; Ilas, J.; Mravljak, J.; Dolenc, M. S.; Stegnar, M.; Kikelj, D., Toward a novel class of antithrombotic compounds with dual function. Discovery of 1,4-benzoxazin-3(4H)-one derivatives possessing thrombin inhibitory and fibrinogen receptor antagonistic activities. *J Med Chem* **2005**, *48* (31)10-3.
122. Mehta, B.; Mehta, M., *Organic Chemistry*. PHI Learning Pvt. Ltd: 2005.
123. Lee, J. C.; Bae, Y. H.; Chang, S., Efficient α -halogenation of carbonyl compounds by *N*-bromosuccinimide and *N*-chlorosuccinimide. *B Kor Chem Soc* **2003**, *24* (4), 407-8.

Chapter IV. References

124. Munde, M.; Lee, M.; Neidle, S.; Arafa, R.; Boykin, D. W.; Liu, Y.; Bailly, C.; Wilson, W. D., Induced fit conformational changes of a "reversed amidine" heterocycle: optimized interactions in a DNA minor groove complex. *J Am Chem Soc* **2007**, *129*, 5688-98.
125. Sangster, J., Octanol-water partition coefficients of simple organic compounds. *J Phys Chem Ref Data* **1989**, *18* (3).
126. Sander, T. OSIRIS property explorer. <http://www.organic-chemistry.org/prog/peo/>.
127. Amarnath, V.; Anthony, D. C.; Amarnath, K.; Valentine, W. M.; Wetterau, L. A.; Graham, D. G., Intermediates in the Paal-Knorr synthesis of pyrroles. *J Org Chem* **1991**, *56*, 6924-31.
128. Zuliani, V.; Cocconcelli, G.; Fantini, M.; Ghiron, C.; Rivara, M., A practical synthesis of 2,4(5)-diarylimidazoles from simple building blocks. *J Org Chem* **2007**, *72*, 4551-3.
129. Ansele, J. H.; Anbazhagan, M.; Brun, R.; Easterbrook, J. D.; Hall, J. E.; Boykin, D. W., O-Alkoxyamidine prodrugs of furamidine: *in vitro* transport and microsomal metabolism as indicators of *in vivo* efficacy in a mouse model of Trypanosoma brucei rhodesiense infection. *J Med Chem* **2004**, *47* (4335-8).
130. Anbazhagan, M.; Boykin, D. W.; Stephens, C. E., Direct conversion of amidoximes to amidines via transfer hydrogenation. *Synthesis* **2003**, *16*, 2467-9.
131. Brieger, G.; Nestruck, T. J., Catalytic Transfer Hydrogenation. *Chem Rev* **1974**, *74* (5), 567-80.
132. Lakner, F. J.; Parker, M. A.; Rogovoy, B.; Khvat, A.; Ivachtchenko, A., Synthesis of novel trisubstituted imidazolines. *Synthesis* **2009**, *2009* (12), 1987-90.
133. Robinson, R., A new synthesis of oxazole derivatives. *J Chem Soc* **1909**, *95*, 2167-74.
134. Wasserman, H. H.; Vinick, F. J., The mechanism of the Robinson-Gabriel synthesis of oxazoles. *J Org Chem* **1973**, *38* (13), 2407-8.
135. Kel'in, A. V.; Kulinkovich, O. G., A new simple synthesis of aryl-substituted 1,4-diketones. *Synthesis* **1996**, *1996* (3), 330-3.
136. (a) Campaigne, E.; Foye, W. O., The synthesis of 2,5-diarylthiophenes. *J Org Chem* **1952**, *17* (10), 1405-12; (b) Jesberger, M.; Davis, T. P.; Barner, L., Applications of Lawesson's reagent in organic and organometallic syntheses. *Synthesis* **2003**, *2003* (13), 1929-58.
137. Shridhar, D. R.; Jogibhukta, M.; Rao, P. S.; Handa, V. K., An improved method for the preparation of 2,5-disubstituted thiophenes. *Synthesis* **1982**, *1982* (12), 1061-2.
138. Mahajan, U. S.; Godinde, R. R.; Mandhare, P. N., Preparation of amidines from amidoximes via transfer hydrogenation. *Synthetic Commun* **2011**, *41* (15), 2195-9.
139. Weller, T.; Alig, L.; Beresini, M.; Blackburn, B.; Bunting, S.; Hadvary, P.; Muller, H. M.; Knopp, D.; Levet-Trafit, B.; Lipari, M. T.; Modi, N. B.; Muller, M.; Refino, C. J.; Schmitt, M.; Schonholzer, P.; Weiss, S.; Steiner, B., Orally active fibrinogen receptor antagonists. 2. Amidoximes as prodrugs of amidines. *J Med Chem* **1996**, *39*, 3139-47.
140. Yoo, S.; Lee, S., Reduction of organic compounds with sodium borohydride-copper (II) sulfate system. *Synlett* **1990**, *1990* (7), 419-20.
141. (a) Schnur, R. C., A generalized and proton-catalyzed synthesis of amidines from thioimidates. *J Org Chem* **1979**, *44* (21), 3726-7; (b) Stephens, C. E.; Tanious, F.; Kim, S.; Wilson, W. D.; Schell, W. A.; Perfect, J. R.; Franzblau, S. G.; Boykin, D. W., Diguanidino and "reversed" diamidino 2,5-diarylfurans as antimicrobial agents. *J Med Chem* **2001**, *44* (1741-8); (c) Shearer, B. G.; Oplinger, J. A.; Lee, S., S-2-

Chapter IV. References

Naphthylmethyl tioacetimidate hydrobromide: a new odoleless reagent for the emild synthesis of substituted acetamidines. *Tetrahedron Lett* **1997**, 38 (2), 179-82.

142. Dabak, K., Synthesis and protection of some amidines. *Turk J Chem* **2002**, 26, 547-50.

143. Pearse, G. A.; Pflaum, R. T., Interaction of metal ions with amidoximes. *J Am Chem Soc* **1959**, 81 (24), 6505-8.

144. Clement, B.; Jung, F., N-hydroxylation of the antiprotozoal drug pentamidine catalyzed by rabbit liver cytochrome P-450 2C3 or human liver microsomes, microsomal retroreduction and further oxidative transformation of the formed amidoximes. *Drug Metab Dispos* **1994**, 22 (3).

145. Edink, E.; Akdemir, A.; Jansen, C.; Elk, R.; Zuiderveld, O.; Kanter, F. J. J.; Muijlwijk-Koezen, J. E.; Smit, A. B.; Leurs, R.; Esch, I., J. P., Structure-based design, synthesis and structure-activity relationships of dibenzosuberyl- and benzoate-substituted tropines as ligands for acetylcholine-binding protein. *Bioorg Med Chem Lett* **2012**, 22, 1448-54.

146. Corson, B. B.; Heintzelman, W. J.; Schwartzman, L. H.; Tiefenthal, H. E.; Lokken, R. J.; Nickels, J. E.; Atwood, G. R.; Pavlik, F. J., Preparation of vinylphenols and isopropenylphenols. *J Org Chem* **1958**, 23 (4), 544-9.

147. Noji, M.; Ohno, T.; Fuji, K.; Futaba, N.; Tajima, H.; Ishii, K., Secondary benzylation using benzyl alcohols catalyzed by lanthanoid, scandium and hafnium triflate. *J Org Chem* **2003**, 68 (24), 9340-8.

148. Goslinski, T.; Golankiewicz, B.; Clercq, E.; Balzarini, J., Synthesis and biological activity of strongly fluorescent tricyclic analogues of acyclovir and ganciclovir. *J Med Chem* **2002**, 45, 5052-5057.

149. Coleman, J. E., Structure and mechanism of alkaline phosphatase. *Annu Rev Biophys Biom* **1992**, 21, 441-83.

150. Kim, E. E.; Wyckoff, H. W., Reaction mechanism of alkaline phosphatase based on crystal structures: two-metal ion catalysis. *J Mol Biol* **1991**, 218, 449-64.

151. Cheng, Y.; Prusoff, W. H., Relation between the inhibition constant (K_i) and the concentration of inhibitor which causes 50 per cent inhibition (I_{50}) of an enzymatic reaction. *Biochem Pharmacol* **1973**, 22, 3099-108.

152. Lazurkin, Y. S.; Frank-Kamenetskii, M. D.; Trifonov, E. N., Melting of DNA: its study and application as a research method. *Biopolymers* **1970**, 9 (11), 1253-306.

153. Shi, X.; Chaires, J. B., Sequence- and structural-selective nucleic acid binding revealed by the melting of mixtures. *Nucleic Acids Res* **2006**, 34 (2).

154. Thomas, R., The denaturation of DNA. *Gene* **1993**, 135 (1-2), 77-9.

155. Wilson, W. D.; Tanious, F. A.; Ding, D.; Kumar, A.; Boykin, D. W.; Colson, P.; Houssier, C.; Bailly, C., Nucleic acid interactions of unfused aromatic cations: evaluation of proposed minor-groove, major-groove and interaction binding modes. *J Am Chem Soc* **1998**, 120, 10310-21.

156. Schildkraut, C., Dependence of the melting temperature of DNA on salt concentration. *Biopolymers* **1965**, 3, 195-208.

157. Gambhir, S. S., Molecular imaging of cancer with positron emission tomography. *Nat Rev Cancer* **2002**, 2, 683-93.

158. Maxwell, C. E., β -Dimethylaminopropiophenone hydrochloride. *Organic Syntheses* **1955**, 23 (Coll. Vol. 3), 305.

159. Macharla, A. K.; Nappunni, R. C.; Marri, M. R.; Peraka, S.; Nama, N., Oxidative bromination of ketones using ammonium bromide and oxone®. *Tetrahedron Lett* **2102**, 53 (2), 191-5.

Chapter IV. References

160. Wan, C.; Gao, L.; Wang, Q.; Zhang, J.; Wang, Z., Simple and efficient preparation of 2,5-disubstituted oxazoles via a metal-free-catalyzed cascade cyclization. *Org Lett* **2010**, *12* (17), 3902-5.
161. Koga, Y.; Kusama, H.; Narasaka, K., Preparations of furans from β -bromo ketones and enol ethers catalyzed by rhenium (I) nitrogen complex. *B Chem Soc Jpn* **1998**, *71* (2), 475-82.
162. Foster, C. E.; Bianchet, M. A.; Talalay, P.; Zhou, Q.; Amzel, L. M., Crystal structure of human quinone reductase type 2, a metalloflavoprotein (PDB ID: 1QR2). *Biochemistry* **1999**, *38* (31), 9881-6.